Discrete Dynamics in Nature and Society

Epidemic Processes on Complex Networks

Lead Guest Editor: Lu-Xing Yang
Guest Editors: Yong Deng and Jose R. C. Piqueira

Epidemic Processes on Complex Networks

Discrete Dynamics in Nature and Society

Epidemic Processes on Complex Networks

Lead Guest Editor: Lu-Xing Yang
Guest Editors: Yong Deng and Jose R. C. Piqueira

Copyright © 2017 Hindawi. All rights reserved.

This is a special issue published in "Discrete Dynamics in Nature and Society." All articles are open access articles distributed under the Creative Commons Attribution License, which permits unrestricted use, distribution, and reproduction in any medium, provided the original work is properly cited.

Editorial Board

Douglas R. Anderson, USA
David Arroyo, Spain
Viktor Avrutin, Germany
Stefan Balint, Romania
Kamel Barkaoui, France
Gian I. Bischi, Italy
Gabriele Bonanno, Italy
Driss Boutat, France
Gabriella Bretti, Italy
Filippo Cacace, Italy
Pasquale Candito, Italy
Cengiz Çinar, Turkey
Carmen Coll, Spain
Alicia Cordero, Spain
Manuel De la Sen, Spain
Luisa Di Paola, Italy
Josef Diblik, Czech Republic
Xiaohua Ding, China
Elmetwally Elabbasy, Egypt
Hassan A. El-Morshedy, Egypt
D. Fournier-Prunaret, France
Genni Fragnelli, Italy
Ciprian G. Gal, USA
Gisèle R Goldstein, USA
Vladimir Gontar, Israel
Chris Goodrich, USA
Pilar R. Gordoa, Spain
Kannan Govindan, Denmark
Luca Guerrini, Italy
Antonio Iannizzotto, Italy
Giuseppe Izzo, Italy
Sarangapani Jagannathan, USA
Jun Ji, USA
Nikos I. Karachalios, Greece
Eric R. Kaufmann, USA
Victor S. Kozyakin, Russia
Mustafa R. S. Kulenovic, USA
Kousuke Kuto, Japan
Aihua Li, USA
Xiaohui Liu, United Kingdom
M. Ángel López, Spain
Ricardo López-Ruiz, Spain
Agustin Martin, Spain
Akio Matsumoto, Japan
Rigoberto Medina, Chile
V. Méndez, Spain
G. Papashinopoulos, Greece
Juan Pavón, Spain
Allan C. Peterson, USA
Andrew Pickering, Spain
Chuanxi Qian, USA
M. Rafei, Netherlands
Mustapha A. Rami, Spain
Aura Reggiani, Italy
Pavel Rehak, Czech Republic
Paolo Renna, Italy
Marko Robnik, Slovenia
Yuriy Rogovchenko, Norway
Silvia Romanelli, Italy
Leonid Shaikhet, Israel
Seenith Sivasundaram, USA
C. Skokos, South Africa
Piergiulio Tempesta, Spain
Tetsuji Tokihiro, Japan
J. R. Torregrosa, Spain
D. F. M. Torres, Portugal
Firdaus Udwadia, USA
Antonia Vecchio, Italy
F. R. Villatoro, Spain
Hubertus Von Bremen, USA
Abdul-Aziz Yakubu, USA
Bo Yang, USA
Guang Zhang, China
Zhengqiu Zhang, China
Lu Zhen, China
Yong Zhou, China
Zuonong Zhu, China

Contents

Hindawi
Discrete Dynamics in Nature and Society
Volume 2017, Article ID 9873678, 1 page
https://doi.org/10.1155/2017/9873678

Editorial

Epidemic Processes on Complex Networks

Lu-Xing Yang,[1] Yong Deng,[2] and Jose Roberto Castilho Piqueira[3]

[1]*Faculty of Electrical Engineering, Mathematics and Computer Science, Delft University of Technology, 2600 GA Delft, Netherlands*
[2]*School of Computer and Information Science, Southwest University, Chongqing 400715, China*
[3]*Polytechnic School, University of Sao Paulo, 05508-900 Sao Paulo, SP, Brazil*

Correspondence should be addressed to Lu-Xing Yang; ylx910920@gmail.com

Received 21 May 2017; Accepted 21 May 2017; Published 27 August 2017

Copyright © 2017 Lu-Xing Yang et al. This is an open access article distributed under the Creative Commons Attribution License, which permits unrestricted use, distribution, and reproduction in any medium, provided the original work is properly cited.

As a fascinating branch of the emerging network science, the mission of the epidemic dynamics on networks is to understand how objects spread in networks and thereby to work out cost-effective strategy for restraining undesirable objects or promoting desirable objects. This special issue contains ten excellent papers about this subject.

The basic function of the epidemic dynamics is to assess the risk of infectious diseases. J. Liu proposed an epidemic model with curing delay and explored its Hopf bifurcation properties. M. De la Sen et al. modeled the propagation of Ebola disease, determining the key factors affecting the global behavior of the model.

Another important role of the epidemic dynamics is to estimate the destructive effect of digital viruses. Z. Zhang et al. suggested a computer virus spreading model with two time delays (the curing delay and the vaccinating delay) and showed the possibility of a Hopf bifurcation. C. Gan et al. established and studied a digital virus model with nonlinear infection rates and external infection sources and developed a dynamic virus-inhibiting strategy. Q. Zhu and C. Cen presented an epidemic model in which different hosts in a network have separate security levels. Based on a novel individual-level virus-countermeasure interacting model, X. Zhang and C. Gan discussed the issue of how to optimally distribute countermeasures in a network. Based on an individual-level disruptive virus spreading model, J. Bi et al. developed a cost-effective dynamic strategy of restraining disruptive viruses.

An interesting application of the epidemic dynamics is to forecast the risk of attacks and the efficiency of security policies. Based on a new epidemic model and aiming at maximizing the utility of the entire system, Q. Shi et al. designed a cost-effective static detection strategy for defending against internal cyberattacks.

The epidemic dynamics can also be used to explore the way that opinions diffuse in social networks. Under an individual-level opinion spreading model, A. Lu uncovered the influence of the network structure on the converging time of opinion spreading.

For any undesirable transmissible object, the spectral radius minimization problem (SRMP) turns out to be crucial to contain its rampancy in a network. Y. Wu et al. studied the SRMP for a class of regular networks and obtained some results that would be instructive in developing heuristic algorithms for the SRMP.

Acknowledgments

We would like to express our great gratitude to all of the authors for their contributions and the reviewers for their serious evaluation of the papers submitted by valuable comments and timely feedback.

Lu-Xing Yang
Yong Deng
Jose Roberto Castilho Piqueira

Hindawi
Discrete Dynamics in Nature and Society
Volume 2017, Article ID 2836865, 16 pages
https://doi.org/10.1155/2017/2836865

Research Article

Optimal and Nonlinear Dynamic Countermeasure under a Node-Level Model with Nonlinear Infection Rate

Xulong Zhang[1] and Chenquan Gan[1,2]

[1]*College of Computer Science, Chongqing University, Chongqing 400044, China*
[2]*School of Communication and Information Engineering, Chongqing University of Posts and Telecommunications, Chongqing 400065, China*

Correspondence should be addressed to Chenquan Gan; gcq2010cqu@163.com

Received 20 January 2017; Accepted 15 May 2017; Published 12 June 2017

Academic Editor: Jose R. C. Piqueira

Copyright © 2017 Xulong Zhang and Chenquan Gan. This is an open access article distributed under the Creative Commons Attribution License, which permits unrestricted use, distribution, and reproduction in any medium, provided the original work is properly cited.

This paper mainly addresses the issue of how to effectively inhibit viral spread by means of dynamic countermeasure. To this end, a controlled node-level model with nonlinear infection and countermeasure rates is established. On this basis, an optimal control problem capturing the dynamic countermeasure is proposed and analyzed. Specifically, the existence of an optimal dynamic countermeasure scheme and the corresponding optimality system are shown theoretically. Finally, some numerical examples are given to illustrate the main results, from which it is found that (1) the proposed optimal strategy can achieve a low level of infections at a low cost and (2) adjusting nonlinear infection and countermeasure rates and tradeoff factor can be conductive to the containment of virus propagation with less cost.

1. Introduction

In order to study the long-term behavior of computer virus and suppress viral spread macroscopically, a large number of dynamical models have been proposed in the past few decades (for the related references, see, e.g., [1–11]). From the perspective of the division scale of computers on networks, these models can be roughly divided into two categories: *compartment-level models* and *node-level models*.

Compartment-level models are those models that regard computers having the same state as an object to study. This work can be traced back to the 1980s. The first compartment-level model is proposed by Kephart and White [1], who followed the suggestions recommended by Cohen [12] and Murray [13]. Since then, multifarious propagation models have been developed (see, e.g., [14–22]). It is worth noticing that Zhu et al. [6] proposed the original compartment-level SICS (susceptible-infected-countermeasured-susceptible) model with linear static countermeasure based on the CMC (Countermeasure Competing) strategy presented by Chen and Carley [23]. However, compartment-level models ignore the effect of network eigenvalue on viral spread. Consequently, node-level models are considered.

Node-level models are those models that regard a single computer as an object to investigate. The first node-level model (i.e., SIS (susceptible-infected-susceptible) model) is proposed by Van Mieghem et al. [7]. Since then, Sahneh and Scoglio [8] presented the node-level SAIS (susceptible-alert-infected-susceptible) model, and Yang et al. [9, 10] considered the node-level SLBS (susceptible-latent-breaking-susceptible) and SIRS (susceptible-infected-recovered-susceptible) models, respectively. Very recently, Gan [11] established the node-level SIES (susceptible-infected-external-susceptible) model. Besides, for the other related work about this topic, one can refer to [24–28] and the references cited therein.

Inspired by the above-mentioned work and based on the compartment-level SICS model, this paper considers a controlled node-level SICS model. Different from the conventional node-level models, this paper mainly addresses the issue of how to effectively distribute dynamic countermeasure by optimal control strategy (for the related references of optimal models, see, e.g., [29–33]). An optimal control

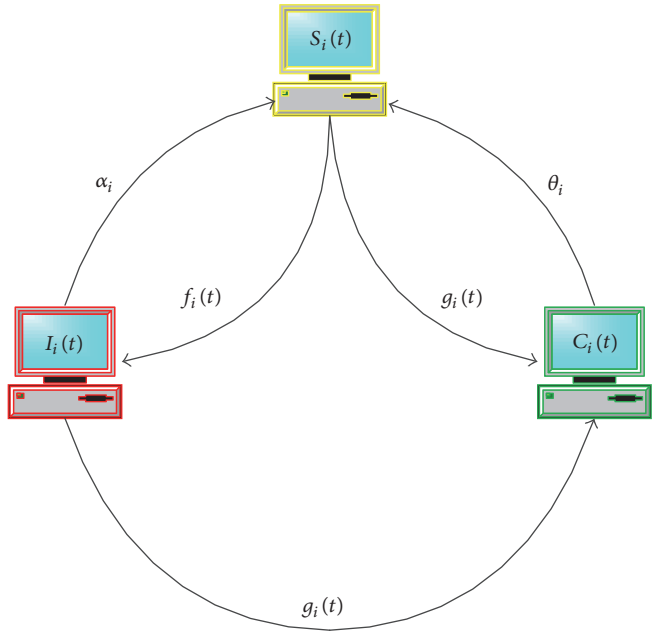

FIGURE 1: The transfer diagram of the controlled node-level SICS model.

problem is proposed and the existence of an optimal control is proved. The corresponding optimality system is also derived. Finally, some numerical examples are made, from which it can be seen that the proposed optimal strategy can achieve a low level of infections at a low cost.

The subsequent materials of this paper are organized as follows. Sections 2 and 3 formulate the controlled node-level model and analyze the optimal control problem, respectively. Numerical examples are provided in Section 4. Finally, Section 5 closes this work.

2. The Controlled Node-Level Model

In this paper, the propagation network of computer virus and countermeasure is represented by a graph $G = (V, E)$ with N nodes labelled $1, 2, \ldots, N$, where each node and edge stand for a computer and a network link, respectively. Thus, the graph G can be described by its adjacency matrix $\mathbf{A} = [a_{ij}]_{N\times N}$, where $a_{ii} = 0$.

As was treated in the traditional SICS model [6], at any time all nodes in the graph G are divided into three groups: S-nodes (susceptible nodes are uninfected but have no immunity), I-nodes (infected nodes), and C-nodes (countermeasured nodes are uninfected and have temporary immunity due to the presence of countermeasures). Let $S_i(t)$, $I_i(t)$, and $C_i(t)$ denote the probability of node i being susceptible, infected, and countermeasured at time t, respectively. Then the vector

$$\left(S_1(t), \ldots, S_N(t), I_1(t), \ldots, I_N(t), C_1(t), \ldots, C_N(t)\right)^T \quad (1)$$

probabilistically captures the state of the network at time t.

For convenience, two important functions, which will be used in the sequel, are defined as follows:

$$f_i(t) = \sum_j \frac{a_{ij}\beta_j I_j(t)}{1 + m_1 I_j(t)}, \quad m_1 \geq 0, \ \beta_j > 0. \quad (2)$$

Clearly, $f_i(t) \leq \sum_j a_{ij}\beta_j I_j(t)$.

$$g_i(t) = \sum_j \frac{a_{ij}\gamma_j(t) C_j(t)}{1 + m_2 C_j(t)}, \quad m_2 \geq 0, \quad (3)$$

where $\gamma_j(t) \in L^2[0, T]$ is a controllable rate, $\underline{\gamma} \leq \gamma_j(t) \leq \overline{\gamma}$, $0 \leq t \leq T$; $\underline{\gamma}$ and $\overline{\gamma}$ are positive constants, $0 < \underline{\gamma} < \overline{\gamma} < 1$.

Now, a set of probabilistic assumptions on the state transition of node i are made (see also Figure 1).

(A1) An S-node i becomes infected at rate $f_i(t)$.

(A2) An S- or I-node i becomes countermeasured at rate $g_i(t)$.

(A3) An I-node i becomes susceptible at a constant rate $\alpha_i > 0$.

(A4) A C-node i loses immunity at constant rate $\theta_i > 0$.

Let Δt be a very small time interval and $o(\Delta t)$ be a higher-order infinitesimal. Assumptions (A1)–(A4) imply that the probabilities of state transition of node i satisfy the following relations:

$$\Pr\left(i \text{ is infected at time } t + \Delta t \mid i \text{ is susceptible at time } t\right) = f_i(t)\Delta t + o(\Delta t),$$

$$\begin{aligned}
&\Pr\left(i \text{ is countermeasured at time } t\right.\\
&\quad \left.+\Delta t \mid i \text{ is susceptible at time } t\right) = g_i(t)\Delta t\\
&\quad + o(\Delta t),\\
&\Pr\left(i \text{ is countermeasured at time } t\right.\\
&\quad \left.+\Delta t \mid i \text{ is infected at time } t\right) = g_i(t)\Delta t + o(\Delta t),\\
&\Pr\left(i \text{ is susceptible at time } t\right.\\
&\quad \left.+\Delta t \mid i \text{ is infected at time } t\right) = \alpha_i \Delta t + o(\Delta t),\\
&\Pr\left(i \text{ is susceptible at time } t\right.\\
&\quad \left.+\Delta t \mid i \text{ is countermeasured at time } t\right) = \theta_i \Delta t\\
&\quad + o(\Delta t).
\end{aligned} \tag{4}$$

Invoking the total probability formulas and letting $\Delta t \to 0$, the controlled node-level model (i.e., controlled node-level SICS model) can be derived.

$$\begin{aligned}
\frac{dS_i(t)}{dt} &= \alpha_i I_i(t) + \theta_i C_i(t) - f_i(t) S_i(t) - g_i(t) S_i(t),\\
\frac{dI_i(t)}{dt} &= -\alpha_i I_i(t) + f_i(t) S_i(t) - g_i(t) I_i(t),\\
\frac{dC_i(t)}{dt} &= -\theta_i C_i(t) + g_i(t)\left(S_i(t) + I_i(t)\right),\\
&\qquad 0 \le t \le T,\ i = 1, 2, \ldots, N,
\end{aligned} \tag{5}$$

with initial condition

$$\begin{aligned}
&\left(S_1(0), \ldots, S_N(0), I_1(0), \ldots, I_N(0), C_1(0), \ldots, C_N(0)\right)^T\\
&\quad \in \widetilde{\Omega},
\end{aligned} \tag{6}$$

where

$$\begin{aligned}
\widetilde{\Omega} = \Big\{&\left(S_1, \ldots, S_N, I_1, \ldots, I_N, C_1, \ldots, C_N\right)^T \in \mathbb{R}_+^{3N} \mid S_i\\
&+ I_i + C_i = 1,\ i = 1, 2, \ldots, N\Big\}.
\end{aligned} \tag{7}$$

The admissible control set is

$$U = \left\{\mathbf{u}(\cdot) \in \left(L^2[0,T]\right)^N \mid \underline{\gamma} \le \gamma_i(\cdot) \le \overline{\gamma},\ 1 \le i \le N\right\}, \tag{8}$$

where $\mathbf{u}(\cdot) = (\gamma_1(\cdot), \ldots, \gamma_N(\cdot))^T$.

3. The Optimal Control Problem

As $S_i(t) + I_i(t) + C_i(t) \equiv 1$, $1 \le i \le N$, system (5) can be reduced to the following system:

$$\begin{aligned}
\frac{dI_i(t)}{dt} &= -\alpha_i I_i(t) + f_i(t)\left(1 - I_i(t) - C_i(t)\right)\\
&\qquad - g_i(t) I_i(t),\\
\frac{dC_i(t)}{dt} &= -\theta_i C_i(t) + g_i(t)\left(1 - C_i(t)\right),\\
&\qquad 0 \le t \le T,\ i = 1, 2, \ldots, N,
\end{aligned} \tag{9}$$

with initial condition

$$\left(I_1(0), \ldots, I_N(0), C_1(0), \ldots, C_N(0)\right)^T \in \Omega, \tag{10}$$

where

$$\begin{aligned}
\Omega = \Big\{&\left(I_1, \ldots, I_N, C_1, \ldots, C_N\right)^T \in \mathbb{R}_+^{2N} \mid I_i + C_i \le 1,\ i\\
&= 1, 2, \ldots, N\Big\}.
\end{aligned} \tag{11}$$

Then system (9) can be written in matrix notation as

$$\frac{d\mathbf{x}(t)}{dt} = \mathbf{f}\left(\mathbf{x}(t), \mathbf{u}(t)\right), \quad 0 \le t \le T, \tag{12}$$

with initial condition $\mathbf{x}(0) \in \Omega$.

Now, the objective is to find a control variable $\mathbf{u}(\cdot) \in U$ so as to minimize both the prevalence of infected computers and the total budget for dynamic countermeasure during the time period $[0, T]$. That is, the following optimal control problem needs to be solved:

$$\underset{\mathbf{u} \in U}{\text{Minimize}}\ J(\mathbf{u}) = \int_0^T L\left(\mathbf{x}(t), \mathbf{u}(t)\right) dt \tag{P}$$

subject to system (12), where

$$L(\mathbf{x}, \mathbf{u}) = \sum_i \left(I_i(t) + \frac{1}{2}\varepsilon_i \gamma_i^2(t)\right), \quad \varepsilon_i > 0, \tag{13}$$

is the Lagrangian and $\varepsilon = (\varepsilon_1, \ldots, \varepsilon_N)^T$ is a tradeoff factor based on the control effect and control cost of dynamic countermeasure.

3.1. Existence of an Optimal Control. First, a lemma, which plays a critical role afterwards, is introduced.

Lemma 1 (see [34, 35]). *We have an optimal control problem*

$$\underset{\mathbf{u} \in U}{\text{Minimize}}\ J(\mathbf{u}) = \int_0^T L\left(\mathbf{x}(t), \mathbf{u}(t)\right) dt \tag{14}$$

subject to

$$\frac{d\mathbf{x}(t)}{dt} = \mathbf{f}\left(\mathbf{x}(t), \mathbf{u}(t)\right), \quad 0 \le t \le T, \tag{15}$$

with $\mathbf{x}(0) \in \Omega$, *where* Ω *is positively invariant for system (15). The problem has an optimal control if the following six conditions hold simultaneously.*

(C1) *There is* $\mathbf{u} \in U$ *such that system (15) is solvable.*

(C2) U *is convex.*

(C3) U *is closed.*

(C4) $\mathbf{f}(\mathbf{x}, \mathbf{u})$ *is bounded by a linear function in* $\mathbf{x}$.

(C5) $L(\mathbf{x}, \mathbf{u})$ *is convex on* U.

(C6) $L(\mathbf{x}, \mathbf{u}) \ge c_1 \|\mathbf{u}\|_2^\rho + c_2$ *for some* $\rho > 1$, $c_1 > 0$, *and* c_2.

In order to prove the existence of an optimal control, six lemmas, one for each condition in Lemma 1, should be proved.

Lemma 2. *There is* $\mathbf{u} \in U$ *such that system (9) or (12) is solvable.*

Proof. Substituting $\mathbf{u} \equiv \overline{\mathbf{u}} \coloneqq (\underbrace{\overline{\gamma}, \ldots, \overline{\gamma}}_{N})^T$ into system (12), one can get the uncontrolled system:

$$\frac{d\mathbf{x}(t)}{dt} = \mathbf{f}(\mathbf{x}(t), \overline{\mathbf{u}}) \tag{16}$$

with $\mathbf{x}(0) \in \Omega$. Then the function $\mathbf{f}(\mathbf{x}, \overline{\mathbf{u}})$ is continuously differentiable, and Ω is positively invariant for the system. Hence, the claimed result follows from the Continuation Theorem for differential equations [36]. □

Lemma 3. *The admissible set* U *is convex.*

Proof. Let

$$\begin{aligned} \mathbf{u}^{(1)} &= \left(\gamma_1^{(1)}, \ldots, \gamma_N^{(1)}\right) \in U, \\ \mathbf{u}^{(2)} &= \left(\gamma_1^{(2)}, \ldots, \gamma_N^{(2)}\right) \in U, \\ & \qquad 0 < \xi < 1. \end{aligned} \tag{17}$$

As $(L^2[0,T])^N$ is a real vector space, one can obtain

$$(1-\xi)\,\mathbf{u}^{(1)} + \xi \mathbf{u}^{(2)} \in \left(L^2[0,T]\right)^N. \tag{18}$$

Then, the convexity of U follows by the observation that

$$\underline{\gamma} \le (1-\xi)\,\gamma_i^{(1)} + \xi \gamma_i^{(2)} \le \overline{\gamma}, \quad 1 \le i \le N. \tag{19}$$

Hence, the claimed result follows. □

Lemma 4. *The admissible set* U *is closed.*

Proof. Let $\mathbf{u} = (\gamma_1, \ldots, \gamma_N)^T$ be a limit point of U and

$$\mathbf{u}^{(n)} = \left(\gamma_1^{(n)}, \ldots, \gamma_N^{(n)}\right)^T, \quad n = 1, 2, \ldots, \tag{20}$$

be a sequence of points in U such that

$$\left\|\mathbf{u}^{(n)} - \mathbf{u}\right\|_2 \coloneqq \left[\int_0^T \left|\mathbf{u}^{(n)}(t) - \mathbf{u}(t)\right|^2 dt\right]^{1/2} < \frac{1}{n}. \tag{21}$$

From the completeness of $(L^2[0,T])^N$, one can get

$$\lim_{n\to\infty} \mathbf{u}^{(n)} = \mathbf{u} \in \left(L^2[0,T]\right)^N. \tag{22}$$

Hence, the closeness of U follows from the observation that

$$\underline{\gamma} \le \gamma_i = \lim_{n\to\infty} \gamma_i^{(n)} \le \overline{\gamma}, \quad 1 \le i \le N. \tag{23}$$

□

Lemma 5. $\mathbf{f}(\mathbf{x}, \mathbf{u})$ *is bounded by a linear function in* $\mathbf{x}$.

Proof. Note that, for system (9) and for $i = 1, 2, \ldots, N$,

$$\begin{aligned} -\frac{\overline{\gamma} N^2}{4} - \alpha_i I_i \le \frac{dI_i}{dt} &\le -\alpha_i I_i + \sum_j a_{ij}\beta_j I_j, \\ -\theta_i C_i \le \frac{dC_i}{dt} &\le -\theta_i C_i + \overline{\gamma} \sum_j a_{ij} C_j. \end{aligned} \tag{24}$$

Thus, the claimed result follows. □

Lemma 6. $L(\mathbf{x}, \mathbf{u})$ *is convex on* U.

Proof. Note that the Hessian matrix of $L(\mathbf{x}, \mathbf{u})$ with respect to $\mathbf{u} \in U$ is as follows:

$$\begin{aligned} &\mathbf{H}_{\mathbf{u}}(L) \\ &= \begin{bmatrix} \frac{\partial^2 L}{\partial \gamma_1^2} & \frac{\partial^2 L}{\partial \gamma_1 \partial \gamma_2} & \cdots & \frac{\partial^2 L}{\partial \gamma_1 \partial \gamma_{N-1}} & \frac{\partial^2 L}{\partial \gamma_1 \partial \gamma_N} \\ \frac{\partial^2 L}{\partial \gamma_2 \partial \gamma_1} & \frac{\partial^2 L}{\partial \gamma_2^2} & \cdots & \frac{\partial^2 L}{\partial \gamma_2 \partial \gamma_{N-1}} & \frac{\partial^2 L}{\partial \gamma_2 \partial \gamma_N} \\ \vdots & \vdots & \ddots & \vdots & \vdots \\ \frac{\partial^2 L}{\partial \gamma_{N-1} \partial \gamma_1} & \frac{\partial^2 L}{\partial \gamma_{N-1} \partial \gamma_2} & \cdots & \frac{\partial^2 L}{\partial \gamma_{N-1}^2} & \frac{\partial^2 L}{\partial \gamma_{N-1} \partial \gamma_N} \\ \frac{\partial^2 L}{\partial \gamma_N \partial \gamma_1} & \frac{\partial^2 L}{\partial \gamma_N \partial \gamma_2} & \cdots & \frac{\partial^2 L}{\partial \gamma_N \partial \gamma_{N-1}} & \frac{\partial^2 L}{\partial \gamma_N^2} \end{bmatrix} \\ &= \begin{bmatrix} \varepsilon_1 & 0 & \cdots & 0 & 0 \\ 0 & \varepsilon_2 & \cdots & 0 & 0 \\ \vdots & \vdots & \ddots & \vdots & \vdots \\ 0 & 0 & \cdots & \varepsilon_{N-1} & 0 \\ 0 & 0 & \cdots & 0 & \varepsilon_N \end{bmatrix}. \end{aligned} \tag{25}$$

For any $t \in [0,T]$, $\mathbf{H}_{\mathbf{u}}(L)$ is real symmetric and its eigenvalues are all positive. Then, $\mathbf{H}_{\mathbf{u}}(L)$ is positive definite. Hence, the convexity of $L(\mathbf{x}, \mathbf{u})$ follows by the result in [37]. □

Lemma 7. $L(\mathbf{x}, \mathbf{u}) \ge c_1 \|\mathbf{u}\|_2^\rho + c_2$ *for some* $\rho > 1$, $c_1 > 0$, *and* c_2.

Proof. Let $\rho = 2$, $c_1 = \min_i\{\varepsilon_i\}/2$, and $c_2 = 0$. Then, $L(\mathbf{x}, \mathbf{u}) \ge (\min_i\{\varepsilon_i\}/2) \times \|\mathbf{u}\|_2^2$. Thus, the proof is complete. □

Now, it is time to examine the main result of this subsection.

Theorem 8. *The optimal control problem* (P) *has a solution.*

Proof. Lemmas 2–7 show that the six conditions in Lemma 1 are all met. Hence, the proof is complete. □

3.2. The Optimality System. In this subsection, a necessary condition for an optimal control of problem (P) is drawn.

Theorem 9. *Suppose* $\mathbf{u}^*(\cdot)$ *is an optimal control for problem* (P) *and* $(I^*(\cdot), C^*(\cdot))^T$ *is the solution to system (9) with*

$\mathbf{u}(\cdot) = \mathbf{u}^*(\cdot)$. *Then, there exist functions* $\lambda_{1i}^*(t)$ *and* $\lambda_{2i}^*(t)$, $0 \le t \le T$, $1 \le i \le N$, *such that*

$$\begin{aligned}
\frac{d\lambda_{1i}^*(t)}{dt} &= -1 + \lambda_{1i}^*(t)\left[\alpha_i + f_i^*(t) + g_i^*(t)\right] \\
&\quad - \frac{\beta_i}{\left(1 + m_1 I_i^*(t)\right)^2} \\
&\quad \cdot \sum_j a_{ij}\lambda_{1j}^*(t)\left(1 - I_j^*(t) - C_j^*(t)\right), \\
\frac{d\lambda_{2i}^*(t)}{dt} &= \lambda_{1i}^*(t) f_i^*(t) + \lambda_{2i}^*(t)\left[\theta_i + g_i^*(t)\right] \\
&\quad + \frac{\gamma_i^*(t)}{\left(1 + m_2 C_i^*(t)\right)^2} \\
&\quad \cdot \sum_j a_{ij}\left[I_j^*(t)\lambda_{1j}^*(t) - \left(1 - C_j^*(t)\right)\lambda_{2j}^*(t)\right], \\
&\qquad 0 \le t \le T,\ i = 1, 2, \ldots, N,
\end{aligned} \tag{26}$$

with transversality conditions

$$\lambda_{1i}^*(T) = \lambda_{2i}^*(T) = 0, \quad i = 1, 2, \ldots, N. \tag{27}$$

Furthermore, one can get

$$\gamma_i^*(t) = \max\left\{\min\left\{\frac{C_i^*(t)}{\varepsilon_i\left(1 + m_2 C_i^*(t)\right)}\sum_j a_{ij}\left[I_j^*(t)\lambda_{1j}^*(t) - \left(1 - C_j^*(t)\right)\lambda_{2j}^*(t)\right], \overline{\gamma}\right\}, \underline{\gamma}\right\}, \tag{28}$$
$$0 \le t \le T,\ i = 1, 2, \ldots, N.$$

Proof. The corresponding Hamiltonian is

$$\begin{aligned}
H(\mathbf{I}, \mathbf{C}, \lambda, \mathbf{u}) &= \sum_i \left(I_i + \frac{1}{2}\varepsilon_i \gamma_i^2\right) + \sum_i \lambda_{1i}\frac{dI_i}{dt} \\
&\quad + \sum_i \lambda_{2i}\frac{dC_i}{dt},
\end{aligned} \tag{29}$$

where λ_{1i}, λ_{2i} are undetermined, $\lambda = (\lambda_{11}, \ldots, \lambda_{1N}, \lambda_{21}, \ldots, \lambda_{2N})^T$.

According to the Pontryagin Minimum Principle [35], there exist functions $\lambda_{1i}^*(t)$ and $\lambda_{2i}^*(t)$, $0 \le t \le T$, $1 \le i \le N$, such that

$$\begin{aligned}
\frac{d\lambda_{1i}^*(t)}{dt} &= -\frac{\partial H\left(\mathbf{I}^*(t), \mathbf{C}^*(t), \lambda^*(t), \mathbf{u}^*(t)\right)}{\partial I_i}, \\
\frac{d\lambda_{2i}^*(t)}{dt} &= -\frac{\partial H\left(\mathbf{I}^*(t), \mathbf{C}^*(t), \lambda^*(t), \mathbf{u}^*(t)\right)}{\partial C_i}, \\
&\qquad 0 \le t \le T,\ i = 1, 2, \ldots, N.
\end{aligned} \tag{30}$$

Thus, system (26) follows by direct calculations. As the terminal cost is unspecified and the final state is free, the transversality conditions hold. By using the optimality condition

$$H\left(\mathbf{I}^*, \mathbf{C}^*, \lambda^*, \mathbf{u}^*\right) = \min_{\mathbf{u}\in U} H\left(\mathbf{I}^*, \mathbf{C}^*, \lambda^*, \mathbf{u}\right), \tag{31}$$

one can obtain that, for $0 \le t \le T$ and for $1 \le i \le N$, either

$$\begin{aligned}
&\frac{\partial H\left(\mathbf{I}^*(t), \mathbf{C}^*(t), \lambda^*(t), \mathbf{u}^*(t)\right)}{\partial \gamma_i} = \varepsilon_i \gamma_i^*(t) \\
&\quad - \frac{C_i^*(t)}{1 + m_2 C_i^*(t)} \\
&\quad \cdot \sum_j a_{ij}\left[I_j^*(t)\lambda_{1j}^*(t) - \left(1 - C_j^*(t)\right)\lambda_{2j}^*(t)\right] = 0
\end{aligned} \tag{32}$$

or $\gamma_i^*(t) = \underline{\gamma}$ or $\gamma_i^*(t) = \overline{\gamma}$. Hence, the proof is complete. □

By combining the above discussions, one can get the optimality system for problem (P) as follows:

$$\begin{aligned}
\frac{dI_i(t)}{dt} &= -\alpha_i I_i(t) + f_i(t)\left(1 - I_i(t) - C_i(t)\right) - g_i(t) I_i(t), \\
\frac{dC_i(t)}{dt} &= -\theta_i C_i(t) + g_i(t)\left(1 - C_i(t)\right), \\
\frac{d\lambda_{1i}(t)}{dt} &= -1 + \lambda_{1i}(t)\left[\alpha_i + f_i(t) + g_i(t)\right] - \frac{\beta_i}{\left(1 + m_1 I_i(t)\right)^2}\sum_j a_{ij}\lambda_{1j}(t)\left(1 - I_j(t) - C_j(t)\right), \\
\frac{d\lambda_{2i}(t)}{dt} &= \lambda_{1i}(t) f_i(t) + \lambda_{2i}(t)\left[\theta_i + g_i(t)\right] + \frac{\gamma_i(t)}{\left(1 + m_2 C_i(t)\right)^2}\sum_j a_{ij}\left[I_j(t)\lambda_{1j}(t) - \left(1 - C_j(t)\right)\lambda_{2j}(t)\right],
\end{aligned}$$

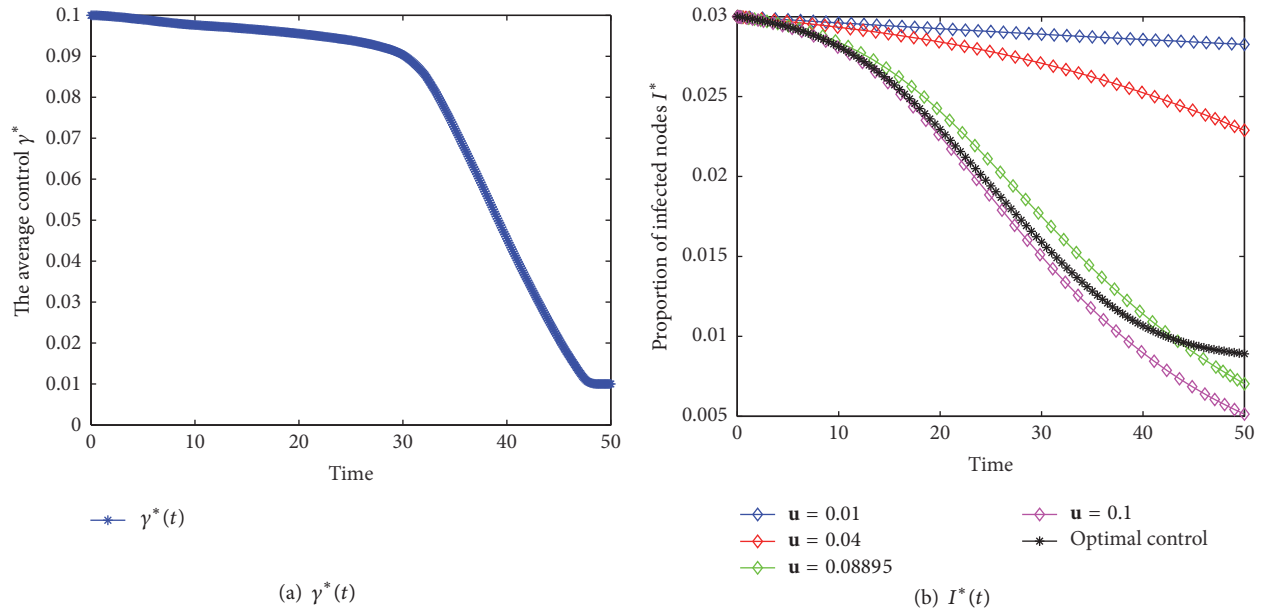

(a) $\gamma^*(t)$ (b) $I^*(t)$

FIGURE 2: $\gamma^*(t)$ and $I^*(t)$ under different control strategies with $m_1 = m_2 = 2$ for Example 1.

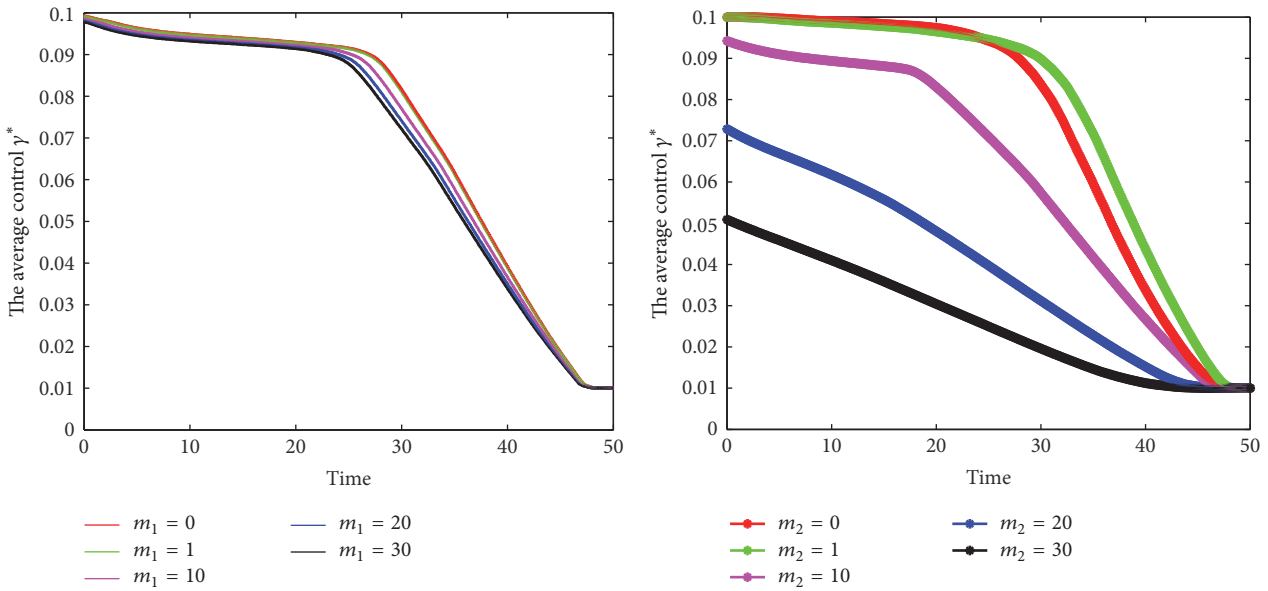

(a) $m_2 = 5$ (b) $m_1 = 5$

FIGURE 3: $\gamma^*(t)$ for different m_1 and m_2 for Example 1.

$$\gamma_i(t) = \max\left\{\min\left\{\frac{C_i(t)}{\varepsilon_i\left(1 + m_2 C_i(t)\right)}\sum_j a_{ij}\left[I_j(t)\lambda_{1j}(t) - \left(1 - C_j(t)\right)\lambda_{2j}(t)\right], \overline{\gamma}\right\}, \underline{\gamma}\right\},$$

$$0 \le t \le T,\ i = 1, 2, \ldots, N, \tag{33}$$

with $(\mathbf{I}(0), \mathbf{C}(0))^T \in \Omega$ and $\lambda(T) = 0$.

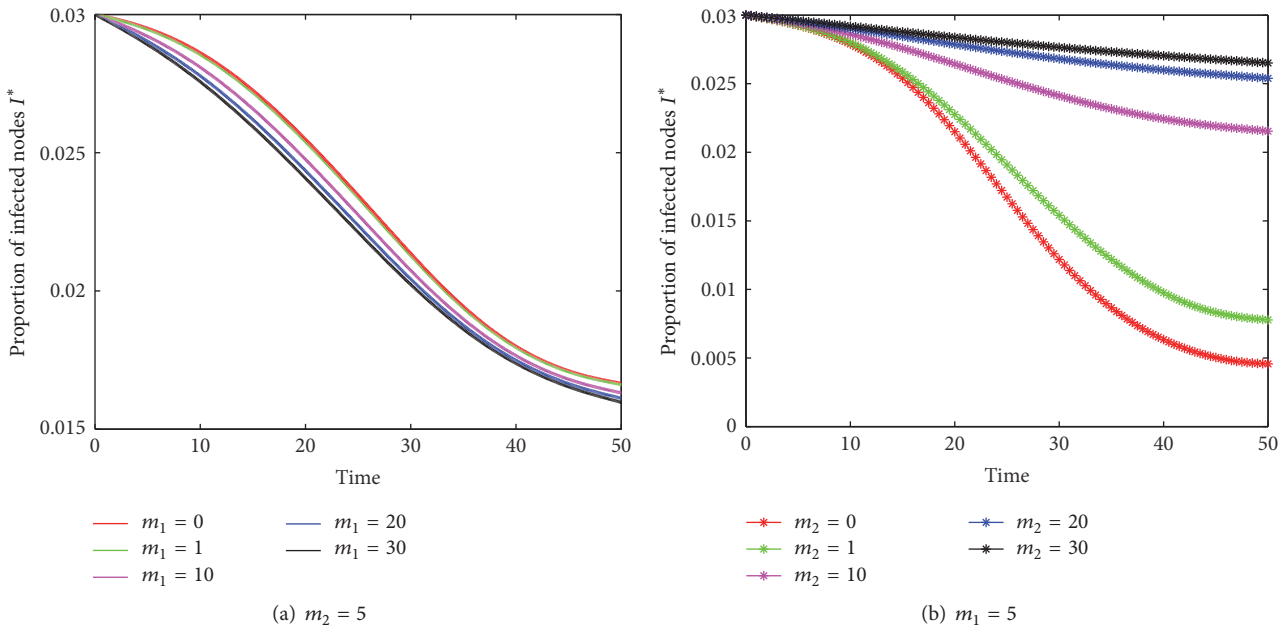

FIGURE 4: $I^*(t)$ for different m_1 and m_2 for Example 1.

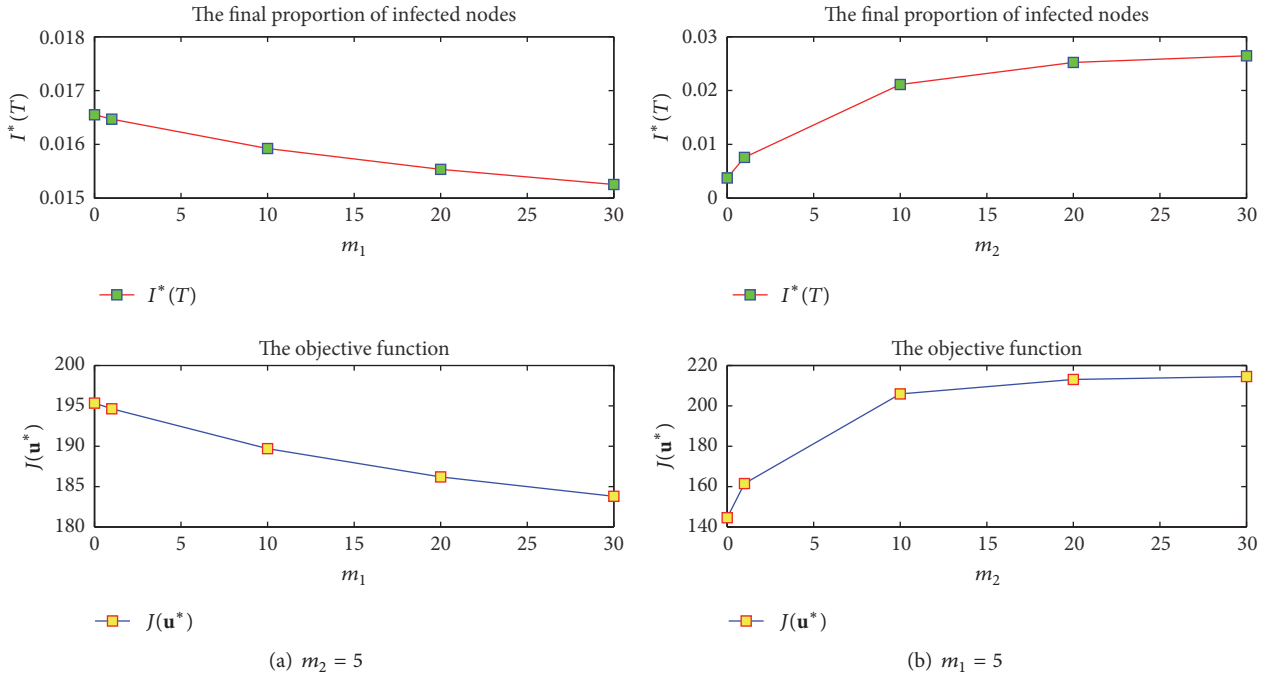

FIGURE 5: The final proportion of infected nodes $I^*(T)$ and the objective function $J(\mathbf{u}^*)$ for different m_1 and m_2 for Example 1.

4. Numerical Examples

In this section, the effectiveness of the optimal dynamic countermeasure will be verified by some numerical examples.

For our purpose, three networks are considered: a synthetic small-world network (WS network [38]), a synthetic scale-free network (BA network [39]), and a partial Facebook network [40], with $N = 150$ nodes, respectively. The parameters of system (33) are set as $\alpha_i = 0.01$, $\beta_i = 0.004887$ (the value of β_i comes from a report on some real infection probabilities in [41]), $\theta_i = 0.02$, $\varepsilon_i = 1$, $\underline{\gamma} = 0.01$, $\overline{\gamma} = 0.1$, and $T = 50$, $1 \le i \le N$, and the initial conditions are set as $I_i(0) = 0.03$ and $C_i(0) = 0.01$, $1 \le i \le N$. The optimality system (33) is solved by invoking the backward-forward Euler

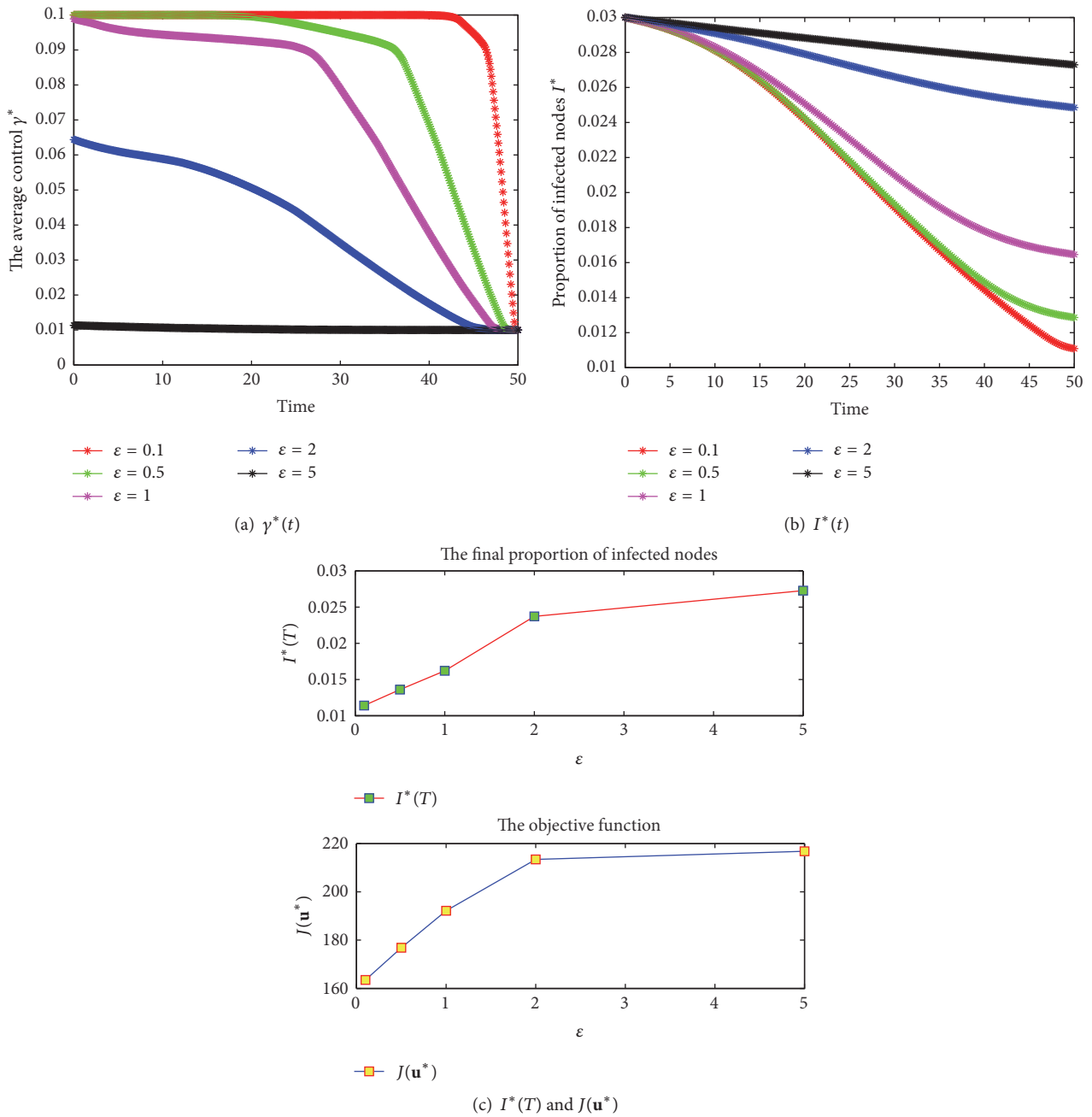

FIGURE 6: $\gamma^*(t)$, $I^*(t)$, $I^*(T)$, and $J(\mathbf{u}^*)$ for different ε with $m_1 = m_2 = 5$ for Example 1.

scheme with step size 0.01. Here we have to point out that some parameter values are chosen hypothetically due to the unavailability of real world data.

Suppose $\mathbf{u}^*(t)$ is an optimal control for problem (P) and $\mathbf{x}^*(t)$ is a solution to the corresponding controlled system. Let $\gamma^*(t)$ and $I^*(t)$ denote the average control and the proportion of infected nodes under $\mathbf{u}^*(t)$, respectively, where

$$\gamma^*(t) = \frac{1}{N}\sum_i \gamma_i^*(t), \qquad I^*(t) = \frac{1}{N}\sum_i I_i^*(t). \tag{34}$$

Example 1. Take a WS network with 150 nodes and 150 links as the propagation network.

Figure 2 exhibits the average control $\gamma^*(t)$ and $I^*(t)$ under different control strategies. Table 1 gives the final proportion of infected nodes and the value of objective function J under different control strategies, where the value of static control $\mathbf{u} = 0.08895$ is an average of several real curing probabilities reported in [42]. From Figure 2 and Table 1, one can conclude that $\mathbf{u}^*$ is indeed the optimal control strategy to minimize the objective function J and reduce virus prevalence to a low level simultaneously.

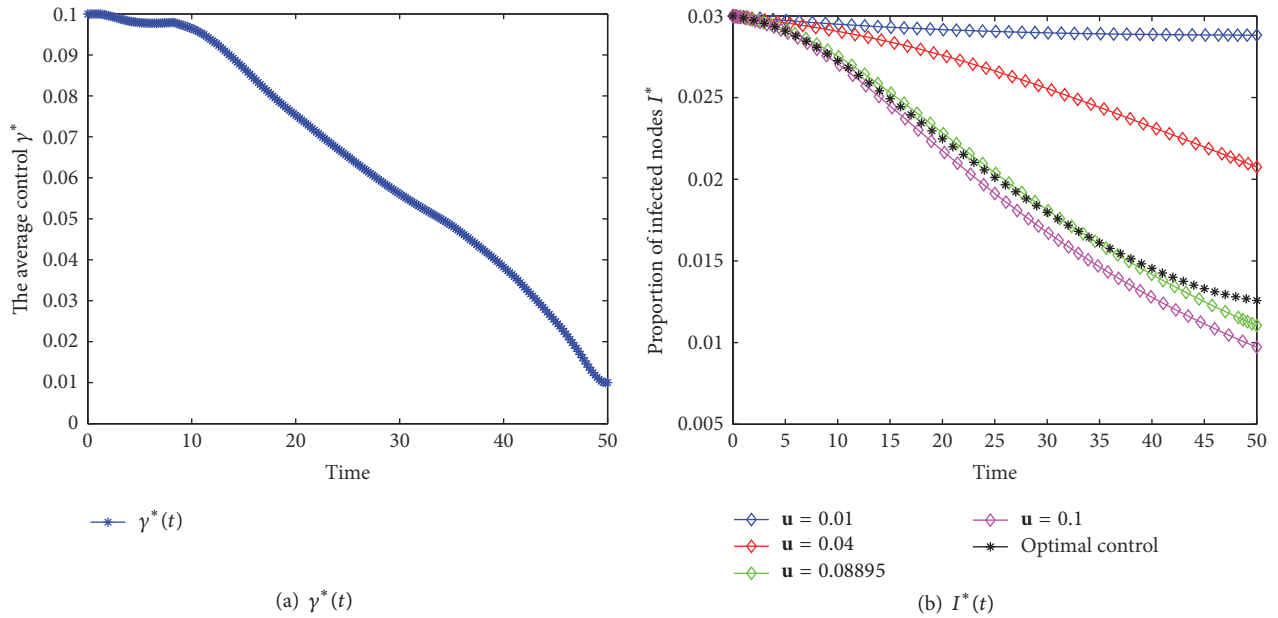

(a) $\gamma^*(t)$ (b) $I^*(t)$

FIGURE 7: $\gamma^*(t)$ and $I^*(t)$ under different control strategies with $m_1 = m_2 = 2$ for Example 2.

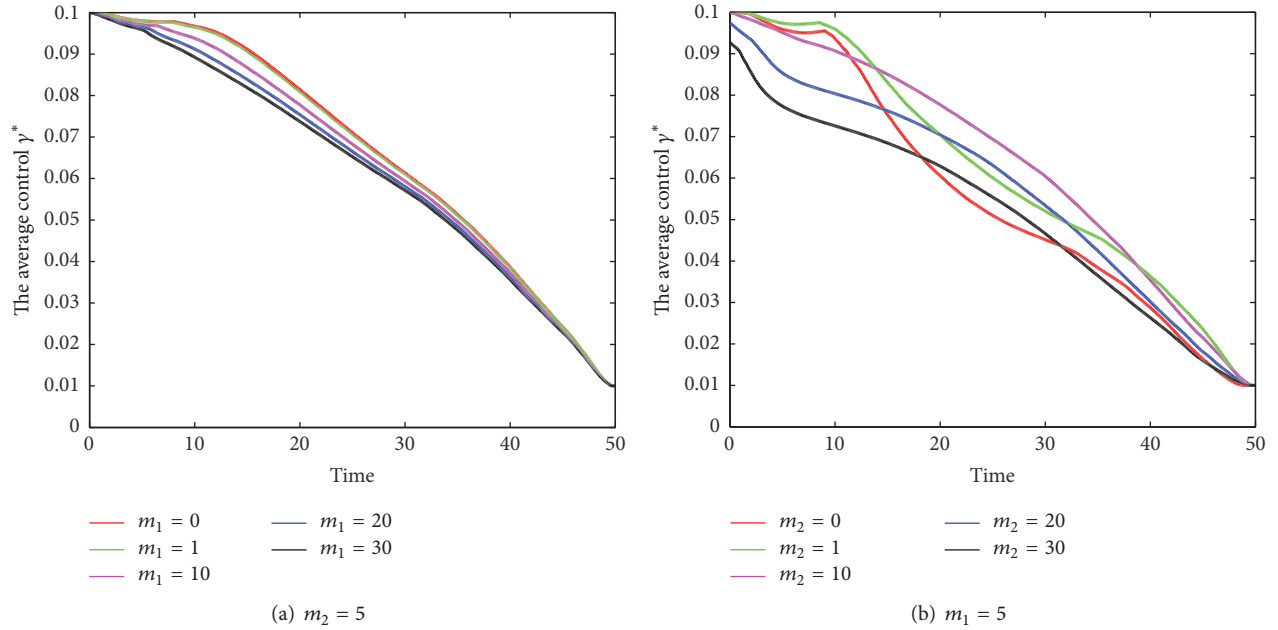

(a) $m_2 = 5$ (b) $m_1 = 5$

FIGURE 8: $\gamma^*(t)$ for different m_1 and m_2 for Example 2.

TABLE 1: $I^*(T)$ and J under different control strategies with $m_1 = m_2 = 2$ for Example 1.

	$\mathbf{u} = \mathbf{u}^*$	$\mathbf{u} = 0.01$	$\mathbf{u} = 0.04$	$\mathbf{u} = 0.08995$	$\mathbf{u} = 0.1$
$I^*(T)$	0.0089	0.0283	0.0231	0.0072	0.0053
$J(\mathbf{u})$	172.55	218.97	211.61	181.14	177.27

Figure 3 demonstrates the average control $\gamma^*(t)$ for different m_1 and m_2. From this figure, one can see that (a) enhancing m_1 and m_2 roughly reduces $\gamma^*(t)$, (b) the smaller m_2 is, the longer $\gamma^*(t)$ stays at $\overline{\gamma}$, and (c) m_2 has a more significant impact on $\gamma^*(t)$ than m_1 does.

Figure 4 displays $I^*(t)$ for different m_1 and m_2. From this figure, it can be seen that (a) lower m_1 favors virus spreading, whereas lower m_2 is conducive to the containment of virus prevalence, (b) m_2 affects $I^*(t)$ more significantly than m_1 does, which implies that dynamic countermeasure plays a

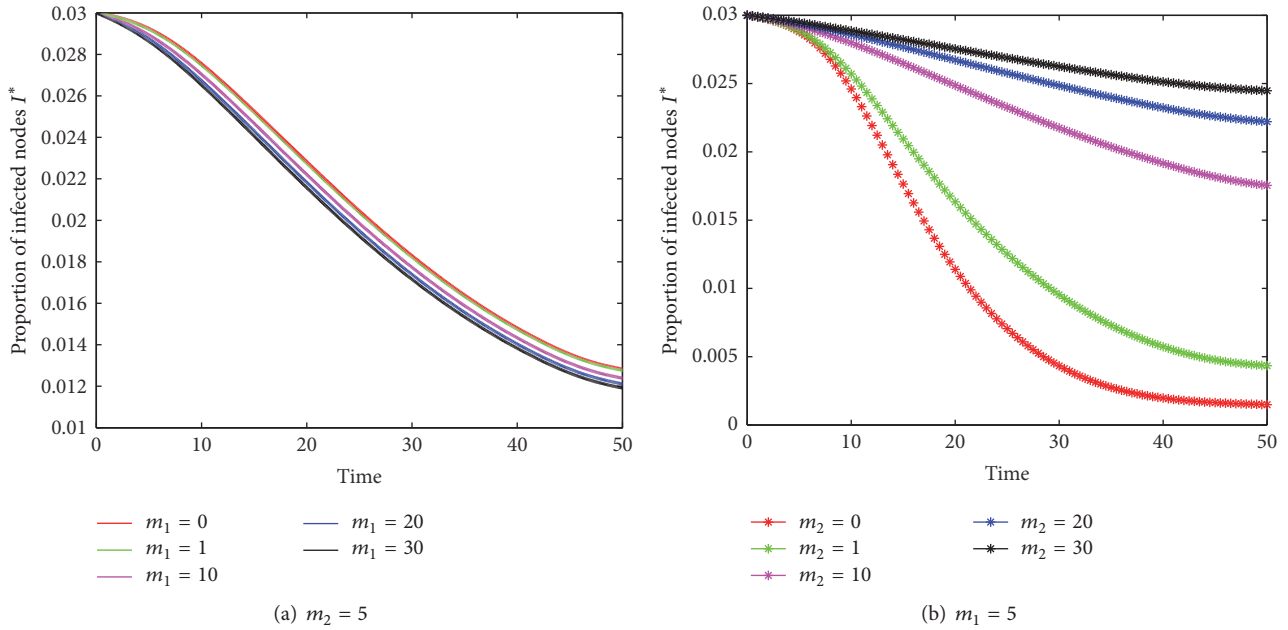

FIGURE 9: $I^*(t)$ for different m_1 and m_2 for Example 2.

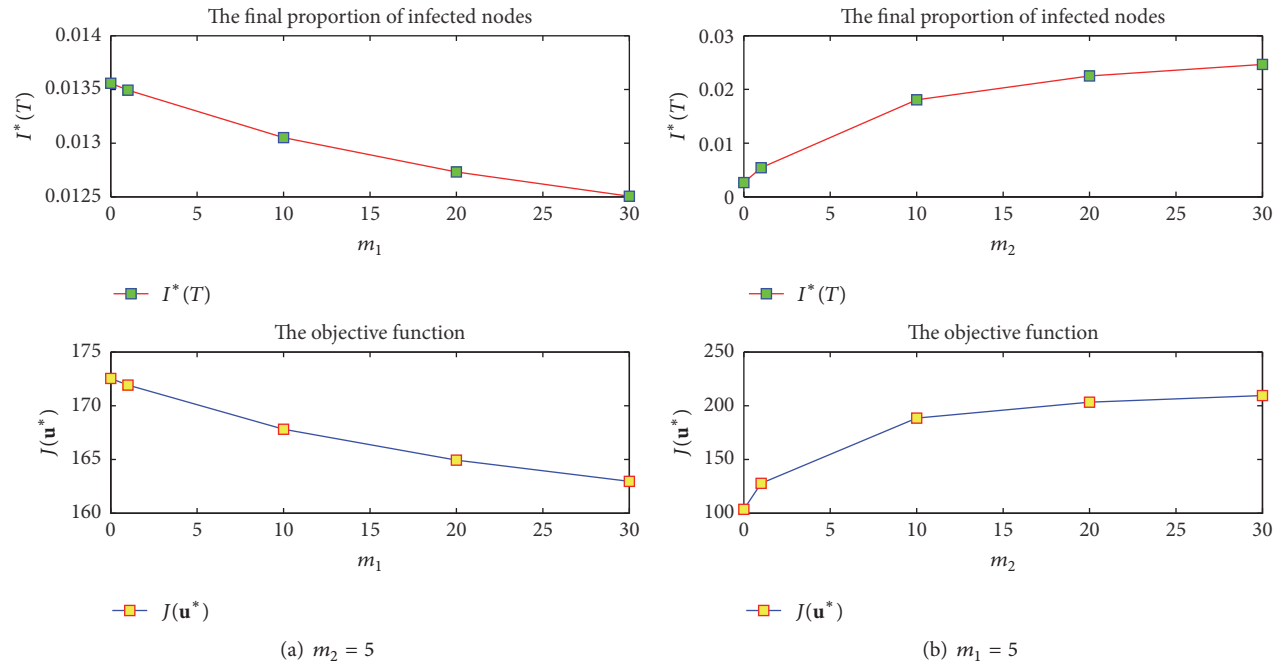

FIGURE 10: $I^*(T)$ and $J(\mathbf{u}^*)$ for different m_1 and m_2 for Example 2.

dominant role in the suppression of virus diffusion, and (c) linear infection rate overestimates virus prevalence, which is in accordance with the result in [7].

Figure 5 depicts the final proportion of infected nodes $I^*(T)$ and the objective function $J(\mathbf{u}^*)$ for varied m_1 and m_2. From this figure, it can be seen that J is decreasing and increasing with respect to m_1 and m_2, respectively, which makes a suggestion that enhancing m_1 and diminishing m_2 are beneficial to the containment of viral spread and reduce J to a low level simultaneously.

Figure 6 shows $\gamma^*(t)$, $I^*(t)$, $I^*(T)$, and $J(\mathbf{u}^*)$ for different ε. From this figure, it is found that decreasing ε is effective on the suppression of virus propagation and attains a lower $J(\mathbf{u}^*)$ simultaneously, although it creates more control cost. This is in good agreement with the fact that when the control effect (i.e., to obtain a low level of infections) is given priority

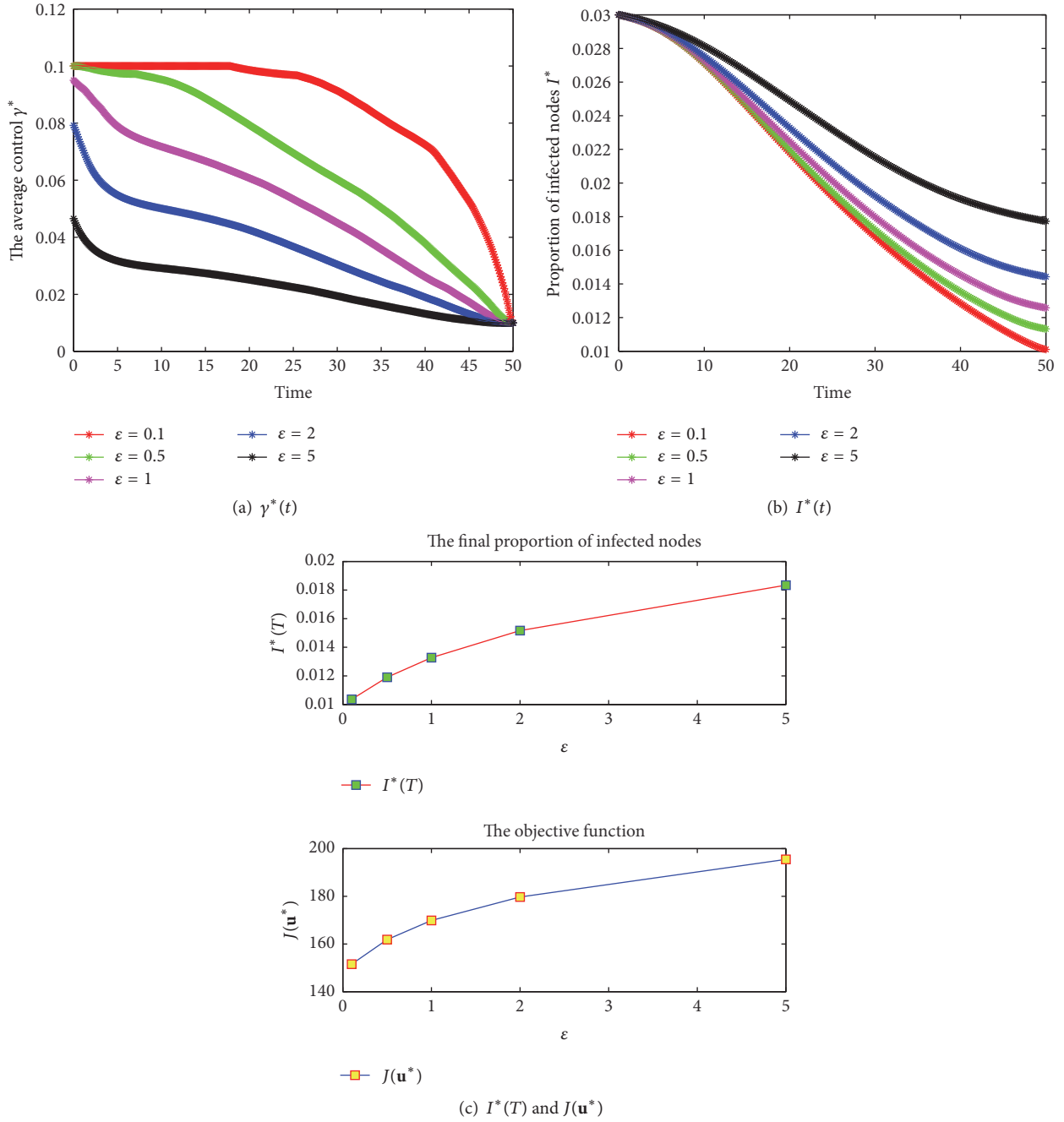

FIGURE 11: $\gamma^*(t)$, $I^*(t)$, $I^*(T)$, and $J(\mathbf{u}^*)$ for different ε with $m_1 = m_2 = 5$ for Example 2.

(i.e., with lower ε), often the decision is made to spend enough control cost. Hence, the tradeoff factor ε plays a critical role in the balance between control effect and control cost.

Example 2. Take a BA network with 150 nodes and 150 links as the propagation network.

Figure 7 displays $\gamma^*(t)$ and $I^*(t)$ under different control strategies. Table 2 shows the values of $I^*(T)$ and $J(\mathbf{u})$ under different control strategies. Figures 8 and 9 depict $\gamma^*(t)$ and $I^*(t)$ for different m_1 and m_2, respectively. Figure 10 demonstrates $I^*(T)$ and $J(\mathbf{u}^*)$ for different m_1 and m_2. Figure 11 exhibits $\gamma^*(t)$, $I^*(t)$, $I^*(T)$, and $J(\mathbf{u}^*)$ for different ε. From them, one can get the same results in Example 1. So they are omitted here for brevity.

Example 3. Take a partial Facebook network with 150 nodes and 603 links as the propagation network.

Figure 12 shows $\gamma^*(t)$ and $I^*(t)$ under different control strategies. Table 3 gives the values of $I^*(T)$ and $J(\mathbf{u})$ under different control strategies. Figures 13 and 14 display $\gamma^*(t)$

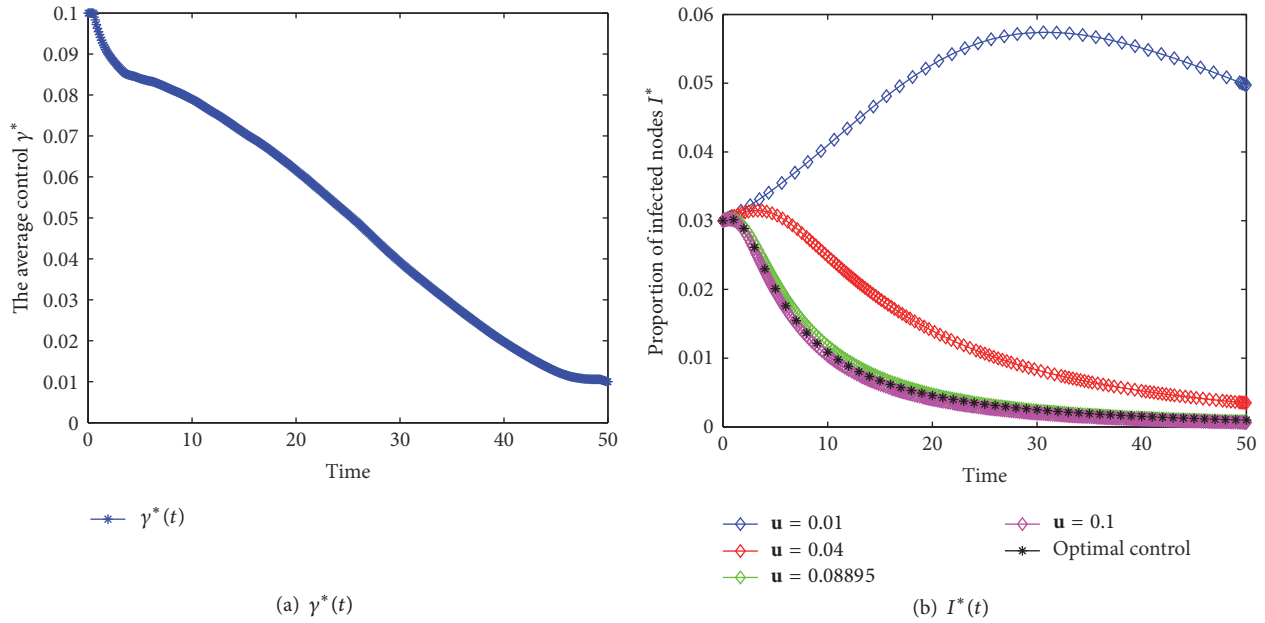

(a) $\gamma^*(t)$ (b) $I^*(t)$

FIGURE 12: $\gamma^*(t)$ and $I^*(t)$ under different control strategies with $m_1 = m_2 = 2$ for Example 3.

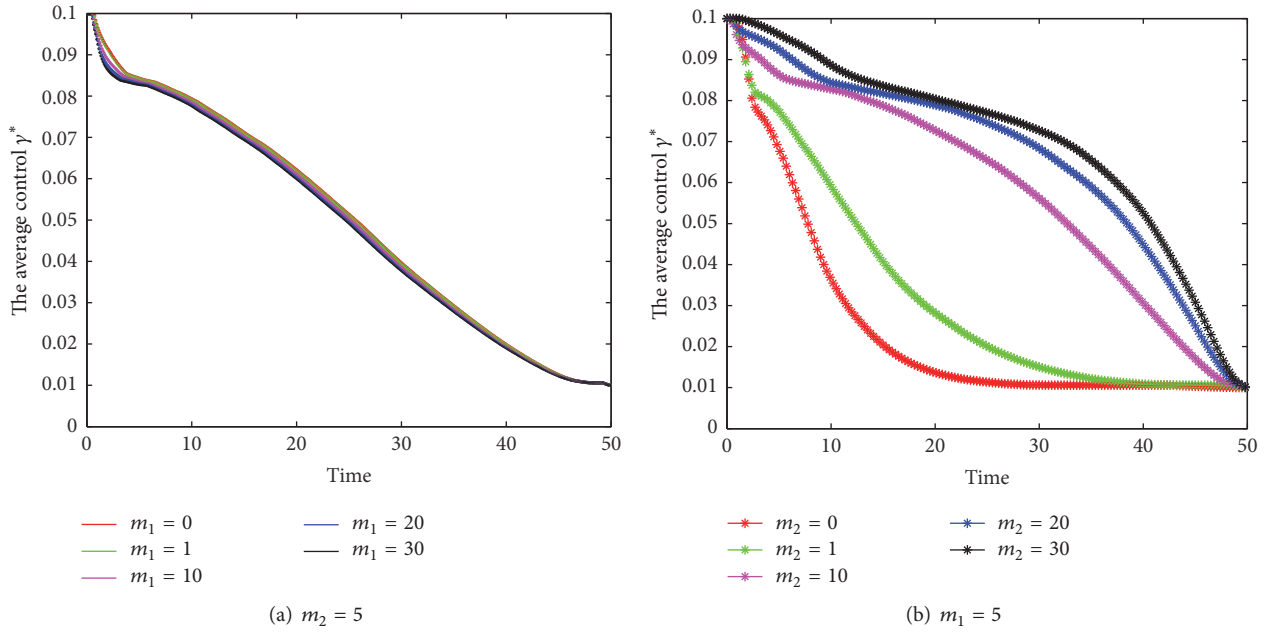

(a) $m_2 = 5$ (b) $m_1 = 5$

FIGURE 13: $\gamma^*(t)$ for different m_1 and m_2 for Example 3.

TABLE 2: $I^*(T)$ and J under different control strategies with $m_1 = m_2 = 2$ for Example 2.

	$\mathbf{u} = \mathbf{u}^*$	$\mathbf{u} = 0.01$	$\mathbf{u} = 0.04$	$\mathbf{u} = 0.08895$	$\mathbf{u} = 0.1$
$I^*(T)$	0.0132	0.0288	0.0208	0.0111	0.0097
$J(\mathbf{u})$	169.84	219.58	202.91	185.27	185.65

TABLE 3: $I^*(T)$ and J under different control strategies with $m_1 = m_2 = 2$ for Example 3.

	$\mathbf{u} = \mathbf{u}^*$	$\mathbf{u} = 0.01$	$\mathbf{u} = 0.04$	$\mathbf{u} = 0.08895$	$\mathbf{u} = 0.1$
$I^*(T)$	0.0013	0.0504	0.0035	0.0008	0.0006
$J(\mathbf{u})$	61.91	373.77	112.31	83.53	86.17

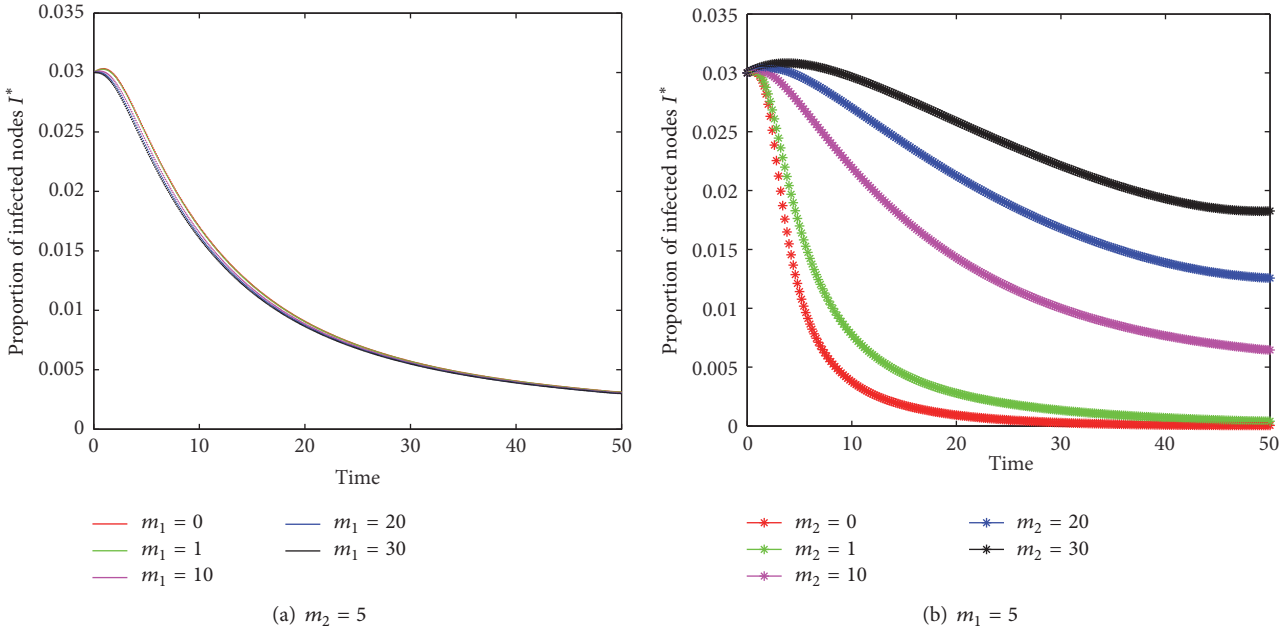

(a) $m_2 = 5$ (b) $m_1 = 5$

FIGURE 14: $I^*(t)$ for different m_1 and m_2 for Example 3.

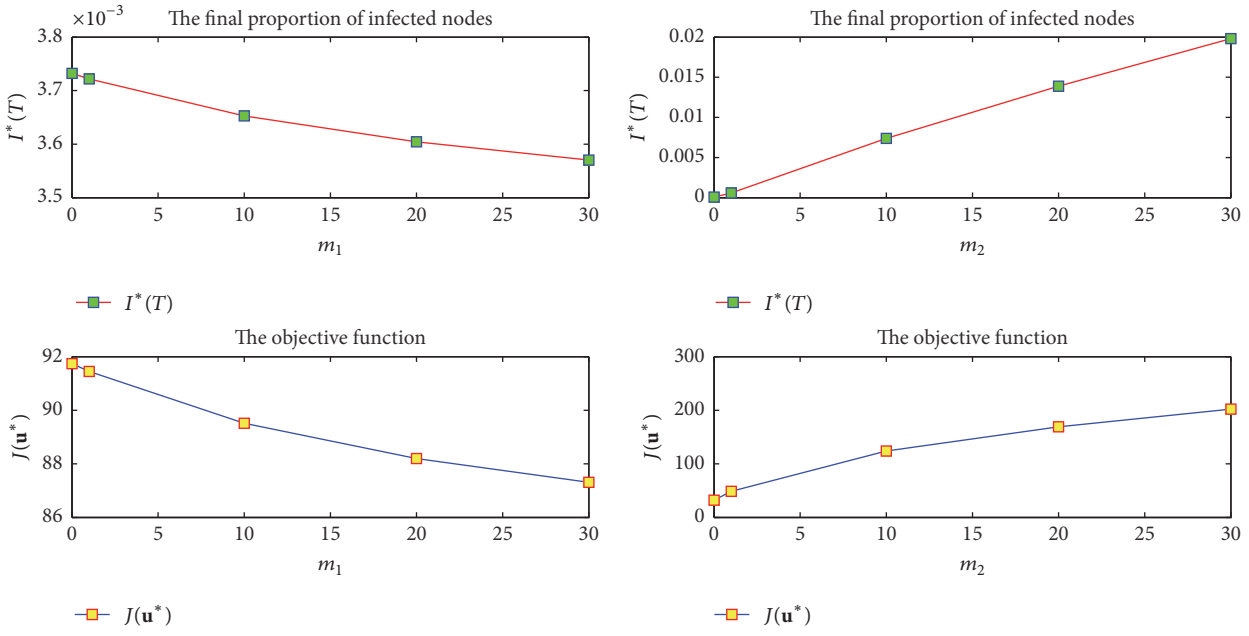

(a) $m_2 = 5$ (b) $m_1 = 5$

FIGURE 15: $I^*(T)$ and $J(\mathbf{u}^*)$ for different m_1 and m_2 for Example 3.

and $I^*(t)$ for different m_1 and m_2, respectively. Figure 15 demonstrates $I^*(T)$ and $J(\mathbf{u}^*)$ for varied m_1 and m_2. Figure 16 depicts $\gamma^*(t)$, $I^*(t)$, $I^*(T)$, and $J(\mathbf{u}^*)$ for different ε.

Most of the results concluded from this example are the same as those in Example 1 except the two phenomena listed as follows: (a) higher m_2 increases $\gamma^*(t)$, which is contrary to the results in Figures 3(b) and 8(b), and (b) m_1 has a negligible impact on $\gamma^*(t)$ and $I^*(t)$. This indicates that the network structure, to some extent, determines the control cost and virus diffusion.

Combining the above numerical examples, the main results are listed below.

(a) $\mathbf{u}^*$ is indeed the optimal control strategy to minimize the objective function J and reduce the infections to a low level simultaneously.

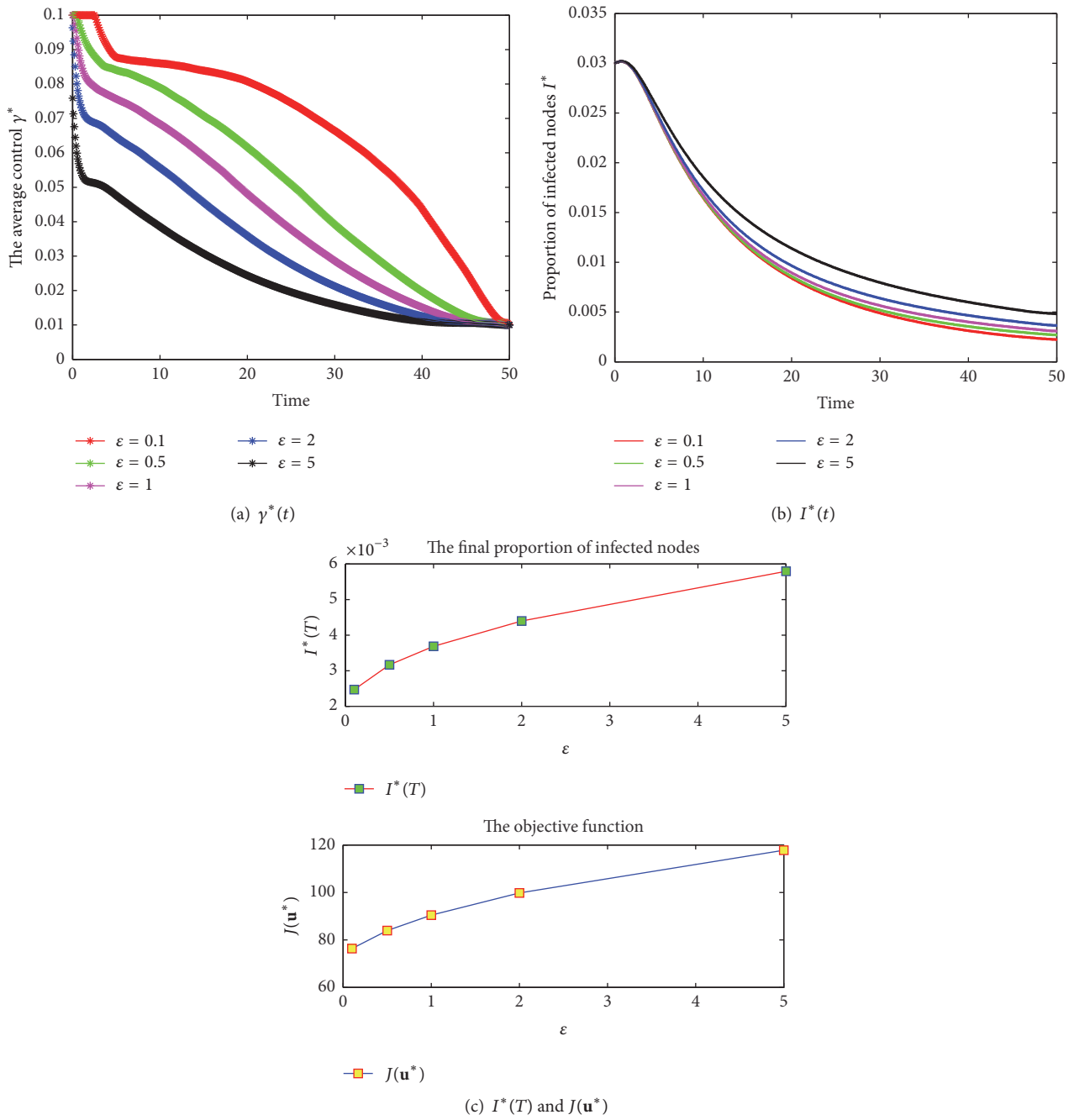

FIGURE 16: $\gamma^*(t)$, $I^*(t)$, $I^*(T)$, and $J(\mathbf{u}^*)$ for different ε with $m_1 = m_2 = 5$ for Example 3.

(b) Linear infection rate overestimates the prevalence of virus.

(c) Enhancing m_1 and diminishing m_2 are conductive to the containment of viral propagation and reduce J to a low level simultaneously.

(d) m_2 has more significant influences on $\gamma^*(t)$, $I^*(t)$, and $J(\mathbf{u}^*)$ than m_1 does.

(e) Decreasing the tradeoff factor ε is beneficial to the suppression of virus spread and obtains a lower $J(\mathbf{u}^*)$ simultaneously, although it brings more control cost.

Additionally, the structure of network, to some extent, determines the virus prevalence and the control cost. Thus, we shall investigate how the network topology affects virus spreading and control cost in the next work.

5. Concluding Remarks

This paper has studied the issue of how to work out an optimal dynamic countermeasure for achieving a low level of infections with a low cost. In this regard, a controlled node-level SICS model with nonlinear infection rate has

been established. Furthermore, an optimal control problem has been proposed. The existence of an optimal control and the corresponding optimality system have also been derived. Additionally, some numerical examples have been given to illustrate the main results. Specifically, it has been found that the proposed optimal countermeasure scheme can achieve a low level of infections at a low cost.

In our opinions, the next work could be made as follows. First, the quadratic cost functions may be generalized to some generic functions. Second, delays [43–45], pulses [46, 47], and random fluctuations [15] may be incorporated to controlled node-level models. Last, but not least, it is worthy to carry out research on the impact of the network topology [9, 25, 48, 49] on the dynamic countermeasure strategy.

Conflicts of Interest

The authors declare that there are no conflicts of interest regarding the publication of this paper.

Acknowledgments

This work is supported by Natural Science Foundation of China (Grant nos. 61572006 and 61503307), Science and Technology Research Program of Chongqing Municipal Education Commission (Grant nos. KJ1500415, KJ1704080, and KJ1704081), and Doctoral Scientific Research Foundation of Chongqing University of Posts and Telecommunications (Grant nos. A2015-02 and A2016-10).

References

[1] J. O. Kephart and S. R. White, "Directed-graph epidemiological models of computer viruses," in *Proceedings of the IEEE Computer Society Symposium on Research in Security and Privacy*, pp. 343–359, Oakland, Calif, USA, May 1991.

[2] J. R. C. Piqueira, A. A. de Vasconcelos, C. E. C. J. Gabriel, and V. O. Araujo, "Dynamic models for computer viruses," *Computers and Security*, vol. 27, no. 7-8, pp. 355–359, 2008.

[3] B. K. Mishra and S. K. Pandey, "Dynamic model of worms with vertical transmission in computer network," *Applied Mathematics and Computation*, vol. 217, no. 21, pp. 8438–8446, 2011.

[4] C. Gan, X. Yang, W. Liu, Q. Zhu, and X. Zhang, "Propagation of computer virus under human intervention: a dynamical model," *Discrete Dynamics in Nature and Society*, vol. 2012, Article ID 106950, 8 pages, 2012.

[5] L.-X. Yang, X. Yang, L. Wen, and J. Liu, "A novel computer virus propagation model and its dynamics," *International Journal of Computer Mathematics*, vol. 89, no. 17, pp. 2307–2314, 2012.

[6] Q. Zhu, X. Yang, L.-X. Yang, and X. Zhang, "A mixing propagation model of computer viruses and countermeasures," *Nonlinear Dynamics*, vol. 73, no. 3, pp. 1433–1441, 2013.

[7] P. Van Mieghem, J. Omic, and R. Kooij, "Virus spread in networks," *IEEE/ACM Transactions on Networking*, vol. 17, no. 1, pp. 1–14, 2009.

[8] F. D. Sahneh and C. M. Scoglio, "Optimal information dissemination in epidemic networks," in *Proceedings of the 51st IEEE Conference on Decision and Control (CDC '12)*, pp. 1657–1662, December 2012.

[9] L.-X. Yang, M. Draief, and X. Yang, "The impact of the network topology on the viral prevalence: a node-based approach," *PLoS ONE*, vol. 10, no. 7, article e0134507, 2015.

[10] L.-X. Yang, M. Draief, and X. Yang, "The optimal dynamic immunization under a controlled heterogeneous node-based SIRS model," *Physica A*, vol. 450, pp. 403–415, 2016.

[11] C. Gan, "Modeling and analysis of the effect of network eigenvalue on viral spread," *Nonlinear Dynamics*, vol. 84, no. 3, pp. 1727–1733, 2016.

[12] F. Cohen, "Computer viruses: theory and experiments," *Computers & Security*, vol. 6, no. 1, pp. 22–35, 1987.

[13] W. H. Murray, "The application of epidemiology to computer viruses," *Computers and Security*, vol. 7, no. 2, pp. 139–145, 1988.

[14] J. R. Piqueira and V. O. Araujo, "A modified epidemiological model for computer viruses," *Applied Mathematics and Computation*, vol. 213, no. 2, pp. 355–360, 2009.

[15] C. Zhang, Y. Zhao, Y. Wu, and S. Deng, "A stochastic dynamic model of computer viruses," *Discrete Dynamics in Nature and Society*, vol. 2012, Article ID 264874, 16 pages, 2012.

[16] J. Amador and J. R. Artalejo, "Stochastic modeling of computer virus spreading with warning signals," *Journal of the Franklin Institute*, vol. 350, no. 5, pp. 1112–1138, 2013.

[17] Y. Yao, X. Feng, W. Yang, W. Xiang, and F. Gao, "Analysis of a delayed Internet worm propagation model with impulsive quarantine strategy," *Mathematical Problems in Engineering*, Article ID 369360, 18 pages, 2014.

[18] C. Gan, X. Yang, W. Liu, and Q. Zhu, "A propagation model of computer virus with nonlinear vaccination probability," *Communications in Nonlinear Science and Numerical Simulation*, vol. 19, no. 1, pp. 92–100, 2014.

[19] L.-X. Yang and X. Yang, "A new epidemic model of computer viruses," *Communications in Nonlinear Science and Numerical Simulation*, vol. 19, no. 6, pp. 1935–1944, 2014.

[20] J. Ren, Y. Xu, and J. Liu, "Investigation of dynamics of a virus-antivirus model in complex network," *Physica A*, vol. 421, pp. 533–540, 2015.

[21] B. K. Mishra, K. Haldar, and D. N. Sinha, "Impact of information based classification on network epidemics," *Scientific Reports*, vol. 6, article 28289, 2016.

[22] J. Ren, J. Liu, and Y. Xu, "Modeling the dynamics of a network-based model of virus attacks on targeted resources," *Communications in Nonlinear Science and Numerical Simulation*, vol. 31, no. 1-3, pp. 1–10, 2016.

[23] L. C. Chen and K. M. Carley, "The impact of countermeasure propagation on the prevalence of computer viruses," *IEEE Transactions on Systems, Man, and Cybernetics B Cybernetics*, vol. 34, no. 2, pp. 823–833, 2004.

[24] Y. Wang, D. Chakrabarti, C. Wang, and C. Faloutsos, "Epidemic spreading in real networks: an eigenvalue viewpoint," in *Proceedings of the 22nd International Symposium on Reliable Distributed Systems (SRDS '03)*, pp. 25–34, Florence, Italy, October 2003.

[25] M. Youssef and C. Scoglio, "An individual-based approach to SIR epidemics in contact networks," *Journal of Theoretical Biology*, vol. 283, no. 1, pp. 136–144, 2011.

[26] Y. Lin, J. C. S. Lui, K. Jung, and S. Lim, "Modelling multi-state diffusion process in complex networks: theory and applications," *Journal of Complex Networks*, vol. 2, no. 4, pp. 431–459, 2014.

[27] C. Nowzari, V. M. Preciado, and G. J. Pappas, "Stability analysis of generalized epidemic models over directed networks," in *Proceedings of the 2014 53rd IEEE Annual Conference on Decision and Control, CDC 2014*, pp. 6197–6202, December 2014.

[28] R. Pastor-Satorras, C. Castellano, P. Van Mieghem, and A. Vespignani, "Epidemic processes in complex networks," *Reviews of Modern Physics*, vol. 87, no. 3, pp. 925–979, 2015.

[29] Q. Zhu, X. Yang, L.-X. Yang, and C. Zhang, "Optimal control of computer virus under a delayed model," *Applied Mathematics and Computation*, vol. 218, no. 23, pp. 11613–11619, 2012.

[30] L. Chen, K. Hattaf, and J. Sun, "Optimal control of a delayed SLBS computer virus model," *Physica A*, vol. 427, pp. 244–250, 2015.

[31] L.-X. Yang, M. Draief, and X. Yang, "The optimal dynamic immunization under a controlled heterogeneous node-based SIRS model," *Physica A. Statistical Mechanics and its Applications*, vol. 450, pp. 403–415, 2016.

[32] C. Zhang and H. Huang, "Optimal control strategy for a novel computer virus propagation model on scale-free networks," *Physica A*, vol. 451, pp. 251–265, 2016.

[33] C. Gan, M. Yang, Z. Zhang, and W. Liu, "Global dynamics and optimal control of a viral infection model with generic nonlinear infection rate," *Discrete Dynamics in Nature and Society*, Article ID 7571017, 9 pages, 2017.

[34] M. I. Kamien and N. L. Schwartz, *Dynamic Optimization: The Calculus of Variations and Optimal Control in Economics and Management*, Elsevier Science, The Netherlands, 2000.

[35] D. Liberzon, *Calculus of Variations and Optimal Control Theory: A Concise Introduction*, Princeton University Press, Princeton, NJ, USA, 2012.

[36] R. C. Robinson, *An Introduction to Dynamical Systems: Continuous and Discrete*, Prentice Hall, New York, NY, USA, 2004.

[37] R. T. Rockafellar, *Convex Analysis*, Princeton Mathematical Series, No. 28, Princeton University Press, Princeton, NJ, USA, 1970.

[38] D. J. Watts and S. H. Strogatz, "Collective dynamics of "small-world" networks," *Nature*, vol. 393, no. 6684, pp. 440–442, 1998.

[39] A.-L. Barabási and R. Albert, "Emergence of scaling in random networks," *Science*, vol. 286, no. 5439, pp. 509–512, 1999.

[40] http://snap.stanford.edu/data/egonets-Facebook.html.

[41] http://green.wangminjie.cn/newsinfo-136730.html.

[42] http://pcedu.pconline.com.cn/pingce/pingcesystem/1109/2527365_all.html.

[43] B. K. Mishra and D. K. Saini, "SEIRS epidemic model with delay for transmission of malicious objects in computer network," *Applied Mathematics and Computation*, vol. 188, no. 2, pp. 1476–1482, 2007.

[44] Y. Yao, X.-w. Xie, H. Guo, G. Yu, F.-X. Gao, and X.-j. Tong, "Hopf bifurcation in an Internet worm propagation model with time delay in quarantine," *Mathematical and Computer Modelling*, vol. 57, no. 11-12, pp. 2635–2646, 2013.

[45] J. Ren and Y. Xu, "Stability and bifurcation of a computer virus propagation model with delay and incomplete antivirus ability," *Mathematical Problems in Engineering*, Article ID 475934, 9 pages, 2014.

[46] Y. Yao, L. Guo, H. Guo, G. Yu, F. Gao, and X. Tong, "Pulse quarantine strategy of internet worm propagation: modeling and analysis," *Computers and Electrical Engineering*, vol. 38, no. 5, pp. 1047–1061, 2012.

[47] L.-X. Yang and X. Yang, "The pulse treatment of computer viruses: a modeling study," *Nonlinear Dynamics*, vol. 76, no. 2, pp. 1379–1393, 2014.

[48] C. Gan, X. Yang, W. Liu, Q. Zhu, J. Jin, and L. He, "Propagation of computer virus both across the Internet and external computers: a complex-network approach," *Communications in Nonlinear Science and Numerical Simulation*, vol. 19, no. 8, pp. 2785–2792, 2014.

[49] Y. Yang, G. Xie, and J. Xie, "Mining important nodes in directed weighted complex networks," *Discrete Dynamics in Nature and Society*, vol. 2017, Article ID 9741824, 7 pages, 2017.

Hindawi
Discrete Dynamics in Nature and Society
Volume 2017, Article ID 9396824, 7 pages
https://doi.org/10.1155/2017/9396824

Research Article

The Impact of Community Structure on the Convergence Time of Opinion Dynamics

An Lu, Chunhua Sun, and Yezheng Liu

School of Management of Hefei University of Technology, Hefei, Anhui Province 230009, China

Correspondence should be addressed to Yezheng Liu; liuyezheng@hfut.edu.cn

Received 14 December 2016; Revised 28 February 2017; Accepted 19 April 2017; Published 1 June 2017

Academic Editor: Lu-Xing Yang

Copyright © 2017 An Lu et al. This is an open access article distributed under the Creative Commons Attribution License, which permits unrestricted use, distribution, and reproduction in any medium, provided the original work is properly cited.

We analyze the convergence time of opinion dynamics in a social network with community structure. Using matrix analysis, we prove that the convergence time is determined by the second largest eigenvalue modulus. This modulus is close to 1 if the social influence matrix is nearly uncoupled. Furthermore, we discuss and analyze the factors of community structure affecting the convergence time.

1. Introduction

Community structure is ubiquitous in reality. It means that many social networks can be divided into some groups such that the connection within each group is dense, while connection between groups is very sparse. Community structure is always relevant to many social and biological phenomena. Previous works have shown that community structure affects the evolution of macroscopic phenomena taking place on a network, such as synchronization [1, 2], the spread of epidemics [3, 4], rumors [5], and opinion dynamics [6–8].

In opinion dynamics, various versions of the opinion models have been proposed. First types are discrete opinion models, among which are the Sznajd model [9], the voter model [10, 11], the majority rule model [12], and the social impact model [13]. Other models are continuous, using concepts and methods based on ideas from statistical physics or control theory. The most famous are bounded confidence model [14, 15] and an earlier model, Degroot model [16], including some agent-based models such as [17].

There are two interesting questions in opinion dynamics. First, under what conditions will the opinions' updating processes converge to a well-defined limit? The second question is about the convergence time or convergence rate problem; that is, how quickly the consensus is reached if opinions can converge ultimately. Previous works have shown that the convergence time is determined by the topology of social network and the updating rule of individuals' opinion. For example, in bounded confidence model [15], the convergence time is determined by bounded confidence parameter, which is expressed by a real number ε, such that an agent, with opinion x, only interacts with its peers whose opinion lies in the range of $[x-\varepsilon,\ x+\varepsilon]$. In another bounded confidence model, Deffuant model [14], the convergence time is only determined by convergence parameter μ. In [18], the authors studied the effects of adding shortcuts connecting randomly chosen pairs of sites in a regular lattice on the consensus time, using a local majority updating rule. They showed that the consensus time dropped sensitively with the addition of a small number of shortcuts. In [19], the author introduced a two-state opinion dynamics model where agents evolve by majority rule, finding that consensus is reached in a time that scales to $\log N$, where N is the number of agents. On finite-dimensional lattices, where a group is a contiguous cluster, the consensus time fluctuates strongly between realizations and grows as a dimension-dependent power of N. The upper critical dimension appears to be larger than 4. In [20] the authors found that, for the voter model, if the network is with an arbitrary but uncorrelated degree distribution, the convergence time T_N scales as $N\mu_1^2/\mu_2$, where μ_k is the kth moment of the degree distribution and N is the size of the network. In [21], the authors found in

a coevolving network that if the number of committed agents added exceeds a critical value, the consensus time growth becomes logarithmic in network size N. Slight changes in the interaction rule can produce strikingly different results of consensus time.

Although it is shown that interaction rules or network topologies have an important impact on the evolution of group opinions, the continuous opinion dynamics issue with community structure is still not well understood. Unlike all the research above, here we mainly discuss the impact of a community structure on convergence time, which applies to situations of how we control the opinion evolution in a social network with community structure. First, through matrix analysis method, we prove that the convergence time is determined by the second largest eigenvalue modulus of social influence matrix. Furthermore, we prove that this modulus is close to 1 if the social influence matrix is nearly uncoupled. Second, in our model the influence of interpersonal is random, which is closer to reality. We propose the concept, distribution of interpersonal influence, which can better describe the interaction situations. We examine this issue from three points of view: the number of nodes connected (including the number of nodes connected between subgroups, the number of nodes connected within subgroups, and the connection density between subgroups), the size of subgroups, and influence distribution. We find that the number of connections between subgroups and the number of subgroups within the subgroups exert a strong influence on the convergence time. In addition, the impact of distribution of influence on the convergence time shows the following fact: the convergence time of the group opinions in an autocratic society is longer than that in a democratic society in average, but various connection patterns may bring much more uncertainty.

The remaining of this paper is organized as follows: in Section 2, we discuss the proposed model in detail. Then in Section 3 we analyze the impact of community structure on the consensus time. Section 4 concludes this paper.

2. Continuous Opinion Dynamics Model

2.1. Notations, Assumptions, and the Opinion Dynamic Model. This section introduces the notations and the assumptions and defines the consensus time of continuous opinion dynamics.

Mathematically, a social network with community structure can be characterized by a big graph in which the nodes represent people, and the edges evaluate their relation strength.

We consider a set of n individuals in a social network. $V = \{1, 2, \ldots, n\}$. A relation $E \subseteq V \times V$ models the interactions between individuals. We assume the relationship is mutual ($(i, j) \in E$ if and only if $(j, i) \in E$). V is the set of vertices and E is a set of edges of undirected graph $G = (V, E)$, describing the social network of individuals. Each individual has an opinion modeled by a real number $x_i(t) \in R$. Initially, individual i has an opinion $x_i(0)$ independent from others. Then, at every time step, the individuals update their opinion by taking a weighted average of their own opinion and opinions of others

$$x_i(t+1) = \sum_{j=1}^{n} a_{ij}(t)\, x_j(t) \tag{1}$$

with the coefficients $a_{ij}(t)$ satisfying

$$\forall i, j \in V, a_{ij}(t) \neq 0 \Longleftrightarrow j \in \{i\} \cup \{N_i(t)\},$$
$$\sum_{j=1}^{n} a_{ij}(t) = 1, \tag{2}$$

where the coefficient a_{ii} denotes the force of self-confidence of individual i and a_{ij} denotes to what extent individual i is affected by individual j. $N_i(t)$ denotes the neighborhood of individual i at time t step.

Let $X(t) = (x_1(t), x_2(t), \ldots, x_n(t))^T$, $A(t) = (a_{ij}(t))_{n\times n}$; thus, the group opinion dynamics can be written as follows:

$$X(t+1) = A(t)\, X(t), \tag{3}$$

where A is a row stochastic and nonnegative matrix. In this following, we call it *social influence matrix* whose entry a_{ij} represents the influence strength from individuals j to i.

In this paper, we assume that (1) G is static and strongly connected; (2) the relationship and interaction between individuals are mutual; (3) every individual has a little self-confidence. Under these conditions, it is easy to find that A is constant and row stochastic matrix. The diagonal entries in A are all positive, and zero-entries in A are symmetric. Using nonnegative matrix theories, we can get some properties as follows.

Proposition 1. *Consensus will be reached ultimately.*

Proof. Under assumption (1), it can easily be seen that A is an irreducible, row stochastic and nonnegative matrix. The summation of each row is equal to 1. Thus, the spectral radius of A denoted by $\rho(A) = 1$. $\alpha_1 = (1, 1, \ldots, 1)^T$ is an eigenvector of $\lambda = 1$. Since all the diagonal entries are positive, using Perron-Frobenius theory, we can get A is primitive. The algebraic multiplicity of $\lambda = 1$ is equal to 1. So the spectrum of A can be denoted by

$$\operatorname{spec}(A) = \{\lambda_i \mid |\lambda_n| \leq |\lambda_{n-1}| \leq \cdots \leq |\lambda_2| < \lambda_1 = 1\}. \tag{4}$$

For any initial opinion vector $X(0) = (x_1(0), x_2(0), \ldots, x_n(0))^T$, it can be written as a linear combination as follows:

$$X(0) = \sum_{i=1}^{n} k_i \alpha_i, \tag{5}$$

where α_i is eigenvector corresponding to the eigenvalue λ_i of A. Thus, for all $t > 0$, α_i^t is an eigenvector corresponding to the eigenvalue λ_i^t of A^t. Since $|\lambda_n| \leq |\lambda_{n-1}| \leq \cdots \leq |\lambda_2| < \lambda_1 = 1$, it follows that

$$\lim_{t\to\infty} X(t) = \lim_{t\to\infty} A^t \cdot X(0) = \lim_{t\to\infty} A^t \sum_{i=1}^{n} k_i \alpha_i$$

$$= \lim_{t\to\infty}\left(\sum_{i=1}^{n} k_i\alpha_i\cdot\lambda_i^t\right) = \lim_{t\to\infty}\left(k_1\alpha_1 + o(1)\right)$$
$$= \left(k_1, k_1, \ldots, k_1\right)^T. \tag{6}$$

So the opinions converge to a constant vector, whose components are all equal. That means the consensus can be reached, and the convergence time is consensus time.

Remark. Assumption (2) is not necessary condition but sufficient for convergence of opinions. For example, if $A = \begin{pmatrix} 0 & 0.5 & 0.5 \\ 1 & 0 & 0 \\ 0 & 1 & 0 \end{pmatrix}$, we can get $\lim_{t\to\infty} A^t = \begin{pmatrix} 0.4 & 0.4 & 0.2 \\ 0.4 & 0.4 & 0.2 \\ 0.4 & 0.4 & 0.2 \end{pmatrix}$, so opinions converge to a fixed vector, but the diagonal of A is not positive. □

Proposition 2. *The convergence time is determined by the second largest eigenvalue modulus* $|\lambda_2|$.

Proof. First we introduce the definition of convergence time:

$$t^* = \inf\left\{t_0 \mid \forall t > t_0, \|X(t) - X\| \le \delta\right\}, \tag{7}$$

where δ can be arbitrarily small, $X(t)$ represents a series of vector, and X is the limit of $X(t)$.

$\|\cdot\|$ represents a vector norm (1-norm, 2-norm, or ∞-norm). If $\|X(t) - X\| < \delta$, it follows that

$$\left\|k_2\alpha_2\cdot\lambda_2^t + o\left(\lambda_2^t\right)\right\| \le \delta; \tag{8}$$

when δ is small enough, $o(\lambda_2^t)$ can be omitted. So (7) can be rewritten as $\|k_2\alpha_2\cdot\lambda_2^t\| \le \delta$.

Thus, we can get

$$t \ge \frac{-c\ln\delta}{\ln\left(1/|\lambda_2|\right)} = \frac{-c\ln\delta}{-\ln|\lambda_2|} \tag{9}$$

satisfying (7). So the convergence time $t^* = -c\ln\delta/-\ln|\lambda_2|$, where c is a constant determined by the initial opinion vector and eigenvector of weighted matrix A.

From the analysis above, it is obvious that the larger $|\lambda_2|$ is, the longer the consensus time is and vice versa. For simplicity, we analyze the convergence time only by the second largest eigenvalue modulus $|\lambda_2|$ or $-\ln|\lambda_2|$. □

Proposition 3. *For a nonnegative row stochastic partitioned matrix* $A = \left(\begin{smallmatrix} B & D \\ E & C \end{smallmatrix}\right)_{n\times n}$, *where* $B = (b_{ij})_{n_1\times n_1}$, $C = (c_{ij})_{n_2\times n_2}$, $n = n_1 + n_2$. *Let* $\sigma(A)$ *be the summation of entries in* D *and* E; *then for any* $\varepsilon > 0$, $\exists\delta > 0$, *if* $|\sigma(A)| < \delta$, *satisfying* $||\lambda_2| - 1| < \varepsilon$.

Proof. First, we prove that if all the entries in a matrix change a little, the eigenvalues of the new matrix will also change. Denote B by

$$\begin{pmatrix} b_{11} & b_{12} & \cdots & b_{1,n_1} \\ b_{21} & b_{22} & \cdots & b_{2,n_1} \\ \vdots & \vdots & \vdots & \vdots \\ b_{n_1,1} & b_{n_1,2} & \cdots & b_{n_1,n_1} \end{pmatrix}; \tag{10}$$

step 1 B is transformed into

$$B^{(1)} = \begin{pmatrix} b_{11} + \Delta^{(1)} & b_{12} & \cdots & b_{1,n_1} \\ b_{21} & b_{22} & \cdots & b_{2,n_1} \\ \vdots & \vdots & \vdots & \vdots \\ b_{n_1,1} & b_{n_1,2} & \cdots & b_{n1,n_1} \end{pmatrix}. \tag{11}$$

Thanks to the continuity of eigenvalues, we can get that, for any $\varepsilon > 0$, there exists $\delta^{(1)} > 0$, if $|\Delta^{(1)}| < \delta^{(1)}$, satisfying $|\lambda(B^{(1)}) - \lambda(B)| < \varepsilon$. For step 2 when $B^{(1)}$ is transformed into

$$B^{(2)} = \begin{pmatrix} b_{11} + \Delta^{(1)} & b_{12} + \Delta^{(2)} & \cdots & b_{1,n1} \\ b_{21} & b_{22} & \cdots & b_{2,n1} \\ \vdots & \vdots & \vdots & \vdots \\ b_{n1,1} & b_{n1,2} & \cdots & b_{n1,n1} \end{pmatrix}, \tag{12}$$

we can get that, $\forall\varepsilon > 0$, $\exists\delta^{(2)} > 0$, if $|\Delta^{(2)}| < \delta^{(2)}$, $|\lambda(B^{(2)}) - \lambda(B^{(1)})| < \varepsilon$. Repeat this process, at the last step, $\exists\delta^{(n_1^2)} > 0$, if $|\Delta^{(n_1^2)}| < \delta^{(n_1^2)}$, $|\lambda(B^{(n_1^2)}) - \lambda(B^{(n_1^2-1)})| < \varepsilon$, so for any $\varepsilon > 0$, there exists $\delta' = \min(\delta^{(1)}, \delta^{(2)}, \ldots, \delta^{(n_1^2)})$, if $|\Delta^{(1)}|, |\Delta^{(2)}|, \ldots, |\Delta^{(n_1^2)}| < \delta'$, satisfying $|\lambda(B^{(n_1^2)}) - \lambda(B)| < n_1^2\varepsilon$.

That is to say, if the matrix perturbation is small enough, the eigenvalues will vary little accordingly. Secondly, let $A' = \left(\begin{smallmatrix} B' & 0 \\ 0 & C' \end{smallmatrix}\right)_{n\times n}$. So it is reducible, and naturally the spectral of A' $\mathrm{spec}(A') = \mathrm{spec}(B') \cup \mathrm{spec}(C')$. If $\sigma(A)$ is small enough, then all the entries in D and E are also small. When $\sigma(A)$ trends toward 0, the entries in B and C must change a little accordingly to keep A as a row stochastic matrix. Without loss of generality, we can assume only one element $d_{11} > 0$ in matrix D (or c_{11} in C). For these reasons, we can obtain that, for any $\varepsilon > 0$, there exists δ, if $d_{11} < \delta$, $|\lambda(A) - \lambda(A')| < \varepsilon$, since $d_{11} < \sigma(A)$; if $\sigma(A) < \delta$, then, $d_{11} < \delta$, $|\lambda(A) - \lambda(A')| < \varepsilon$ or specially $||\lambda_2| - 1| < \varepsilon$. That is to say, if $\sigma(A) \to 0$, then the second largest eigenvalue modulus is nearly 1. The inverse of Proposition 3 has been proved by [22]. If second largest eigenvalue is sufficiently close to 1, then A is nearly uncoupled.

A social network with community structure means partitioned matrix A with $\sigma(A)$ is very small. According to the above analysis, if individuals in different subgroups of a society rarely interact with each other, then λ_2 will be very close to 1. As a result, it is hard to reach a consensus. □

3. The Impact of Community Structure on Convergence Time

Although we have some analytical results of the second largest eigenvalue modulus of the social influence matrix with community structure, the exact results depend on entries of this matrix. Different network structures or different influence distributions will affect the second largest eigenvalue modulus, which in turn affects the convergence time of the group opinion. Therefore, the analysis of the impact of community structure on the convergence of time includes the following three aspects: the number of connection nodes, the size of subgroups, and the distribution of interpersonal influence.

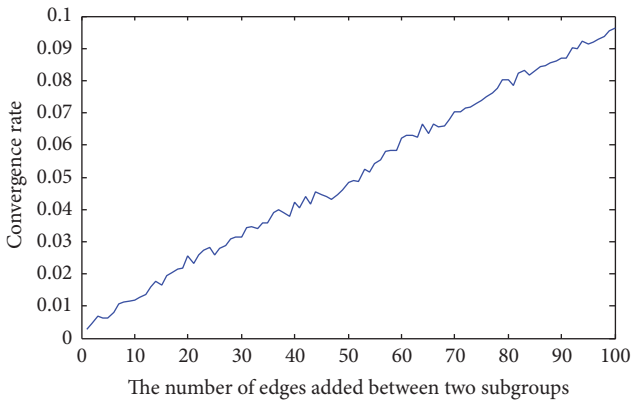

Figure 1: The relationship between the number of edges added between two subgroups and the convergence time.

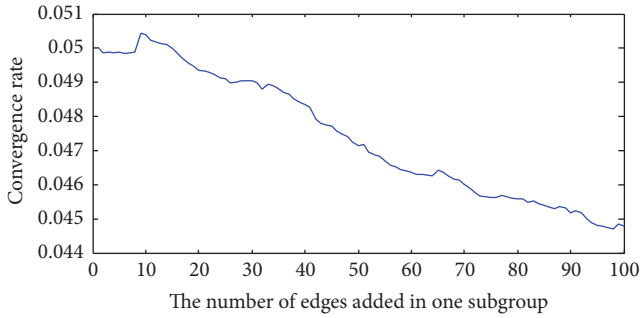

Figure 2: The relationship between the number of edges added in one subgroup and the convergence time.

3.1. The Number of Connection Nodes. First of all, using the famous WS model [23], we build a social network containing two subgroups, respectively. Each social network is a small world. To ensure the whole network is linked, the nodes between subgroups are connected sparsely and randomly. And then we investigate whether the increasing of connection can influence the convergence time.

Figure 1 shows that the convergence rate of opinion evolution is highly dependent on the connection pattern between subgroups. If the number of connections or connection densities between subgroups increases, the convergence rate of the group opinions is faster. At the beginning, when there is only one connection between subgroups, there is almost no connection between two subgroups, and the convergence rate is almost zero. This is the result of the aforementioned Proposition 3, and in this case, the social influence matrix associated the social network is nearly uncoupled. So consensus is hardly reached. However, when the number of connections (or densities) between the groups increases, for example, when the number of nodes increases to 10 pairs, the second largest eigenvalue modulus $|\lambda_2|$ will reduce from 0.9972 to 0.9881. When the number of connections nodes goes up to 100, $|\lambda_2|$ will drop to 0.9081 accordingly.

However, the convergence rate in Figure 2 declines with the rise of the number of internal connections in one subgroup. But the rate of weakening is much slower than

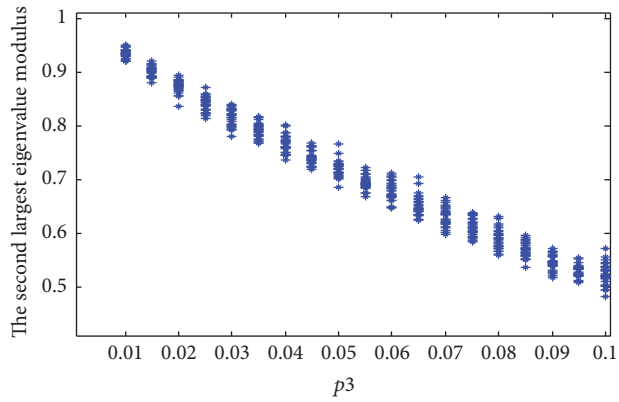

Figure 3: Example of the frequency of interaction between different subgroups impact on the second largest eigenvalue modulus, with $n_1 = 100$, $n_2 = 50$, $p_1 = 0.2$, and $p_2 = 0.4$ (repeatedly calculating 30 times).

that in Figure 1. In Figure 2, with the ascent in the internal connection of the subgroup (from the beginning of the connection density 0.1 is 0.9512; the second largest eigenvalue modulus decreases slightly to 0.9561 when the number of connected nodes ascends to 100 pairs).

In Figure 3, we explore the impact of two subgroups interaction frequency on the consensus time. Frequency of interaction in the first subgroup is denoted by p_1, and the second is p_2. The interaction frequency between subgroups is denoted by p_3, which is the proportion of positive entries to all the entries in D and E (or the connection density between different subgroups).

In Figure 3, it is easily to be observed that if the parameter p_3 goes up, the second largest eigenvalue modulus will fall off. Thus, the consensus time will be shorter with the increasing frequency of interaction between subgroups.

3.2. The Size of Subgroups. In this section, we examine the impact of the size of subgroups on the convergence time. For a fixed size, for example, 150, of the social network, Figure 4 shows that $|\lambda_2|$ will be the largest when n_1 is close to n_2. More precisely, if $p_1 = p_2$, when $n_1 = n_2 = 75$, $|\lambda_2|$ will be the largest. That is to say, if a social network has a small subgroup and a large subgroup simultaneously, it will always be easy to reach a consensus. On the contrary, if the sizes of two subgroups are about the same, it is difficult to reach a consensus.

Simulation results show that the second largest eigenvalue modulus is negatively correlated to the size of the corresponding graph of A, as well as the density (or average degrees) of the underling graph. For convenience, they are roughly denoted by

$$|\lambda_2| = f(n, p),$$
$$\frac{\partial f}{\partial n} < 0, \tag{13}$$
$$\frac{\partial f}{\partial p} < 0.$$

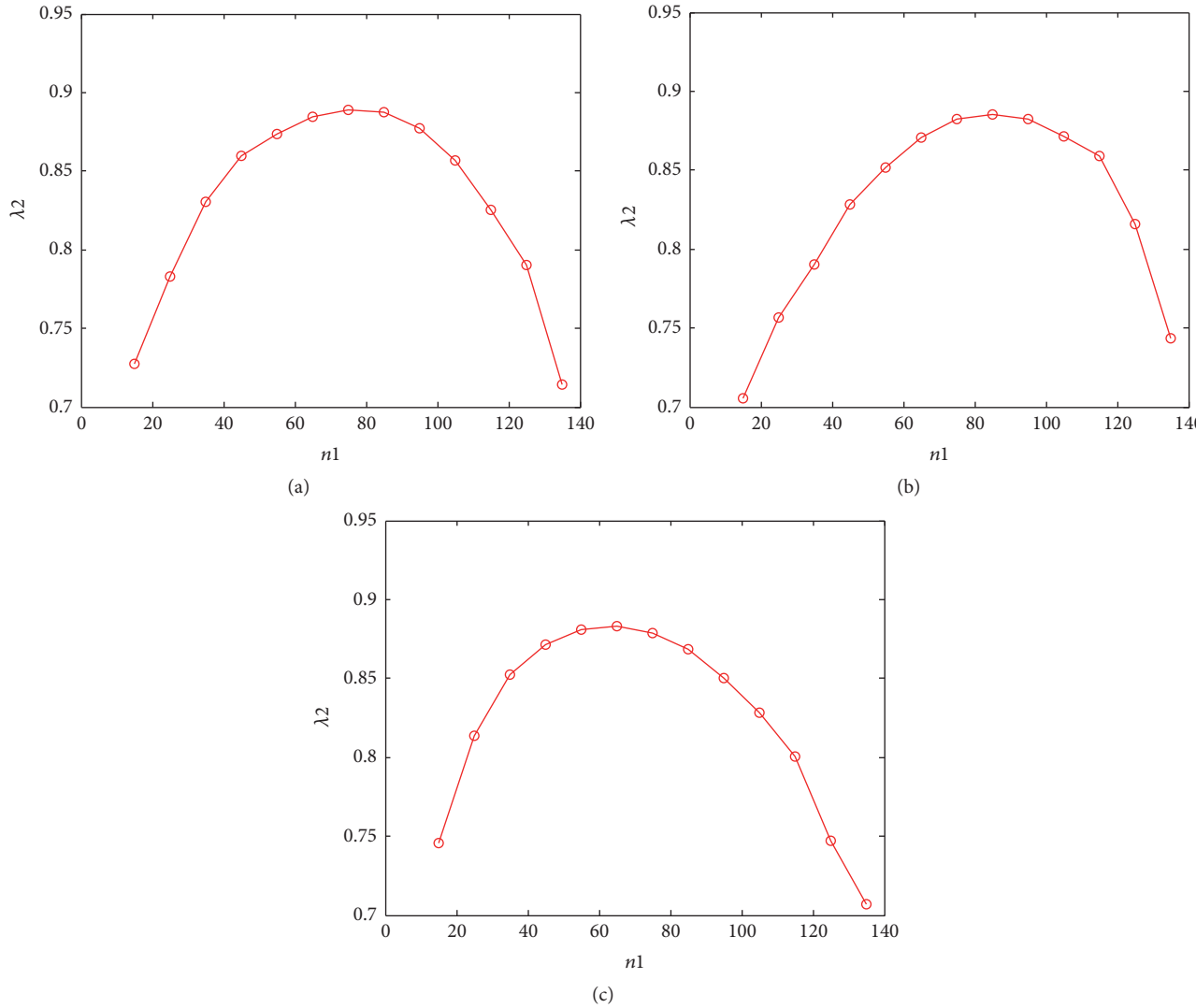

FIGURE 4: The relationship between the size of subgroups and the second largest eigenvalue modulus. x-axis is the size of one subgroup and y-axis is the second largest eigenvalue modulus. Here we assume the size of G is 150, $p_3 = 0.02$, in (a), $p_1 = p_2 = 0.2$; in (b), $p_1 = 0.2$, $p_2 = 0.4$; in (c), $p_1 = 0.4$, $p_2 = 0.2$.

If the interaction between subgroups is very small, A is nearly uncoupled; using Proposition 3 we can get

$$\operatorname{spec}(A) \approx \operatorname{spec}(B) \cup \operatorname{spec}(C); \tag{14}$$

thus,

$$\begin{aligned} |\lambda_2|(A) &\approx \max\left(|\lambda_2|(B), |\lambda_2|(C)\right), \\ \text{i.e.,}\ |\lambda_2|(A) &\approx \max\left(f(n_1, p), f(n - n_1, p)\right) \\ &= f\left(\min\left(n_1, n - n_1\right), p\right). \end{aligned} \tag{15}$$

So for fixed n, if $n_1 = n/2$, $\min(n_1, n-n_1)$ can be the largest, accordingly $|\lambda_2|$ is the largest.

3.3. The Distribution of Interpersonal Influence. Finally, we study three different distributions of influence strength of individuals. In Figure 5 Case 1, power law distribution represents an autocratic society, where minority-influential individuals or opinion leaders exist, and the latter two both represent a democratic society. In Case 2, the influence of individuals follows normal distribution. In Case 3, all individuals are affected by their neighbors with the same influence. Repeatedly calculating 1000 times, we can get the distribution of convergence rate as illustrated in Figure 5. It can be seen that, in an autocratic society (Case 1), the convergence of rate is slow with high probability, but sometimes is very fast. This is due to the asymmetry and heterogeneity of the power law distribution. If a few influential nodes belonging to different subgroups connect with each other, it will accelerate the convergence of groups opinions. On the contrary, if influential nodes form links only by inner-group, it will slightly slow down the convergence of group opinions. Thus, to some extent, the convergence time or convergence rate of group opinions is uncertain in this case. In a democratic society (Case 2 and Case 3), the convergence

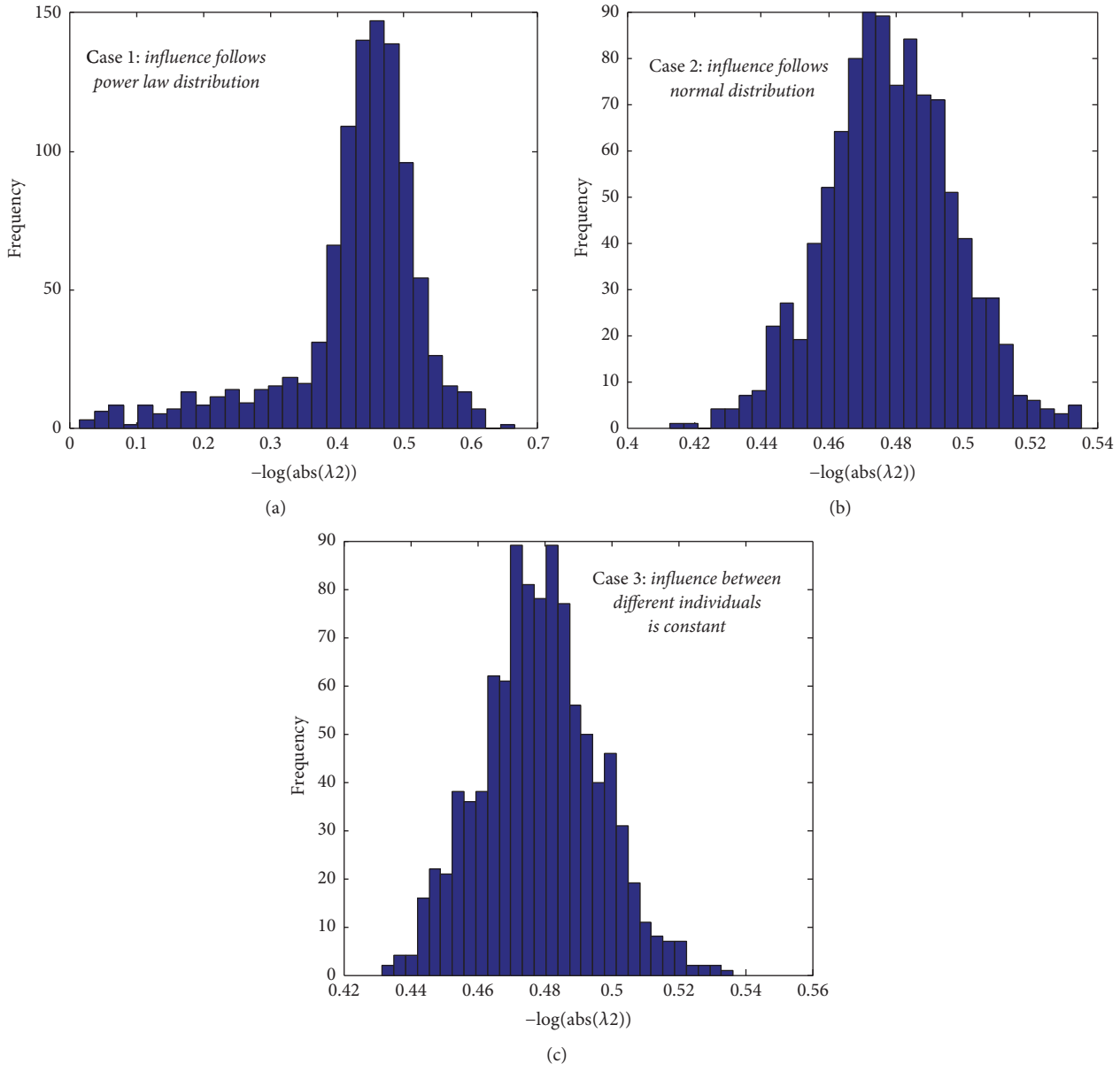

FIGURE 5: The distribution of convergence rate of group opinion is determined by the distribution of influence. x-axis is the convergence rate $-\log(|\lambda_2|)$ and y-axis is the frequency (total frequency is 1000). (a) represents autocratic society; (b) and (c) represent democratic society.

time follows a narrow-range distribution. In general, the average convergence rate is faster than that of Case 1. In Case 3, the influence matrix can be expressed as $A = (D+I)^{-1}M_A$, where M_A is the adjacency matrix of the graph. In this case, all the eigenvalues are real, and the second largest eigenvalue is determined by the maximum degree of the graph.

4. Conclusions

Based on the framework of the Degroot model, this paper studies the impact of the community structure topology on the consensus time by introducing the second largest eigenvalues modulus of social influence matrix. We prove that if the interaction between subgroups is tiny, then the consensus time will be very long. This means that opinions profiles in a social network with community structure are difficult to reach a consensus.

In order to study how the community structure impacts on the convergence time (or the convergence rate), using the second largest eigenvalue modulus, we examine this issue from three points of view: the number of nodes connected (including the number of subgroups connected, the number of subgroups within the connection, and the connection density), subgroup size, and influence distribution. We find that increasing the number of connections between subgroups can accelerate the convergence of group opinions, while increasing the number of subgroups within the subgroups slows the convergence rate. The closer the subgroups' size is,

the longer the convergence time of the group opinions is. On the other hand, the smaller the size of the subgroup is, the shorter the convergence time is. Thus, the community structure depends not only on the density of the subgroups but also on the relative size of the subgroups. In addition, the impact of distribution of influence strength on the convergence time shows that the convergence time of group opinions in an autocratic society is longer than that in a democratic society in average, but may involve more uncertainty, which depends on the various connection pattern.

The implication of all the above is network intervene [24]. In order to accelerate the consensus, we must strengthen the communication of individuals in different subgroups. On the contrary, to maintain the discrepancy of group opinions, we can strengthen the communication of individuals in the same subgroups. Another effective way to control opinion evolution is to vary the size of subgroups.

Conflicts of Interest

The authors declare that they have no conflicts of interest.

Acknowledgments

This work was supported by State Key Development Program of Basic Research of China (2013CB329603) and the Humanity and Social Science Foundation of Ministry of Education (15YJC630111).

References

[1] S. H. Strogatz, "Exploring complex networks," *Nature*, vol. 410, no. 6825, pp. 268–276, 2001.

[2] S. Boccaletti, V. Latora, Y. Moreno, M. Chavez, and D.-U. Hwang, "Complex networks: structure and dynamics," *Physics Reports. A Review Section of Physics Letters*, vol. 424, no. 4-5, pp. 175–308, 2006.

[3] R. Pastor-Satorras and A. Vespignani, "Epidemic spreading in scale-free networks," *Physical Review Letters*, vol. 86, no. 14, pp. 3200–3203, 2001.

[4] R. Pastor-Satorras, C. Castellano, P. Van Mieghem, and A. Vespignani, "Epidemic processes in complex networks," *Reviews of Modern Physics*, vol. 87, no. 3, pp. 925–979, 2015.

[5] M. Nekovee, Y. Moreno, G. Bianconi, and M. Marsili, "Theory of rumour spreading in complex social networks," *Physica A: Statistical Mechanics and Its Applications*, vol. 374, no. 1, pp. 457–470, 2007.

[6] F. Amblard and G. Deffuant, "The role of network topology on extremism propagation with the relative agreement opinion dynamics," *Physica A: Statistical Mechanics and its Applications*, vol. 343, no. 1-4, pp. 725–738, 2004.

[7] S. Boccalett et al., "The structure and dynamics of multilayer networks," *Physics Reports*, vol. 544, no. 1, pp. 1–122, 2014.

[8] M. Meadows and D. Cliff, *The Relative Agreement Model of Opinion Dynamics in Populations with Complex Social Network Structure: The Fourth International Workshop on Complex Networks*, Berlin, Germany, 2013.

[9] K. Sznajd-Weron and J. Sznajd, "Opinion evolution in closed community," *International Journal of Modern Physics C*, vol. 11, no. 6, pp. 1157–1165, 2000.

[10] P. Clifford and A. Sudbury, "A model for spatial conflict," *Biometrika*, vol. 60, pp. 581–588, 1973.

[11] R. Holley and T. M. Ligget, "Ergodic thermos for weakly interacting system and the voter model," *The Annals of Probability*, vol. 3, no. 4, pp. 643–663, 1975.

[12] S. Galam, "Majority rule, hierarchical structures, and democratic totalitarianism: A statistical approach," *Journal of Mathematical Psychology*, vol. 30, no. 4, pp. 426–434, 1986.

[13] B. Latané, "The psychology of social impact," *American Psychologist*, vol. 36, no. 4, pp. 343–356, 1981.

[14] G. Deffuant, D. Neau, F. Amblard, and G. Weisbuch, "Mixing beliefs among interacting agents," *Advances in Complex Systems*, vol. 3, no. 04, pp. 87–98, 2000.

[15] R. Hegselmann and U. Krause, "Opinion dynamics and bounded confidence models, analysis, and simulations," *Journal of Artificial Societies and Social Simulation*, vol. 5, no. 3, 2002, http://jasss.soc.surrey.ac.uk/9/1/8.html.

[16] M. H. DeGroot, "Reaching a consensus," *Journal of the American Statistical Association*, vol. 69, no. 345, pp. 118–121, 1974.

[17] R. Olfati-Saber and R. M. Murray, "Consensus problems in networks of agents with switching topology and time-delays," *Institute of Electrical and Electronics Engineers. Transactions on Automatic Control*, vol. 49, no. 9, pp. 1520–1533, 2004.

[18] P.-P. Li, D.-F. Zheng, and P. M. Hui, "Dynamics of opinion formation in a small-world network," *Physical Review E—Statistical, Nonlinear, and Soft Matter Physics*, vol. 73, no. 5, Article ID 056128, 2006.

[19] P. L. Krapivsky and S. Redner, "Dynamics of majority rule in two-state interacting spins systems," *Physica Review Letter*, vol. 90, no. 23, Article ID 238701, 2003.

[20] V. Sood and S. Redner, "Voter model on heterogeneous graphs," *Physical Review Letters*, vol. 94, no. 17, Article ID 178701, 2005.

[21] P. Singh, S. Sreenivasan, B. K. Szymanski, and G. Korniss, "Accelerating consensus on coevolving networks: The effect of committed individuals," *Physical Review E—Statistical, Nonlinear, and Soft Matter Physics*, vol. 85, no. 4, Article ID 046104, 2012.

[22] D. J. Hartfiel and C. D. Meyer, "On the structure of stochastic matrices with a subordinant eigenvalue near 1," *Linear Algebra and its Applications*, vol. 272, pp. 193–203, 1998.

[23] D. J. Watts and S. H. Strogatz, "Collective dynamics of 'small-world' networks," *Nature*, vol. 393, no. 6684, pp. 440–442, 1998.

[24] T. W. Valente, "Network interventions," *Science*, vol. 336, no. 6090, pp. 49–53, 2012.

Hindawi
Discrete Dynamics in Nature and Society
Volume 2017, Article ID 5743801, 9 pages
https://doi.org/10.1155/2017/5743801

Research Article

A Dynamic Programming Model for Internal Attack Detection in Wireless Sensor Networks

Qiong Shi,[1] Li Qin,[2] Lipeng Song,[1] Rongping Zhang,[1] and Yanfeng Jia[1]

[1]*School of Computer Science and Control Engineering, North University of China, Taiyuan, Shan'xi 030051, China*
[2]*School of Instrument and Electronics, North University of China, Taiyuan, Shan'xi 030051, China*

Correspondence should be addressed to Qiong Shi; shiqiong0641@nuc.edu.cn

Received 10 March 2017; Accepted 9 May 2017; Published 1 June 2017

Academic Editor: Lu-Xing Yang

Copyright © 2017 Qiong Shi et al. This is an open access article distributed under the Creative Commons Attribution License, which permits unrestricted use, distribution, and reproduction in any medium, provided the original work is properly cited.

Internal attack is a crucial security problem of WSN (wireless sensor network). In this paper, we focus on the internal attack detection which is an important way to locate attacks. We propose a state transition model, based on the continuous time Markov chain (CTMC), to study the behaviors of the sensors in a WSN under internal attack. Then we conduct the internal attack detection model as the epidemiological model. In this model, we explore the detection rate as the rate of a compromised state transition to a response state. By using the Bellman equation, the utility for the state transitions of a sensor can be written in standard forms of dynamic programming. It reveals a natural way to find the optimal detection rate that is by maximizing the total utility of the compromised state of the node (the sum of current utility and future utility). In particular, we encapsulate the current state, survivability, availability, and energy consumption of the WSN into an information set. We conduct extensive experiments and the results show the effectiveness of our solutions.

1. Introduction

WSN (wireless sensor network) is always vulnerable because it is usually deployed in hostile environments [1]. The attack behaviors in WSN are mainly divided into two types: external attack and internal attack. For the improvement of hardware performance, which makes the public cryptography possible, the external attacks in WSN can be prevented effectively with the security structure based on cryptography [2–4]. Thus, the focus of the study is about internal attack such as detection, revocation, and tolerance of the compromised nodes and replicated nodes that have been physically captured. Normally, there are three ways to detect internal attacks: analyzing the attack behavior [5–8], detecting the compromised nodes [9–13], and verifying replica attack [14–17].

In a WSN, the states of a sensor are typically distinguished into healthy, compromised, responsive, or fail state. At any time, a sensor stays precisely at one of the four states. For the existence of internal attacks, the sensor transits among the states in its lifecycle. In this paper, we leverage the continuous time Markov chain (CTMC) to model the state transition of sensors. In addition, we built up an internal attack detection model for WSN based on classical SIR epidemiological model. The model described the behaviors of the sensors in a WSN under internal attacks.

Thereafter, we can detect the internal attacks over the models. According to our study, the detection rate can be viewed as the rate of the transitions from a compromised state to a responsive state. In this way, the system responds immediately when a sensor changes its state to a compromised state; that is, the node has been attacked. Traditionally, the existing studies on internal attack detection in WSN focus on more efficient detection methods and higher detection rates [18–20], while the detection rate is actually not the higher the better in practice, especially when it is constrained with limits of network characteristics of a WSN such as power and computing capability. In contrast, we are more concerned with the trade-off between detection rate and network characteristics.

Therefore, we proposed a solution to find the optimal detection rate rather than choose the highest rate. By using the Bellman equation, the utility for the state transitions of a sensor can be written in standard forms of dynamic programming. In addition, we encapsulate the four parameters, that is,

current state, survivability, availability, and energy consumption, into information set. The information set is a good indicator for achieving the balance between network characteristics and security. We can find the optimal detection rate by maximizing the total utility. Extensive experiments have been conducted to show the effectiveness of our solutions. The experimental results show that our solution can indeed improve the survivability of WSN and therefore guide the design of WSN.

The rest of this paper is organized as follows. In Section 2, we give related work and outline the perspectives and approaches in the existing literatures. In Section 3, we propose the state transition model of internal attack and internal attack detection model, based on CTMC and epidemiological model, respectively. Thereafter, we establish dynamic programming model via the Bellman equation to find the optimal detection rate. In Sections 4 and 5, we present the numerical simulation study for our methods. Finally, we conclude our study in the paper and the future work in Section 6.

2. Related Work

The epidemiological model has been widely used to analyze the spread of malware in wired networks [21–25]. In literature [26], the impact of the network topology on the viral prevalence was studied and author proposed a node-based approach. In literature [27], epidemic processes were studied in complex networks. In literature [28], a theoretical assessment approach was proposed on the impact of patch forwarding on the prevalence of computer virus.

In recent years, application of the epidemiological model in WSN has become increasingly widespread [29]. The analyses based on the simulation and experiment research show that the epidemiological model can effectively describe the dynamic propagation of malware when the number of nodes in the network is large enough. In literature [30], the attack behavior of malware was studied by combining the epidemiological model with a loss equation. In literature [31], the reactive diffusion equation model of malware propagation was proposed based on the theory of epidemiological diseases.

Normally the state of the sensors in a WSN is either healthy, compromised, responsive, or failed. At any time, a sensor stays precisely at one of the four states. The state of a sensor will transit to other types if it suffers an internal attack. Therefore, we use the CTMC to model the state transition of a sensor, though the decision of the "malicious attacker" is not random in the attacked WSN, while the attack time is randomly distributed. The lifecycle of sensors can be regarded as a dynamic system, so the stochastic process can be used to establish the corresponding model. In some related papers, the Markov chain [32] is also widely used to simulate the spread of malware in WSN.

3. Model and Methods

3.1. State Transition Model. The various epidemic models are actually state transition models. These states are mutually exclusive: every sensor is in a precisely specific state at any time. The sensor transits diversely among different states during its lifecycle.

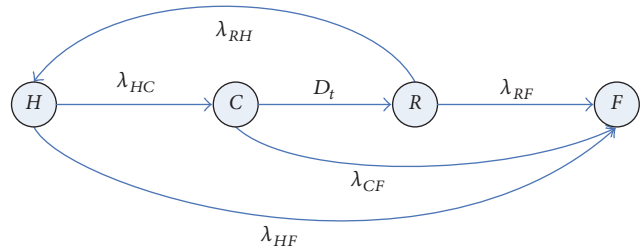

Figure 1: The value of D_t for several planning horizons.

The state transition of a node in WSN can be modeled with a CTMC. Figure 1 depicts the state transition diagram of a node under an internal attack. A circled node in the diagram stands for a state which is either healthy, compromised, responsive, or failed, which are marked with H, C, R, or F, respectively. Each arc in the diagram associates with a rate $\lambda_{ij}, i, j \in \{H, C, R, F\}$, which indicates the rate of the transition from state i to state j when the node suffered an internal attack.

State transition processes are as follows: a node in WSN in H was functioning correctly at the beginning. We suppose that the healthy sensor becomes a compromised node under an attack; that is, the state of the sensor turns to C from H. When the compromised state has been detected, the state of it will change to R; otherwise, the state of it will change to F or remain at C. If a sensor stays in R, a response action will be carried out. If we get an acknowledgement from the node, then it moves to H. Otherwise, it will be viewed as F. The response actions include software rejuvenation and reconfiguration as a countermeasure against attacks. Since a WSN is usually deployed in hostile environments or areas, the sensors could be failed for the influence of environment and outage of power.

3.2. Internal Attack Detection Model. We explore the impact of detection rate on sensors under internal attack and metrics by combining a classical epidemiological model and an economic behavioral model based on a forward-looking, representative agent. Detection efforts determine the detection rate that will determine nodes from C to R by some specific rate. It will affect the survivability and availability of nodes. The survivability and availability of one single node will have influence on the entire cluster and network.

There are four types of nodes in the WSN. Assume we have N sensors in total, and let H_t, C_t, R_t, and F_t be the number of healthy nodes, compromised nodes, responsive nodes, and failed nodes, respectively. Then we have the following differential equations:

$$\frac{dH_t}{dt} = -\lambda_{HC} H_t C_t + \lambda_{RH} R_t - \lambda_{HF} H_t,$$

$$\frac{dC_t}{dt} = \lambda_{HC} H_t C_t - D_t C_t - \lambda_{CF} C_t,$$

$$\frac{dR_t}{dt} = D_t C_t - \lambda_{RH} R_t - \lambda_{RF} R_t,$$
$$\frac{dF_t}{dt} = \lambda_{RF} R_t + \lambda_{CF} C_t + \lambda_{HF} H_t. \tag{1}$$

Equations (1) formalize four-state transition processes when a sensor in the WSN is under an internal attack. D_t in the equations is the detection rate, that is, the rate that nodes detected in C at every interval. The transition rate from C to R is taken as the detection rate D_t; that is, $\lambda_{CR} = D_t$. In other words, response measures should be taken immediately as long as the node is recognized as C. However, the other types of state transition do not depend on the detection rate.

The above model (model 1) illustrates the dynamic evolution process of WSN under internal attack within a certain period. The dynamics of internal attack detection model cannot be analyzed thoroughly in a short period of time, so we will focus on the process of the long-term dynamic evolution on the WSN. With the power of WSN limited and deployed in harsh environments, a large number of redundant sensors are normally deployed in WSN for the sensors cannot be able to be repaired once they transited to the failure state. After the sensor fails, the redundant node will be the suitable alternatives. We will call it "death" and "birth"; we will put forward model 2:

$$\frac{dH_t}{dt} = N_0 - \lambda_{HC} H_t C_t + \lambda_{RH} R_t - \lambda_{HF} H_t,$$
$$\frac{dC_t}{dt} = \lambda_{HC} H_t C_t - D_t C_t - \lambda_{CF} C_t, \tag{2}$$
$$\frac{dR_t}{dt} = D_t C_t - \lambda_{RH} R_t - \lambda_{RF} R_t.$$

Assume the immutability of the sum of the sensors (including H_t, C_t, R_t, and F_t, excluding abundant nodes), N_0 is the number of the "births", and it is equal to the number of "deaths," namely the abundant nodes which replaced the "death". To simplify the counting process, let $\lambda_{HF} = \lambda_{CF} = \lambda_{RF} = \lambda$.

Dynamic analysis is carried out on model 2 and both the existence and stability of the equilibrium point will be discussed. According to (2), we find the steady state as follows:

(i) $E_0 = (1, 0, 0)$.

(ii) Interior equilibrium point $E^*(H_t^*, R_t^*, C_t^*)$

$$H_t^* = \frac{\lambda + D_t}{\lambda_{HC}},$$
$$R_t^* = \frac{D_t(\lambda_{HC} - \lambda - D_t)}{\lambda_{HC}(D_t + \lambda + \lambda_{RH})}, \tag{3}$$
$$C_t^* = \frac{(\lambda_{HC} - \lambda - D_t)(\lambda + \lambda_{RH})}{\lambda_{HC}(D_t + \lambda + \lambda_{RH})}.$$

The Jacobi matrix of the model is acquired:

$$J = \begin{pmatrix} -\lambda_{HC} C_t - \lambda & -\lambda_{HC} H_t & \lambda_{RH} \\ \lambda_{HC} C_t & \lambda_{HC} H_t - D_t - \lambda & 0 \\ 0 & D_t & -\lambda_{RH} - \lambda \end{pmatrix}. \tag{4}$$

(1) The Jacobian corresponding to $E_0(1, 0, 0)$ is that

$$J_0 = \begin{pmatrix} -\lambda & -\lambda_{HC} & \lambda_{RH} \\ 0 & \lambda_{HC} - D_t - \lambda & 0 \\ 0 & D_t & -\lambda_{RH} - \lambda \end{pmatrix} \tag{5}$$

and, thus, the eigenvalues of the Jacobian at $E_0(1, 0, 0)$ must have negative real parts, which are equivalent to $\lambda_1 = -\lambda < 0$, $\lambda_2 = \lambda_{HC} - D_t - \lambda < 0$, and $\lambda_3 = -\lambda_{RH} - \lambda < 0$.

(2) The Jacobian corresponding to $E^*(H_t^*, R_t^*, C_t^*)$ is that

$$J^* = \begin{pmatrix} -\frac{(\lambda_{HC} - \lambda - D_t)(\lambda + \lambda_{RH})}{D_t + \lambda + \lambda_{RH}} - \lambda & -\lambda - D_t & \lambda_{RH} \\ \frac{(\lambda_{HC} - \lambda - D_t)(\lambda + \lambda_{RH})}{D_t + \lambda + \lambda_{RH}} & 0 & 0 \\ 0 & D_t & -\lambda_{RH} - \lambda \end{pmatrix}. \tag{6}$$

The eigenvalues of the Jacobian at $E^*(H_t^*, R_t^*, C_t^*)$ are obtained $\lambda_1 = -\lambda < 0$ and λ_2 and λ_3 meet $(\lambda')^2 + (\lambda_{RH} + \lambda + (\lambda_{HC} - \lambda - D_t)(\lambda + \lambda_{RH})/(D_t + \lambda + \lambda_{RH}))\lambda' + ((\lambda_{HC} - \lambda - D_t)(\lambda + \lambda_{RH})/(D_t + \lambda + \lambda_{RH}))D_t = 0$, because $\lambda_{HC} - \lambda - D_t > 0$, then $\lambda_2\lambda_3 > 0$, $\lambda_2 + \lambda_3 < 0$, and thus $\lambda_2 < 0$, $\lambda_3 < 0$.

By using linear analysis, we can find that E^* is always stable.

Model 1, which is the key of the article, is the basis of the model behind and simulation test. The dynamics analysis is only carried out on model 2.

3.3. Dynamic Programming. We next present a dynamic programming paradigm to find the optimal detection rate. The method is based on an interesting observation that the highest detection rate does not always act as the best choice. So many factors influence the detection rate in WSN, such as availability, survivability, and energy. Suppose we have a healthy sensor under attack. The sensor still can provide service even though it transits to C due to the attack. However, the service will break off if the sensor, currently staying in C, moves to R. The service continues when the sensor restores to a healthy state successfully. The availability of the WSN declines when the sensor in R is doing that recovery. The utility of C is greater than R and the compromised nodes might as well have not been detected in this case. So higher detection rate does not always mean better utility. Moreover, higher detection rate means more energy consumption, which violates the efficiency rules in WSNs. Above all, we focus on the optimal rate instead of the highest one. All the factors we were concerned about have been abstracted to be part of the information set.

We propose a new objective, namely, utility, measuring the quality of the information set. The detection rate will

maximize the expected net value of the present utility, while influencing current utility and expected utility in future periods. To model this dynamic maximization, we define utility within a period and define the probability of transiting across states. We switch to a discrete-time formulation, with time incremented in days and transition probabilities reformulated below on the basis of (1).

Suppose that we have complete statistics about the current value of utility, including the negative utilities, with its information set including knowledge about survivability, availability, energy consumption, and H_t, C_t, R_t, and F_t.

Let $u_t(S)$ be the current utility of a sensor at time t in S ($S \in \{H, C, R, F\}$). Then, the utility of the sensor in C at time t is formally defined as follows:

$$u_t\left(C, D_t\right) = \left(bD_t - D_t^2\right)^{\gamma} - a. \tag{7}$$

The utility function u_t is a hybrid indicator measuring the content of the information set that has been mentioned before, which can simplify the model and enhance the generality of it. The utility function is concave and unimodal. The coefficients, a and b, in (7) can be adjusted according to the application.

According to (1), the transition probabilities between a pair of states are written as follows:

$$\begin{aligned} P_{HC} &= 1 - e^{(-\lambda_{HC} C_t)}, \\ P_{RH} &= 1 - e^{(-\lambda_{RH})}, \\ P_{HF} &= 1 - e^{(-\lambda_{HF})}, \\ P_{CR} &= D_t, \\ P_{CF} &= 1 - e^{(-\lambda_{CF})}, \\ P_{RF} &= 1 - e^{(-\lambda_{RF})}. \end{aligned} \tag{8}$$

The detection rate is determined by the current utility, at time t, and the expected utility at time $t + 1$, of compromised nodes. We use the Bellman equation to calculate the optimal detection rate and utility equations can be written as standard forms of dynamic programming

$$\begin{aligned} &V_t(H) \\ &\quad = u_t(H) \\ &\qquad + \delta\left[P_{HH} V_{t+1}(H) + P_{HC} V_{t+1}(C) + P_{HF} V_{t+1}(F)\right], \end{aligned} \tag{9}$$

$$\begin{aligned} &V_t(C) \\ &\quad = u_t\left(C, D_t\right) \\ &\qquad + \delta\left[P_{CC} V_{t+1}(C) + P_{CR} V_{t+1}(R) + P_{CF} V_{t+1}(F)\right], \end{aligned} \tag{10}$$

$$\begin{aligned} &V_t(R) \\ &\quad = u_t(R) \\ &\qquad + \delta\left[P_{RR} V_{t+1}(R) + P_{RF} V_{t+1}(F) + P_{RH} V_{t+1}(H)\right], \end{aligned} \tag{11}$$

$$V_t(F) = u_t(F) + \delta\left[P_{FF} V_{t+1}(F)\right]. \tag{12}$$

In the equation system, $V_t(S)$ $(S = H, C, R, F)$ is the utility for a sensor staying in S at time t and δ is the discount factor. $u_t(S)$ is current utility. $V_{t+1}(S)$ is the expected utility and P_{ij} stands for the transition probabilities between states (see (8)). The second term of the right member in each equation indicates that the utility of the future $(t + 1)$ moments is discounted to the present (t) utility.

Since the utilities are written in the standard form of dynamic programming, we can optimize the detection rate D_t dynamically with a planning horizon of length τ. If $t = 0$, then D_0 is chosen to solve the problem formalized by (9)–(12). In period $t = 1$, the system updates knowledge on information set and uses (9)–(12) to optimize anew over the next τ planning periods. The process continues in this way. For example, if $\tau = 7$, then on February 1 the horizon is through February 8, but on February 2 the horizon extends to February 9, and so on:

$$\begin{aligned} V_t(C) = \max\{&u_t\left(C, D_t\right) \\ &+ \delta\left[P_{CC} V_{t+1}(C) + P_{CR} V_{t+1}(R) + P_{CF} V_{t+1}(F)\right]\}. \end{aligned} \tag{13}$$

In (13), if we take the maximum value of (10), the optimal D_t can be obtained. So partial derivative of (13) is formalized as

$$\frac{\partial u_t\left(C, D_t\right)}{\partial D_t} = \delta\left[-\frac{\partial P_{CC}}{\partial D_t} V_{t+1}(C) - \frac{\partial P_{CR}}{\partial D_t} V_{t+1}(R)\right]. \tag{14}$$

The left member in (14) stands for the gain of utility, at time t, for a unit increase of the detection rate. The right member in (14) is the expected benefit from a unit increase of the detection rate at time t, which comes from future discounts.

If $t = \tau$, we have $t + 1 = \tau + 1$. Each utility at $\tau + 1$ is 0, since $\tau + 1$ exceeds the planning horizon.

The optimal detection rate D_t is determined by the information set at time t and its effects on the future values of H, C, R, and F. It is reasonable to assume that the system adapts to forecasts on the basis of the current information set.

The optimal detection rate can be reached with the equation system (9)–(14) by using backward induction over the planning period $[0, \tau]$.

4. Experiments

In this section we present the experimental studies of our models. In the experiments, we simulate two different WSNs that are under internal attacks and conduct three groups of experiments with them. The first group of experiments is designed to find the optimal detection rate D_t by using the dynamic programming paradigm. In the second group, we verify the models. In the third one, we present comparative studies by varying the value of detection rate D_t.

4.1. Experimental Setup. We simulate two different WSNs in the experiments:

(1) For the first WSN, the number of healthy sensors is much larger than that of compromised sensors, where $H_t = 0.9$, $C_t = 0.1$, $R_t = 0$, and $F_t = 0$.

Table 1: The parameters in models.

Parameter	Description
δ	Discount factor
λ_{HC}	Compromised rate
λ_{CR}	Responsive rate
λ_{RH}	Recovery rate
λ_{CF}	Failure from compromised rate
λ_{HF}	Failure rate
λ_{RF}	Failure from responsive rate

Table 2: The parameter value.

Parameter	Value
γ	0.25
a	1
b	0.5
δ	0.9
λ_{HC}	0.1
λ_{CR}	D_t, 0.3, 0.9
λ_{RH}	0.8
λ_{CF}	0.000278
λ_{HF}	0.01
λ_{RF}	0.0417

(2) In the second one, the number of healthy sensors is almost the same as that of compromised sensors, where $H_t = 0.6$, $C_t = 0.4$, $R_t = 0$, and $F_t = 0$.

The settings of the parameters of the models are summarized in Tables 1 and 2. Particularly, the utilities of H, C, R, and F fall in $[0, 1]$. To note is that the parameters can be changed according to various application scenarios.

5. Experimental Results

The Optimal Detection Rate. In the first group of experiments, we are to find the optimal detection rate D_t. In this experiment, the current utilities of H, F, and R are initially set to 1, 0, and 0.6, respectively. We evaluated the detection rate D_t for the two WSNs. As we can see from Figure 2, there is no significant difference of the detection rates between the two WSNs. The results show that the ratio of healthy sensors and the compromised sensors have little influence on the detection rate D_t and the value of D_t gradually converges to 0.75 after $\tau = 5$. The optimal value of D_t will be obtained when $\tau = 9$, where the optimal values for both WSNs fall into $[0.74, 0.75]$.

Verifying the Models. We apply the optimal detection rate $D_t = 0.75$ in second group of experiments. Figures 3–6 plot the change in the number of sensors in H, C, R, and F for WSNs in nine days. As we can see from Figure 3, the number of sensors in H decreases when t is in $[0, 1]$. After the decline, there is a sudden increase and the number of healthy sensors gradually converges to a constant value after $t = 4$. For example, the ratio of healthy sensors is around 0.9. Since

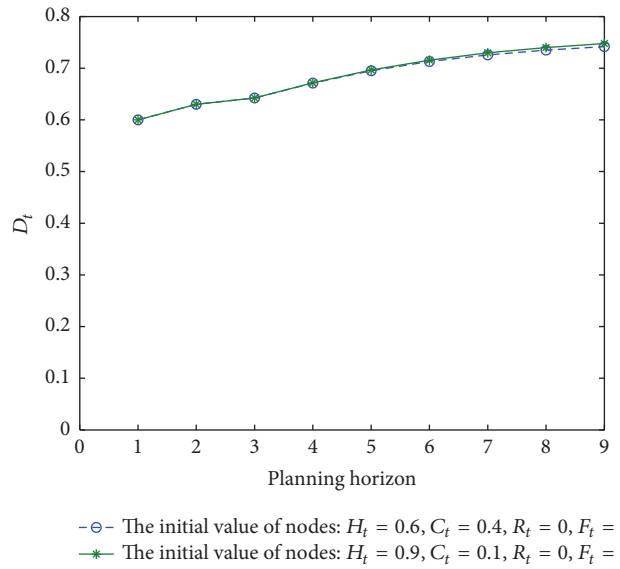

Figure 2: The value of D_t for several planning horizons.

we have more healthy sensors, the WSN is therefore robust. In contrast, as shown by Figure 4, the number of sensors in C drops quickly to 0. The results justify the effectiveness of our detection mechanism and the optimal detection rate is very effective for the transition of compromised nodes (detection rate in the model is transition rate). From Figure 5, we observe that the number of responsive sensors jumps quickly to a peak at $t = 1$ and then gradually decreases to 0. When t is in $[0, 1]$, the number of nodes in C is greatest and it is the period of most numbers of nodes from C to R. So the number of nodes in R increases quickly and reaches the peak. In Figure 6, we can see that the number of failed sensors increases monotonically as the time is elapsing. This is because a WSN is usually deployed in hostile environments and the sensors cannot get repaired once they failed. From Figures 3–6, we observe that there are big deviations between the dashed lines and solid line at beginning, but the deviation drops off gradually to 0 as time is increasing. It means that each of the WSNs used in our experiments converges to a steady state regardless of the initial condition during an observation period. Therefore, we can conclude that our model is general enough and it is applicable to a large range of WSNs.

Comparative Studies. In Section 3, we have made an assumption that the optimal detection rate is better than the highest one. To justify this assumption, in this group of experiments, we census the number of sensors being in ($H, C, R,$ and F) by varying the detection rate D_t. In the previous simulation, we have got the optimal detection rate $D_t = 0.75$ and we have also proved that our model is valid for both WSNs. So we can conduct the comparative experiments over only one WSN. We use the WSN with $H_t = 0.9$, $C_t = 0.1$, $R_t = 0$, and $F_t = 0$. In the literature [33], the author chose five empirical values at the transition rate from C to R, and we select the highest value 0.3 as D_t. In addition, we select another detection rate,

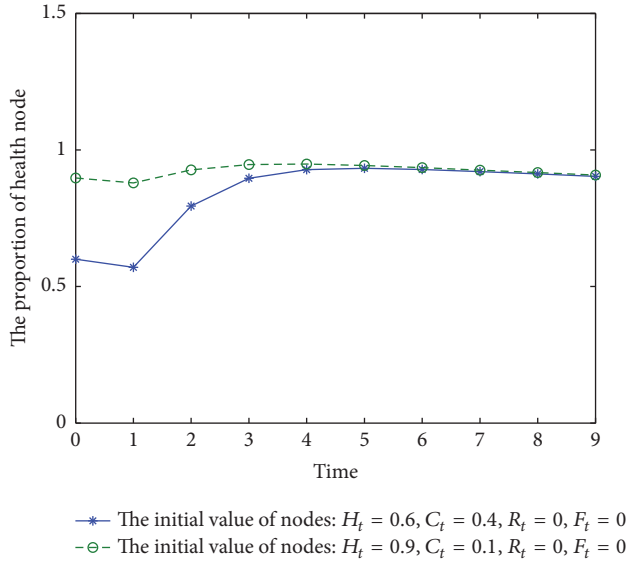

Figure 3: The proportion of healthy sensors.

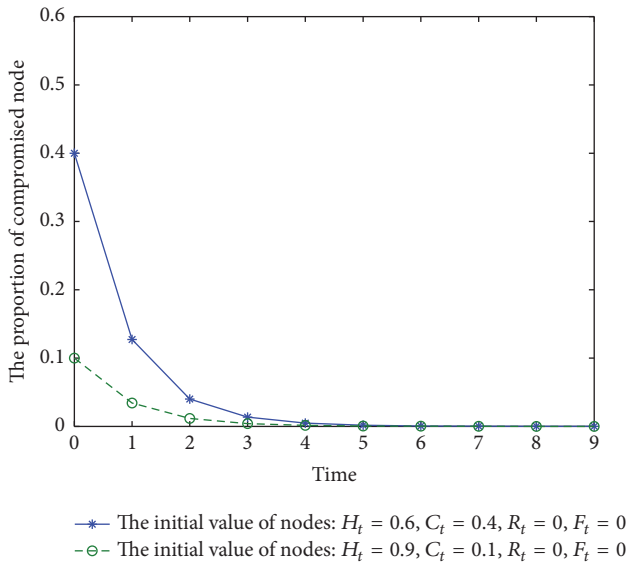

Figure 4: The proportion of compromised sensors.

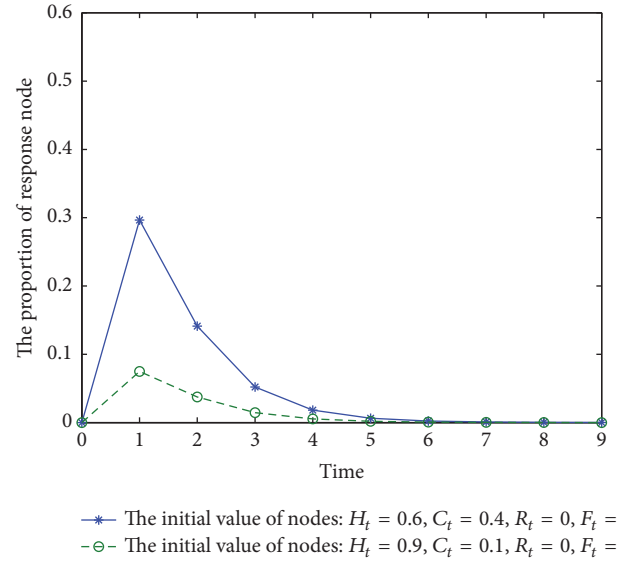

Figure 5: The proportion of responsive sensors.

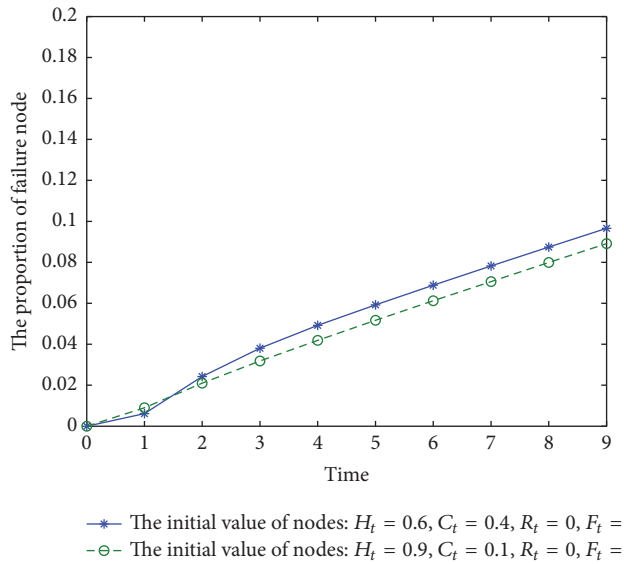

Figure 6: The proportion of failed sensors.

$D_t = 0.9$, to compare with. We plot the results in Figures 7–10, where the blue solid line represents the results $D_t = 0.75$, the green dashed line represents the results $D_t = 0.3$, and the red dashed line represents the results for $D_t = 0.9$.

As shown in Figure 7, there is a drop at the beginning for each line, but the blue solid one rises immediately when $t = 1$. The other two lines, $D_t = 0.9$ and $D_t = 0.3$, get to rise until $t = 2$. This shows that our model can make the WSN more robust, since it gets restored faster. Figure 8 shows the number of compromised sensors. We observe that the higher the detection rate D_t the faster the line drops. The red dotted line and the blue solid line move gradually close to zero after $t = 2$, which means that the reliability of the WSN is getting improved. We can also observe that the blue solid line converges in almost the same speed with the red dashed line. In other words, our model and $D_t = 0.9$ have the same performances, which are much better than that of $D_t = 0.3$. Figure 9 plots the number of the responsive sensors. As we can see from the figure, the blue solid line is completely below the other red dashed line. It is clear that optimal detection rate is better than the higher one. Although it only beats by $D_t = 0.3$ at $t = 1$, it gets improved fast after that time. In addition, we observe the blue solid line drops first, which indicates the recovery process starts earlier than other choices. Figure 10 plots the change of the failed sensors, where the three lines show similar trend. To note is that the WSN has more failed nodes when the detection rate D_t goes larger. when D_t is 0.75 and D_t is 0.3, the number of failure nodes is similar.

We have compared our solution with other ones from the recovery time, the recovery rate, the number of the final

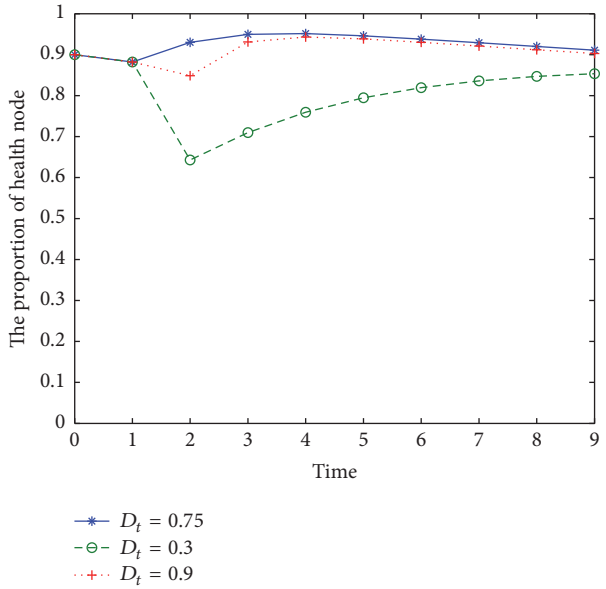

Figure 7: The proportion of responsive sensors.

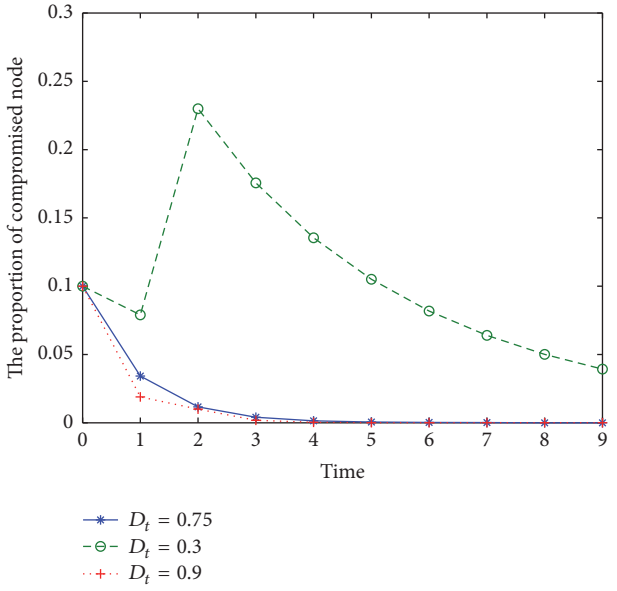

Figure 8: The proportion of compromised sensors.

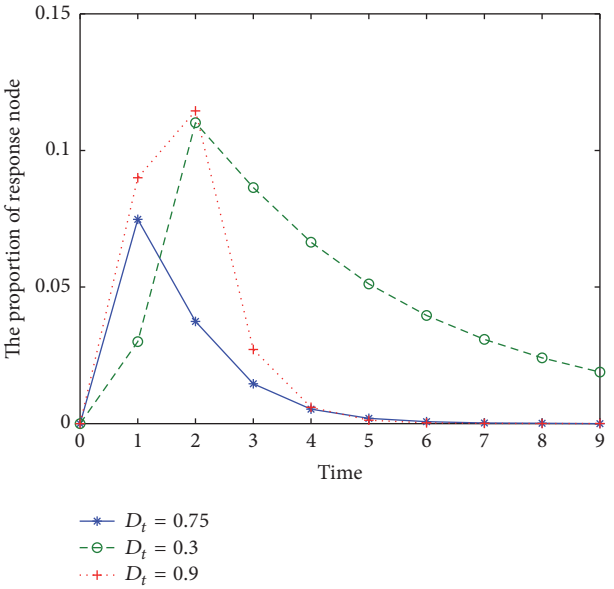

Figure 9: The proportion of responsive sensors.

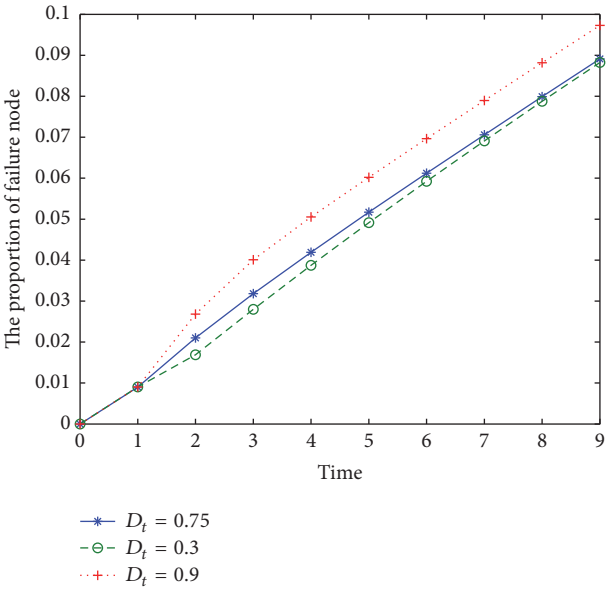

Figure 10: The proportion of failed sensors.

failed nodes, and the energy consumption. In general, the simulation results show that our solution outperforms the other ones. It justifies our observation that the highest detection rate is not always servers as the best choice.

6. Conclusion

In this work, we investigated the problem of finding the detection rate of WSN under internal attacks. Firstly, we established a state transition model of sensors based on the CTMC. The model described the behaviors of sensors in a WSN under attacked nodes and the transition between states. We are the first to observe that detection rate is irrelevant to other state transitions except the transition from C to R. Therefore, we take the detection rate as the transition rate from C to R. Secondly, we modeled the state transition process of the sensors in a WSN under internal attacks by using the epidemic model and make a formal description about this model. Thirdly, by using the dynamic programming paradigm (Bellman equation), we can easily find the optimal detection rate for WSN under internal attacks. In addition, we encapsulated the influencing factors into an information set which captures the current utility and the utility in future time. In this way, the detection rate can be optimized by maximizing the total utility of the current and future utility

discount in C. The experimental studies justified the validity of our models.

In the future, we would like to quantize the influencing factors with respect to survivability, availability, and energy consumption in order to improve the accuracy and practicability of detection rate. Moreover, it is more meaningful to set the parameters applied in the simulation according to a real world application. In addition, we will introduce the immune state into the model and refer to the SIRS model [34, 35] for further study. Therefore, it will accelerate the design of WSN and then improve the availability and survivability of WSN.

Conflicts of Interest

The authors declare that they have no conflicts of interest.

Acknowledgments

This work is supported by the National Sciences Foundation of China (61379125).

References

[1] Y. Wang, G. Attebury, and B. Ramamurthy, "A survey of security issues in wireless sensor networks," *IEEE Communications Surveys and Tutorials*, vol. 8, no. 2, pp. 2–22, 2006.

[2] A. Liu and P. Ning, "TinyECC: a configurable library for elliptic curve cryptography in wireless sensor networks," in *Proceedings of the 7th International Conference on Information Processing in Sensor Networks (IPSN '08)*, pp. 245–256, St. Louis, Mo, USA, April 2008.

[3] H. D. Wang, B. Sheng, C. C. Tan, and Q. Li, "Comparing symmetric–key and public–key based security schemes in sensor networks: a case study of user access control," in *Proceedings of the 28th International Conference on Distributed Computing Systems (ICDCS '08)*, pp. 11–18, China, 2008.

[4] R. H. Wang, W. Du, X. Liu, and P. Ning, "ShortPK: a short–term public key scheme for broadcast authentication in sensor networks," *ACM Transactions on Sensor Networks*, vol. 6, no. 1, article 9, pp. 1–29, 2009.

[5] P. Ballarini, L. Mokdad, and Q. Monnet, "Modeling tools for detecting DoS attacks in WSNs," *Security and Communication Networks*, vol. 6, no. 4, pp. 420–436, 2013.

[6] Y. Zhang, W. Liu, W. Lou, and Y. Fang, "Location–based compromise–tolerant security mechanisms for wireless sensor networks," *IEEE Journal on Selected Areas in Communications*, vol. 24, no. 2, pp. 247–260, 2006.

[7] Y. Chen, J. Yang, W. Trappe, and R. P. Martin, "Detecting and localizing identity–based attacks in wireless and sensor networks," *IEEE Transactions on Vehicular Technology*, vol. 59, no. 5, pp. 2418–2434, 2010.

[8] J. Katiravan, D. N, and D. N, "A two level detection of routing layer attacks in hierarchical wireless sensor networks using learning based energy prediction," *KSII Transactions on Internet and Information Systems*, vol. 9, no. 11, pp. 4644–4661, 2015.

[9] A. Ahmed, K. Abu Bakar, M. . Channa, K. Haseeb, and A. W. Khan, "A survey on trust based detection and isolation of malicious nodes in ad–hoc and sensor networks," *Frontiers in Computer Science*, vol. 9, no. 2, pp. 280–296, 2015.

[10] Y. Zhang, J. Yang, W. Li, L. Wang, and L. Jin, "An authentication scheme for locating compromised sensor nodes in WSNs," *Journal of Network and Computer Applications*, vol. 33, no. 1, pp. 50–62, 2010.

[11] A. Al-Riyami, N. Zhang, and J. Keane, "An adaptive early node compromise detection scheme for hierarchical wsns," *IEEE Access*, vol. 4, pp. 4183–4206, 2016.

[12] N. Labraoui, M. Gueroui, and L. Sekhri, "A risk–aware reputation–based trust management in wireless sensor networks," *Wireless Personal Communications*, vol. 87, no. 3, pp. 1037–1055, 2016.

[13] A. Le, J. Loo, A. Lasebae, M. Aiash, and Y. Luo, "6LoWPAN: a study on QoS security threats and countermeasures using intrusion detection system approach," *International Journal of Communication Systems*, vol. 25, no. 9, pp. 1189–1212, 2012.

[14] B. Zhu, S. Setia, S. Jajodia, S. Roy, and L. Wang, "Localized multicast: efficient and distributed replica detection in large–scale sensor networks," *IEEE Transactions on Mobile Computing*, vol. 9, no. 7, pp. 913–926, 2010.

[15] Y. P. Zeng, J. N. Cao, S. G. Zhang, S. Guo, and L. Xie, "Random–walk based approach to detect clone attacks in wireless sensor networks," *IEEE Journal on Selected Areas in Communications*, vol. 28, no. 5, pp. 677–691, 2010.

[16] W. T. Zhu, J. Zhou, R. H. Deng, and F. Bao, "Detecting node replication attacks in wireless sensor networks: a survey," *Journal of Network and Computer Applications*, vol. 35, no. 3, pp. 1022–1034, 2012.

[17] W. Z. Khan, M. S. Hossain, M. Y. Aalsalem, N. M. Saad, and M. Atiquzzaman, "A cost analysis framework for claimer reporter witness based clone detection schemes in WSNs," *Journal of Network and Computer Applications*, vol. 63, pp. 68–85, 2016.

[18] S. S. Wang, K. Q. Yan, and C. Liu, "An integrated intrusion detection system for cluster-based wireless sensor networks," *Expert Systems with Applications*, vol. 38, no. 12, pp. 15234–15243, 2011.

[19] I. Almomani, B. Al-Kasasbeh, and M. AL-Akhras, "WSN-DS: a Dataset for intrusion detection systems in wireless sensor networks," *Journal of Sensors*, vol. 2016, article 4731953, pp. 1–16, 2016.

[20] N. Labraoui, M. Gueroui, and M. Aliouat, "Secure DV-Hop localization scheme against wormhole attacks in wireless sensor networks," *European Transactions on Telecommunications*, vol. 23, no. 4, pp. 303–316, 2012.

[21] L. Song, J. Zhen, G. Sun, J. Zhang, and X. Han, "Influence of removable devices on computer worms: dynamic analysis and control strategies," *Computers and Mathematics with Applications*, vol. 61, no. 7, pp. 1823–1829, 2011.

[22] P. Van Mieghem, J. Omic, and R. Kooij, "Virus spread in networks," *IEEE/ACM Transactions on Networking*, vol. 17, no. 1, pp. 1–14, 2009.

[23] F. D. Sahneh, C. Scoglio, and P. Van Mieghem, "Generalized epidemic mean–field model for spreading processes over multilayer complex networks," *IEEE/ACM Transactions on Networking*, vol. 21, no. 5, pp. 1609–1620, 2013.

[24] X. Yang, Y. Zhu, J. Hong, L.-X. Yang, Y. Wu, and Y. Y. Tang, "The rationality of four metrics of network robustness: a viewpoint of robust growth of generalized meshes," *PLoS ONE*, vol. 11, no. 8, Article ID e0161077, 2016.

[25] L.-X. Yang and X. Yang, "A new epidemic model of computer viruses," *Communications in Nonlinear Science and Numerical Simulation*, vol. 19, no. 6, pp. 1935–1944, 2014.

[26] L.-X. Yang, M. Draief, and X. Yang, "The impact of the network topology on the viral prevalence: a node–based approach," *PLoS ONE*, vol. 10, no. 7, article e0134507, 2015.

[27] R. Pastor-Satorras, C. Castellano, P. Van Mieghem, and A. Vespignani, "Epidemic processes in complex networks," *Reviews of Modern Physics*, vol. 87, no. 3, pp. 925–979, 2015.

[28] L.-X. Yang, X. Yang, and Y. Wu, "The impact of patch forwarding on the prevalence of computer virus: a theoretical assessment approach," *Applied Mathematical Modelling*, vol. 43, pp. 110–125, 2017.

[29] L. Feng, L. Song, Q. Zhao, and H. Wang, "Modeling and stability analysis of worm propagation in wireless sensor network," *Mathematical Problems in Engineering*, Article ID 129598, Art. ID 129598, 8 pages, 2015.

[30] M. H. R. Khouzani, S. Sarkar, and E. Altman, "Optimal control of epidemic evolution," in *Proceedings of the IEEE International Conference on Computer Communications (INFOCOM '11)*, pp. 1683–1691, April 2011.

[31] Z. B. He and X. M. Wang, "A spatial–temporal model for the malware propagation in MWSNs based on the reaction–diffusion equations," in *Proceedings of the WAIM 2012 Workshops*, pp. 45–56.

[32] S. Shen, L. Huang, J. Liu, A. C. Champion, S. Yu, and Q. Cao, "Reliability evaluation for clustered WSNs under malware propagation," *Sensors*, vol. 16, no. 6, article no. 855, 2016.

[33] S. Parvin, F. K. Hussain, J. S. Park, and D. S. Kim, "A survivability model in wireless sensor networks," *Computers and Mathematics with Applications*, vol. 64, no. 12, pp. 3666–3682, 2012.

[34] L.-X. Yang, M. Draief, and X. Yang, "The optimal dynamic immunization under a controlled heterogeneous node–based SIRS model," *Physica A.*, vol. 450, pp. 403–415, 2016.

[35] L. Yang, M. Draief, and X. Yang, "Heterogeneous virus propagation in networks: a theoretical study," *Mathematical Methods in the Applied Sciences*, vol. 40, no. 5, pp. 1396–1413, 2017.

Hindawi
Discrete Dynamics in Nature and Society
Volume 2017, Article ID 8609082, 11 pages
https://doi.org/10.1155/2017/8609082

Research Article

A Novel Computer Virus Propagation Model under Security Classification

Qingyi Zhu[1] and Chen Cen[2]

[1]*College of Cyber-Security and Information Law, Chongqing University of Posts and Telecommunications, Chongqing 400065, China*
[2]*College of Computer Science, Chongqing University of Posts and Telecommunications, Chongqing 400065, China*

Correspondence should be addressed to Qingyi Zhu; zhuqy@cqupt.edu.cn

Received 28 February 2017; Revised 30 April 2017; Accepted 2 May 2017; Published 25 May 2017

Academic Editor: Jose R. C. Piqueira

Copyright © 2017 Qingyi Zhu and Chen Cen. This is an open access article distributed under the Creative Commons Attribution License, which permits unrestricted use, distribution, and reproduction in any medium, provided the original work is properly cited.

In reality, some computers have specific security classification. For the sake of safety and cost, the security level of computers will be upgraded with increasing of threats in networks. Here we assume that there exists a threshold value which determines when countermeasures should be taken to level up the security of a fraction of computers with low security level. And in some specific realistic environments the propagation network can be regarded as fully interconnected. Inspired by these facts, this paper presents a novel computer virus dynamics model considering the impact brought by security classification in full interconnection network. By using the theory of dynamic stability, the existence of equilibria and stability conditions is analysed and proved. And the above optimal threshold value is given analytically. Then, some numerical experiments are made to justify the model. Besides, some discussions and antivirus measures are given.

1. Introduction

With the rapid development of the Internet, the spread of computer virus has brought a lot of potential safety problems, which not only caused huge waste to the network resources but also harmed the interests of individuals and the masses. The traditional way of antivirus is constantly updating the virus library of antivirus software. But it is a passive mechanism to prevent viruses. In this context, the macroscopical study of computer virus propagation is regarded as a very important approach to antivirus and has received more and more attention from scholars.

In 1991, Kephart and White firstly used the model of biological infectious virus to study the spread of computer viruses [1]. Since then, a lot of dynamical models of computer virus have been presented. These models can be simply divided into two broad categories: homogeneous models and heterogeneous models according to according to whether the network is fully connected or not.

In recent years, more and more scholars have begun to study heterogeneous models. Kjaergaard and his partners followed the time evolution of information propagation through communication networks by using the susceptible-infected (SI) model with empirical data on contact sequences [2]. Castellano and Pastor-Satorras studied the threshold of epidemic models in quenched networks with degree distribution given by a power-law for the susceptible-infected-susceptible (SIS) model [3]. Zhu et al. investigated a new epidemic SIS model with nonlinear infectivity, as well as birth and death of nodes and edges [4]. Taking into account the power-law degree distribution of the Internet, Yang et al. proposed a novel epidemic model of computer viruses and presented the spreading threshold for the model [5]. L.-X. Yang and X. Yang proposed an epidemic model of computer viruses over a reduced scale-free network [6]. Yang and his partners proposed a node-based susceptible-latent-breaking-susceptible (SLBS) model which addresses the impact of the structure of the viral propagation network on the viral prevalence [7]. To understand the impact of available information in the control of malicious network epidemics, Mishra and three others proposed a 1-n-n-1 type differential epidemic model, where the differentiability allows

a symptom based classification [8]. All these models assume that the spread of viruses can only be through the topological neighbors.

In fact, a lot of viruses can propagate without dependence on the topology, such as Code Red (2001), Slammer (2003), Blaster (2003), Witty (2004), and Conficker (2009). By probing the entire IPv4 space or localized IP addresses, these viruses can infect an arbitrary vulnerable computer. In this condition, the propagation network can be regarded as fully connected. Besides, there are still some fully interconnected networks, such as virtual cluster in cloud [9–12]. So the study of homogeneous models is also an important branch of computer virus dynamical models. A portion of infected external computers could enter the Internet and removable storage media could carry viruses, based on the two facts. Gan et al. established a series of dynamical models [13–16]. Amador and Artalejo investigated the dynamics of computer virus spreading by considering a stochastic SIRS model where immune computers send warning signals to reduce the propagation of the virus among the rest of computers in the network [17]. Liu and Zhong presented and analyzed an SDIRS model describing the propagation of web malware based on the assumption of homogeneity [18]. Yuan and three others presented a nonlinear force of infection function for e-SEIR model to study the crowding and psychological effects in network virus prevalence [19].

In order to protect the security and stability of information systems, the concept of information security classified protection is proposed and has been a basic strategy of construction of national information. But to our knowledge, nearly all previous models describing the spread of computer viruses ignore the impacts of security classifications. In order to study how these factors affect the spread of computer viruses on the Internet, this paper proposes a novel computer virus propagation model. A thorough analysis of this model shows that some equilibria existed and are globally asymptotically stable in a specific situation. Besides, some simulation experiments are performed to examine the conclusion got from this model. In the end, some effective strategies for controlling virus spreading are recommended.

The subsequent materials are organized in this fashion: The idea of modeling is introduced in Section 2. The new model is established in Section 3. The analysis of four equilibria is addressed in Section 4. The local and global stabilities of these equilibria are investigated in Sections 5 and 6, respectively. Simulation experiments and some discussions are presented in Section 7. Finally, this work is outlined in Section 8.

2. Idea of Modeling

In a security classification network, blindly increasing the security level of computer will result in both waste of resource and increase of cost. Therefore, reinforcing the security level of computer must be targeted. About security classification of computer, the influential criteria are "Trusted Computer System Evaluation Criteria (TcsEC)" issued by United States Department of Defense [20]. By using these criteria, computers in the network can be divided into four divisions. From high to low, they are Levels A, B, C, and D, respectively.

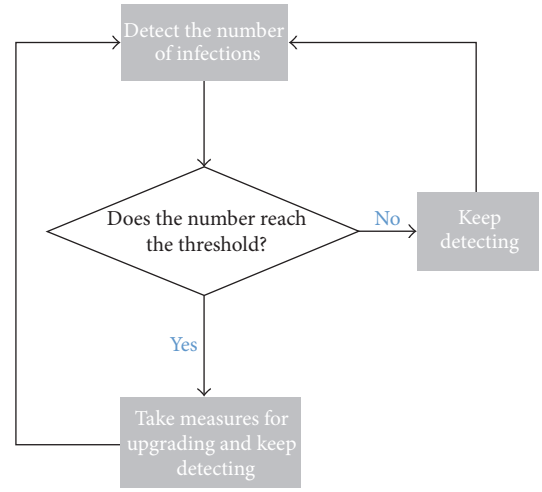

Figure 1: Flow diagram of upgrading.

Low Security Level: Divisions D and C. In this level, it is reserved for those systems that have been evaluated but that fail to meet the requirements for a higher evaluation class. Classes in this level provide for discretionary (need-to-know) protection and it can only provide a review of protection.

High Security Level: Divisions B and A. The security-relevant sections of a system are mentioned throughout this document as the Trusted Computing Base (TCB) [21]. Computers in this level must carry the sensitivity labels with most data structures in the system and the system developer should provide the security policy model based on TCB. By using formal security verification methods, this level requires that each operation in the system must have a formal documentation and can only be made by the administrator.

Obviously, computers with low security level are more likely to be infected by virus. This is the first breakthrough point for modeling.

In the network with security classification, administrators usually do not take any measures to upgrade the computers with low security level if there are only few threats for the sake of cost. With the increase of the infected computers number in the network, the administrators will upgrade the security level of computers ultimately. Here we assume that there exists a threshold value. If the number of infected computers is above the threshold value, some countermeasures will be taken to level up the security of a fraction of computers with low security level. Further, assume that the probability of taking upgrading measures for one uninfected computer is proportional to the number of infected computers. The flow diagram in Figure 1 can briefly express these operations. How the threshold value and the fraction of upgraded computers affect the propagation of computer virus is the concern in this paper.

3. Model Formulation

According to the situation of computer virus infection and the level of computer security, all computers in the network are divided into three compartments.

(a) S_l-compartment: the set of uninfected or susceptible computers in low security level

(b) S_h-compartment: the set of uninfected or susceptible computers in high security level

(c) I-compartment: the set of infected computers

For the modeling purpose, a series of parameters are introduced and some assumptions are made.

(1) One can assume that the average probabilities per unit time of S_l and S_h computers connecting to the network are b_l and b_h, respectively.

(2) Every computer in the system is got out for some reasons with the average probability per unit time μ, where μ is positive constant.

(3) Due to possible contact with infected computers in the network, every S_l and S_h computer is infected with the average probabilities β_l and β_h per unit time, respectively, where β_l and β_h are positive constant and $\beta_l > \beta_h$.

(4) Assume that one I computer becomes an S_l computer (or an S_h computer) with the average probability per unit time γ_l (or γ_h), where γ_l, γ_h are positive constants.

(5) As mentioned in Section 2, the upgrading probability of an S_l computer is denoted by a piecewise function $f(I)$. The expression of $f(I)$ is as follows:

$$f(I) = \begin{cases} 0, & \text{if } 0 \leqslant I < I_{\max}, \\ \alpha I, & \text{if } I \geqslant I_{\max}. \end{cases} \tag{1}$$

$I_{\max}$ denotes the threshold value and α denotes the a fraction of upgrading computers.

Let $S_l(t)$, $S_h(t)$, and $I(t)$ denote, at time t, the average numbers of S_l-, S_h-, and I-compartment computers, respectively. Let $N(t)$ denote the total number of all computers in the system at time t. Unless otherwise stated in the following content, they will be abbreviated as N, S_l, S_h, and I, respectively. Then, $S_l + S_h + I = N$. The collection of the above parameters and assumptions can be schematically depicted in Figure 2, from which the dynamical model is formulated as the following differential system:

$$\begin{aligned} \dot{S}_l &= b_l + \gamma_l I - f(I) S_l - \beta_l S_l I - \mu S_l, \\ \dot{S}_h &= b_h + \gamma_h I + f(I) S_l - \beta_h S_h I - \mu S_h, \\ \dot{I} &= \beta_l S_l I + \beta_h S_h I - \gamma_l I - \gamma_h I - \mu I. \end{aligned} \tag{2}$$

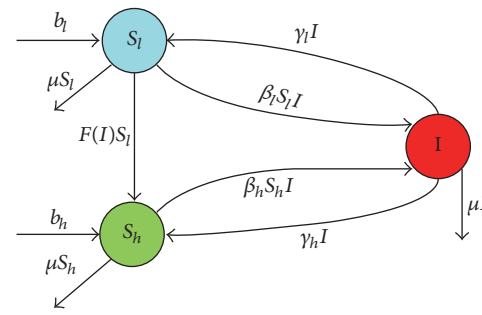

Figure 2: Transition diagram of the new model.

Considering that $S_l + S_h + I = N$, system (2) can be reduced to the following system:

$$\begin{aligned} \dot{N} &= b_l + b_h - \mu N, \\ \dot{S}_h &= b_h + \gamma_h I + f(I)(N - S_h - I) - \beta_h S_h I - \mu S_h, \\ \dot{I} &= \beta_l (N - S_h - I) I + \beta_h S_h I - \gamma_l I - \gamma_h I - \mu I. \end{aligned} \tag{3}$$

Solving the first equations of system (3), it is easy to obtain $\lim_{t\to\infty} N = N^* = (b_l + b_h)/\mu$. Therefore, system (3) can be reduced to the following limiting system [22, 23]:

$$\begin{aligned} \dot{S}_h &= b_h + \gamma_h I + f(I)(N^* - S_h - I) - \beta_h S_h I - \mu S_h, \\ \dot{I} &= \beta_l (N^* - S_h - I) I + \beta_h S_h I - \gamma_l I - \gamma_h I - \mu I. \end{aligned} \tag{4}$$

The feasible region for system (4) is

$$\Omega = \{(S_h, I) \mid S_h \geqslant 0,\ I \geqslant 0,\ 0 \leqslant S_h + I \leqslant N^*\}, \tag{5}$$

which is positively invariant.

4. Equilibria

In this section, all equilibria of system (4) are calculated. To obtain all potential equilibria, system (4) can be written as

$$\begin{aligned} b_h + \gamma_h I - \beta_h S_h I - \mu S_h &= 0, \\ \beta_l (N^* - S_h - I) I + \beta_h S_h I - \gamma_l I - \gamma_h I - \mu I &= 0, \\ &\text{if } 0 \leqslant I < I_{\max}, \end{aligned} \tag{6}$$

$$\begin{aligned} b_h + \gamma_h I + \alpha I (N^* - S_h - I) - \beta_h S_h I - \mu S_h &= 0, \\ \beta_l (N^* - S_h - I) I + \beta_h S_h I - \gamma_l I - \gamma_h I - \mu I &= 0, \\ &\text{if } I \geqslant I_{\max}. \end{aligned} \tag{7}$$

From (6) the fact that there always exists a virus-free equilibrium can be got:

$$E_0^* = \left(S_{h0}^* = \frac{b_h}{\mu},\ I_0^* = 0\right), \tag{8}$$

and the basic reproduction number is

$$R_0 = \frac{\beta_l b_l + \beta_h b_h}{\mu(\gamma_l + \gamma_h + \mu)}. \tag{9}$$

Let

$$\begin{aligned} C &= \mu(\gamma_l + \gamma_h + \mu) - \beta_l b_l - \beta_h b_h \\ &= \mu(\gamma_l + \gamma_h + \mu)(1 - R_0), \end{aligned} \tag{10}$$

$$A_1 = \beta_l \beta_h, \tag{11}$$

$$B_1 = \beta_l \beta_h N^* - \beta_l \gamma_h - \beta_l \mu - \beta_h \gamma_l - \beta_h \mu,$$

$$\Delta_1 = B_1^2 - 4A_1 C,$$

$$A_2 = \beta_l \beta_h + \alpha \beta_h, \tag{12}$$

$$\begin{aligned} B_2 = {} & (\beta_l \beta_h + \alpha \beta_h) N^* - \beta_l \gamma_h - \beta_l \mu - \beta_h \gamma_l - \beta_h \mu \\ & - \alpha(\gamma_l + \gamma_h + \mu), \end{aligned}$$

$$\Delta_2 = B_2^2 - 4A_2 C.$$

The quadratic equation of I can be got from system (6) and (7) as follows:

$$A_1 I^2 - B_1 I + C = 0 \quad \text{if } 0 \leqslant I < I_{\max}, \tag{13}$$

$$A_2 I^2 - B_2 I + C = 0, \quad \text{if } I \geqslant I_{\max}. \tag{14}$$

Considering that $I_1^* = (B_1 + \sqrt{\Delta_1})/2A_1$, $I_2^* = (B_1 - \sqrt{\Delta_1})/2A_1$ are the roots of (13) and $I_3^* = (B_2 + \sqrt{\Delta_2})/2A_2$, $I_4^* = (B_2 - \sqrt{\Delta_2})/2A_2$ are the roots of (14) ($I_1^* \neq I_3^*$), the solution of (6) and (7) can be got as follows:

$$\begin{aligned} I_1^* &= \frac{B_1 + \sqrt{\Delta_1}}{2A_1}, \\ S_{h1}^* &= \frac{b_h + \gamma_h I_1^*}{\mu + \beta_h I_1^*}, \\ I_2^* &= \frac{B_1 - \sqrt{\Delta_1}}{2A_1}, \\ S_{h2}^* &= \frac{b_h + \gamma_h I_2^*}{\mu + \beta_h I_2^*}, \\ I_3^* &= \frac{B_2 + \sqrt{\Delta_2}}{2A_2}, \\ S_{h3}^* &= \frac{b_h + \gamma_h I_3^* + \alpha I_3^* (N - I_3^*)}{\mu + \beta_h I_3^*}, \\ I_4^* &= \frac{B_2 - \sqrt{\Delta_2}}{2A_2}, \\ S_{h4}^* &= \frac{b_h + \gamma_h I_4^* + \alpha I_4^* (N - I_4^*)}{\mu + \beta_h I_4^*}. \end{aligned} \tag{15}$$

(13) and (14) can be deduced as follows:

$$\begin{aligned} & A_1 (I_1^{*2} - I_3^{*2}) - B_1 (I_1^* - I_3^*) - \alpha \beta_h I_3^{*2} \\ & \quad + (B_2 - B_1) I_3^* = 0, \\ & (I_1^* - I_3^*)[A_1 (I_1^* + I_3^*) - B_1] \\ & \quad = I_3^* [\alpha \beta_h I_3^* - (B_2 - B_1)], \\ & (I_1^* - I_3^*)[A_1 (I_1^* + I_3^*) - B_1] \\ & \quad = I_3^* [\alpha \beta_h I_3^* - \alpha \beta_h N^* + \alpha(\gamma_l + \gamma_h + \mu)], \\ & (I_1^* - I_3^*)[A_1 (I_1^* + I_3^*) - B_1] \\ & \quad = \alpha I_3^* [\beta_h I_3^* - \beta_h N^* + \beta_l (N^* - I_3^* - S_{h3}^*)], \\ & (I_1^* - I_3^*)[A_1 (I_1^* + I_3^*) - B_1] \\ & \quad = \alpha I_3^* (\beta_l - \beta_h)(N^* - I_3^* - S_{h3}^*), \end{aligned} \tag{16}$$

because of $\beta_l > \beta_h$ and $I_3^* + S_{h3}^* \leqslant N^*$, $\alpha I_3^* (\beta_l - \beta_h)(N^* - I_3^* - S_{h3}^*) \geqslant 0$. Then

$$(I_1^* - I_3^*)[A_1 (I_1^* + I_3^*) - B_1] \geqslant 0. \tag{17}$$

Assuming $I_1^* < I_3^*$, then $A_1(I_1^* + I_3^*) - B_1 > 2A_1 I_1^* - B_1 = \sqrt{\Delta_1} > 0$ and $(I_1^* - I_3^*)[A_1(I_1^* + I_3^*) - B_1] < 0$, which contradicts with (17). So $I_1^* > I_3^*$. In the same way, one can get

$$I_2^* < I_4^* < I_3^* < I_1^*. \tag{18}$$

Theorem 1. *There are only two viral equilibria $E_1^* = (S_{h1}^*, I_1^*)$ (or $E_3^* = (S_{h3}^*, I_3^*)$) and $E_2^* = (S_{h2}^*, I_2^*)$ (or $E_4^* = (S_{h4}^*, I_4^*)$) in this model if*

(1) $R_0 < 1$;

(2) $B_1 > 0, \Delta_1 > 0$ (*or* $B_2 > 0,\ \Delta_2 > 0$);

(3) $I_1^* > I_{\max}$ (*or* $I_2^* > I_{\max}$).

Proof. System (13) has two real roots if $\Delta_1 > 0$. From (10) one can get that $C > 0$ if $R_0 < 1$; then $C/A_1 > 0$. So the fact that $I_1^* > 0,\ I_2^* > 0$ if $B_1 > 0$ can be got (in the same way, the fact that $I_1^* > 0,\ I_2^* > 0$ can be got if $B_2 > 0, \Delta_2 > 0$) and there are only two viral equilibria E_1^*, E_2^* (or E_3^*, E_4^*) if $I_1^* > I_{\max}$ (or $I_2^* > I_{\max}$) from (18). □

Theorem 2. *System (4) has only three viral equilibria $E_2^* = (S_{h2}^*, I_2^*)$, $E_3^* = (S_{h3}^*, I_3^*)$, and $E_4^* = (S_{h4}^*, I_4^*)$ if*

(1) $R_0 < 1$;

(2) $B_1 > 0,\ \Delta_1 > 0$;

(3) $B_2 > 0,\ \Delta_2 > 0$;

(4) $I_2^* < I_{\max} \leqslant I_4^*$.

Proof. Like the proof of Theorem 1, it does not need to be stated. □

Theorem 3. *System (4) has only one viral equilibrium* $E_1^* = (S_{h1}^*, I_1^*)$ *(or* $E_3^* = (S_{h3}^*, I_3^*)$*) if*

(1) $R_0 > 1$;

(2) $I_1^* < I_{\max}$ *(or* $I_3^* \geqslant I_{\max}$*).*

Proof. One can get $C < 0$ if $R_0 > 1$ and $\Delta_1 > 0$, $\Delta_2 > 0$, $C/A_1 < 0$, $C/A_2 < 0$. So $I_1^* > 0$, $I_2^* < 0$ and $I_3^* > 0$, $I_4^* < 0$. Then the fact that only E_1^* (or E_3^*) existed if $I_1^* < I_{\max}$ (or $I_3^* \geqslant I_{\max}$) from (18) can be got. □

5. The Local Stability Analysis

To examine the local stability of the equilibria of system (4), its Jacobian matrices should be got as follows:

$$J_1 = \begin{pmatrix} -\beta_h I - \mu & \gamma_h - \beta_h S_h \\ -\beta_l I + \beta_h I & \beta_l N^* - \beta_l S_h - 2\beta_l I + \beta_h S_h - \gamma_l - \gamma_h - \mu \end{pmatrix}, \quad \text{if } 0 \leqslant I < I_{\max},$$

$$J_2 = \begin{pmatrix} -\beta_h I - \mu - \alpha I & \gamma_h - \beta_h S_h + \alpha (N^* - S_h - 2I) \\ -\beta_l I + \beta_h I & \beta_l N^* - \beta_l S_h - 2\beta_l I + \beta_h S_h - \gamma_l - \gamma_h - \mu \end{pmatrix}, \quad \text{if } I \geqslant I_{\max}. \tag{19}$$

Theorem 4. E_0^* *is locally asymptotically stable if* $R_0 < 1$.

Proof. The associated characteristic equation of E_0^* can be got from J_1 as follows:

$$(\lambda + \mu)\left(\lambda + \gamma_l + \gamma_h + \mu - \beta_l \frac{b_l}{\mu} - \beta_h \frac{b_h}{\mu}\right). \tag{20}$$

Then

$$\begin{aligned} \lambda_1 &= -\mu < 0, \\ \lambda_2 &= -\gamma_l - \gamma_h - \mu + \beta_l \frac{b_l}{\mu} + \beta_h \frac{b_h}{\mu} \\ &= (\gamma_l + \gamma_h + \mu)(R_0 - 1). \end{aligned} \tag{21}$$

Based on the Lyapunov theorem [24], only if $R_0 < 1$ are all eigenvalues of (17) negative. At this situation, E_0^* is locally asymptotically stable. □

Theorem 5. E_1^* *(or* E_3^**) is locally asymptotically stable if system (4) follows Theorem 1 or 2 or 3.*

Proof. The associated characteristic equations of E_1^* can be got from J_1 as follows:

$$\lambda^2 + k_1 \lambda + k_2 = 0, \tag{22}$$

where

$$\begin{aligned} k_1 &= \beta_l I_1^* + \beta_h I_1^* + \mu > 0, \\ k_2 &= I_1^* [\beta_l (\beta_h I_1^* + \mu) - (\beta_l - \beta_h)(\beta_h S_{h1}^* - \gamma_h)] \\ &= I_1^* \left[2\beta_l \beta_h I_1^* + \beta_l \mu - \beta_l \beta_h S_{h1}^* + \beta_l \gamma_h + \beta_2^2 S_{h1}^* \right. \\ &\quad \left. - \beta_h \gamma_h - \beta_l \beta_h I_1^* + \beta_l \beta_h N^* - \beta_l \beta_h N^* \right] \\ &= I_1^* [2\beta_l \beta_h I_1^* + \beta_l \mu + \beta_l \gamma_h - \beta_h \gamma_h \\ &\quad + \beta_h (\beta_l N^* - \beta_l S_{h1}^* - \beta_l I_1^* + \beta_h S_{h1}^*) - \beta_l \beta_h N^*] \\ &= I_1^* [2\beta_l \beta_h I_1^* + \beta_l \mu + \beta_l \gamma_h - \beta_h \gamma_h \\ &\quad + \beta_h (\gamma_l + \gamma_h + \mu) - \beta_l \beta_h N^*] = I_1^* [2\beta_l \beta_h I_1^* + \beta_l \mu \\ &\quad + \beta_l \gamma_h + \beta_h \gamma_l + \beta_h \mu - \beta_l \beta_h N^*] \\ &= I_1^* \left(2A_1 \frac{B_1 + \sqrt{\Delta_1}}{2A_1} - B_1\right) = I_1^* \sqrt{\Delta_1} > 0. \end{aligned} \tag{23}$$

The associated characteristic equations of E_3^* can be got from J_2 as follows:

$$\lambda^2 + k_3 \lambda + k_4 = 0, \tag{24}$$

where

$$\begin{aligned} k_3 &= \alpha I_3^* + \beta_l I_3^* + \beta_h I_3^* + \mu > 0, \\ k_4 &= I_3^* [\beta_l (\alpha I_3^* + \beta_h I_3^* + \mu) \\ &\quad - (\beta_l - \beta_h)(\alpha S_{h3}^* + 2\alpha I_3^* - \alpha N^* + \beta_h S_{h3}^* - \gamma_h)] \\ &= I_3^* [2(\beta_l \beta_h + \beta_h \alpha) I_3^* \\ &\quad + \alpha (\beta_l N^* - \beta_l I_3^* - \beta_l S_{h3}^* + \beta_h S_{h3}^*) \\ &\quad + \beta_h (\beta_l N^* - \beta_l I_3^* - \beta_l S_{h3}^* + \beta_h S_{h3}^*) + \beta_l \mu + \beta_l \gamma_h \\ &\quad - \beta_h \gamma_h - N^* (\beta_l \beta_h + \beta_h \alpha)] = I_3^* [2A_2 I_3^* \\ &\quad + \alpha (\gamma_l + \gamma_h + \mu) + \beta_h (\gamma_l + \gamma_h + \mu) + \beta_l \mu + \beta_l \gamma_h \\ &\quad - \beta_h \gamma_h - N^* (\beta_l \beta_h + \beta_h \alpha)] = I_3^* [2A_2 I_3^* - B_2] \\ &= I_3^* \left[2A_2 \frac{B_2 + \sqrt{\Delta_2}}{2A_2} - B_2\right] = I_3^* \sqrt{\Delta_2} > 0. \end{aligned} \tag{25}$$

$k_1 > 0$, $k_2 > 0$ (or $k_3 > 0$, $k_4 > 0$); the Hurwitz criterion follows [24], so E_1^* (or E_3^*) is locally asymptotically stable. □

6. The Global Stability Analysis

This section will discuss the global stability of the equilibrium of system (4). To get global stability, let us investigate the following lemmas.

Lemma 6. *For system (4), there is no periodic solution in the interior of* Ω.

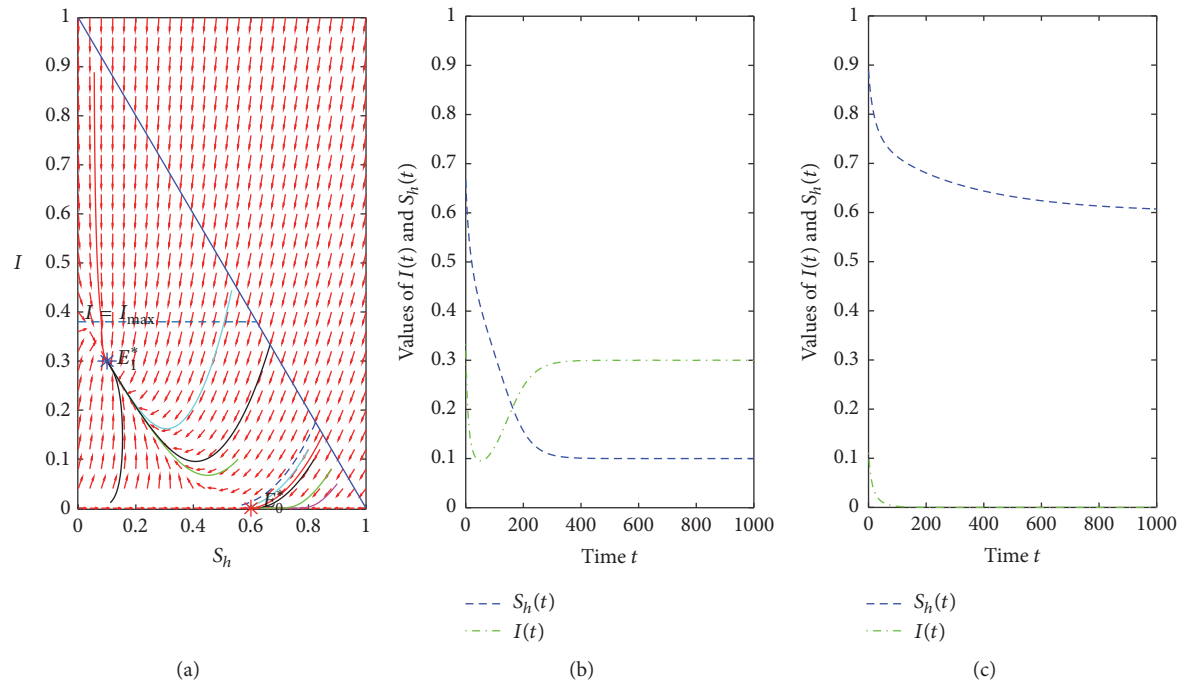

Figure 3: Trajectory figure and time plots of Example 1.

Proof. Let

$$\begin{aligned} G(S_h, I) &= b_h + \gamma_h I + f(I)(N^* - S_h - I) - \beta_h S_h I \\ &\quad - \mu S_h, \\ H(S_h, I) &= \beta_l (N^* - S_h - I) I + \beta_h S_h I - \gamma_l I - \gamma_h I \\ &\quad - \mu I, \\ B(S_h, I) &= \frac{1}{I}, \end{aligned} \tag{26}$$

and then

$$\begin{aligned} &\frac{\partial (GB)}{\partial S_h} + \frac{\partial (HB)}{\partial I} = -\beta_h - \frac{\mu}{I} - \beta_l < 0, \\ &\qquad\qquad \text{if } 0 \leqslant I < I_{\max}, \\ &\frac{\partial (GB)}{\partial S_h} + \frac{\partial (HB)}{\partial I} = -\beta_h - \frac{\mu}{I} - \beta_l - \alpha < 0, \\ &\qquad\qquad \text{if } I \geqslant I_{\max}. \end{aligned} \tag{27}$$

Thus, the claimed result follows from the Bendixson-Dulac criterion [24]. □

Lemma 7. *For system (4), there is no periodic solution that passes through a point on $\partial\Omega$, the boundary of Ω.*

Proof. Consider an arbitrary point $(\bar{S}_h, \bar{I})$, on the boundary of Ω. From (5), $\partial\Omega$ consists of the following three possibilities:

(a) $\bar{S}_h = 0$. Then $\dot{S}_h|_{(\bar{S}_h, \bar{I})} = b_h + \gamma_h \bar{I} > 0$, if $0 \leqslant I < I_{\max}$, and $\dot{S}_h|_{(\bar{S}_h, \bar{I})} = b_h + \gamma_h \bar{I} + \alpha \bar{I}(N^* - \bar{I}) > 0$, if $I_{\max} \leqslant I \leqslant N^*$.

(b) $\bar{I} = 0, 0 \leqslant \bar{S}_h \leqslant N^*$. Then $\dot{I}|_{(\bar{S}_h, \bar{I})} = 0$.

(c) $\bar{S}_h + \bar{I} = N^*$. Then $(d(\bar{S}_h + \bar{I})/dt)|_{(\bar{S}_h, \bar{I})} = -b_l - \gamma_l \bar{I} < 0$.

In view of the orbit smoothness, combining the above discussions can get the claimed result. □

In view of Lemmas 6 and 7 and Theorems 3–5, the main result of this section can be got as follows.

Table 1: Related instructions.

N	Not existing
E	Only existing
EL	Existing and locally asymptotically stable
EG	Existing and globally asymptotically stable

7. Numerical Examples and Discussions

In this section, some numerical examples are used to verify the results obtained in the previous section.

Example 1. Suppose $\beta_l = 0.24$, $\beta_h = 0.08$, $\gamma_l = 0.146$, $\gamma_h = 0.003$, $b_l = 0.0012$, $b_h = 0.0018$, $\mu = 0.003$, $\alpha = 0.005$, and $I_{\max} = 0.38$. In this situation, $R_0 < 1$, $I_1^* < I_{\max}$. Some trajectories of initial points are displayed in Figure 3(a) and the time plots about two of them are shown in Figures 3(b) and 3(c). In Figure 3(a), the blue dashed line divides Ω into Ω_1 (above the blue dashed line) and Ω_2 (under the blue dashed line). The initial points in Ω_1 are finally stable at E_1^* and in Ω_2 are finally stable at E_0^*, which complies with the third rows of Table 2. And the abbreviation notations of Table 2 are shown in Table 1.

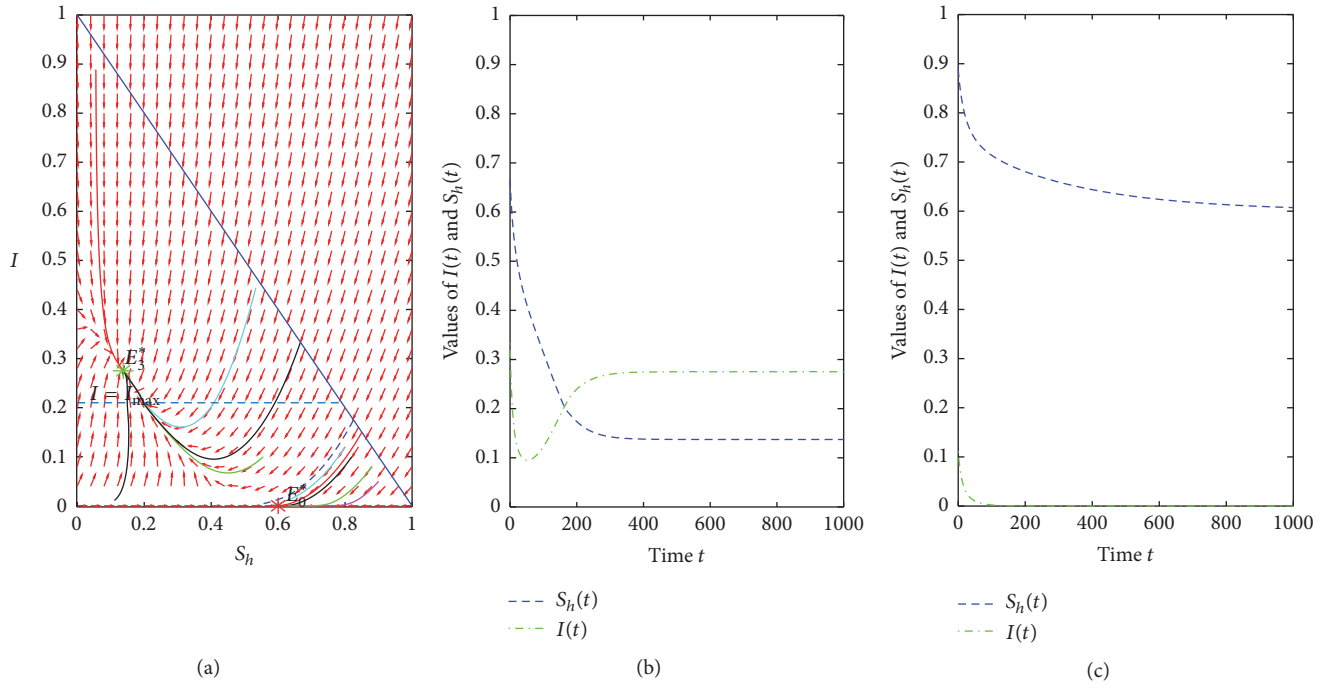

Figure 4: Trajectory figure and time plots of Example 2.

Table 2: Main result of Section 6.

Conditions			E_0^*	E_1^*	E_2^*	E_3^*	E_4^*
$R_0 < 1$			EG	N	N	N	N
$R_0 < 1$	$B_1 > 1,\ B_2 > 1,\ \Delta_1 > 0,\ \Delta_2 > 0$	$I_1^* < I_{\max}$	EL	EL	E	N	N
		$I_3^* \geqslant I_{\max} > I_2^*$	EL	N	E	EL	E
		$I_2^* > I_{\max}$	EL	N	N	EL	E
$R_0 > 1$		$I_1^* < I_{\max}$	E	EG	E	N	N
		$I_3^* \geqslant I_{\max}$	E	N	N	EG	E

Example 2. Suppose $\beta_l = 0.24$, $\beta_h = 0.08$, $\gamma_l = 0.146$, $\gamma_h = 0.003$, $b_l = 0.0012$, $b_h = 0.0018$, $\mu = 0.003$, $\alpha = 0.005$, and $I_{\max} = 0.21$. In this situation, $R_0 < 1$, $I_3^* > I_{\max}$. Some trajectories of initial points are displayed in Figure 4(a) and the time plots about two of them are shown in Figures 4(b) and 4(c). In Figure 4(a), the blue dashed line divides Ω into Ω_1 (above the blue dashed line) and Ω_2 (under the blue dashed line). The initial points in Ω_1 are finally stable at E_3^* and in Ω_2 are finally stable at E_0^*, which complies with lines 4-5 of Table 2.

Example 3. Suppose $\beta_l = 0.24$, $\beta_h = 0.08$, $\gamma_l = 0.146$, $\gamma_h = 0.043$, $b_l = 0.0012$, $b_h = 0.0018$, $\mu = 0.003$, $\alpha = 0.005$, and $I_{\max} = 0.21$. In this situation, $R_0 < 1$ and there is only E_0^* in the system. Some trajectories of initial points are displayed in Figure 5(a) and the time plots about two of them are shown in Figures 5(b) and 5(c). The initial points in are finally stable at E_0^*, which complies with line 2 of Table 2.

Example 4. Suppose $\beta_l = 0.3$, $\beta_h = 0.09$, $\gamma_l = 0.056$, $\gamma_h = 0.043$, $b_l = 0.0012$, $b_h = 0.0018$, $\mu = 0.003$, $\alpha = 0.06$, and $I_{\max} = 0.38$. In this situation, $R_0 > 1$, $I_1^* < I_{\max}$. Some trajectories of initial points are displayed in Figure 6(a) and the time plots about two of them are shown in Figures 6(b) and 6(c). The initial points in are finally stable at E_1^*, which complies with line 6 of Table 2.

Example 5. Suppose $\beta_l = 0.3$, $\beta_h = 0.09$, $\gamma_l = 0.056$, $\gamma_h = 0.043$, $b_l = 0.0012$, $b_h = 0.0018$, $\mu = 0.003$, $\alpha = 0.06$, and $I_{\max} = 0.2$. In this situation, $R_0 > 1$, $I_3^* > I_{\max}$. Some trajectories of initial points are displayed in Figure 7(a) and the time plots about two of them are shown in Figures 7(b) and 7(c). The initial points in are finally stable at E_3^*, which complies with the last row of Table 2.

By introducing random factors and model adaptive behavior, a series of simulations run are used to approximate closer to actual worm propagation due to the unavailability of real-world data. Hosts (used IP addresses) here appear as abstractions in the simulations. Instead of modeling various operating systems and services, each host is simply considered to be one of the following: susceptible nodes with

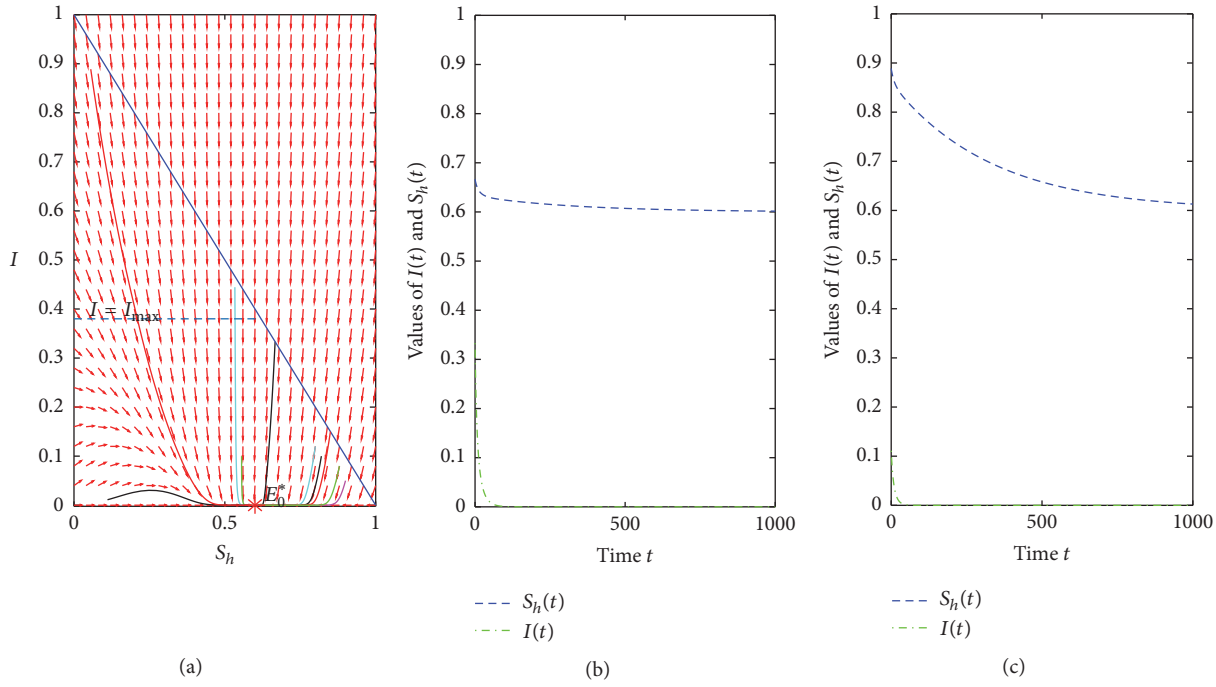

Figure 5: Trajectory figure and time plots of Example 3.

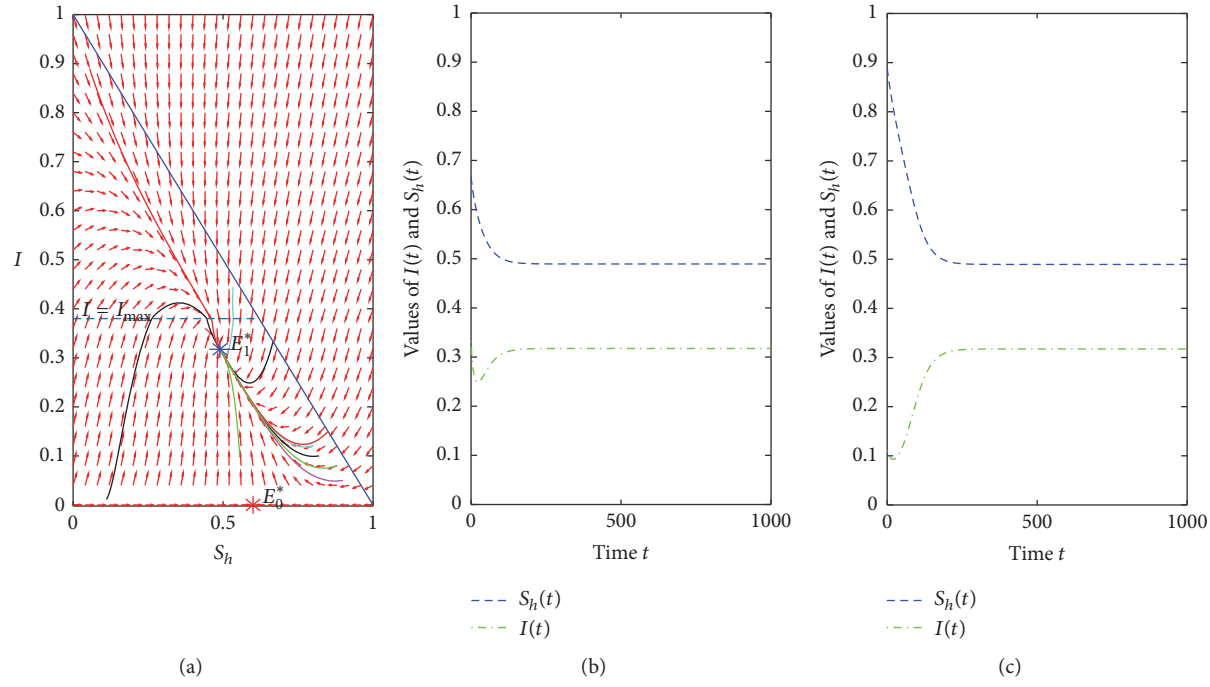

Figure 6: Trajectory figure and time plots of Example 4.

high security level, susceptible nodes with low security level, and infected nodes. Here a complete network with initial 10000 nodes is applied for numerical evaluation. And we focus on how the mechanisms of security classification and intervention affect the propagation of network viruses. So we simulate three scenarios for the spread of viruses: (1) non-SC non-INTVIN scenario, (2) with SC non-INTVIN scenario, and (3) with SC and INTVIN scenario (see Figure 8), where SC and INTVIN are short for security classification and intervention, respectively. And the parameters I_{max} and α determine when to intervene and the strength of interventions, respectively. For evaluation purpose, the values of the

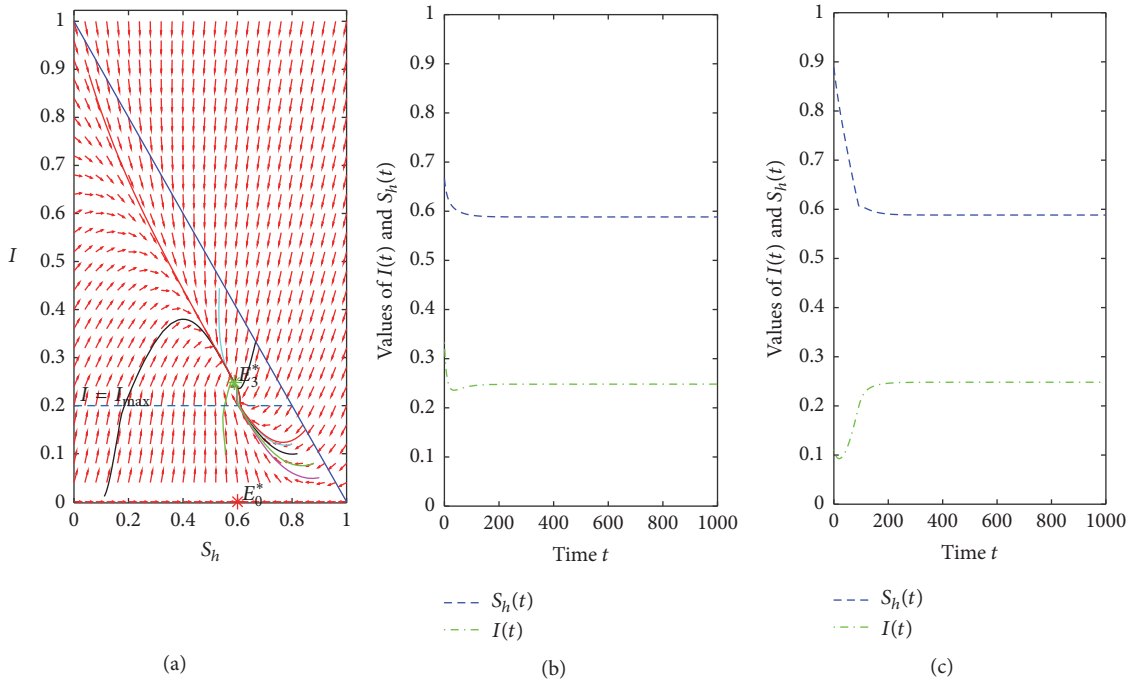

Figure 7: Trajectory figure and time plots of Example 5.

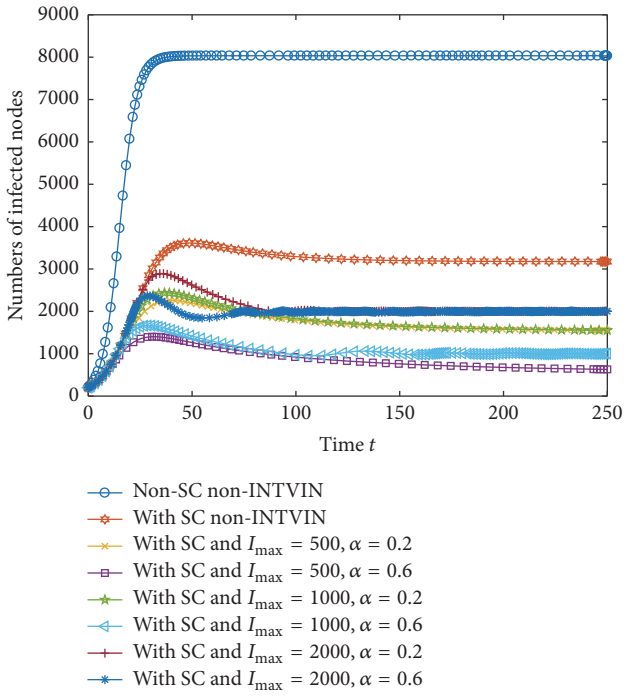

Figure 8: Time evolution of the infected nodes in different scenarios.

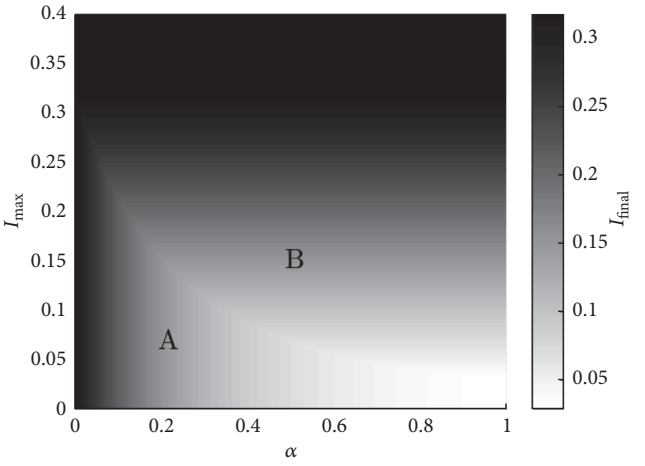

Figure 9: Influence of I_{max} and α on I_{final}. I_{max} and I_{final} are the proportions of infected nodes in all nodes. Moreover, I_{final} is the average of 100 values for $t > 10000$. Here all other parameters are the same as Figure 8.

model parameters are set as follows: $\beta_l = 0.3$, $\beta_h = 0.09$, $\gamma_l = 0.056$, $\gamma_h = 0.043$, $b_l = 0.0012$, $b_h = 0.0018$, $\mu = 0.003$, and other parameters are shown in Figure 8. In general, simulation results show that the intervention mechanism proposed in this paper can be applied to curbing the spread of virus effectively. Moreover, a large number of simulations are conducted to study how the combination of I_{max} and α affects the propagation scale (see Figure 9). Obviously, the earlier (the lower I_{max}) and stronger (the higher α) the intervention is introduced, the fewer the nodes finally get infected. We divide the parameter subspace $\{(\alpha, I_{max}): \alpha > 0, I_{max} > 0\}$ into two parts, numbered as A and B (as shown in Figure 9). Simulation results lead the following conclusion.

(1) If $(\alpha, I_{\max}) \in A$, the value of I_{final} (defined in Figure 9) only depends on the value of α. So in Figure 8 the number of infected nodes in scenarios with $I_{\max} = 500$ is the same as the one with $I_{\max} = 1000$, where $\alpha = 0.2$, and it is higher than the one with $I_{\max} = 500$ and $\alpha = 0.6$. More precisely, the value of I_{final} decreases as α increasing.

(2) If $(\alpha, I_{\max}) \in B$, the value of I_{final} only depends on the value of $I_{\max}$ (4). So in Figure 8 the number of infected nodes in scenarios with $\alpha = 0.2$ is the same as the one with $\alpha = 0.6$, where $I_{\max} = 2000$, and it is higher than the one with $I_{\max} = 1000$ and $\alpha = 0.6$. Note that I_{final} does not always decrease with the increase of $I_{\max}$, because the intervention is never involved for large $I_{\max}$ (see the dark black part for $I_{\max} > 0.3$ in Figure 9).

Remark 6. The simulations here do not take into account latency issues, hop-count, bandwidth limitations, and transfer times or connectivity issues. Since the scale of simulated network is quite small compared with the real Internet, all parameters are assumed on that scale. But the scale factor can also make the real-world more complex.

Table 2 suggests that, to eradicate viruses from the Internet, one should take necessary actions to control the system parameters so that R_0^* is well below 1 and not let system meet the lines 3–5 of Table 2. After simple calculations, the following can be got:

$$\begin{aligned}
\frac{\partial R_0}{\partial \beta_l} &= \frac{b_l}{\mu(\gamma_l + \gamma_h + \mu)} > 0,\\
\frac{\partial R_0}{\partial \beta_h} &= \frac{b_h}{\mu(\gamma_l + \gamma_h + \mu)} > 0,\\
\frac{\partial R_0}{\partial b_1} &= \frac{\beta_1}{\mu(\gamma_l + \gamma_h + \mu)} > 0,\\
\frac{\partial R_0}{\partial b_h} &= \frac{\beta_h}{\mu(\gamma_l + \gamma_h + \mu)} > 0,\\
\frac{\partial R_0}{\partial \mu} &= -\frac{\gamma_l + \gamma_h + 2\mu}{\mu^2(\gamma_l + \gamma_h + \mu)^2} < 0,\\
\frac{\partial R_0}{\partial \gamma_l} &= -\frac{1}{\mu(\gamma_l + \gamma_h + \mu)^2} < 0,\\
\frac{\partial R_0}{\partial \gamma_h} &= -\frac{1}{\mu(\gamma_l + \gamma_h + \mu)^2} < 0.
\end{aligned} \tag{28}$$

Thus, R_0 is increasing with $\beta_l, \beta_h, b_l, b_h$ and is decreasing with μ, γ_l, γ_h.

Based on the above discussions, an incomplete list of effective measures for users to contain the virus prevalence is presented below:

(1) Timely acquire the updated versions of the antivirus software, so that the two infecting probabilities, β_l and β_h, are both reduced and the curing probabilities, γ_l and γ_h, are enhanced.

(2) Do not connect computers to the Internet when unnecessary, so that the recruitment rate, μ, is lowered.

(3) For both cost and security, let the threshold value of computer virus lead administrator to take measures to upgrade the security level approaching the value of stable infections in the stage of taking measures.

8. Conclusions

In this paper, we presented a novel intervention mechanism to restrain the virus spreading under the framework of security classification. The model reflects a realistic scenario how the intervention is applied when the number of infected nodes reaches the intervention threshold. Theoretical analysis and numerical evaluation are used to study how $I_{\max}$, α affect the propagation behaviors. The main results are listed as follows: (1) The dynamic behaviors of computer virus under security classification are different with common circumstance. Obviously, much higher security computers will lead to fewer infections. (2) The earlier and the stronger the intervention is introduced, the fewer the nodes finally get infected. (3) According to the brief parameter analysis, some other effective measures in reality are presented. Viewed from a real-world perspective, in order to make better use of this intervention mechanism, one of the most important things is how to detect the exact number of infected nodes. Although an in-depth discussion of this is outside this paper's scope, we are forced to point out that the measured value is below the actual one. In this case, the actual value of intervention threshold must be set below the theoretical one.

Our future work will be focused on studying such intervention mechanism in heterogeneous networks, such as small-world network and scale-free network.

Conflicts of Interest

The authors declare that there are no conflicts of interest regarding the publication of this paper.

Acknowledgments

This work is supported by Chongqing Engineering Research Center of Mobile Internet Data Application, Scientific and Technological Research Program of Chongqing Municipal Education Commission (Grant nos. KJ1500415, KJ1400414, KJ1500434, and KJ1704080), Doctoral Scientific Research Foundation of Chongqing University of Posts and Telecommunications (Grant no. A2015-02), and the National Natural Science Foundation of China (no. 61672004).

References

[1] J. O. Kephart and S. R. White, "Directed-graph epidemiological models of computer viruses," in *Proceedings of the IEEE Computer Society Symposium on Research in Security and Privacy*, pp. 343–359, Oakland, Calif, USA, May 1991.

[2] M. Kjaergaard, S. Brander, and F. M. Poulsen, "Small but slow world: how network topology and burstiness slow down spreading," *Physical Review E*, vol. 83, no. 83, pp. 602–608, 2010.

[3] C. Castellano and R. Pastor-Satorras, "Thresholds for epidemic spreading in networks," *Physical Review Letters*, vol. 105, no. 21, Article ID 218701, 2010.

[4] G. Zhu, X. Fu, and G. Chen, "Global attractivity of a network-based epidemic SIS model with nonlinear infectivity," *Communications in Nonlinear Science and Numerical Simulation*, vol. 17, no. 6, pp. 2588–2594, 2012.

[5] L.-X. Yang, X. Yang, J. Liu, Q. Zhu, and C. Gan, "Epidemics of computer viruses: a complex-network approach," *Applied Mathematics and Computation*, vol. 219, no. 16, pp. 8705–8717, 2013.

[6] L.-X. Yang and X. Yang, "The spread of computer viruses over a reduced scale-free network," *Physica A: Statistical Mechanics and Its Applications*, vol. 396, pp. 173–184, 2014.

[7] L.-X. Yang, M. Draief, and X. Yang, "The impact of the network topology on the viral prevalence: a node-based approach," *PLoS ONE*, vol. 10, no. 9, Article ID e0134507, 2015.

[8] B. K. Mishra, K. Haldar, and D. N. Sinha, "Impact of information based classification on network epidemics," *Scientific Reports*, vol. 6, Article ID 28289, 2016.

[9] Z. Fu, X. Sun, Q. Liu, L. Zhou, and J. Shu, "Achieving efficient cloud search services: multi-keyword ranked search over encrypted cloud data supporting parallel computing," *IEICE Transactions on Communications*, vol. E98B, no. 1, pp. 190–200, 2015.

[10] Q. Liu, W. Cai, J. Shen, Z. Fu, X. Liu, and N. Linge, "A speculative approach to spatial-temporal efficiency with multi-objective optimization in a heterogeneous cloud environment," *Security and Communication Networks*, vol. 9, no. 17, pp. 4002–4012, 2016.

[11] G. Juve and E. Deelman, "Wrangler: Virtual cluster provisioning for the cloud," in *Proceedings of 20th ACM International Symposium on High-Performance Parallel and Distributed Computing, HPDC'11*, pp. 277-278, San Jose, Calif, USA, June 2011.

[12] L. H. Zeng, B. F. Zhang, and L. H. Zhang, "Virtual cluster constructing based on cloud computing platform," *Microelectronics Computer*, vol. 27, no. 8, pp. 31–39, 2010.

[13] C. Gan, X. Yang, and Q. Zhu, "Propagation of computer virus under the influences of infected external computers and removable storage media: modeling and analysis," *Nonlinear Dynamics*, vol. 78, no. 2, pp. 1349–1356, 2014.

[14] C. Gan and X. Yang, "Theoretical and experimental analysis of the impacts of removable storage media and antivirus software on viral spread," *Communications in Nonlinear Science and Numerical Simulation*, vol. 22, no. 1–3, pp. 611–622, 2014.

[15] C. Gan, X. Yang, W. Liu, and Q. Zhu, "A propagation model of computer virus with nonlinear vaccination probability," *Communications in Nonlinear Science and Numerical Simulation*, vol. 19, no. 1, pp. 92–100, 2014.

[16] C. Gan, "Modeling and analysis of the effect of network eigenvalue on viral spread," *Nonlinear Dynamics*, vol. 84, no. 3, pp. 1727–1733, 2016.

[17] J. Amador and J. R. Artalejo, "Stochastic modeling of computer virus spreading with warning signals," *Journal of the Franklin Institute. Engineering and Applied Mathematics*, vol. 350, no. 5, pp. 1112–1138, 2013.

[18] W. Liu and S. Zhong, "Web malware spread modelling and optimal control strategies," *Scientific Reports*, vol. 7, Article ID 42308, 2017.

[19] H. Yuan, G. Liu, and G. Chen, "On modeling the crowding and psychological effects in network-virus prevalence with nonlinear epidemic model," *Applied Mathematics and Computation*, vol. 219, no. 5, pp. 2387–2397, 2012.

[20] L. Qiu, Y. Zhang, F. Wang, H. R. Mahajan, and M. Kyung, "Trusted computer system evaluation criteria," Classified Information, 2007.

[21] J. Noorman, P. Agten, W. Daniels et al., "Sancus: low-cost trustworthy extensible networked devices with a zero-software trusted computing base," in *Proceedings of the Usenix Conference on Security*, pp. 479–494, 2013.

[22] L.-X. Yang and X. Yang, "The effect of infected external computers on the spread of viruses: a compartment modeling study," *Physica A. Statistical Mechanics and Its Applications*, vol. 392, no. 24, pp. 6523–6535, 2013.

[23] H. R. Thieme, "Asymptotically autonomous differential equations in the plane," *The Rocky Mountain Journal of Mathematics*, vol. 24, no. 1, pp. 351–380, 1994.

[24] R. C. Robinson, *An Introduction to Dynamical System: Continuous and Discrete*, Prentice Hall, New Jersey, NJ, USA, 2004.

Hindawi
Discrete Dynamics in Nature and Society
Volume 2017, Article ID 2340549, 9 pages
https://doi.org/10.1155/2017/2340549

Research Article

Bifurcation of a Delayed SEIS Epidemic Model with a Changing Delitescence and Nonlinear Incidence Rate

Juan Liu

Department of Mathematics and Physics, Bengbu University, Bengbu 233030, China

Correspondence should be addressed to Juan Liu; liujuan7216@163.com

Received 16 February 2017; Accepted 28 March 2017; Published 9 May 2017

Academic Editor: Lu-Xing Yang

Copyright © 2017 Juan Liu. This is an open access article distributed under the Creative Commons Attribution License, which permits unrestricted use, distribution, and reproduction in any medium, provided the original work is properly cited.

This paper is concerned with a delayed SEIS (Susceptible-Exposed-Infectious-Susceptible) epidemic model with a changing delitescence and nonlinear incidence rate. First of all, local stability of the endemic equilibrium and the existence of a Hopf bifurcation are studied by choosing the time delay as the bifurcation parameter. Directly afterwards, properties of the Hopf bifurcation are determined based on the normal form theory and the center manifold theorem. At last, numerical simulations are carried out to illustrate the obtained theoretical results.

1. Introduction

The outbreak of infectious diseases had not only caused the loss of billions of lives but also badly damaged the social economy in a short time, which brought much pain to human society [1]. Thus, it has been an increasingly urgent issue to understand how to prevent or slow down the transmission of infectious diseases. To this end, many mathematical models have been proposed for describing the spread process of infectious diseases [2–10]. However, all the epidemic models above do not consider the change of delitescence of the infectious diseases. Considering that the diversity of the delitescence period in each infected individual who is infected with disease virus is mainly due to the variation of the virus and the distinct constitution of different people for some disease, such as H1N1 disease, Wang proposed the following SEIS epidemic model with a changing delitescence and a nonlinear incidence rate [11]:

$$\begin{aligned}
\frac{dS(t)}{dt} &= A - dS(t) - \frac{\beta S(t) I(t)}{1+\alpha I(t)} + \gamma I(t),\\
\frac{dE(t)}{dt} &= \mu \frac{\beta S(t) I(t)}{1+\alpha I(t)} - (d+\varepsilon) E(t),\\
\frac{dI(t)}{dt} &= (1-\mu) \frac{\beta S(t) I(t)}{1+\alpha I(t)} + \varepsilon E(t)\\
&\quad - (d+\gamma+\delta) I(t),
\end{aligned} \tag{1}$$

where $S(t)$, $E(t)$, and $I(t)$ denote the numbers of the susceptible, exposed, and infectious populations at time t, respectively. A is the recruitment rate of the susceptible population; d is the natural death rate of the population; δ is the death rate due to the disease of the infected population; ε is the rate at which the exposed population becomes infectious; γ is the rate at which the infected population returns to the susceptible population because of the treatment; μ is the rate at which the infected population becomes the exposed one; and $1-\mu$ is the rate at which the infected population becomes infectious directly. $\beta SI/(1+\alpha I)$ is the nonlinear incidence rate, where β measures the infection force of the disease and α measures the inhibition effect from the behavioral change of the susceptible population. Wang investigated global stability of system (1).

In fact, many infectious diseases have different kinds of delays during their spreading process in the population, such as latent period delay [9, 12–16], immunity period delay [17, 18], and infection period delay [19]. The time delay may induce Hopf bifurcation and periodic solutions. The

occurrence of a Hopf bifurcation means that the state of the epidemic disease prevalence changes from an equilibrium to a limit cycle. Therefore, the time delay can influence the dynamics of infectious diseases. So it is necessary and useful to investigate system (1) with time delay. Based on this fact and taking the period used to cure the infectious population, we consider the following delayed epidemic system:

$$\begin{aligned}
\frac{dS(t)}{dt} &= A - dS(t) - \frac{\beta S(t) I(t)}{1+\alpha I(t)} + \gamma I(t-\tau),\\
\frac{dE(t)}{dt} &= \mu\frac{\beta S(t) I(t)}{1+\alpha I(t)} - (d+\varepsilon) E(t),\\
\frac{dI(t)}{dt} &= (1-\mu)\frac{\beta S(t) I(t)}{1+\alpha I(t)} + \varepsilon E(t) - (d+\delta) I(t)\\
&\quad - \gamma I(t-\tau),
\end{aligned} \tag{2}$$

where τ is the time delay due to the period that is used to cure the infectious population. That is, we assume that all the infectious populations will survive after time τ. The initial conditions for system (2) are

$$\begin{aligned}
(\phi_1(\theta), \phi_2(\theta), \phi_3(\theta)) \in C = C\left([-\tau, 0], R_+^3\right),\\
\phi_1(\theta) > 0,\ \phi_2(\theta) > 0,\ \phi_3(\theta) > 0,
\end{aligned} \tag{3}$$

where $R_+^3 = (S, E, I) \in R_+^3$.

The outline of this paper is as follows. In the next section, stability of the endemic equilibrium is analyzed and the critical value of the time delay at which a Hopf bifurcation occurs is obtained. In Section 3, direction and stability of the Hopf bifurcation are investigated. In Section 4, the obtained theoretical results are verified by some numerical simulations. Finally, this work is summarized in Section 5.

2. Stability of the Endemic Equilibrium and Existence of Hopf Bifurcation

By a direct computation, we know that if (I) $b_2 = 0$ and $b_0/b_1 < 0$, (II) $b_1^2 - 4b_0b_2 > 0$ and $b_0/b_2 < 0$, (III) $b_1^2 - 4b_0b_2 > 0$, $b_0 = 0$ and $b_1/b_2 < 0$, or (IV) $b_1^2 - 4b_0b_2 = 0$ and $b_1/b_2 < 0$, then system (2) has a unique endemic equilibrium $P_*(S_*, E_*, I_*)$, where

$$\begin{aligned}
S_* &= \frac{(d+\varepsilon)(d+\gamma+\delta)(1+\alpha I_*)}{\beta(1-\mu)(d+\varepsilon) + \mu\beta\varepsilon},\\
E_* &= \frac{(\mu\beta S_* I_*)}{((d+\varepsilon)(1+\alpha I_*))},
\end{aligned} \tag{4}$$

and I_* is the unique positive root of the following equation:

$$b_2 I^2 + b_1 I + b_0 = 0, \tag{5}$$

where

$$\begin{aligned}
b_0 &= d(d+\varepsilon)(d+\gamma+\varepsilon) - A\beta((1-\mu)(d+\varepsilon) + \mu\varepsilon),\\
b_1 &= (d+\varepsilon)(2d\alpha+\beta)(d+\gamma+\varepsilon)\\
&\quad - \beta((1-\mu)(d+\varepsilon) + \mu\varepsilon)(A\alpha+\gamma),\\
b_2 &= \alpha(d+\varepsilon)(d\alpha+\beta)(d+\gamma+\varepsilon).
\end{aligned} \tag{6}$$

Let $u_1(t) = S(t) - S_*$, $u_2(t) = E(t) - E_*$, $u_3(t) = I(t) - I_*$. We can rewrite system (2) as the following form:

$$\begin{aligned}
\dot{u}_1(t) &= a_{11}u_1(t) + a_{13}u_3(t) + b_{13}u_3(t-\tau)\\
&\quad + \sum_{i+j\geq 2}\frac{1}{i!\,j!} f_{ij}^{(1)} u_1^i(t)\, u_3^j(t),\\
\dot{u}_2(t) &= a_{21}u_1(t) + a_{22}u_2(t) + a_{23}u_3(t)\\
&\quad + \sum_{i+j\geq 2}\frac{1}{i!\,j!} f_{ij}^{(2)} u_1^i(t)\, u_3^j(t),\\
\dot{u}_3(t) &= a_{31}u_1(\mathrm{t}) + a_{32}u_2(t) + a_{33}u_3(t) + b_{33}u_3(t-\tau)\\
&\quad + \sum_{i+j\geq 2}\frac{1}{i!\,j!} f_{ij}^{(3)} u_1^i(t)\, u_3^j(t),
\end{aligned} \tag{7}$$

where

$$\begin{aligned}
a_{11} &= -\left(d + \frac{\beta I_*}{1+\alpha I_*}\right),\\
a_{13} &= -\frac{\beta S_*}{1+\alpha I_*},\\
b_{13} &= \gamma,\\
a_{21} &= \frac{\mu\beta I_*}{1+\alpha I_*},\\
a_{22} &= -(d+\varepsilon),\\
a_{23} &= \frac{\mu\beta S_*}{1+\alpha I_*},\\
a_{31} &= \frac{(1-\mu)\beta I_*}{1+\alpha I_*},\\
a_{32} &= \varepsilon,\\
a_{33} &= \frac{(1-\mu)\beta I_*}{1+\alpha I_*} - (d+\delta),
\end{aligned}$$

$$
\begin{aligned}
b_{33} &= -\gamma,\\
f_{ij}^{(k)} &= \frac{\partial^{i+j} f^{(k)}\left(S_*, E_*, I_*\right)}{\partial u_1^i(t)\,\partial u_3^j(t)},\\
f^{(1)} &= A - d u_1(t) - \frac{\beta u_1(t) u_3(t)}{1+\alpha u_3(t)} + \gamma u_3(t-\tau),\\
f^{(2)} &= \mu\frac{\beta u_1(t) u_3(t)}{1+\alpha u_3(t)} - (d+\varepsilon) u_2(t),\\
f^{(3)} &= (1-\mu)\frac{\beta u_1(t) u_3(t)}{1+\alpha u_3(t)} + \varepsilon u_2(t) - (d+\delta) u_3(t)\\
&\quad - \gamma u_3(t-\tau).
\end{aligned}
\tag{8}
$$

Then we obtain the linearized system of system (2)

$$
\begin{aligned}
\dot{u}_1(t) &= a_{11}u_1(t) + a_{13}u_3(t) + b_{13}u_3(t-\tau),\\
\dot{u}_2(t) &= a_{21}u_1(t) + a_{22}u_2(t) + a_{23}u_3(t),\\
\dot{u}_3(t) &= a_{31}u_1(t) + a_{32}u_2(t) + a_{33}u_3(t)\\
&\quad + b_{33}u_3(t-\tau).
\end{aligned}
\tag{9}
$$

The characteristic equation is

$$
\begin{aligned}
&\lambda^3 + A_2\lambda^2 + A_1\lambda + A_0 + \left(B_2\lambda^2 + B_1\lambda + B_0\right)e^{-\lambda\tau}\\
&\quad = 0,
\end{aligned}
\tag{10}
$$

where

$$
\begin{aligned}
A_0 &= a_{13}\left(a_{22}a_{31} - a_{21}a_{32}\right) + a_{11}\left(a_{23}a_{32} - a_{22}a_{33}\right),\\
A_1 &= a_{11}a_{22} + a_{22}a_{33} + a_{11}a_{33}\\
A_2 &= -\left(a_{11} + a_{22} + a_{33}\right),\\
B_0 &= b_{13}\left(a_{22}a_{31} - a_{21}a_{32}\right) - a_{11}a_{22}b_{33},\\
B_1 &= b_{33}\left(a_{11} + a_{22}\right) - a_{13}b_{13},\\
B_2 &= -b_{33}.
\end{aligned}
\tag{11}
$$

When $\tau = 0$, (10) reduces to

$$
\lambda^3 + \left(A_2 + B_2\right)\lambda^2 + \left(A_1 + B_1\right)\lambda + A_0 + B_0 = 0. \tag{12}
$$

Routh-Hurwitz criterion implies that P_* is locally asymptotically stable without delay if condition (H_1) holds.

(H_1) $A_2 + B_2 > 0$, $(A_2 + B_2)(A_1 + B_1) > A_0 + B_0 > 0$.

For $\tau > 0$, substituting $\lambda = i\omega$ $(\omega > 0)$ into (10), we obtain

$$
\begin{aligned}
B_1\omega\sin\tau\omega + \left(B_0 - B_2\omega^2\right)\cos\tau\omega &= A_2\omega^2 - A_0,\\
B_1\omega\cos\tau\omega - \left(B_0 - B_2\omega^2\right)\sin\tau\omega &= \omega^3 - A_1\omega.
\end{aligned}
\tag{13}
$$

Then

$$
\omega^6 + a_2\omega^4 + a_1\omega^2 + a_0 = 0, \tag{14}
$$

where

$$
\begin{aligned}
a_0 &= A_0^2 - B_0^2,\\
a_1 &= A_1^2 - 2A_0A_2 - B_1^2 + 2B_0B_2,\\
A_2 &= A_2^2 - 2A_1 - B_2^2.
\end{aligned}
\tag{15}
$$

Let $\omega^2 = v$; then

$$
v^3 + a_2v^2 + a_1v + a_0 = 0, \tag{16}
$$

where $f(v) = v^3 + a_2v^2 + a_1v + a_0$. According to the analysis about the distribution of roots of (16) in Song et al. [20], we have the following result.

Lemma 1. *For the polynomial equation (16),*

(1) *if $a_0 < 0$, then (16) has at least one positive root;*

(2) *if $a_0 \geq 0$ and $\triangle = a_2^2 - 3a_1 \leq 0$, then (16) has no positive roots;*

(3) *if $a_0 \geq 0$ and $\triangle = a_2^2 - 3a_1 > 0$, then (16) has positive roots if and only if $v_1^* = (-a_2 + \sqrt{\triangle})/3 > 0$ and $f(v_1^*) \leq 0$.*

Next, we assume that the coefficients in (16) satisfy the following condition.

(H_2) (i) $a_0 < 0$ or (ii) $a_0 \geq 0$, $\triangle = a_2^2 - 3a_1 > 0$, $v_1^* = (-a_2 + \sqrt{\triangle})/3 > 0$, and $f(v_1^*) \leq 0$.

Thus, (14) has at least one positive root such that (10) has a pair of purely imaginary roots $\pm i\omega_0$. The corresponding critical value τ_0 can be obtained from (13)

$$
\begin{aligned}
\tau_0 &= \frac{1}{\omega_0}\\
&\quad\cdot \arccos\frac{\left(B_1 - A_2B_2\right)\omega_0^4 + \left(A_2B_0 + A_0B_2 - A_1B_1\right)\omega_0^2 - A_0B_0}{B_1^2\omega_0^2 + \left(B_0 - B_2\omega_0^2\right)^2}.
\end{aligned}
\tag{17}
$$

Taking derivative with respect to τ on both sides of (10), we obtain

$$
\begin{aligned}
\left[\frac{d\lambda}{d\tau}\right]^{-1} &= -\frac{3\lambda^2 + 2A_2\lambda + A_1}{\lambda\left(\lambda^3 + A_2\lambda^2 + A_1\lambda + A_0\right)}\\
&\quad + \frac{2B_2\lambda + B_1}{\lambda\left(B_2\lambda^2 + B_1\lambda + B_0\right)} - \frac{\tau}{\lambda}.
\end{aligned}
\tag{18}
$$

Further, we have

$$
\operatorname{Re}\left[\frac{d\lambda}{d\tau}\right]_{\tau=\tau_0}^{-1} = \frac{f'\left(\omega_0^2\right)}{B_1^2\omega_0^2 + \left(B_0 - B_2\omega_0^2\right)^2}. \tag{19}
$$

Thus, if the condition (H_3): $f'(\omega_0^2) \neq 0$ holds, then $\operatorname{Re}[d\lambda/d\tau]_{\tau=\tau_0}^{-1} \neq 0$. Then, based on the Hopf bifurcation theorem in [21], we have the following.

Theorem 2. *For system (2), if the conditions (H_1)–(H_3) hold, then the endemic equilibrium $E_*(S_*, E_*, I_*)$ of system (2) is asymptotically stable for $\tau \in [0, \tau_0)$ and system (2) undergoes a Hopf bifurcation at the endemic equilibrium $E_*(S_*, E_*, I_*)$ when $\tau = \tau_0$, where τ_0 is defined in (17).*

3. Direction and Stability of the Hopf Bifurcation

Let $\tau = \tau_0 + \mu$, $\mu \in R$; then $\mu = 0$ is the Hopf bifurcation value of system (2). Rescaling the time delay $t \to (t/\tau)$, then system (2) can be transformed into an FDE in $C = C([-1, 0], R^3)$ as follows:

$$\dot{u}(t) = L_\mu u_t + F(\mu, u_t), \tag{20}$$

where

$$\begin{aligned} L_\mu \phi = {} & (\tau_0 + \mu) \begin{pmatrix} a_{11} & 0 & a_{13} \\ a_{21} & a_{22} & a_{23} \\ a_{31} & a_{32} & a_{33} \end{pmatrix} \phi(0) \\ & + (\tau_0 + \mu) \begin{pmatrix} 0 & 0 & b_{13} \\ 0 & 0 & 0 \\ 0 & 0 & b_{33} \end{pmatrix} \phi(-1), \end{aligned} \tag{21}$$

$$F(\mu, \phi) = (\tau_0 + \mu)(F_1, F_2, F_3)^T,$$

where F_1, F_2, and F_3 are defined by Appendix A.

By the Riesz representation theorem, there exists a 3×3 matrix function $\eta(\theta, \mu)$, $\theta \in [-1, 0]$, whose components are of bounded variation, such that

$$L_\mu \phi = \int_{-1}^{0} d\eta(\theta, \mu) \phi(\theta), \quad \phi \in C([-1, 0], R^3). \tag{22}$$

In fact, we choose

$$\begin{aligned} \eta(\theta, \mu) = {} & (\tau_0 + \mu) \begin{pmatrix} a_{11} & 0 & a_{13} \\ a_{21} & a_{22} & a_{23} \\ a_{31} & a_{32} & a_{33} \end{pmatrix} \phi(0) \\ & + (\tau_0 + \mu) \begin{pmatrix} 0 & 0 & b_{13} \\ 0 & 0 & 0 \\ 0 & 0 & b_{33} \end{pmatrix} \phi(-1). \end{aligned} \tag{23}$$

For $\phi \in C([-1, 0], R^3)$, we define

$$\begin{aligned} A(\mu)\phi &= \begin{cases} \dfrac{d\phi(\theta)}{d\theta}, & -1 \le \theta < 0, \\ \displaystyle\int_{-1}^{0} d\eta(\theta, \mu)\phi(\theta), & \theta = 0, \end{cases} \\ R(\mu)\phi &= \begin{cases} 0, & -1 \le \theta < 0, \\ F(\mu, \phi), & \theta = 0. \end{cases} \end{aligned} \tag{24}$$

Then system (20) is equivalent to

$$\dot{u}(t) = A(\mu) u_t + R(\mu) u_t. \tag{25}$$

For $\varphi \in C^1([0, 1]), (R^3)^*$, the adjoint operator A^* of A is defined as

$$A^*(\varphi) = \begin{cases} -\dfrac{d\varphi(s)}{ds}, & 0 < s \le 1, \\ \displaystyle\int_{-1}^{0} d\eta^T(s, 0)\varphi(-s), & s = 0, \end{cases} \tag{26}$$

and a bilinear inner product is defined by

$$\begin{aligned} \langle \varphi(s), \phi(\theta) \rangle = {} & \overline{\varphi}(0)\phi(0) \\ & - \int_{\theta=-1}^{0} \int_{\xi=0}^{\theta} \overline{\varphi}(\xi - \theta)\, d\eta(\theta)\, \phi(\xi)\, d\xi, \end{aligned} \tag{27}$$

where $\eta(\theta) = \eta(\theta, 0)$.

Let $q(\theta) = (1, q_2, q_3)^T e^{i\omega_0\tau_0\theta}$ be the eigenvector of $A(0)$ belonging to $+i\omega_0\tau_0$ and $q^*(s) = D(1, q_2^*, q_3^*)e^{i\omega_0\tau_0 s}$ be the eigenvector of $A^*(0)$ belonging to $-i\omega_0\tau_0$. By a direct computation, we can get

$$\begin{aligned} q_2 &= \frac{a_{21} + a_{23}q_3}{i\omega_0 - a_{22}}, \\ q_3 &= \frac{i\omega_0 - a_{11}}{a_{13} + b_{13}e^{-i\tau_0\omega_0}}, \\ q_2^* &= -\frac{a_{32}q_3}{i\omega_0 + a_{22}}, \\ q_3^* &= \frac{\left(a_{13} + b_{13}e^{i\tau_0\omega_0}\right)(i\omega_0 + a_{22})}{a_{23}a_{32} - (i\omega_0 + a_{22})\left(i\omega_0 + a_{33} + b_{33}e^{i\tau_0\omega_0}\right)}. \end{aligned} \tag{28}$$

From (27), we can get

$$\begin{aligned} & \langle q^*(s), q(\theta) \rangle \\ & \quad = \overline{D}\left[1 + q_2\overline{q}_2^* + q_3\overline{q}_3^* + \tau_0 e^{-i\tau_0\omega_0} q_3 \left(b_{13} + b_{33}\overline{q}_3^*\right)\right]. \end{aligned} \tag{29}$$

Then we choose

$$\overline{D} = \left[1 + q_2\overline{q}_2^* + q_3\overline{q}_3^* + \tau_0 e^{-i\tau_0\omega_0} q_3 \left(b_{13} + b_{33}\overline{q}_3^*\right)\right]^{-1}. \tag{30}$$

such that $\langle q^*, q \rangle = 1$.

Next, we can obtain the coefficients g_{20}, g_{11}, g_{02}, and g_{21} by using the method introduced in [21] and a computation process similar to that in [22–24]. The expressions of g_{20}, g_{11}, g_{02}, and g_{21} are defined by Appendix B.

Then, we can get the following coefficients which determine the properties of the Hopf bifurcation:

$$\begin{aligned} C_1(0) &= \frac{i}{2\tau_0\omega_0}\left(g_{11}g_{20} - 2|g_{11}|^2 - \frac{|g_{02}|^2}{3}\right) + \frac{g_{21}}{2}, \\ \mu_2 &= -\frac{\operatorname{Re}\{C_1(0)\}}{\operatorname{Re}\{\lambda'(\tau_0)\}}, \\ \beta_2 &= 2\operatorname{Re}\{C_1(0)\}, \\ T_2 &= -\frac{\operatorname{Im}\{C_1(0)\} + \mu_2 \operatorname{Im}\{\lambda'(\tau_0)\}}{\tau_0\omega_0}. \end{aligned} \tag{31}$$

In conclusion, we have the following results.

Theorem 3. *For system (2), if $\mu_2 > 0$ ($\mu_2 < 0$), then the Hopf bifurcation is supercritical (subcritical). If $\beta_2 < 0$ ($\beta_2 > 0$), then the bifurcating periodic solutions are stable (unstable). If $T_2 > 0$ ($T_2 < 0$), then the bifurcating periodic solutions increase (decrease).*

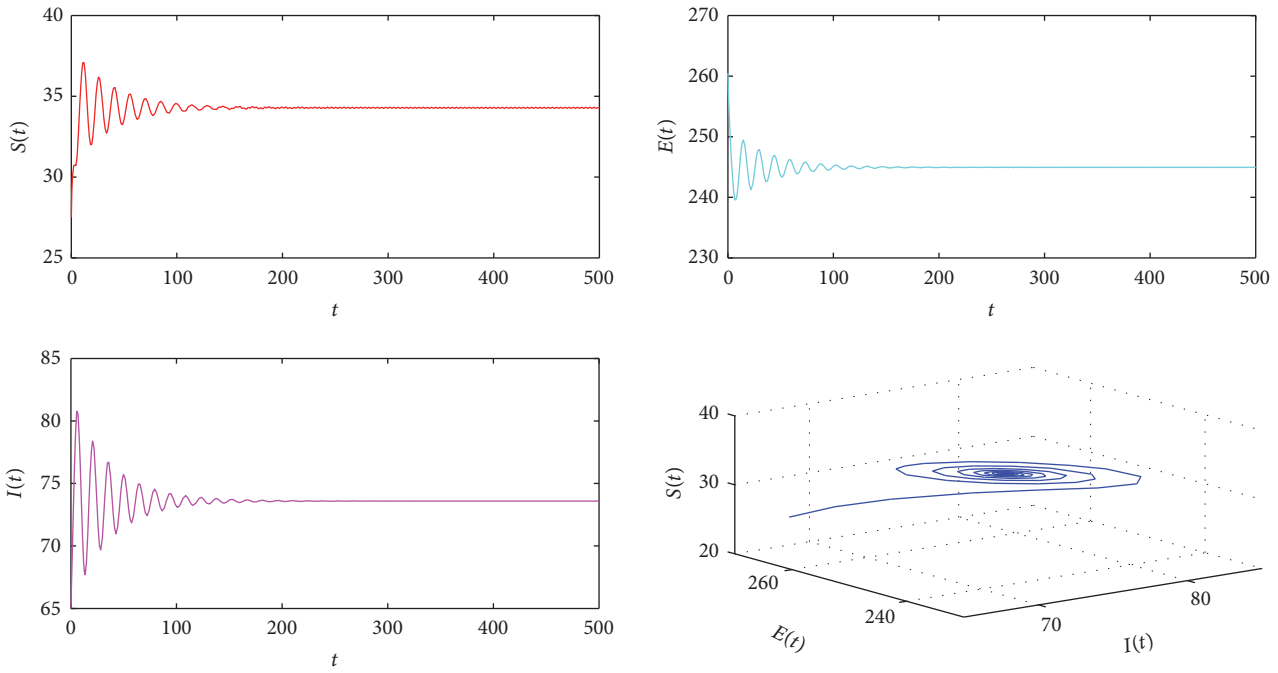

FIGURE 1: P_* is locally asymptotically stable for $\tau = 4.475 < \tau_0 = 5.1686$ with initial values "27.5, 260.5, 65."

4. Numerical Simulations

In order to verify the efficiency of the obtained results in the paper, we carry out some numerical simulations in this section. By extracting some values from [11] and considering the conditions for the existence of the Hopf bifurcation, we consider the special case of system (2) with the parameters $A = 5$, $d = 0.01$, $\beta = 0.5$, $\alpha = 0.4$, $\gamma = 0.5$, $\mu = 0.65$, $\varepsilon = 0.1$, and $\delta = 0.02$, Then, system (2) becomes the following form:

$$\begin{aligned}
\frac{dS(t)}{dt} &= 5 - 0.01S(t) - \frac{0.5S(t)I(t)}{1 + 0.4I(t)} + 0.5I(t-\tau),\\
\frac{dE(t)}{dt} &= \frac{0.325S(t)I(t)}{1 + 0.4I(t)} - 0.11E(t),\\
\frac{dI(t)}{dt} &= \frac{0.175S(t)I(t)}{1 + 0.4I(t)} + 0.1E(t) - 0.03I(t)\\
&\quad - 0.5I(t-\tau),
\end{aligned} \tag{32}$$

$$0.0014I^2 - 0.0999I - 0.2584 = 0, \tag{33}$$

from which we can obtain the unique positive root $I_* = 73.8562$ and then we get the unique endemic equilibrium $P_*(34.3750, 245.5930, 73.8562)$. Then, we can obtain $\omega_0 = 0.3950$, $\tau_0 = 5.1686$, and $\lambda'(\tau_0) = 0.0012 - 0.0759i$. Thus, based on Theorem 2, we know that the endemic equilibrium $P_*(34.3750, 245.5930, 73.8562)$ is locally asymptotically stable when $\tau < \tau_0 = 5.1686$, which can be illustrated by Figures 1 and 2. In this case, the disease can be controlled easily. Once the value of the delay passes through the critical value $\tau_0 = 5.1686$, then the endemic equilibrium $P_*(34.3750, 245.5930, 73.8562)$ loses its stability and a Hopf bifurcation occurs, and a family of periodic solutions bifurcate from the endemic equilibrium $P_*(34.3750, 245.5930, 73.8562)$. This property can be shown as in Figures 3 and 4. In this case, the disease will be out of control.

In addition, according to (31), we get $C_1(0) = -1.0027 - 0.9244i$, $\mu_2 = 835.5833 > 0$, $\beta_2 = -2.0054 < 0$, and $T_2 = 31.5171 > 0$. Therefore, we can conclude that the Hopf bifurcation is supercritical and the bifurcating periodic solutions are stable and increase. Since the bifurcating periodic solutions are stable, it can be concluded that the populations in system (32) can coexist from the view of ecology. Based on this fact, we can conclude that the time delay is harmful for system (32).

5. Conclusions

We generalize a delayed SEIS (Susceptible-Exposed-Infectious-Susceptible) epidemic model with a changing delitescence and nonlinear incidence rate in this paper by introducing the time delay due to the period that is used to cure the infectious population into the SEIS model considered in the literature [11]. Compared with the literature [11], we mainly consider the effect of the time delay on the model.

The main results are given in terms of local stability and Hopf bifurcation. Stability of the endemic equilibrium is investigated by analyzing the corresponding characteristic equation. By choosing the time delay as a bifurcation parameter, sufficient conditions have been established for local existence of Hopf bifurcation at the endemic equilibrium. Then, with the help of the normal form theory and the

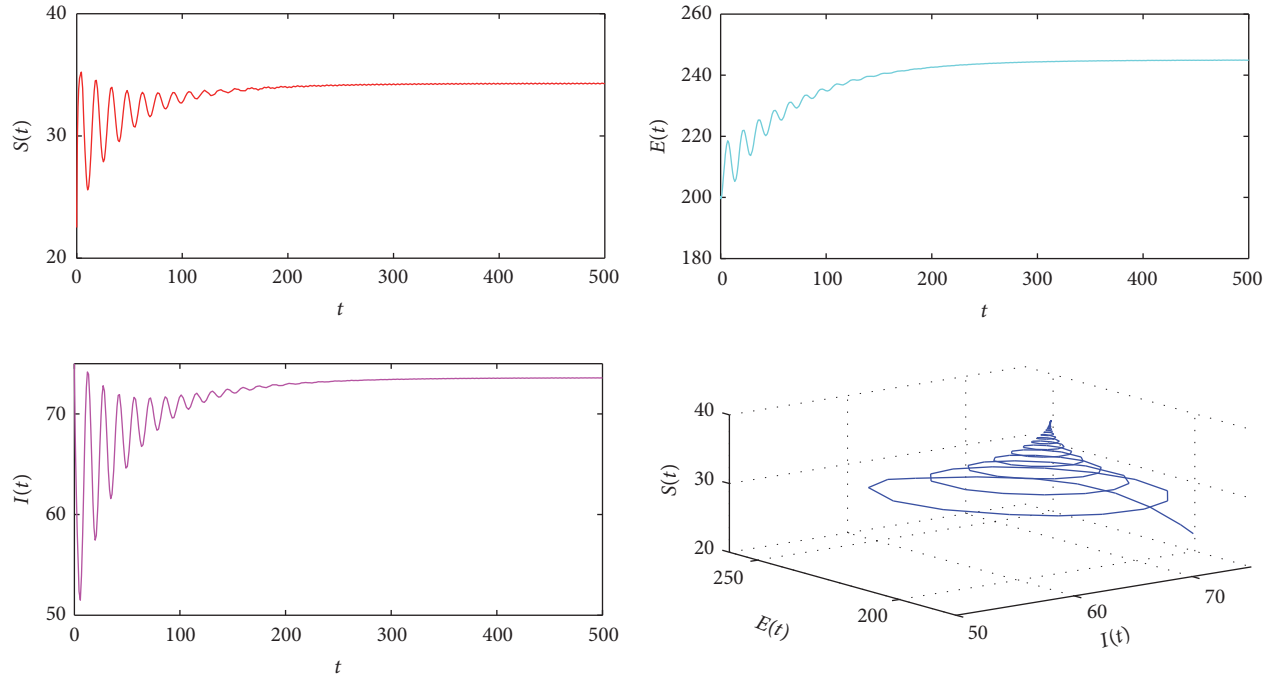

FIGURE 2: P_* is locally asymptotically stable for $\tau = 4.475 < \tau_0 = 5.1686$ with initial values "22, 200, 75."

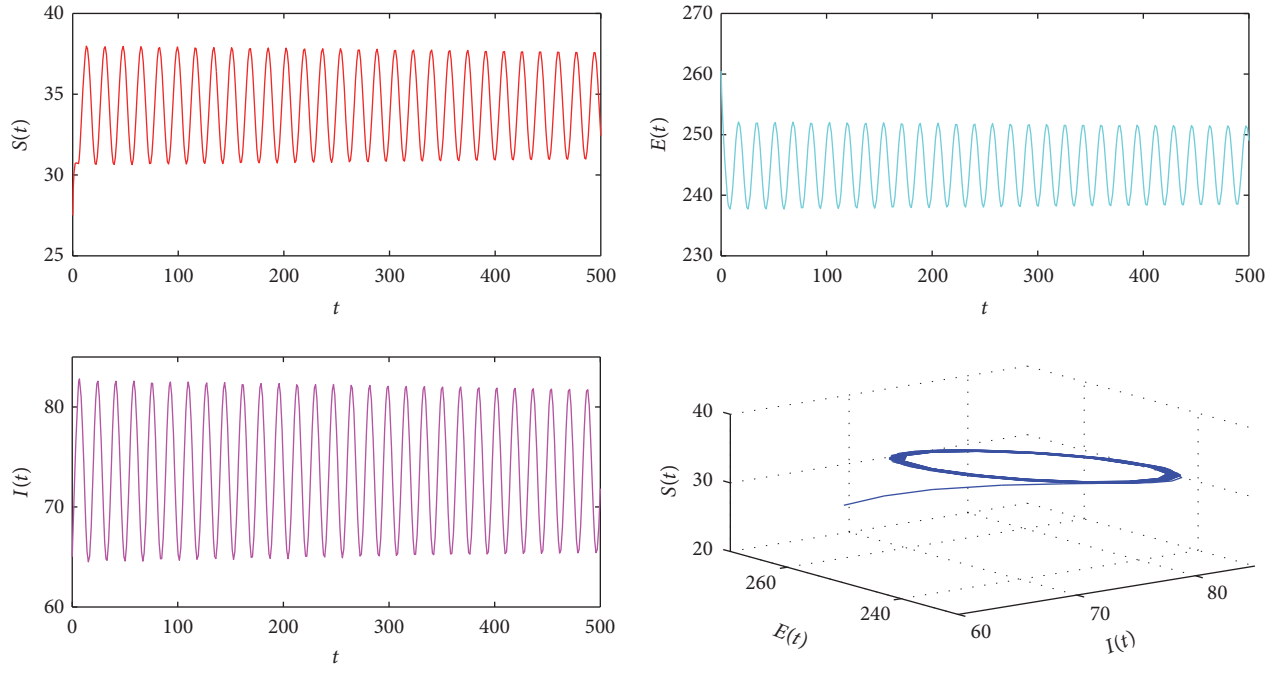

FIGURE 3: P_* becomes unstable and a Hopf bifurcation occurs when $\tau = 5.485 > \tau_0 = 5.1686$ with initial values "27.5, 260.5, 65."

center manifold theorem due to Hassard et al. [21], direction and stability of the Hopf bifurcation are determined. Finally, through numerical simulations, it can be concluded that the period used to cure the infectious population plays an important role in the disease spreading and the disease may be controlled by shortening the period used to cure the infectious population.

Appendix

A. The Expressions of F_1, F_2, and F_3

$$F_1 = g_1\phi_3^2(0) + g_2\phi_1(0)\phi_3(0) + g_3\phi_1(0)\phi_3^2(0) + g_4\phi_3^3(0) + \cdots,$$

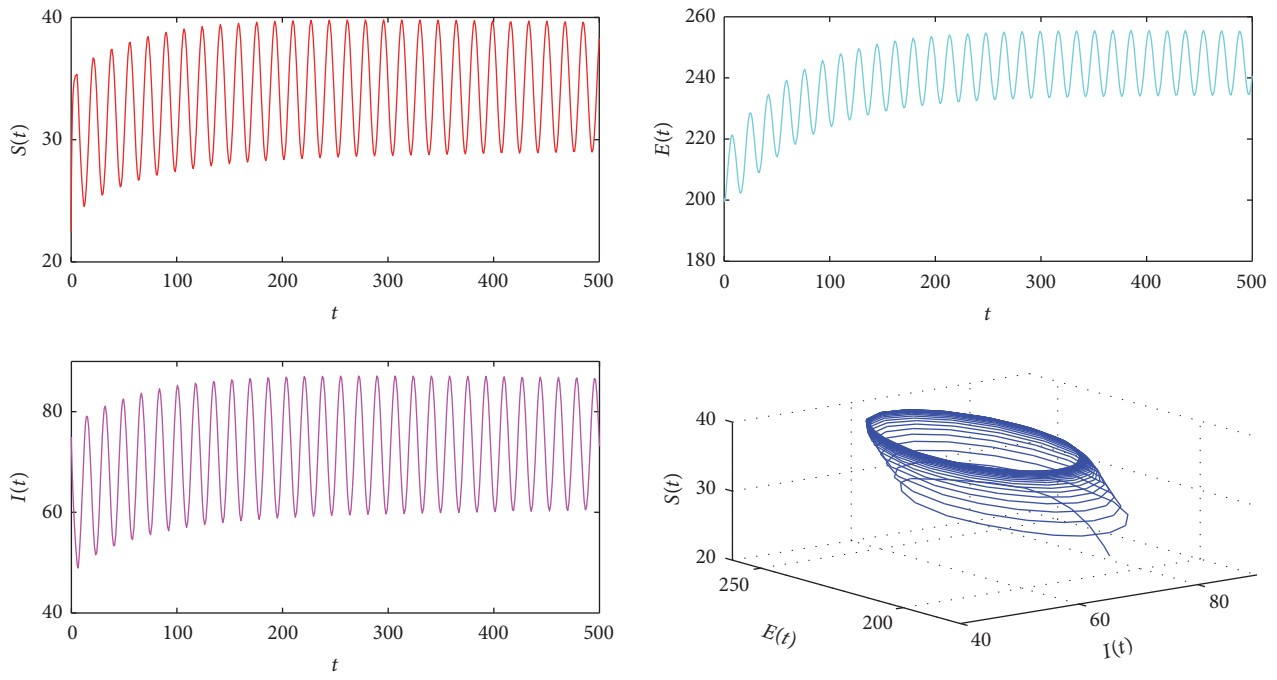

FIGURE 4: P_* becomes unstable and a Hopf bifurcation occurs when $\tau = 5.485 > \tau_0 = 5.1686$ with initial values "22, 200, 75."

$$F_2 = h_1\phi_3^2(0) + h_2\phi_1(0)\phi_3(0) + h_3\phi_1(0)\phi_3^2(0) + h_4\phi_3^3(0) + \cdots,$$

$$F_3 = k_1\phi_3^2(0) + k_2\phi_1(0)\phi_3(0) + k_3\phi_1(0)\phi_3^2(0) + k_4\phi_3^3(0) + \cdots,$$

$$g_1 = \frac{\alpha\beta S_*}{(1+\alpha I_*)^3},$$

$$g_2 = -\frac{\beta}{(1+\alpha I_*)^2},$$

$$g_3 = \frac{\alpha\beta}{(1+\alpha I_*)^3},$$

$$g_4 = -\frac{\alpha^2\beta S_*}{(1+\alpha I_*)^4},$$

$$h_1 = -\frac{\mu\alpha\beta S_*}{(1+\alpha I_*)^3},$$

$$h_2 = \frac{\mu\beta}{(1+\alpha I_*)^2},$$

$$h_3 = -\frac{\mu\alpha\beta}{(1+\alpha I_*)^3},$$

$$h_4 = \frac{\mu\alpha^2\beta S_*}{(1+\alpha I_*)^4},$$

$$k_1 = -\frac{(1-\mu)\alpha\beta S_*}{(1+\alpha I_*)^3},$$

$$k_2 = \frac{(1-\mu)\beta}{(1+\alpha I_*)^2},$$

$$k_3 = -\frac{(1-\mu)\alpha\beta}{(1+\alpha I_*)^3},$$

$$k_4 = \frac{(1-\mu)\alpha^2\beta S_*}{(1+\alpha I_*)^4}. \tag{A.1}$$

B. The Expressions of g_{20}, g_{11}, g_{02}, and g_{21}

$$g_{20} = 2\tau_0\overline{D}\left(g_1\left(q^{(3)}(0)\right)^2 + g_2q^{(1)}(0)q^{(3)}(0) + \overline{q}_2^*\left(h_1\left(q^{(3)}(0)\right)^2 + h_2q^{(1)}(0)q^{(3)}(0)\right) + \overline{q}_3^*\left(k_1\left(q^{(3)}(0)\right)^2 + k_2q^{(1)}(0)q^{(3)}(0)\right)\right),$$

$$g_{11} = \tau_0\overline{D}\left(2g_1q^{(3)}(0)\overline{q}^{(3)}(0) + g_2\left(q^{(1)}(0)\overline{q}^{(3)}(0) + \overline{q}^{(1)}(0)\cdot q^{(3)}(0)\right) + \overline{q}_2^*\left(2h_1q^{(3)}(0)\overline{q}^{(3)}(0) + h_2\left(q^{(1)}(0)\overline{q}^{(3)}(0) + \overline{q}^{(1)}(0)q^{(3)}(0)\right)\right) + \overline{q}_3^*\left(2k_1q^{(3)}(0)\overline{q}^{(3)}(0) + k_2\left(q^{(1)}(0)\overline{q}^{(3)}(0) + \overline{q}^{(1)}(0)q^{(3)}(0)\right)\right)\right),$$

$$g_{02} = 2\tau_0\overline{D}\left(g_1\left(\overline{q}^{(3)}(0)\right)^2 + g_2\overline{q}^{(1)}(0)\overline{q}^{(3)}(0)\right)$$

$$+\overline{q}_2^*\left(h_1\left(\overline{q}^{(3)}(0)\right)^2+h_2\overline{q}^{(1)}(0)\,\overline{q}^{(3)}(0)\right)+\overline{q}_3^*\left(k_1\left(\overline{q}^{(3)}(0)\right)^2+k_2\overline{q}^{(1)}(0)\,\overline{q}^{(3)}(0)\right)\Big),$$

$$g_{21}=2\tau_0\overline{D}\Big(g_1\left(2W_{11}^{(3)}(0)\,q^{(3)}(0)+W_{20}^{(3)}(0)\,\overline{q}^{(3)}(0)\right)+g_2\left(W_{11}^{(1)}(0)\,q^{(3)}(0)+\frac{1}{2}W_{20}^{(1)}(0)\,\overline{q}^{(3)}(0)+W_{11}^{(3)}(0)\,q^{(1)}(0)+\frac{1}{2}W_{20}^{(3)}(0)\,\overline{q}^{(1)}(0)\right)+g_3\left(\overline{q}^{(1)}(0)\left(q^{(3)}(0)\right)^2+2q^{(1)}(0)\cdot q^{(3)}(0)\,\overline{q}^{(3)}(0)\right)+3g_4\left(q^{(3)}(0)\right)^2\overline{q}^{(3)}(0)+\overline{q}_2^*\left(h_1\left(2W_{11}^{(3)}(0)\,q^{(3)}(0)+W_{20}^{(3)}(0)\,\overline{q}^{(3)}(0)\right)+h_2\left(W_{11}^{(1)}(0)\,q^{(3)}(0)+\frac{1}{2}W_{20}^{(1)}(0)\,\overline{q}^{(3)}(0)+W_{11}^{(3)}(0)\,q^{(1)}(0)+\frac{1}{2}W_{20}^{(3)}(0)\,\overline{q}^{(1)}(0)\right)+h_3\left(\overline{q}^{(1)}(0)\left(q^{(3)}(0)\right)^2+2q^{(1)}(0)\,q^{(3)}(0)\,\overline{q}^{(3)}(0)\right)+3h_4\left(q^{(3)}(0)\right)^2\overline{q}^{(3)}(0)\Big)+\overline{q}_3^*\left(k_1\left(2W_{11}^{(3)}(0)\,q^{(3)}(0)+W_{20}^{(3)}(0)\,\overline{q}^{(3)}(0)\right)+k_2\left(W_{11}^{(1)}(0)\,q^{(3)}(0)+\frac{1}{2}W_{20}^{(1)}(0)\,\overline{q}^{(3)}(0)+W_{11}^{(3)}(0)\,q^{(1)}(0)+\frac{1}{2}W_{20}^{(3)}(0)\,\overline{q}^{(1)}(0)\right)+k_3\left(\overline{q}^{(1)}(0)\left(q^{(3)}(0)\right)^2+2q^{(1)}(0)\,q^{(3)}(0)\,\overline{q}^{(3)}(0)\right)+3k_4\left(q^{(3)}(0)\right)^2\overline{q}^{(3)}(0)\Big)\Big),$$

$$W_{20}(\theta)=\frac{ig_{20}q(0)}{\tau_0\omega_0}e^{i\tau_0\omega_0\theta}+\frac{i\overline{g}_{02}\overline{q}(0)}{3\tau_0\omega_0}e^{-i\tau_0\omega_0\theta}+E_1e^{2i\tau_0\omega_0\theta},$$

$$W_{11}(\theta)=-\frac{ig_{11}q(0)}{\tau_0\omega_0}e^{i\tau_0\omega_0\theta}+\frac{i\overline{g}_{11}\overline{q}(0)}{\tau_0\omega_0}e^{-i\tau_0\omega_0\theta}+E_2,$$

$$E_1=\begin{pmatrix}2i\omega_0-a_{11} & 0 & -a_{13}-b_{13}e^{-2i\tau_0\omega_0}\\ -a_{21} & 2i\omega_0-a_{22} & -a_{23}\\ -a_{31} & -a_{32} & 2i\omega_0-a_{33}-b_{33}e^{-2i\tau_0\omega_0}\end{pmatrix}^{-1}\times\begin{pmatrix}E_1^{(1)}\\ E_1^{(2)}\\ E_1^{(3)}\end{pmatrix},$$

$$E_2=-\begin{pmatrix}a_{11} & a_{12} & a_{13}+b_{13}\\ a_{21} & a_{22} & a_{23}\\ a_{31} & a_{32} & a_{33}+b_{33}\end{pmatrix}^{-1}\times\begin{pmatrix}E_2^{(1)}\\ E_2^{(2)}\\ E_2^{(3)}\end{pmatrix},$$

$$E_1^{(1)}=g_1\left(q^{(3)}(0)\right)^2+g_2q^{(1)}(0)\,q^{(3)}(0),$$

$$E_1^{(2)}=h_1\left(q^{(3)}(0)\right)^2+h_2q^{(1)}(0)\,q^{(3)}(0),$$

$$E_1^{(3)}=k_1\left(q^{(3)}(0)\right)^2+k_2q^{(1)}(0)\,q^{(3)}(0),$$

$$E_2^{(1)}=2g_1q^{(3)}(0)\,\overline{q}^{(3)}(0)+g_2\left(q^{(1)}(0)\,\overline{q}^{(3)}(0)+\overline{q}^{(1)}(0)\,q^{(3)}(0)\right),$$

$$E_2^{(2)}=2h_1q^{(3)}(0)\,\overline{q}^{(3)}(0)+h_2\left(q^{(1)}(0)\,\overline{q}^{(3)}(0)+\overline{q}^{(1)}(0)\,q^{(3)}(0)\right),$$

$$E_2^{(3)}=2k_1q^{(3)}(0)\,\overline{q}^{(3)}(0)+k_2\left(q^{(1)}(0)\,\overline{q}^{(3)}(0)+\overline{q}^{(1)}(0)\,q^{(3)}(0)\right).\tag{B.1}$$

Conflicts of Interest

The author declares that there are no conflicts of interest regarding the publication of this paper.

Acknowledgments

This work was supported by Natural Science Foundation of the Higher Education Institutions of Anhui Province (KJ2015A144).

References

[1] T. Zhang, X. Meng, T. Zhang, and Y. Song, "Global dynamics for a new high-dimensional SIR model with distributed delay," *Applied Mathematics and Computation*, vol. 218, no. 24, pp. 11806–11819, 2012.

[2] Y. Xiao, T. Zhao, and S. Tang, "Dynamics of an infectious diseases with media/psychology induced non-smooth incidence," *Mathematical Biosciences and Engineering. MBE*, vol. 10, no. 2, pp. 445–461, 2013.

[3] W. Qin, S. Tang, and R. A. Cheke, "Nonlinear pulse vaccination in an SIR epidemic model with resource limitation," *Abstract and Applied Analysis*, vol. 2013, Article ID 670263, 13 pages, 2013.

[4] T. Zhang, R. Kang, K. Wang, and J. Liu, "Global dynamics of an SEIR epidemic model with discontinuous treatment," *Advances in Difference Equations*, vol. 2015: Article 361, 16 pages, 2015.

[5] X. Wang, "An SIRS Epidemic Model with Vital Dynamics and a Ratio-Dependent Saturation Incidence Rate," *Discrete Dynamics in Nature and Society*, vol. 2015, Article ID 720682, 9 pages, 2015.

[6] Y. Tian and X. Liu, "Global dynamics of a virus dynamical model with general incidence rate and cure rate," *Nonlinear Analysis. Real World Applications*, vol. 16, pp. 17–26, 2014.

[7] D. Zhao and S. Yuan, "Persistence and stability of the disease-free equilibrium in a stochastic epidemic model with imperfect vaccine," *Advances in Difference Equations*, vol. 2016: Article ID 280, 14 pages, 2016.

[8] L. Liu, "A delayed SIR model with general nonlinear incidence rate," *Advances in Difference Equations*, vol. 2015: Article 329, 11 pages, 2015.

[9] Y. N. Xiao and L. S. Chen, "An SIS epidemic model with stage structure and a delay," *Acta Mathematicae Applicatae Sinica*, vol. 18, pp. 607–618, 2002.

[10] Q. Liu and P. Van Mieghem, "Evaluation of an analytic, approximate formula for the time-varying SIS prevalence in different networks," *Physica A. Statistical Mechanics and its Applications*, vol. 471, pp. 325–336, 2017.

[11] J. Wang, "Analysis of an SEIS Epidemic Model with a Changing Delitescence," *Abstract and Applied Analysis*, vol. 2012, Article ID 318150, 10 pages, 2012.

[12] Y. Enatsu, E. Messina, Y. Muroya, Y. Nakata, E. Russo, and A. Vecchio, "Stability analysis of delayed SIR epidemic models with a class of nonlinear incidence rates," *Applied Mathematics and Computation*, vol. 218, no. 9, pp. 5327–5336, 2012.

[13] F.-F. Zhang, Z. Jin, and G.-Q. Sun, "Bifurcation analysis of a delayed epidemic model," *Applied Mathematics and Computation*, vol. 216, no. 3, pp. 753–767, 2010.

[14] W. Wang and L. Chen, "Stability and Hopf Bifurcation Analysis of an Epidemic Model by Using the Method of Multiple

Scales," *Mathematical Problems in Engineering*, vol. 2016: Article 2034136, 8 pages, 2016.

[15] J.-J. Wang, J.-Z. Zhang, and Z. Jin, "Analysis of an SIR model with bilinear incidence rate," *Nonlinear Analysis. Real World Applications*, vol. 11, no. 4, pp. 2390–2402, 2010.

[16] J.-Z. Zhang, Z. Jin, Q.-X. Liu, and Z.-Y. Zhang, "Analysis of a delayed SIR model with nonlinear incidence rate," *Discrete Dynamics in Nature and Society*, vol. 2008, Article ID 636153, 16 pages, 2008.

[17] L. Wen and X. Yang, "Global stability of a delayed SIRS model with temporary immunity," *Chaos, Solitons & Fractals*, vol. 38, no. 1, pp. 221–226, 2008.

[18] Y. N. Kyrychko and K. B. Blyuss, "Global properties of a delayed SIR model with temporary immunity and nonlinear incidence rate," *Nonlinear Analysis. Real World Applications*, vol. 6, no. 3, pp. 495–507, 2005.

[19] P. Yongzhen, S. Li, C. Li, and S. Chen, "The effect of constant and pulse vaccination on an SIR epidemic model with infectious period," *Applied Mathematical Modelling. Simulation and Computation for Engineering and Environmental Systems*, vol. 35, no. 8, pp. 3866–3878, 2011.

[20] Y. Song, M. Han, and J. Wei, "Stability and Hopf bifurcation analysis on a simplified BAM neural network with delays," *Physica D. Nonlinear Phenomena*, vol. 200, no. 3-4, pp. 185–204, 2005.

[21] B. D. Hassard, N. D. Kazarinoff, and Y. H. Wan, *Theory and Applications of Hopf Bifurcation*, Cambridge University Press, Cambridge, UK, 1981.

[22] M. Ferrara, L. Guerrini, and G. M. Bisci, "Center Manifold Reduction and Perturbation Method in a Delayed Model with a Mound-Shaped Cobb-Douglas Production Function," *Abstract and Applied Analysis*, vol. 2013, Article ID 738460, 6 pages, 2013.

[23] X.-Y. Meng, H.-F. Huo, X.-B. Zhang, and H. Xiang, "Stability and Hopf bifurcation in a three-species system with feedback delays," *Nonlinear Dynamics*, vol. 64, no. 4, pp. 349–364, 2011.

[24] C. Xu, X. Tang, and M. Liao, "Stability and bifurcation analysis of a six-neuron BAM neural network model with discrete delays," *Neurocomputing*, vol. 74, no. 5, pp. 689–707, 2011.

Hindawi
Discrete Dynamics in Nature and Society
Volume 2017, Article ID 1382980, 8 pages
https://doi.org/10.1155/2017/1382980

Research Article

The Minimum Spectral Radius of an Edge-Removed Network: A Hypercube Perspective

Yingbo Wu,[1] Tianrui Zhang,[1] Shan Chen,[2] and Tianhui Wang[1]

[1]*School of Software Engineering, Chongqing University, Chongqing 400044, China*
[2]*School of Mechanical Engineering, Chongqing University, Chongqing 400044, China*

Correspondence should be addressed to Yingbo Wu; wyb@cqu.edu.cn

Received 15 December 2016; Revised 17 February 2017; Accepted 28 March 2017; Published 19 April 2017

Academic Editor: Yong Deng

Copyright © 2017 Yingbo Wu et al. This is an open access article distributed under the Creative Commons Attribution License, which permits unrestricted use, distribution, and reproduction in any medium, provided the original work is properly cited.

The spectral radius minimization problem (SRMP), which aims to minimize the spectral radius of a network by deleting a given number of edges, turns out to be crucial to containing the prevalence of an undesirable object on the network. As the SRMP is NP-hard, it is very unlikely that there is a polynomial-time algorithm for it. As a result, it is proper to focus on the development of effective and efficient heuristic algorithms for the SRMP. For that purpose, it is appropriate to gain insight into the pattern of an optimal solution to the SRMP by means of checking some regular networks. Hypercubes are a celebrated class of regular networks. This paper empirically studies the SRMP for hypercubes with two/three/four missing edges. First, for each of the three subproblems of the SRMP, a candidate for the optimal solution is presented. Second, it is shown that the candidate is optimal for small-sized hypercubes, and it is shown that the proposed candidate is likely to be optimal for medium-sized hypercubes. The edges in each candidate are evenly distributed over the network, which may be a common feature of all symmetric networks and hence is instructive in designing effective heuristic algorithms for the SRMP.

1. Introduction

The epidemic modeling is recognized as an effective approach to the understanding of propagation process of objects over a network [1, 2]. For instance, epidemic models help us understand the key factors that affect the prevalence of malware [3–8]. The speed and extent of spread of an epidemic on a network depend largely on the structure of the network; whether the epidemic goes viral depends on whether the spectral radius of the network exceeds a threshold [9–14]. Therefore, reducing the spectral radius of a network by removing a set of edges is an effective approach to the containment of the prevalence of an undesirable epidemic on the network. The spectral radius minimization problem (SRMP) aims to remove a given number of edges of a network so that the spectral radius of the resulting network attains the minimum. As the SRMP is NP-hard [15], it is much unlikely that there be a polynomial-time algorithm for it. As thus, a number of heuristic algorithms for the SRMP have been proposed [15–19]. In most situations, these heuristics are ineffective, because they produce nonoptimal solutions rather than optimal solutions. For the purpose of developing effective heuristic algorithms for the SRMP, it is appropriate to gain insight into the pattern of an optimal solution to the SRMP by means of checking some regular networks. Recently, Yang et al. [20] studied the SRMP for 2D tori.

Hypercubes are a class of regular networks [21]. Due to remarkable advantages in communication [22–25], fault tolerant communication [26–30], fault diagnosis [31–34], and parallel computation [35, 36], hypercubes have been widely adopted as the underlying interconnection network in multicomputer systems [37]. To our knowledge, the SRMP for hypercubes is still unsolved.

This paper addresses three subproblems of the SRMP, where two/three/four edges are removed from a hypercube, respectively. First, for each of the three subproblems of the SRMP, a candidate optimal solution is presented. Second, it is shown that the candidate is optimal for small-sized hypercubes, and it is shown that the proposed candidate is likely to be optimal for medium-sized hypercubes. The edges

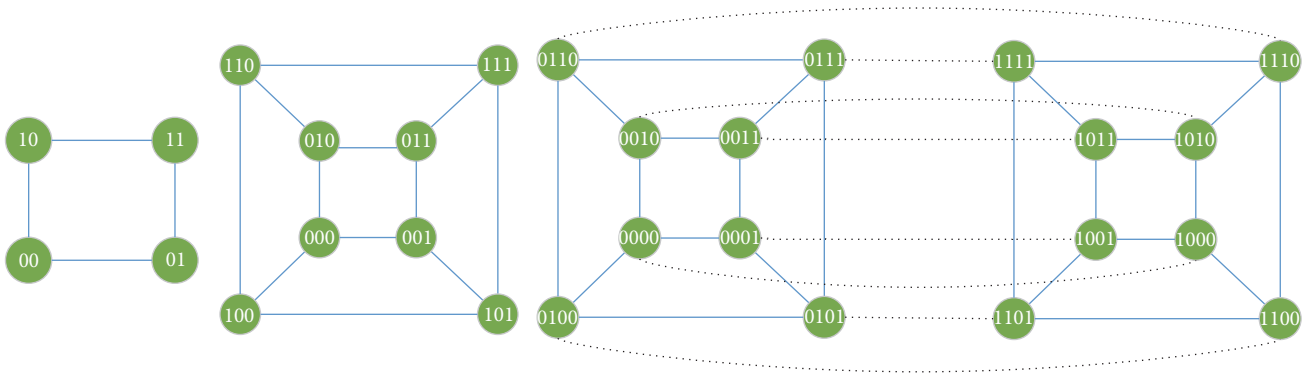

Figure 1: Three examples of H_n.

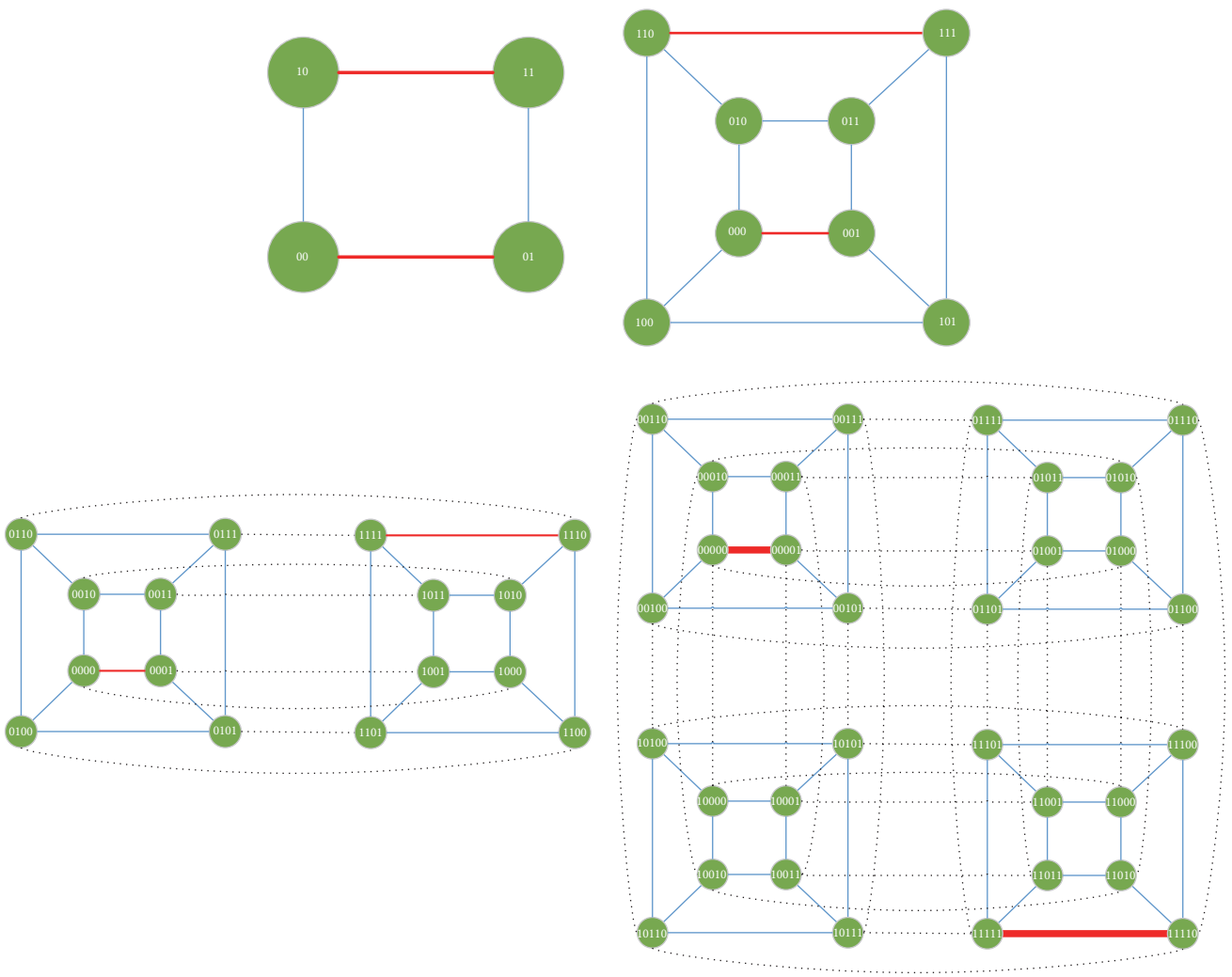

Figure 2: The proposed candidate in H_n.

in each candidate are evenly distributed over the network, which may be a common feature of all symmetric networks and hence is instructive in designing effective heuristic algorithms for the SRMP.

The remaining materials are organized in this fashion: the preliminary knowledge is given in Section 2. Section 3 presents the main results of this work. Finally, Section 4 summarizes this work.

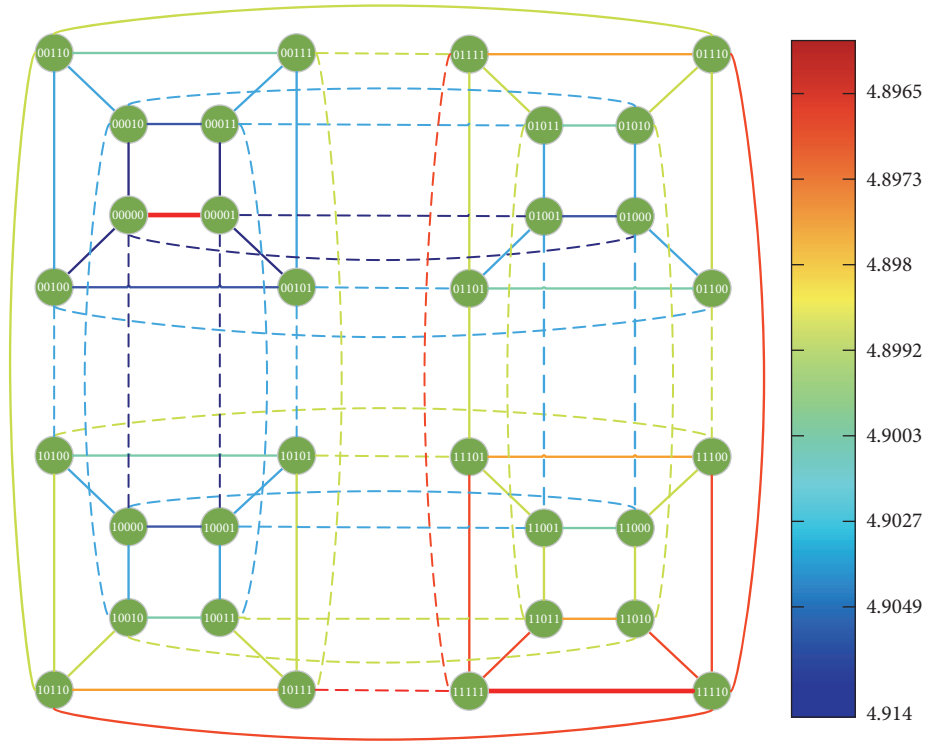

FIGURE 3: Assume that the red edge in the upper-left 3D subcube of H_5 is the first deleted edge and each of the remaining edges is a candidate for the second deleted edge. The spectral radius of the surviving network formed by deleting each of the candidate edges from H_5 is shown.

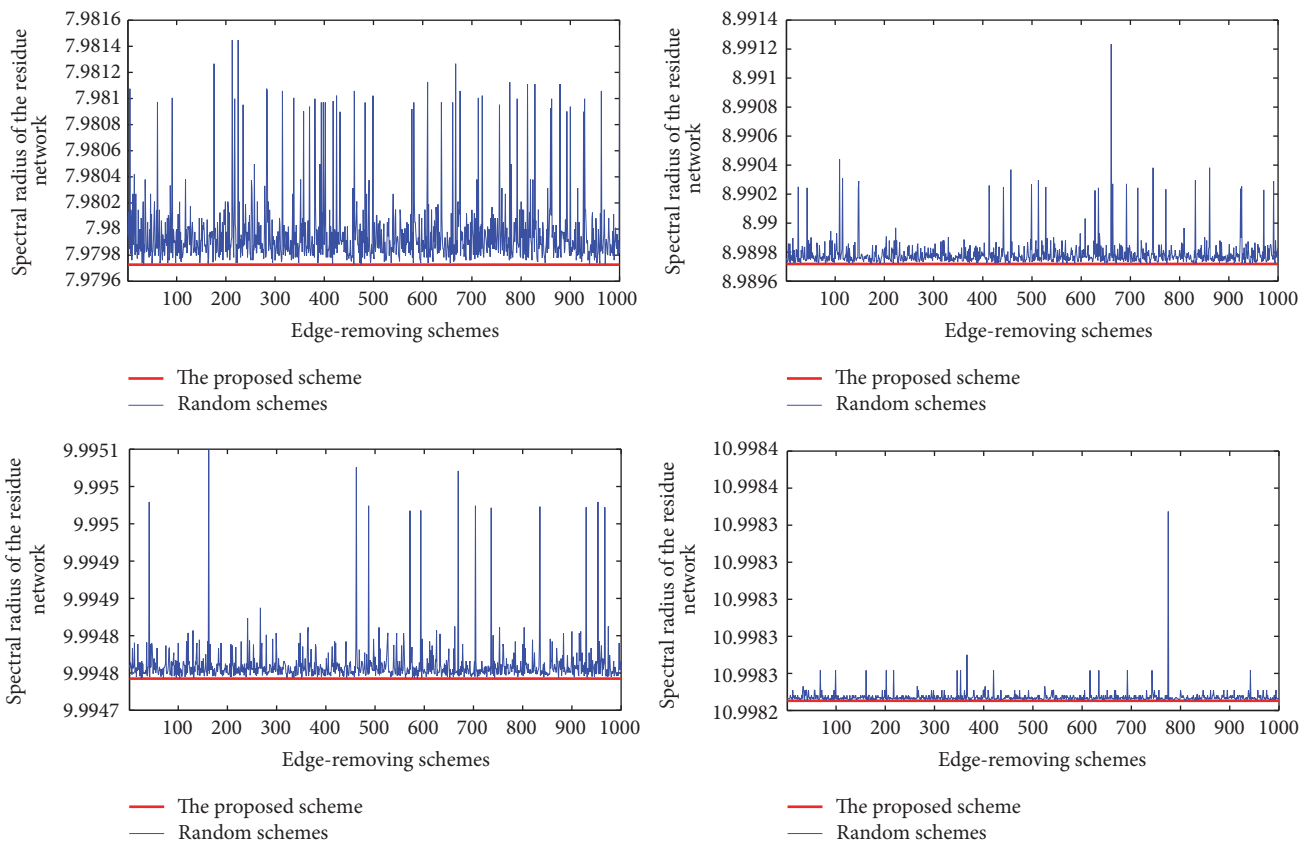

FIGURE 4: The proposed candidate (red) versus 10^3 random candidates (blue).

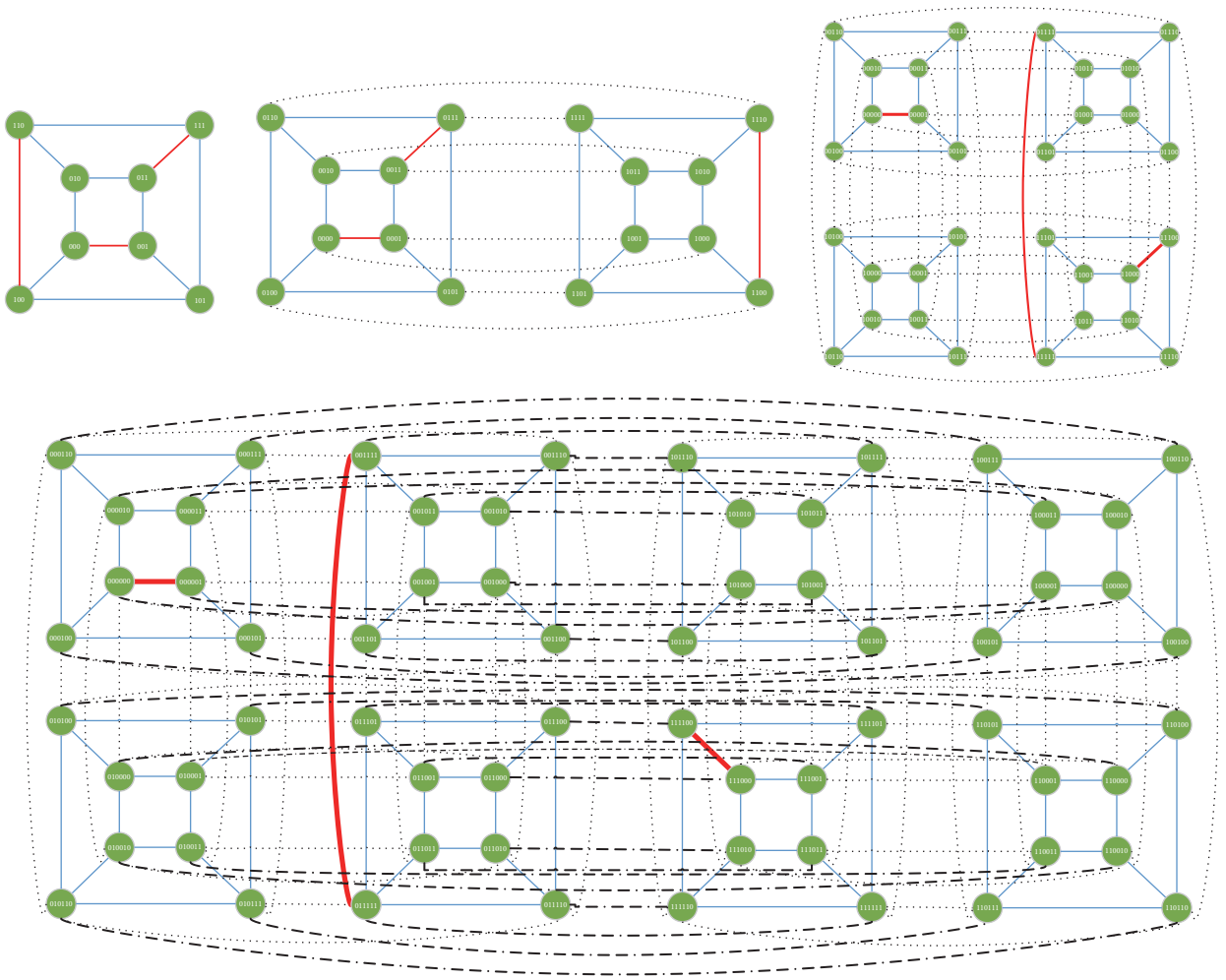

Figure 5: The proposed candidate in H_n.

2. Preliminaries

For fundamental knowledge on the spectral radius of a network, see [38, 39]. The SRMP is formulated as follows: given a network $G = (V, E)$ and a positive integer k, find a set of k edges of G so that the surviving network obtained by removing the set of edges from the network achieves the minimum spectral radius.

An n-dimensional cube (n-D cube, for short), denoted by H_n, is a network $G = (V, E)$, where there is a one-to-one correspondance ϕ from V to the set of all 0-1 binary strings of length n so that node u is adjacent to node v if and only if $\phi(u)$ differs from $\phi(v)$ in exactly one bit position. In what follows, it is always assumed that the nodes of a hypercube have been labelled with 0-1 strings in this way. See Figure 1 for three small-sized hypercubes.

An n-D cube can also be defined in a recursive way as follows. (1) A 0-D cube is a graph on a single node. (2) For $n \geq 1$, an n-D cube is built from two copies of an $(n-1)$-D cube in this way: connect each node in one copy to the same node in the other copy.

3. Main Results

This section considers the optimal scheme of deleting two/three/four edges from H_n, respectively.

3.1. Deleting Two Edges. Firstly, we consider a subproblem of the SRMP, denoted by SRMP-H2, for which two edges will be deleted from a hypercube. Let us present a candidate for the optimal solution to the SRMP-H2 as follows, where n denotes the dimension of the hypercube:

$$e_1 = \left\{0^n, 0^{n-1}1\right\},$$
$$e_2 = \left\{1^n, 1^{n-1}0\right\}. \tag{1}$$

Figure 2 shows the proposed candidate in H_2, H_3, H_4, and H_5, respectively.

For $2 \leq n \leq 7$, it follows by exhaustive search that the proposed candidate is optimal. For instance, assume that the red edge in the upper-left 3D subcube of H_5 is the first deleted edge, and each of the remaining edges is a candidate for

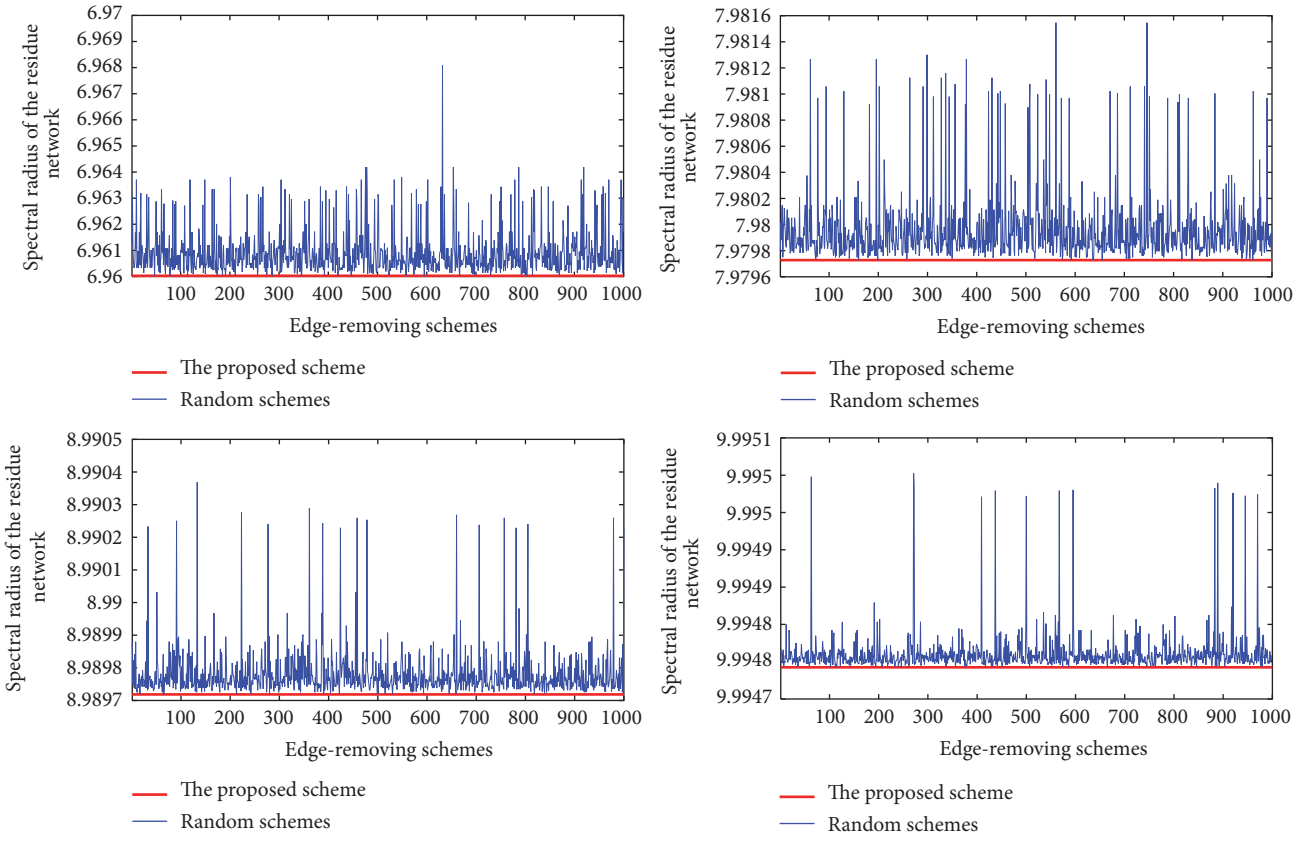

Figure 6: The proposed candidate (red) versus 10^3 random candidates (blue).

the second deleted edge. The spectral radius of the surviving network formed by deleting each of the candidate edges from H_5 is shown in Figure 3. It can be seen that the larger the distance between the two edges, the smaller the spectral radius of the surviving network. At the extreme, the proposed candidate is optimal.

For $8 \leq n \leq 11$, the proposed candidate is compared with 10^3 random candidates in terms of the spectral radius of the surviving network; see Figure 4. It is concluded that the proposed candidate is optimal among these candidates.

Therefore, we propose the following conjecture.

Conjecture 1. *For all $n \geq 2$, the proposed candidate is an optimal solution to the SRMP-H2.*

3.2. Deleting Three Edges. Secondly, we consider a subproblem of the SRMP problem, denoted by SRMP-H3, for which three edges will be removed from a hypercube. Let us present a candidate for the optimal solution to the SRMP-H3 as follows, where n denotes the dimension of the hypercube, $c = \lfloor (n+1)/3 \rfloor$:

$$\begin{aligned} e_1 &= \left\{0^n, 0^{n-1}1\right\}, \\ e_2 &= \left\{0^{n-2c}1^{2c}, 0^{n-2c-1}1^{2c+1}\right\}, \\ e_3 &= \left\{1^{n-c-1}0^{c+1}, 1^{n-c}0^c\right\}. \end{aligned} \tag{2}$$

Figure 5 shows the proposed candidate in H_3, H_4, H_5, and H_6, respectively.

For $2 \leq n \leq 6$, it follows by exhaustive search that the proposed candidate is optimal. For $7 \leq n \leq 10$, the proposed candidate is compared with 10^3 random candidates; see Figure 6. It is concluded that the proposed candidate is optimal among these candidates. Therefore, we propose the following conjecture.

Conjecture 2. *For all $n \geq 3$, the proposed candidate is an optimal solution to the SRMP-H3.*

3.3. Deleting Four Edges. Finally, consider a subproblem of the SRMP, denoted by SRMP-H4, for which four edges will be deleted from a hypercube. Let us present a candidate to the optimal solution to the SRMP-H4 as follows, where n denotes the dimension of the hypercube, $c = \lfloor (n-1)/3 \rfloor$:

If $n \equiv 0, 2 \bmod 3$, then

$$\begin{aligned} e_1 &= \left\{0^n, 0^{n-1}1\right\}, \\ e_2 &= \left\{0^{n-2c-2}1^{2c+2}, 0^{n-2c-2}1^{2c+1}0\right\}, \\ e_3 &= \left\{1^{n-2c-2}0^c1^{c+1}0, 1^{n-2c-2}0^c1^c0^2\right\}, \\ e_4 &= \left\{1^{n-c-2}0^{c+1}1, 1^{n-c-2}0^c1^2\right\}. \end{aligned} \tag{3}$$

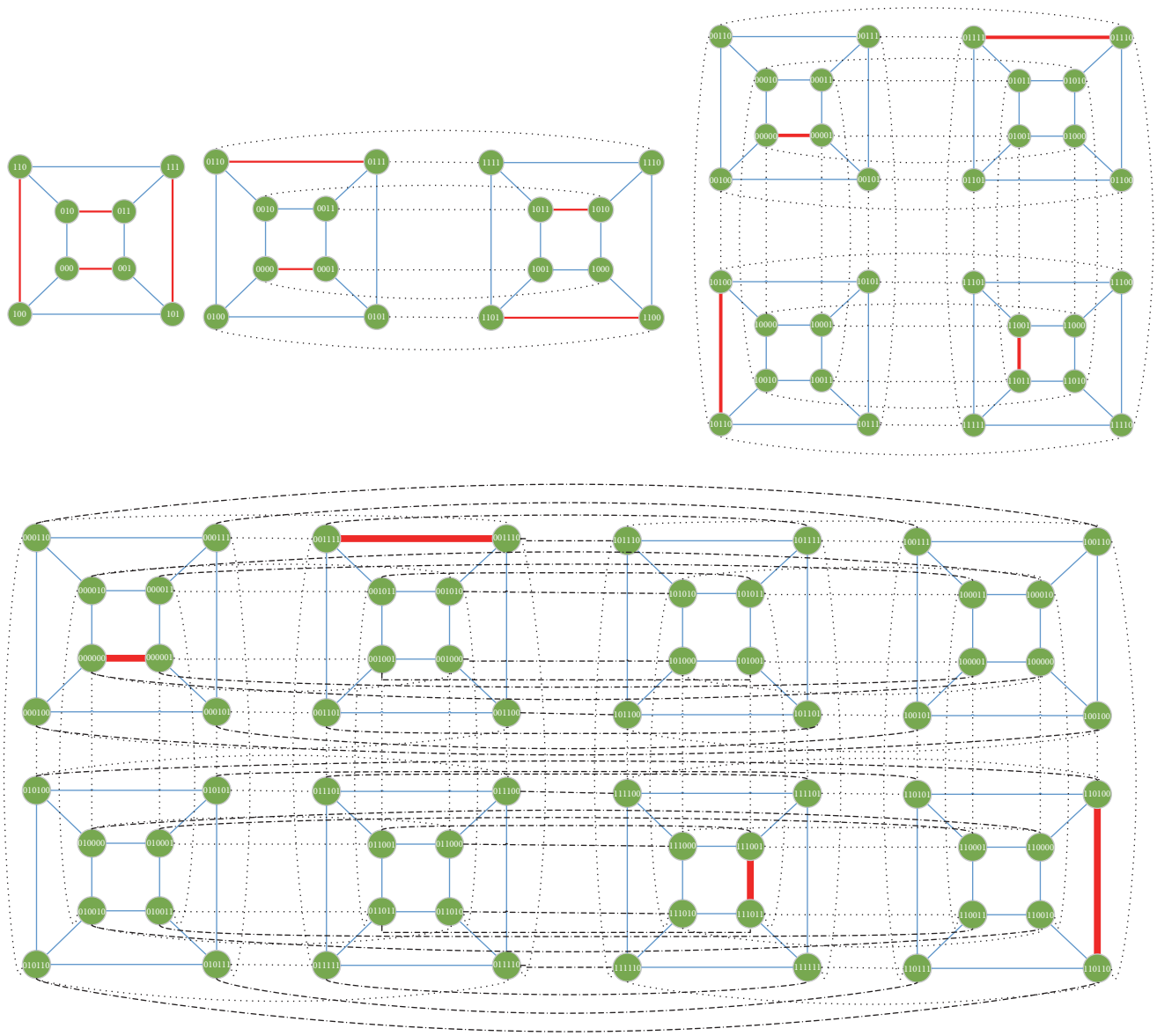

Figure 7: The proposed candidate in H_n.

If $n \equiv 1 \bmod 3$, then

$$\begin{aligned} e_1 &= \left\{0^n, 0^{n-1}1\right\}, \\ e_2 &= \left\{0^{n-2c-1}1^{2c+1}, 0^{n-2c-1}1^{2c}0\right\}, \\ e_3 &= \left\{1^{n-2c-1}0^c1^{c+1}, 1^{n-2c-1}0^c1^c0\right\}, \\ e_4 &= \left\{1^{n-c-1}0^{c+1}, 1^{n-c-1}0^c1\right\}. \end{aligned} \tag{4}$$

Figure 7 shows the proposed candidate in H_3, H_4, H_5, and H_6, respectively.

For $3 \leq n \leq 6$, it follows by exhaustive search that the proposed candidate is an optimal solution to the SRMP-H4 problem. For $7 \leq n \leq 10$, the proposed candidate is compared with 10^3 random candidates; see Figure 8. It is concluded that the proposed candidate is optimal among these candidates. Therefore, we propose the following conjecture.

Conjecture 3. *For all $n \geq 3$, the proposed candidate is an optimal solution to the SRMP-H4.*

4. Summary

This paper has addressed the spectral radius minimization problem for hypercubes. Given the number of edges to be deleted, a candidate for the optimal solution has been presented. For small-sized hypercubes, the proposed candidate has been shown to be optimal. For medium-sized hypercubes, it has been shown that the proposed candidate is likely to be optimal. Due to the symmetry of hypercubes, there are multiple optimal solutions for each of the subproblems. The

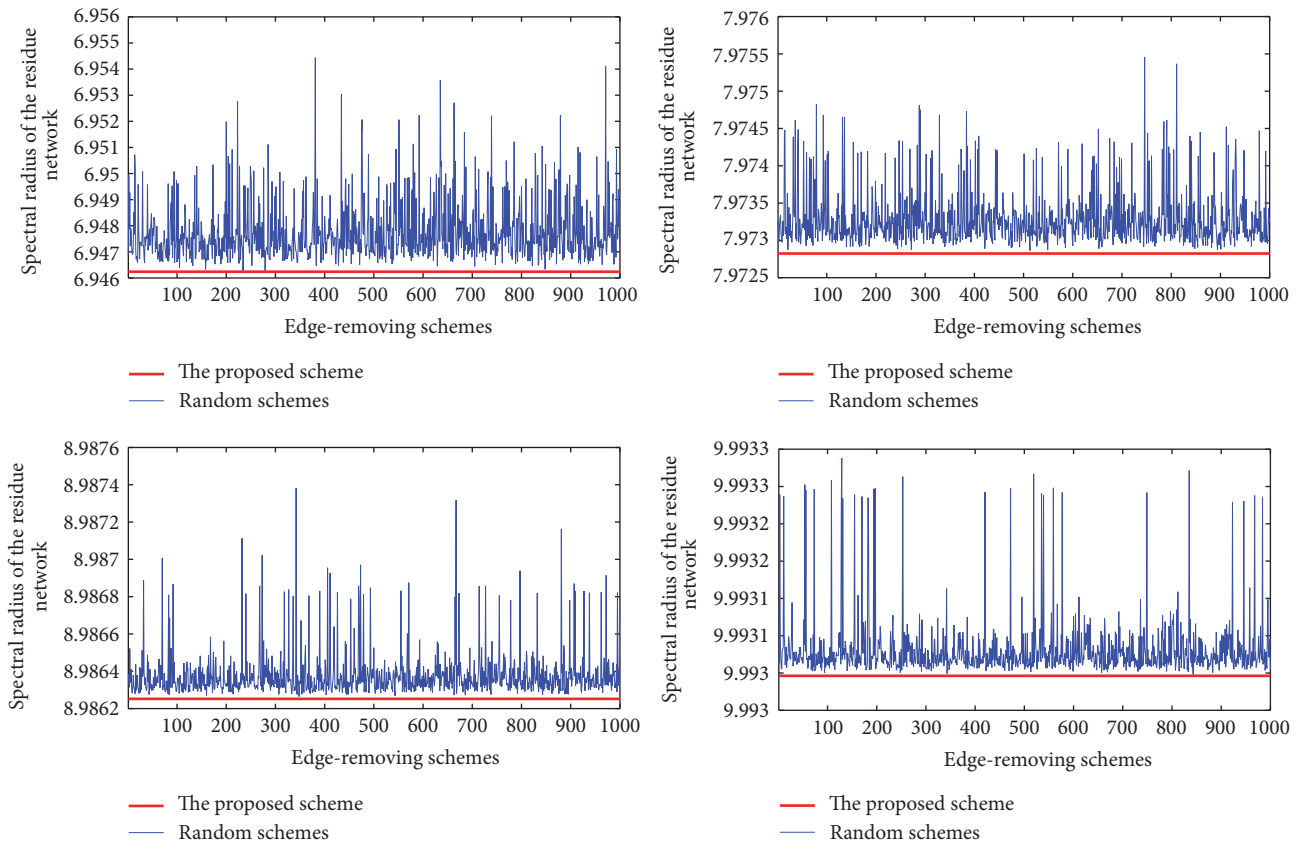

FIGURE 8: The proposed candidate (red) versus 10^3 random candidates (blue).

experimental results show that, up to isomorphism, all of the optimal solutions are identical. By observing the pattern of the proposed candidate, it has been speculated that, for any symmetric network, the edges in an optimal solution are always evenly distributed.

Towards this direction, some researches are yet to be done. First, the proposed conjectures need a proof. Second, this work should be extended to asymmetric networks such as the hypercube-like networks [40, 41], the small-world networks [42], the scale-free networks [43, 44], and the general networks [45, 46]. Last, the effectiveness of heuristics for the spectral radius minimization problem must be improved.

Conflicts of Interest

The authors declare that there are no conflicts of interest regarding the publication of this paper.

Acknowledgments

This work was supported by Science and Technology Support Program of China (Grant no. 2015BAF05B03), Natural Science Foundation of China (Grants nos. 61572006, 71301177), Basic and Advanced Research Program of Chongqing (Grant no. cstc2013jcyjA1658), and Fundamental Research Funds for the Central Universities (Grant no. 106112014CDJZR008823).

References

[1] Z. Ma, Y. Zhou, and J. Wu, *Modeling and Dynamics of Infectious Diseases*, Higher Education Press, Beijing, China, 2009.

[2] M. Draief and L. Massoulié, *Epidemics and Rumours in Complex Networks*, Cambridge University Press, 2010.

[3] J. O. Kephart and S. R. White, "Directed-graph epidemiological models of computer viruses," in *Proceedings of the IEEE Computer Society Symposium on Research of Security and Privacy*, pp. 343–359, 1991.

[4] J. O. Kephart, S. R. White, and D. M. Chess, "Computers and epidemiology," *IEEE Spectrum*, vol. 30, no. 5, pp. 20–26, 1993.

[5] C. Gao, J. Liu, and N. Zhong, "Network immunization with distributed autonomy-oriented entities," *IEEE Transactions on Parallel and Distributed Systems*, pp. 1222–1229, 2011.

[6] L.-X. Yang, X. Yang, J. Liu, Q. Zhu, and C. Gan, "Epidemics of computer viruses: a complex-network approach," *Applied Mathematics and Computation*, vol. 219, no. 16, pp. 8705–8717, 2013.

[7] C. Gao and J. Liu, "Modeling and restraining mobile virus propagation," *IEEE Transactions on Mobile Computing*, vol. 12, no. 3, pp. 529–541, 2013.

[8] L.-X. Yang and X. Yang, "A novel virus-patch dynamic model," *PLoS ONE*, vol. 10, no. 9, Article ID e0137858, 2015.

[9] M. Draief, A. Ganesh, and L. Massoulié, "Thresholds for virus spread on networks," *The Annals of Applied Probability*, vol. 18, no. 2, pp. 359–378, 2008.

[10] P. Van Mieghem, J. Omic, and R. Kooij, "Virus spread in networks," *IEEE/ACM Transactions on Networking*, vol. 17, no. 1, pp. 1–14, 2009.

[11] P. Van Mieghem, "The N-intertwined SIS epidemic network model," *Computing*, vol. 93, no. 2–4, pp. 147–169, 2011.

[12] F. D. Sahneh, F. N. Chowdhury, and C. M. Scoglio, "On the existence of a threshold for preventive behavioral responses to suppress epidemic spreading," *Scientific Reports*, vol. 2, article 00632, 2012.

[13] F. D. Sahneh, C. Scoglio, and P. Van Mieghem, "Generalized epidemic mean-field model for spreading processes over multilayer complex networks," *IEEE/ACM Transactions on Networking*, vol. 21, no. 5, pp. 1609–1620, 2013.

[14] L. X. Yang and X. Yang, "The effect of network topology on the spread of computer viruses: a modelling study," *International Journal of Computer Mathematics*, 2016.

[15] P. Van Mieghem, D. Stevanović, F. Kuipers et al., "Decreasing the spectral radius of a graph by link removals," *Physical Review E —Statistical, Nonlinear, and Soft Matter Physics*, vol. 84, no. 1, Article ID 016101, 2011.

[16] J. G. Restrepo, E. Ott, and B. R. Hunt, "Approximating the largest eigenvalue of network adjacency matrices," *Physical Review E. Statistical, Nonlinear, and Soft Matter Physics*, vol. 76, no. 5, 056119, 6 pages, 2007.

[17] A. Milanese, J. Sun, and T. Nishikawa, "Approximating spectral impact of structural perturbations in large networks," *Physical Review E - Statistical, Nonlinear, and Soft Matter Physics*, vol. 81, no. 4, Article ID 046112, 2010.

[18] P. Van Mieghem, H. Wang, X. Ge, S. Tang, and F. A. Kuipers, "Influence of assortativity and degree-preserving rewiring on the spectra of networks," *European Physical Journal B*, vol. 76, no. 4, pp. 643–652, 2010.

[19] C. Li, H. Wang, and P. Van Mieghem, "Degree and principal eigenvectors in complex networks," *Lecture Notes in Computer Science (including subseries Lecture Notes in Artificial Intelligence and Lecture Notes in Bioinformatics)*, vol. 7289, no. 1, pp. 149–160, 2012.

[20] X. Yang, P. Li, L.-X. Yang, and Y. Wu, "Reducing the spectral radius of a torus network by link removal," *PLoS ONE*, vol. 11, no. 5, Article ID e0155580, 2016.

[21] J. Xu, *A First Course in Graph Theory*, Science Press, 2015.

[22] Y. Saad and M. H. Schultz, "Data communication in hypercubes," *Journal of Parallel and Distributed Computing*, vol. 6, no. 1, pp. 115–135, 1989.

[23] T. Bier and K.-F. Loe, "Embedding of binary trees into hypercubes," *Journal of Parallel and Distributed Computing*, vol. 6, no. 3, pp. 679–691, 1989.

[24] V. Heun and E. W. Mayr, "Efficient dynamic embeddings of binary trees into hypercubes," *Journal of Algorithms. Cognition, Informatics and Logic*, vol. 43, no. 1, pp. 51–84, 2002.

[25] C.-N. Lai, "Optimal construction of all shortest node-disjoint paths in hypercubes with applications," *IEEE Transactions on Parallel and Distributed Systems*, vol. 23, no. 6, pp. 1129–1134, 2012.

[26] P. J. Yang, S. B. Tien, and C. S. Raghavendra, "Reconfiguration of rings and meshes in faulty hypercubes," *Journal of Parallel and Distributed Computing*, vol. 22, no. 1, pp. 96–106, 1994.

[27] D. Xiang, Y. Zhang, and J.-G. Sun, "Unicast-based fault-tolerant multicasting in wormhole-routed hypercubes," *Journal of Systems Architecture*, vol. 54, no. 12, pp. 1164–1178, 2008.

[28] W. Yang and J. Meng, "Generalized measures of fault tolerance in hypercube networks," *Applied Mathematics Letters*, vol. 25, no. 10, pp. 1335–1339, 2012.

[29] T.-L. Kung, C.-K. Lin, and L.-H. Hsu, "On the maximum number of fault-free mutually independent Hamiltonian cycles in the faulty hypercube," *Journal of Combinatorial Optimization*, vol. 27, no. 2, pp. 328–344, 2014.

[30] J.-J. Liu and Y.-L. Wang, "Hamiltonian cycles in hypercubes with faulty edges," *Information Sciences. An International Journal*, vol. 256, pp. 225–233, 2014.

[31] S.-L. Peng, C.-K. Lin, J. J. Tan, and L.-H. Hsu, "The g-good-neighbor conditional diagnosability of hypercube under PMC model," *Applied Mathematics and Computation*, vol. 218, no. 21, pp. 10406–10412, 2012.

[32] M.-C. Yang, "Conditional diagnosability of matching composition networks under the MM* model," *Information Sciences*, vol. 233, pp. 230–243, 2013.

[33] C.-K. Lin, T.-L. Kung, and J. J. Tan, "An algorithmic approach to conditional-fault local diagnosis of regular multiprocessor interconnected systems under the PMC model," *IEEE Transactions on Computers*, vol. 62, no. 3, pp. 439–451, 2013.

[34] P.-L. Lai, "Adaptive system-level diagnosis for hypercube multiprocessors using a comparison model," *Information Sciences*, vol. 252, pp. 118–131, 2013.

[35] K. W. Ryu and J. Jájá, "Efficient algorithms for list ranking and for solving graph problems on the hypercube," *IEEE Transactions on Parallel and Distributed Systems*, vol. 1, no. 1, pp. 83–90, 1990.

[36] O. H. Ibarra and M. H. Kim, "Fast parallel algorithms for solving triangular systems of linear equations on the hypercube," *Journal of Parallel and Distributed Computing*, vol. 20, no. 3, pp. 303–316, 1994.

[37] A. Grama, A. Gupta, G. Karypis, and V. Kumar, *Introduction to Parallel Computing*, The Benjamin/Cummings Publishing Company, Inc., 2nd edition, 1994.

[38] P. Van Mieghem, *Graph Spectra for Complex Networks*, Cambridge University Press, 2012.

[39] D. Stevanovic, *Spectral Radius of Graphs*, Elsevier, 2015.

[40] J. Fan, X. Jia, X. Liu, S. Zhang, and J. Yu, "Efficient unicast in bijective connection networks with the restricted faulty node set," *Information Sciences*, vol. 181, no. 11, pp. 2303–2315, 2011.

[41] J. Fan, X. Jia, B. Cheng, and J. Yu, "An efficient fault-tolerant routing algorithm in bijective connection networks with restricted faulty edges," *Theoretical Computer Science*, vol. 412, no. 29, pp. 3440–3450, 2011.

[42] D. J. Watts and S. H. Strogatz, "Collective dynamics of 'small-world' networks," *Nature*, vol. 393, no. 6684, pp. 440–442, 1998.

[43] A.-L. Barabási and R. Albert, "Emergence of scaling in random networks," *American Association for the Advancement of Science. Science*, vol. 286, no. 5439, pp. 509–512, 1999.

[44] R. Albert and A.-L. Barabási, "Statistical mechanics of complex networks," *Reviews of Modern Physics*, vol. 74, no. 1, pp. 47–97, 2002.

[45] L.-X. Yang, M. Draief, and X. Yang, "The impact of the network topology on the viral prevalence: a node-based approach," *PLoS ONE*, vol. 10, no. 7, Article ID e0134507, 2015.

[46] L.-X. Yang, X. Yang, and Y. Wu, "The impact of patch forwarding on the prevalence of computer virus: a theoretical assessment approach," *Applied Mathematical Modelling. Simulation and Computation for Engineering and Environmental Systems*, vol. 43, pp. 110–125, 2017.

Hindawi
Discrete Dynamics in Nature and Society
Volume 2017, Article ID 3536125, 17 pages
https://doi.org/10.1155/2017/3536125

Research Article

Stability and Hopf Bifurcation Analysis for a Computer Virus Propagation Model with Two Delays and Vaccination

Zizhen Zhang,[1] Yougang Wang,[1] Dianjie Bi,[1] and Luca Guerrini[2]

[1]*School of Management Science and Engineering, Anhui University of Finance and Economics, Bengbu 233030, China*
[2]*Department of Management, Marche Polytechnic University, Piazza Martelli 8, 60121 Ancona, Italy*

Correspondence should be addressed to Zizhen Zhang; zzzhaida@163.com

Received 5 January 2017; Accepted 23 February 2017; Published 20 March 2017

Academic Editor: Lu-Xing Yang

Copyright © 2017 Zizhen Zhang et al. This is an open access article distributed under the Creative Commons Attribution License, which permits unrestricted use, distribution, and reproduction in any medium, provided the original work is properly cited.

A further generalization of an SEIQRS-V (susceptible-exposed-infectious-quarantined-recovered-susceptible with vaccination) computer virus propagation model is the main topic of the present paper. This paper specifically analyzes effects on the asymptotic dynamics of the computer virus propagation model when two time delays are introduced. Sufficient conditions for the asymptotic stability and existence of the Hopf bifurcation are established by regarding different combination of the two delays as the bifurcation parameter. Moreover, explicit formulas that determine the stability, direction, and period of the bifurcating periodic solutions are obtained with the help of the normal form theory and center manifold theorem. Finally, numerical simulations are employed for supporting the obtained analytical results.

1. Introduction

Computer viruses, including conventional viruses and network worms, can propagate among computers with no human awareness and popularization of Internet has been the major propagation channel of viruses [1, 2]. The past few decades have witnessed the great financial losses caused by computer viruses. Therefore, it is of considerable importance to investigate the laws describing propagation of computer viruses in order to provide some help with preventing computer viruses. For that purpose and in view of the fact that propagation of computer viruses among computers resembles that of biological viruses among a population, many dynamical models describing propagation of computer viruses across the Internet have been established by the scholars at home and abroad, such as conventional models [3–8], stochastic models [9–12], and delayed models [13–18]. There are also some other computer virus models [19–21] combined with network theory to investigate the impact of the network topology, the patch forwarding, and the network eigenvalue on the viral prevalence.

As is known, vaccination is regarded as one of the most effective measures of preventing computer viruses and the awareness that there exist many infected computers would enhance the probability that the user of a susceptible computer will make his computer vaccinated [22, 23]. However, the mentioned models above neglect the influence of vaccination strategy on the propagation of computer viruses. Recently, considering the importance of vaccination, Kumar et al. [24] proposed the following SEIQRS-V computer virus propagation model:

$$\begin{aligned}
\frac{dS(t)}{dt} &= A - \beta S(t) I(t) - dS(t) - \rho S(t) + \theta R(t) \\
&\quad + \chi V(t), \\
\frac{dE(t)}{dt} &= \beta S(t) I(t) - dE(t) - \gamma E(t), \\
\frac{dI(t)}{dt} &= \gamma E(t) - dI(t) - \alpha I(t) - \delta I(t) - \eta I(t), \\
\frac{dQ(t)}{dt} &= \delta I(t) - dQ(t) - \alpha Q(t) - \varepsilon Q(t), \\
\frac{dR(t)}{dt} &= \varepsilon Q(t) - dR(t) - \theta R(t) + \eta I(t), \\
\frac{dV(t)}{dt} &= \rho S(t) - dV(t) - \chi V(t),
\end{aligned} \tag{1}$$

where $S(t)$, $E(t)$, $I(t)$, $Q(t)$, $R(t)$, and $V(t)$ denote the numbers of the uninfected computers, the exposed computers, the infected computers, the quarantined computers, recovered computers, and vaccinated computers at time t, respectively. A is the birth rate of new computers in the network; d is the death rate of the computers due to the reason other than the attack of viruses; α is the death rate of computers due to the attack of viruses; β is the contact rate of the uninfected computers; ρ, θ, χ, γ, δ, η, and ε are the transition rates between the states in system (1).

Obviously, system (1) neglects the delays in the procedure of viruses' propagation and it is investigated under the assumption that the transition between the states is instantaneous. This is not reasonable with reality. For example, it needs a period to clean the viruses in the infected and quarantined computers for antivirus software and there is usually a temporary immunity period for the recovered and the vaccinated computers because of the effect of the antivirus software. In addition, a stability switch occurs even when an ignored delay is small for a dynamical system. Based on this, we introduce two delays into system (1) and get the following delayed system:

$$\begin{aligned}
\frac{dS(t)}{dt} &= A - \beta S(t) I(t) - dS(t) - \rho S(t) + \theta R(t-\tau_2) \\
&\quad + \chi V(t-\tau_2), \\
\frac{dE(t)}{dt} &= \beta S(t) I(t) - dE(t) - \gamma E(t), \\
\frac{dI(t)}{dt} &= \gamma E(t) - dI(t) - \alpha I(t) - \delta I(t) - \eta I(t-\tau_1), \\
\frac{dQ(t)}{dt} &= \delta I(t) - dQ(t) - \alpha Q(t) - \varepsilon Q(t-\tau_1), \\
\frac{dR(t)}{dt} &= \varepsilon Q(t-\tau_1) - dR(t) - \theta R(t-\tau_2) \\
&\quad + \eta I(t-\tau_1), \\
\frac{dV(t)}{dt} &= \rho S(t) - dV(t) - \chi V(t-\tau_2),
\end{aligned} \tag{2}$$

where τ_1 is the time delay due to the period that antivirus software uses to clean the viruses in the infected and quarantined computers and τ_2 is the time delay due to the temporary immunity period of the recovered and the vaccinated computers.

To the best of our knowledge, until now, there is no good analysis on system (2). Therefore, it is meaningful to analyze the proposed system with two delays.

The rest of this paper is organized as follows. In the next section, we analyze the threshold of Hopf bifurcation of system (2) by regarding different combination of the two delays as the bifurcation parameter. In Section 3, by means of the normal form theory and center manifold theorem, direction and stability of the Hopf bifurcation for $\tau_1 > 0$ and $\tau_2 > 0$ are investigated. Simulation results of system (2) are shown in Section 4. Finally, we finish the paper with conclusions in Section 5.

2. Analysis of Hopf Bifurcation

By direct computation, we know that if $AR_0(d+\chi) > d^2 + (\rho+\chi)d$ and $\beta(d+\theta)(d+\alpha+\varepsilon) > R_0\theta\varepsilon\delta + R_0\theta\eta(d+\alpha+\varepsilon)$, then system (2) has a unique viral equilibrium $P_*(S_*, E_*, I_*, Q_*, R_*, V_*)$, where

$$\begin{aligned}
S_* &= \frac{(d+\gamma)(d+\alpha+\delta+\eta)}{\beta\gamma} = \frac{1}{R_0}, \\
E_* &= \frac{d+\alpha+\delta+\eta}{\gamma} I_*, \\
R_* &= \frac{\varepsilon\delta + \eta(d+\alpha+\varepsilon)}{(d+\theta)(d+\alpha+\varepsilon)} I_*, \\
V_* &= \frac{\rho}{(d+\chi)R_0}, \\
Q_* &= \frac{\delta}{d+\alpha+\varepsilon} I_*, \\
I_* &= \frac{(d+\theta)(d+\alpha+\varepsilon)\left[d^2 + (\rho+\chi)d - AR_0(d+\chi)\right]}{(d+\chi)\left[R_0\theta\varepsilon\delta + (d+\alpha+\varepsilon)(R_0\theta\eta - \beta d - \beta\theta)\right]}, \\
R_0 &= \frac{\beta\gamma}{(d+\gamma)(d+\alpha+\delta+\eta)}.
\end{aligned} \tag{3}$$

The linearized section of system (2) at $P_*(S_*, E_*, I_*, Q_*, R_*, V_*)$ is as follows:

$$\begin{aligned}
\frac{dS(t)}{dt} &= a_1 S(t) + a_2 I(t) + c_1 R(t-\tau_2) + c_2 V(t-\tau_2), \\
\frac{dE(t)}{dt} &= a_3 S(t) + a_4 E(t) + a_5 I(t), \\
\frac{dI(t)}{dt} &= a_6 E(t) - a_7 I(t) + b_1 I(t-\tau_1), \\
\frac{dQ(t)}{dt} &= a_8 I(t) + a_9 Q(t) + b_2 Q(t-\tau_1), \\
\frac{dR(t)}{dt} &= a_{10} R(t) + b_3 I(t-\tau_1) + b_4 Q(t-\tau_1) \\
&\quad + c_3 R(t-\tau_2), \\
\frac{dV(t)}{dt} &= a_{11} S(t) + a_{12} V(t) + c_4 V(t-\tau_2),
\end{aligned} \tag{4}$$

where

$$\begin{aligned}
a_1 &= -(\beta I_* + d + \rho), \\
a_2 &= -\beta S_*, \\
a_3 &= \beta I_*, \\
a_4 &= -(d+\gamma),
\end{aligned}$$

$$
\begin{aligned}
a_5 &= \beta S_*, \\
a_6 &= \gamma, \\
a_7 &= -(d+\alpha+\delta), \\
a_8 &= \delta, \\
a_9 &= -(d+\alpha), \\
a_{10} &= -d, \\
a_{11} &= \rho, \\
a_{12} &= -d, \\
b_1 &= -\eta, \\
b_2 &= -\varepsilon, \\
b_3 &= \eta, \\
b_4 &= \varepsilon, \\
c_1 &= \theta, \\
c_2 &= \chi, \\
c_3 &= -\theta, \\
c_4 &= -\chi.
\end{aligned} \tag{5}
$$

Then, the characteristic equation for system (4) can be obtained:

$$
\begin{aligned}
&\lambda^6 + A_5\lambda^5 + A_4\lambda^4 + A_3\lambda^3 + A_2\lambda^2 + A_1\lambda + A_0 \\
&\quad + \left(B_5\lambda^5 + B_4\lambda^4 + B_3\lambda^3 + B_2\lambda^2 + B_1\lambda + B_0\right)e^{-\lambda\tau_1} \\
&\quad + \left(C_5\lambda^5 + C_4\lambda^4 + C_3\lambda^3 + C_2\lambda^2 + C_1\lambda + C_0\right)e^{-\lambda\tau_2} \\
&\quad + \left(D_4\lambda^4 + D_3\lambda^3 + D_2\lambda^2 + D_1\lambda + D_0\right)e^{-\lambda(\tau_1+\tau_2)} \\
&\quad + \left(E_3\lambda^3 + E_2\lambda^2 + E_1\lambda + E_0\right)e^{-\lambda(\tau_1+2\tau_2)} \\
&\quad + \left(F_4\lambda^4 + F_3\lambda^3 + F_2\lambda^2 + F_1\lambda + F_0\right)e^{-2\lambda\tau_1} \\
&\quad + \left(G_4\lambda^4 + G_3\lambda^3 + G_2\lambda^2 + G_1\lambda + G_0\right)e^{-2\lambda\tau_2} \\
&\quad + \left(H_3\lambda^3 + H_2\lambda^2 + H_1\lambda + H_0\right)e^{-\lambda(2\tau_1+\tau_2)} \\
&\quad + \left(I_2\lambda^2 + I_1\lambda + I_0\right)e^{-2\lambda(\tau_1+\tau_2)} = 0,
\end{aligned} \tag{6}
$$

with

$$
\begin{aligned}
A_0 &= a_9a_{12}\left(a_1a_4a_7a_{10} + a_2a_3a_6a_{10} - a_1a_5a_6a_{10} - a_3a_6b_3c_1\right), \\
A_1 &= a_5a_6\left(a_1a_9\left(a_{10}+a_{12}\right) + a_{10}a_{12}\left(a_1+a_9\right)\right) + a_3a_6b_3c_1\left(a_9+a_{12}\right) - a_2a_3a_6\left(a_9a_{10} + a_9a_{12} + a_{10}a_{12}\right) - a_1a_4a_7a_9\left(a_{10}+a_{12}\right) - a_{10}a_{12}\left(a_1a_4\left(a_7+a_9\right) + a_7a_9\left(a_1+a_4\right)\right), \\
A_2 &= a_2a_3a_6\left(a_9+a_{10}+a_{12}\right) + a_1a_4a_7a_9 - a_3a_6b_3c_1 - a_5a_6\left(a_1a_9 + a_{10}a_{12} + \left(a_1+a_9\right)\left(a_{10}+a_{12}\right)\right) + a_{10}a_{12}\left(a_1a_4 + a_7a_9 + \left(a_1+a_4\right)\left(a_7+a_9\right)\right) + \left(a_{10}+a_{12}\right)\left(a_1a_4\left(a_7+a_9\right) + a_7a_9\left(a_1+a_4\right)\right), \\
A_3 &= a_5a_6\left(a_1+a_9+a_{10}+a_{12}\right) - a_2a_3a_6 - a_1a_4\left(a_7+a_9\right) - a_7a_9\left(a_1+a_4\right) - a_{10}a_{12}\left(a_1+a_4+a_7+a_9\right) - \left(a_{10}+a_{12}\right)\left(a_1a_4 + a_7a_9 + \left(a_1+a_4\right)\left(a_7+a_9\right)\right), \\
A_4 &= a_1a_4 + a_7a_9 + a_{10}a_{12} - a_5a_6 + \left(a_1+a_4\right)\left(a_7+a_9\right) + \left(a_{10}+a_{12}\right)\left(a_1+a_4+a_7+a_9\right), \\
A_5 &= -\left(a_1+a_4+a_7+a_9+a_{10}+a_{12}\right), \\
B_0 &= a_1a_4a_{10}a_{12}\left(a_7b_2 + a_9b_1\right) - a_6a_{10}a_{12}b_2\left(a_1a_5 + a_2a_3\right), \\
B_1 &= a_5a_6b_2\left(a_1a_{10} + a_1a_{12} + a_{10}a_{12}\right) - a_2a_3a_6b_2\left(a_{10}+a_{12}\right) - \left(a_7b_2 + a_9b_1\right)\left(a_1a_4\left(a_{10}+a_{12}\right) + a_{10}a_{12}\left(a_1+a_4\right)\right) - a_1a_4a_{10}a_{12}\left(b_1+b_2\right) \\
B_2 &= \left(a_7b_2 + a_9b_1\right)\left(a_1a_4 + a_{10}a_{12} + \left(a_1+a_4\right)\left(a_{10}+a_{12}\right)\right) + a_2a_3a_6b_2 + \left(b_1+b_2\right)\cdot\left(a_1a_4\left(a_{10}+a_{12}\right) + a_{10}a_{12}\left(a_1+a_4\right)\right), \\
B_3 &= a_5a_6b_2 - \left(a_7b_2 + a_9b_1\right)\left(a_1+a_4+a_{10}+a_{12}\right) - \left(b_1+b_2\right)\left(a_1a_4 + a_{10}a_{12} + \left(a_1+a_4\right)\left(a_{10}+a_{12}\right)\right), \\
B_4 &= a_7b_2 + a_9b_1 + \left(b_1+b_2\right)\left(a_1+a_4+a_{10}+a_{12}\right), \\
B_5 &= -\left(b_1+b_2\right), \\
C_0 &= a_1a_4a_7a_9\left(a_{10}c_4 + a_{12}c_3\right) + a_9a_{10}a_{11}c_2\left(a_4a_7 - a_5a_6\right) + a_6a_9\left(a_{10}c_4 + a_{12}c_3\right)\left(a_2a_3 - a_1a_5\right), \\
C_1 &= a_9\left(c_3+c_4\right)\left(a_1a_5a_6 - a_2a_3a_6 - a_1a_4a_7\right) + a_5a_6a_{11}c_2\left(a_9+a_{10}\right) + a_6\left(a_1a_5 - a_2a_3 + a_5a_9\right)\cdot\left(a_{10}c_4 + a_{12}c_3\right) - a_{11}c_2\left(a_4a_7\left(a_9+a_{10}\right) + a_9a_{10}\left(a_4+a_7\right)\right),
\end{aligned}
$$

$$
\begin{aligned}
C_2 &= (c_3 + c_4)(a_1a_4(a_7 + a_9) + a_7a_9(a_1 + a_4)) \\
&\quad + (a_{10}c_4 + a_{12}c_3)(a_1a_4 + a_7a_9 + (a_1 + a_4)(a_7 + a_9)) \\
&\quad - a_5a_6(a_{10}c_4 + a_{12}c_3 - a_{11}c_2) + a_6(c_3 + c_4)(a_2a_3 \\
&\quad - a_1a_5 - a_5a_9) + a_{11}c_2(a_4a_7 + a_9a_{10} \\
&\quad + (a_4 + a_7)(a_9 + a_{10})), \\
C_3 &= a_5a_6(c_3 + c_4) - a_{11}c_2(a_4 + a_7 + a_9 + a_{10}) - (a_{10}c_4 \\
&\quad + a_{12}c_3)(a_1 + a_4 + a_7 + a_9) - (c_3 + c_4)(a_1a_4 + a_7a_9 \\
&\quad + (a_1 + a_4)(a_7 + a_9)), \\
C_4 &= a_{10}c_4 + a_{11}c_2 + a_{12}c_3 + (c_3 + c_4)(a_1 + a_4 + a_7 \\
&\quad + a_9), \\
C_5 &= -(c_3 + c_4), \\
D_0 &= a_4(a_1a_{10}c_4 + a_1a_{12}c_3 + a_{10}a_{11}c_2)(a_7b_2 + a_9b_1) \\
&\quad + a_6(a_3a_8a_{12}b_4c_4 - a_5a_{10}a_{11}b_2c_2) - a_6b_2(a_1a_5 \\
&\quad - a_2a_3)(a_{10}c_4 + a_{12}c_3), \\
D_1 &= (c_3 + c_4)(a_5b_2(a_1a_5 - a_2a_3) - a_1a_4(a_7b_2 + a_9b_1)) \\
&\quad + a_6(a_5a_{11}b_2c_2 - a_3a_8b_4c_4) + a_5a_6b_2(a_{10}c_4 + a_{12}c_3) \\
&\quad - a_{11}c_2(a_4a_{10}(b_1 + b_2) + (a_4 + a_{10})(a_7b_2 + a_9b_1)) \\
&\quad - (a_{10}c_4 + a_{12}c_3)(a_1a_4(b_1 + b_2) \\
&\quad + (a_1 + a_4)(a_7b_2 + a_9b_1)), \\
D_2 &= (a_{10}c_4 + a_{12}c_3)(a_7b_2 + a_9b_1 + (b_1 + b_2)(a_1 + a_4)) \\
&\quad + (c_3 + c_4)(a_1a_4(b_1 + b_2) + (a_1 + a_4)(a_7b_2 + a_9b_1)) \\
&\quad + a_{11}c_2(a_7b_2 + a_9b_1 + (a_4 + a_{10})(b_1 + b_2)) \\
&\quad - a_5a_6b_2(c_3 + c_4), \\
D_3 &= -(c_3 + c_4)(a_7b_2 + a_9b_1 + (b_1 + b_2)(a_1 + a_4)) \\
&\quad - (b_1 + b_2)(a_{10}c_4 + a_{11}c_2 + a_{12}c_3), \\
D_4 &= (b_1 + b_2)(c_3 + c_4), \\
E_0 &= a_4c_3(a_7b_2 + a_9b_1)(a_1c_4 + a_{11}c_2) + a_6b_2c_3c_4(a_2a_3 \\
&\quad - a_1a_5) - a_6(a_3a_9b_3c_1c_4 + a_5a_{11}b_2c_2c_3), \\
E_1 &= a_6c_4(a_5b_2c_3 + a_3b_3c_1) - a_{11}c_2c_3(b_1(a_4 + a_9) \\
&\quad + b_2(a_4 + a_7)) - c_3c_4(a_1a_4(b_1 + b_2) \\
&\quad + (a_1 + a_4)(a_7b_2 + a_9b_1)), \\
E_2 &= c_3c_4(a_7b_2 + a_9b_1 + (a_1 + a_4)(b_1 + b_2)) \\
&\quad + a_{11}c_2c_3(b_1 + b_2), \\
E_3 &= -c_3c_4(b_1 + b_2), \\
F_0 &= a_1a_4a_{10}a_{12}b_1b_2, \\
F_1 &= -b_1b_2(a_1a_4(a_{10} + a_{12}) + a_{10}a_{12}(a_1 + a_4)), \\
F_2 &= b_1b_2(a_1a_4 + a_{10}a_{12} + (a_1 + a_4)(a_{10} + a_{12})), \\
F_3 &= -b_1b_2(a_1 + a_4 + a_{10} + a_{12}), \\
F_4 &= b_1b_2, \\
G_0 &= a_9c_3c_4(a_1a_4a_7 - a_1a_5a_6 + a_2a_3a_6) \\
&\quad + a_4a_7a_9a_{11}c_2c_3, \\
G_1 &= a_{11}c_2c_3(a_4a_7 + a_4a_9 + a_7a_9) + a_5a_6c_3c_4(a_1 + a_9) \\
&\quad - c_3c_4(a_1a_4(a_7 + a_9) + a_7a_9(a_1 + a_4)), \\
G_2 &= c_3c_4(a_1a_4 + a_7a_9 + (a_1 + a_4)(a_7 + a_9)) \\
&\quad + a_{11}c_2c_3(a_4 + a_7 + a_9) - a_5a_6c_3c_4, \\
G_3 &= c_3c_4(a_1 + a_4 + a_7 + a_9) + a_{11}c_2c_3, \\
G_4 &= c_3c_4, \\
H_0 &= a_4b_1b_2(a_1(a_{10}c_4 + a_{12}c_3) + a_{10}a_{11}c_2) \\
&\quad - a_3a_6a_{12}b_2b_3c_1, \\
H_1 &= a_3a_6b_2b_3c_1 - b_1b_2(a_1a_4(c_3 + c_4) \\
&\quad + a_{11}c_2(a_4 + a_{10})) - b_1b_2(a_1 + a_4)(a_{10}c_4 + a_{12}c_3), \\
H_2 &= b_1b_2(a_{10}c_4 + a_{11}c_2 + a_{12}c_3 + (a_1 + a_4)(c_3 + c_4)), \\
H_3 &= -b_1b_2(c_3 + c_4), \\
I_0 &= a_4b_1b_2c_3(a_{11}c_2 + a_1c_4) - a_3a_6b_2b_3c_1c_4, \\
I_1 &= b_1b_2c_3c_4(a_1 + a_4) + a_{11}b_1b_2c_2c_3, \\
I_2 &= b_1b_2c_3c_4.
\end{aligned} \tag{7}
$$

Case 1 ($\tau_1 = \tau_2 = 0$). When $\tau_1 = \tau_2 = 0$, (6) becomes

$$
\begin{aligned}
&\lambda^6 + A_{15}\lambda^5 + A_{14}\lambda^4 + A_{13}\lambda^3 + A_{12}\lambda^2 + A_{11}\lambda + A_{10} \\
&\quad = 0,
\end{aligned} \tag{8}
$$

where

$$
\begin{aligned}
A_{10} &= A_0 + B_0 + C_0 + D_0 + E_0 + F_0 + G_0 + H_0 + I_0, \\
A_{11} &= A_1 + B_1 + C_1 + D_1 + E_1 + F_1 + G_1 + H_1 + I_1, \\
A_{12} &= A_2 + B_2 + C_2 + D_2 + E_2 + F_2 + G_2 + H_2 + I_2, \\
A_{13} &= A_3 + B_3 + C_3 + D_3 + E_3 + F_3 + G_3 + H_3, \\
A_{14} &= A_4 + B_4 + C_4 + D_4 + E_4 + F_4 + G_4, A_{15} \\
&\quad = A_5 + B_5 + C_5.
\end{aligned} \tag{9}
$$

Clearly, $D_1 = A_{15} = \beta I_* + \rho + \gamma + \delta + \eta + \varepsilon + \theta + \chi + 2\alpha + 6d > 0$. Thus, if condition (H_1) (see (10)) holds, then system (2) without delay is locally asymptotically stable:

$$
\begin{aligned}
D_2 &= \det\begin{pmatrix} A_{15} & 1 \\ A_{13} & A_{14} \end{pmatrix} > 0,\\
D_3 &= \det\begin{pmatrix} A_{15} & 1 & 0 \\ A_{13} & A_{14} & A_{15} \\ A_{11} & A_{12} & A_{13} \end{pmatrix} > 0,\\
D_4 &= \det\begin{pmatrix} A_{05} & 1 & 0 & 0 \\ A_{03} & A_{14} & A_{15} & 1 \\ A_{01} & A_{12} & A_{13} & A_{14} \\ 0 & A_{10} & A_{11} & A_{12} \end{pmatrix} > 0,\\
D_5 &= \det\begin{pmatrix} A_{15} & 1 & 0 & 0 & 0 \\ A_{13} & A_{14} & A_{15} & 1 & 0 \\ A_{11} & A_{12} & A_{13} & A_{14} & A_{15} \\ 0 & A_{10} & A_{11} & A_{12} & A_{13} \\ 0 & 0 & 0 & A_{10} & A_{11} \end{pmatrix} > 0,\\
D_6 &= A_{10} > 0.
\end{aligned}
\tag{10}
$$

Case 2 ($\tau_1 > 0; \tau_2 = 0$). Equation (6) equals

$$
\begin{aligned}
&\lambda^6 + A_{25}\lambda^5 + A_{24}\lambda^4 + A_{23}\lambda^3 + A_{22}\lambda^2 + A_{21}\lambda + A_{20}\\
&\quad + \left(B_{25}\lambda^5 + B_{24}\lambda^4 + B_{23}\lambda^3 + B_{22}\lambda^2 + B_{21}\lambda + B_{20}\right)\\
&\quad \cdot e^{-\lambda\tau_1} + \left(F_{24}\lambda^4 + F_{23}\lambda^3 + F_{22}\lambda^2 + F_{21}\lambda + F_{20}\right)\\
&\quad \cdot e^{-2\lambda\tau_1} = 0,
\end{aligned}
\tag{11}
$$

where

$$
\begin{aligned}
A_{20} &= A_0 + C_0 + G_0,\\
A_{21} &= A_1 + C_1 + G_1,\\
A_{22} &= A_2 + C_2 + G_2,\\
A_{23} &= A_3 + C_3 + G_3,\\
A_{24} &= A_4 + C_4 + G_4,\\
A_{25} &= A_5 + G_5,\\
B_{20} &= B_0 + D_0 + E_0,\\
B_{21} &= B_1 + D_1 + E_1,\\
B_{22} &= B_2 + D_2 + E_2,\\
B_{23} &= B_3 + D_3 + E_3,\\
B_{24} &= B_4 + D_4 + E_4,\\
B_{25} &= B_5.
\end{aligned}
\tag{12}
$$

Multiplying $e^{\lambda\tau_1}$ on left and right of (11), one has

$$
\begin{aligned}
&B_{25}\lambda^5 + B_{24}\lambda^4 + B_{23}\lambda^3 + B_{22}\lambda^2 + B_{21}\lambda + B_{20} + \lambda^6\\
&\quad + \left(A_{25}\lambda^5 + A_{24}\lambda^4 + A_{23}\lambda^3 + A_{22}\lambda^2 + A_{21}\lambda\right.\\
&\quad \left. + A_{20}\right)e^{\lambda\tau_1} + \left(F_{24}\lambda^4 + F_{23}\lambda^3 + F_{22}\lambda^2 + F_{21}\lambda\right.\\
&\quad \left. + F_{20}\right)e^{-\lambda\tau_1} = 0.
\end{aligned}
\tag{13}
$$

Assume that $\lambda = i\omega_1$ ($\omega_1 > 0$) is the root of (13):

$$
\begin{aligned}
L_{21}(\omega_1)\cos\tau_1\omega_1 - L_{22}(\omega_1)\sin\tau_1\omega_1 &= L_{23}(\omega_1),\\
L_{24}(\omega_1)\sin\tau_1\omega_1 + L_{25}(\omega_1)\cos\tau_1\omega_1 &= L_{26}(\omega_1),
\end{aligned}
\tag{14}
$$

with

$$
\begin{aligned}
L_{21}(\omega_1) &= \left(A_{24} + F_{24}\right)\omega_1^4 - \omega_1^6 - \left(A_{22} + F_{22}\right)\omega_1^2\\
&\quad + A_{20} + F_{20},\\
L_{22}(\omega_1) &= A_{25}\omega_1^5 - \left(A_{23} - F_{23}\right)\omega_1^3 + \left(A_{21} - F_{21}\right)\omega_1,\\
L_{23}(\omega_1) &= B_{22}\omega_1^2 - B_{24}\omega_1^4 - B_{20},\\
L_{24}(\omega_1) &= \left(A_{24} - F_{24}\right)\omega_1^4 - \omega_1^6 - \left(A_{22} - F_{22}\right)\omega_1^2\\
&\quad + A_{20} - F_{20},\\
L_{25}(\omega_1) &= A_{25}\omega_1^5 - \left(A_{23} + F_{23}\right)\omega_1^3 + \left(A_{21} + F_{21}\right)\omega_1,\\
L_{26}(\omega_1) &= B_{23}\omega_1^3 - B_{25}\omega_1^5 - B_{21}\omega_1.
\end{aligned}
\tag{15}
$$

Thus, one can obtain the expressions of $\cos\tau_1\omega_1$ and $\sin\tau_1\omega_1$ as follows:

$$
\begin{aligned}
&\cos\tau_1\omega_1\\
&\quad = \frac{L_{22}(\omega_1)\times L_{26}(\omega_1) + L_{23}(\omega_1)\times L_{24}(\omega_1)}{L_{21}(\omega_1)\times L_{24}(\omega_1) + L_{22}(\omega_1)\times L_{25}(\omega_1)},\\
&\sin\tau_1\omega_1\\
&\quad = \frac{L_{21}(\omega_1)\times L_{26}(\omega_1) - L_{23}(\omega_1)\times L_{25}(\omega_1)}{L_{21}(\omega_1)\times L_{24}(\omega_1) + L_{22}(\omega_1)\times L_{25}(\omega_1)}.
\end{aligned}
\tag{16}
$$

Then, we can get

$$
\cos^2\tau_1\omega_1 + \sin^2\tau_1\omega_1 = 1. \tag{17}
$$

Suppose that (H_{21}) (see (17)) has at least one positive root.

If condition (H_{21}) holds, then there exists $\omega_{10} > 0$ such that (13) has a pair of purely imaginary roots $\pm i\omega_{10}$. For ω_{10},

$$
\begin{aligned}
\tau_{10} &= \frac{1}{\omega_{10}}\\
&\quad \times \arccos\left\{\frac{L_{22}(\omega_{10})\times L_{26}(\omega_{10}) + L_{23}(\omega_{10})\times L_{24}(\omega_{10})}{L_{21}(\omega_{10})\times L_{24}(\omega_{10}) + L_{22}(\omega_{10})\times L_{25}(\omega_{10})}\right\}.
\end{aligned}
\tag{18}
$$

Differentiating (13) with respect to τ_1, one has

$$
\left[\frac{d\lambda}{d\tau_1}\right]^{-1} = \frac{F_{21}(\lambda)}{F_{22}(\lambda)} - \frac{\tau_1}{\lambda}, \tag{19}
$$

where

$$F_{21}(\lambda) = 5B_{25}\lambda^4 + 4B_{24}\lambda^4 + 3B_{23}\lambda^2 + 2B_{22}\lambda + B_{21} + \left(6\lambda^5 + 5A_{25}\lambda^4 + 4A_{24}\lambda^3 + 3A_{23}\lambda^2 + 2A_{22}\lambda + A_{21}\right)e^{\lambda\tau_1} + \left(4F_{24}\lambda^3 + 3F_{23}\lambda^2 + 2F_{22}\lambda + F_{21}\right)\cdot e^{-\lambda\tau_1}, \quad (20)$$

$$F_{22}(\lambda) = \left(4F_{24}\lambda^4 + 3F_{23}\lambda^3 + 2F_{22}\lambda^2 + F_{21}\lambda\right)e^{-\lambda\tau_1} - \left(\lambda^7 + A_{25}\lambda^6 + A_{24}\lambda^5 + A_{23}\lambda^4 + A_{22}\lambda^3 + A_{21}\lambda^2 + A_{20}\lambda\right)e^{\lambda\tau_1}.$$

Thus,

$$\mathrm{Re}\left[\frac{d\lambda}{d\tau_1}\right]^{-1}_{\lambda=i\omega_{10}} = \frac{G_{2R}\times H_{2R} + G_{2I}\times H_{2I}}{H_{2R}^2 + H_{2I}^2}, \quad (21)$$

with

$$G_{2R} = 5B_{25}\omega_{10}^4 - 3B_{23}\omega_{10}^2 + B_{21} + \left(5A_{25}\omega_{10}^4 - 3\left(A_{23} + F_{23}\right)\omega_{10}^2 + A_{21} + F_{21}\right)\cos\tau_{10}\omega_{10} - \left(6\omega_{10}^5 - 4\left(A_{24} - F_{24}\right)\omega_{10}^3 + 2\left(A_{22} - F_{22}\right)\omega_{10}\right)\cdot\sin\tau_{10}\omega_{10},$$

$$G_{2I} = 2B_{22}\omega_{10} - 4B_{24}\omega_{10}^3 + \left(5A_{25}\omega_{10}^4 - 3\left(A_{23} - F_{23}\right)\omega_{10}^2 + A_{21} - F_{21}\right)\sin\tau_{10}\omega_{10} + \left(6\omega_{10}^5 - 4\left(A_{24} + F_{24}\right)\omega_{10}^3 + 2\left(A_{22} + F_{22}\right)\omega_{10}\right)\cdot\cos\tau_{10}\omega_{10}, \quad (22)$$

$$H_{2R} = \left(\left(F_{21} + A_{20}\right)\omega_{10} + A_{24}\omega_{10}^5 - \omega_{10}^7 - \left(3F_{23} + A_{22}\right)\omega_{10}^3\right)\sin\tau_{10}\omega_{10} + \left(\left(4F_{24} - A_{23}\right)\omega_{10}^4 - \left(2F_{22} - A_{21}\right)\omega_{10}^2 - A_{25}\omega_{10}^6\right)\cos\tau_{10}\omega_{10},$$

$$H_{2I} = \left(\left(F_{21} - A_{20}\right)\omega_{10} - A_{24}\omega_{10}^5 + \omega_{10}^7 - \left(3F_{23} - A_{22}\right)\omega_{10}^3\right)\cos\tau_{10}\omega_{10} - \left(\left(4F_{24} + A_{23}\right)\omega_{10}^4 - \left(2F_{22} - A_{21}\right)\omega_{10}^2 - A_{25}\omega_{10}^6\right)\sin\tau_{10}\omega_{10}.$$

Thus, if condition (H_{22}) $G_{2R}\times H_{2R} + G_{2I}\times H_{2I} \neq 0$ holds, then $\mathrm{Re}[d\lambda/d\tau_1]_{\lambda=i\omega_{10}} \neq 0$. Based on the Hopf bifurcation theorem in [25], we have the following results.

Theorem 1. *Suppose that conditions* (H_1), (H_{21}), *and* (H_{22}) *hold for system (2). The viral equilibrium* $P_*(S_*, E_*, I_*, Q_*, R_*, V_*)$ *is locally asymptotically stable when* $\tau_1 \in [0, \tau_{10})$ *and a Hopf bifurcation occurs at the viral equilibrium* $P_*(S_*, E_*, I_*, Q_*, R_*, V_*)$ *when* $\tau_1 = \tau_{10}$.

Case 3 ($\tau_1 = 0; \tau_2 > 0$). Equation (6) becomes

$$\lambda^6 + A_{35}\lambda^5 + A_{34}\lambda^4 + A_{33}\lambda^3 + A_{32}\lambda^2 + A_{31}\lambda + A_{30} + \left(C_{35}\lambda^5 + C_{34}\lambda^4 + C_{33}\lambda^3 + C_{32}\lambda^2 + C_{31}\lambda + C_{30}\right)\cdot e^{-\lambda\tau_2} + \left(G_{34}\lambda^4 + G_{33}\lambda^3 + G_{32}\lambda^2 + G_{31}\lambda + G_{30}\right)\cdot e^{-2\lambda\tau_2} = 0, \quad (23)$$

where

$$\begin{aligned}
A_{30} &= A_0 + B_0 + F_0,\\
A_{31} &= A_1 + B_1 + F_1,\\
A_{32} &= A_2 + B_2 + F_2,\\
A_{33} &= A_3 + B_3 + F_3,\\
A_{34} &= A_4 + B_4 + F_4,\\
A_{35} &= A_5 + B_5,\\
C_{30} &= C_0 + D_0 + H_0,\\
C_{31} &= C_1 + D_1 + H_1,\\
C_{32} &= C_2 + D_2 + H_2,\\
C_{33} &= C_3 + D_3 + H_3,\\
C_{34} &= C_4 + D_4,\\
C_{35} &= C_5,\\
G_{30} &= E_0 + G_0 + I_0,\\
G_{31} &= E_1 + G_1 + I_1,\\
G_{32} &= E_2 + G_2 + I_2,\\
G_{33} &= E_3 + G_3,\\
G_{34} &= G_4.
\end{aligned} \quad (24)$$

Multiplying $e^{\lambda\tau_2}$ on left and right of (23), one has

$$C_{35}\lambda^5 + C_{34}\lambda^4 + C_{33}\lambda^3 + C_{32}\lambda^2 + C_{31}\lambda + C_{30} + \left(\lambda^6 + A_{35}\lambda^5 + A_{34}\lambda^4 + A_{33}\lambda^3 + A_{32}\lambda^2 + A_{31}\lambda + A_{30}\right)e^{\lambda\tau_2} + \left(G_{34}\lambda^4 + G_{33}\lambda^3 + G_{32}\lambda^2 + G_{31}\lambda + G_{30}\right)e^{-\lambda\tau_2} = 0. \quad (25)$$

Let $\lambda = i\omega_2$ ($\omega_2 > 0$) be the root of (25):

$$\begin{aligned}
L_{31}(\omega_2)\cos\tau_2\omega_2 - L_{32}(\omega_2)\sin\tau_2\omega_2 &= L_{33}(\omega_2),\\
L_{34}(\omega_2)\sin\tau_2\omega_2 + L_{35}(\omega_2)\cos\tau_2\omega_2 &= L_{36}(\omega_2),
\end{aligned} \quad (26)$$

with

$$\begin{aligned}
L_{31}(\omega_2) &= (A_{34}+G_{34})\omega_2^4 - \omega_2^6 - (A_{32}+G_{32})\omega_2^2 \\
&\quad + A_{30} + G_{30}, \\
L_{32}(\omega_2) &= A_{35}\omega_2^5 - (A_{33}-G_{33})\omega_2^3 \\
&\quad + (A_{31}-G_{31})\omega_2, \\
L_{33}(\omega_2) &= C_{32}\omega_2^2 - C_{34}\omega_2^4 - C_{30}, \\
L_{34}(\omega_2) &= (A_{34}-G_{34})\omega_2^4 - \omega_2^6 - (A_{32}-G_{32})\omega_2^2 \\
&\quad + A_{30} - G_{30}, \\
L_{35}(\omega_2) &= A_{35}\omega_2^5 - (A_{33}+G_{33})\omega_2^3 \\
&\quad + (A_{31}+G_{31})\omega_2, \\
L_{36}(\omega_2) &= C_{33}\omega_2^3 - C_{35}\omega_2^5 - C_{31}\omega_2.
\end{aligned} \tag{27}$$

Then,

$$\begin{aligned}
&\cos\tau_2\omega_2 \\
&\quad = \frac{L_{32}(\omega_2)\times L_{36}(\omega_2) + L_{33}(\omega_2)\times L_{34}(\omega_2)}{L_{31}(\omega_2)\times L_{34}(\omega_2) + L_{32}(\omega_2)\times L_{35}(\omega_2)}, \\
&\sin\tau_2\omega_2 \\
&\quad = \frac{L_{31}(\omega_2)\times L_{36}(\omega_2) - L_{33}(\omega_2)\times L_{35}(\omega_2)}{L_{31}(\omega_2)\times L_{34}(\omega_2) + L_{32}(\omega_2)\times L_{35}(\omega_2)}.
\end{aligned} \tag{28}$$

And the equation following equation regarding τ_2 can be obtained:

$$\cos^2\tau_2\omega_2 + \sin^2\tau_2\omega_2 = 1. \tag{29}$$

Suppose that (H_{31}) (see (29)) has at least one positive root.

If condition (H_{31}) holds, then there exists $\omega_{20} > 0$ such that (25) has a pair of purely imaginary roots $\pm i\omega_{20}$. For ω_{20},

$$\begin{aligned}
\tau_{20} &= \frac{1}{\omega_{20}} \\
&\quad \times \arccos\left\{\frac{L_{32}(\omega_{20})\times L_{36}(\omega_{20}) + L_{33}(\omega_{20})\times L_{34}(\omega_{20})}{L_{31}(\omega_{20})\times L_{34}(\omega_{20}) + L_{32}(\omega_{20})\times L_{35}(\omega_{20})}\right\}.
\end{aligned} \tag{30}$$

Differentiate both sides of (25) with respect to τ_2. Then,

$$\left[\frac{d\lambda}{d\tau_2}\right]^{-1} = \frac{F_{31}(\lambda)}{F_{32}(\lambda)} - \frac{\tau_2}{\lambda}, \tag{31}$$

where

$$\begin{aligned}
F_{31}(\lambda) &= 5C_{35}\lambda^4 + 4C_{34}\lambda^4 + 3C_{33}\lambda^2 + 2C_{32}\lambda + C_{31} \\
&\quad + \left(6\lambda^5 + 5A_{35}\lambda^4 + 4A_{34}\lambda^3 + 3A_{33}\lambda^2 + 2A_{32}\lambda\right. \\
&\quad \left. + A_{31}\right)e^{\lambda\tau_2} + \left(4G_{34}\lambda^3 + 3G_{33}\lambda^2 + 2G_{32}\lambda + G_{31}\right) \\
&\quad \cdot e^{-\lambda\tau_2}, \\
F_{32}(\lambda) &= \left(4G_{34}\lambda^4 + 3G_{33}\lambda^3 + 2G_{32}\lambda^2 + G_{31}\lambda\right)e^{-\lambda\tau_2} \\
&\quad - \left(\lambda^7 + A_{35}\lambda^6 + A_{34}\lambda^5 + A_{33}\lambda^4 + A_{32}\lambda^3 + A_{31}\lambda^2\right. \\
&\quad \left. + A_{30}\lambda\right)e^{\lambda\tau_2}.
\end{aligned} \tag{32}$$

Thus,

$$\mathrm{Re}\left[\frac{d\lambda}{d\tau_2}\right]^{-1}_{\lambda=i\omega_{20}} = \frac{G_{3R}\times H_{3R} + G_{3I}\times H_{3I}}{H_{3R}^2 + H_{3I}^2}, \tag{33}$$

with

$$\begin{aligned}
G_{3R} &= 5C_{35}\omega_{20}^4 - C_{33}\omega_{20}^2 + C_{31} + \left(5A_{35}\omega_{20}^4\right. \\
&\quad \left. - 3(A_{33}+G_{33})\omega_{20}^2 + A_{31} + G_{31}\right)\cos\tau_{20}\omega_{20} \\
&\quad - \left(6\omega_{20}^5 - 4(A_{34}+G_{34})\omega_{20}^3 + 2(A_{32}+G_{32})\omega_{20}\right) \\
&\quad \cdot \sin\tau_{20}\omega_{20}, \\
G_{3I} &= 2C_{22}\omega_{20} - 4C_{24}\omega_{20}^3 + \left(5A_{35}\omega_{20}^4\right. \\
&\quad \left. - 3(A_{33}+G_{33})\omega_{20}^2 + A_{31} - G_{31}\right)\sin\tau_{20}\omega_{20} \\
&\quad + \left(6\omega_{20}^5 - 4(A_{34}+G_{34})\omega_{20}^3 + 2(A_{32}+G_{32})\omega_{20}\right) \\
&\quad \cdot \cos\tau_{20}\omega_{20}, \\
H_{3R} &= \left((G_{31}+A_{30})\omega_{20} + A_{34}\omega_{20}^5 - \omega_{20}^7\right. \\
&\quad \left. - (3G_{33}+A_{32})\omega_{20}^3\right)\sin\tau_{20}\omega_{20} \\
&\quad + \left((4G_{34}-A_{33})\omega_{20}^4 - (2G_{32}-A_{31})\omega_{20}^2\right. \\
&\quad \left. - A_{35}\omega_{20}^6\right)\cos\tau_{20}\omega_{20}, \\
H_{3I} &= \left((G_{31}-A_{30})\omega_{20} - A_{34}\omega_{20}^5 + \omega_{20}^7\right. \\
&\quad \left. - (3G_{33}-A_{32})\omega_{20}^3\right)\cos\tau_{20}\omega_{20} \\
&\quad + \left((4G_{34}+A_{33})\omega_{20}^4 - (2G_{32}+A_{31})\omega_{20}^2\right. \\
&\quad \left. - A_{35}\omega_{20}^6\right)\sin\tau_{20}\omega_{20}.
\end{aligned} \tag{34}$$

Similar to Case 2, we know that if condition (H_{32}) $G_{3R}\times H_{3R} + G_{3I}\times H_{3I} \neq 0$ holds, then $\mathrm{Re}\,[d\lambda/d\tau_2]_{\lambda=i\omega_{20}} \neq 0$. In conclusion, we have the following results.

Theorem 2. *Suppose that conditions* (H_1), (H_{31}), *and* (H_{32}) *hold for system (2). The viral equilibrium* $P_*(S_*, E_*, I_*,$

$Q_*, R_*, V_*)$ *is locally asymptotically stable when* $\tau_2 \in [0, \tau_{20})$ *and a Hopf bifurcation occurs at the viral equilibrium* $P_*(S_*, E_*, I_*, Q_*, R_*, V_*)$ *when* $\tau_2 = \tau_{20}$.

Case 4 ($\tau_1 > 0; \tau_2 \in (0, \tau_{20})$). Regarding τ_1 as the bifurcation parameter when $\tau_2 \in (0, \tau_{20})$, multiplying by $e^{\lambda\tau_1}$, (6) becomes

$$\begin{aligned} &B_5\lambda^5 + B_4\lambda^4 + B_3\lambda^3 + B_2\lambda^2 + B_1\lambda + B_0 + \left(D_4\lambda^4 \right.\\ &\quad + D_3\lambda^3 + D_2\lambda^2 + D_1\lambda + D_0\left.\right)e^{-\lambda\tau_2} + \left(E_3\lambda^3 + E_2\lambda^2 \right.\\ &\quad + E_1\lambda + E_0\left.\right)e^{-2\lambda\tau_2} + \left(\lambda^6 + A_5\lambda^5 + A_4\lambda^4 + A_3\lambda^3 \right.\\ &\quad + A_2\lambda^2 + A_1\lambda + A_0\left.\right)e^{\lambda\tau_1} + \left(C_5\lambda^5 + C_4\lambda^4 + C_3\lambda^3 \right.\\ &\quad + C_2\lambda^2 + C_1\lambda + C_0\left.\right)e^{\lambda(\tau_1-\tau_2)} + \left(F_4\lambda^4 + F_3\lambda^3 \right.\\ &\quad + F_2\lambda^2 + F_1\lambda + F_0\left.\right)e^{-\lambda\tau_1} + \left(G_4\lambda^4 + G_3\lambda^3 + G_2\lambda^2 \right.\\ &\quad + G_1\lambda + G_0\left.\right)e^{\lambda(\tau_1-2\tau_2)} + \left(H_3\lambda^3 + H_2\lambda^2 + H_1\lambda \right.\\ &\quad + H_0\left.\right)e^{-\lambda(\tau_1+\tau_2)} + \left(I_2\lambda^2 + I_1\lambda + I_0\right)e^{-\lambda(\tau_1+2\tau_2)}. \end{aligned} \tag{35}$$

Let $\lambda = i\omega_1^*$ ($\omega_1^* > 0$) be the root of (35), and for the convenience we still denote ω_1^* as ω_1; then,

$$\begin{aligned} L_{41}(\omega_1)\cos\tau_1\omega_1 - L_{42}(\omega_1)\sin\tau_1\omega_1 &= L_{43}(\omega_1), \\ L_{44}(\omega_1)\sin\tau_1\omega_1 + L_{45}(\omega_1)\cos\tau_1\omega_1 &= L_{46}(\omega_1), \end{aligned} \tag{36}$$

where

$$\begin{aligned} L_{41}(\omega_1) &= (A_4 + F_4)\omega_1^4 - \omega_1^6 - (A_2 + F_2)\omega_1^2 + A_0 \\ &\quad + F_0 + \left(C_4\omega_1^4 - (C_2 + H_2)\omega_1^2 + C_0 + H_0\right)\cos\tau_2\omega_1 \\ &\quad + \left(C_5\omega_1^5 - (C_3 + H_3)\omega_1^3 + (C_1 + H_1)\omega_1\right)\sin\tau_2\omega_1 \\ &\quad + \left(G_4\omega_1^4 - (G_2 + I_2)\omega_1^2 + G_0 + I_0\right)\cos 2\tau_2\omega_1 \\ &\quad + \left((G_1 + I_1)\omega_1 - G_3\omega_1^3\right)\sin 2\tau_2\omega_1, \\ L_{42}(\omega_1) &= A_5\omega_1^5 - (A_3 - F_3)\omega_1^3 + (A_1 - F_1)\omega_1 \\ &\quad + \left(C_5\omega_1^5 - (C_3 - H_3)\omega_1^3 + (C_1 - H_1)\omega_1\right)\cos\tau_2\omega_1 \\ &\quad - \left(C_4\omega_1^4 - (C_2 - H_2)\omega_1^2 + C_0 - H_0\right)\sin\tau_2\omega_1 \\ &\quad + \left((G_1 - I_1)\omega_1 - G_3\omega_1^3\right)\cos 2\tau_2\omega_1 \\ &\quad - \left(G_4\omega_1^4 - (G_2 - I_2)\omega_1^2 + G_0 - I_0\right)\sin 2\tau_2\omega_1, \\ L_{43}(\omega_1) &= B_2\omega_1^2 - B_4\omega_1^4 - B_0 \\ &\quad + \left(D_3\omega_1^3 - D_1\omega_1\right)\sin\tau_2\omega_1 \\ &\quad + \left(D_2\omega_1^2 - D_4\omega_1^4 - D_0\right)\cos\tau_2\omega_1 \\ &\quad + \left(E_3\omega_1^3 - E_1\omega_1\right)\sin\tau_2\omega_1 + \left(E_2\omega_1^2 - E_0\right)\cos\tau_2\omega_1, \\ L_{44}(\omega_1) &= (A_4 - F_4)\omega_1^4 - \omega_1^6 - (A_2 - F_2)\omega_1^2 + A_0 \\ &\quad - F_0 + \left(C_4\omega_1^4 - (C_2 - H_2)\omega_1^2 + C_0 - H_0\right)\cos\tau_2\omega_1 \\ &\quad + \left(C_5\omega_1^5 - (C_3 - H_3)\omega_1^3 + (C_1 - H_1)\omega_1\right)\sin\tau_2\omega_1 \\ &\quad + \left(G_4\omega_1^4 - (G_2 - I_2)\omega_1^2 + G_0 - I_0\right)\cos 2\tau_2\omega_1 \\ &\quad + \left((G_1 - I_1)\omega_1 - G_3\omega_1^3\right)\sin 2\tau_2\omega_1, \\ L_{45}(\omega_1) &= A_5\omega_1^5 - (A_3 + F_3)\omega_1^3 + (A_1 + F_1)\omega_1 \\ &\quad + \left(C_5\omega_1^5 - (C_3 + H_3)\omega_1^3 + (C_1 + H_1)\omega_1\right)\cos\tau_2\omega_1 \\ &\quad - \left(C_4\omega_1^4 - (C_2 + H_2)\omega_1^2 + C_0 + H_0\right)\sin\tau_2\omega_1 \\ &\quad + \left((G_1 + I_1)\omega_1 - G_3\omega_1^3\right)\cos 2\tau_2\omega_1 \\ &\quad - \left(G_4\omega_1^4 - (G_2 + I_2)\omega_1^2 + G_0 + I_0\right)\sin 2\tau_2\omega_1, \\ L_{46}(\omega_1) &= B_3\omega_1^3 - B_3\omega_1^3 - B_1\omega_1 \\ &\quad + \left(D_3\omega_1^3 - D_1\omega_1\right)\cos\tau_2\omega_1 \\ &\quad - \left(D_2\omega_1^2 - D_4\omega_1^4 - D_0\right)\sin\tau_2\omega_1 \\ &\quad + \left(E_3\omega_1^3 - E_1\omega_1\right)\cos\tau_2\omega_1 - \left(E_2\omega_1^2 - E_0\right)\sin\tau_2\omega_1. \end{aligned} \tag{37}$$

Thus,

$$\begin{aligned} &\cos\tau_1\omega_1 \\ &\quad = \frac{L_{42}(\omega_1)\times L_{46}(\omega_1) + L_{43}(\omega_1)\times L_{44}(\omega_1)}{L_{41}(\omega_1)\times L_{44}(\omega_1) + L_{42}(\omega_1)\times L_{45}(\omega_1)}, \\ &\sin\tau_1\omega_1 \\ &\quad = \frac{L_{41}(\omega_1)\times L_{46}(\omega_1) - L_{43}(\omega_1)\times L_{45}(\omega_1)}{L_{41}(\omega_1)\times L_{44}(\omega_1) + L_{42}(\omega_1)\times L_{45}(\omega_1)}. \end{aligned} \tag{38}$$

Then, we get

$$\cos^2\tau_1\omega_1 + \sin^2\tau_1\omega_1 = 1. \tag{39}$$

Suppose that (H_{41}) (see (39)) has at least one positive root.

If (H_{41}) holds, then there exists $\omega_{10} > 0$ such that (35) has a pair of purely imaginary roots $\pm i\omega_{10}^*$. For ω_{10}^*,

$$\begin{aligned} \tau_{10}^* &= \frac{1}{\omega_{10}^*} \\ &\quad \times \arccos\left\{\frac{L_{42}(\omega_{10}^*)\times L_{46}(\omega_{10}^*) + L_{43}(\omega_{10}^*)\times L_{44}(\omega_{10}^*)}{L_{41}(\omega_{10}^*)\times L_{44}(\omega_{10}^*) + L_{42}(\omega_{10}^*)\times L_{45}(\omega_{10}^*)}\right\}. \end{aligned} \tag{40}$$

Differentiating both sides of (25) with respect to τ_2,

$$\left[\frac{d\lambda}{d\tau_1}\right]^{-1} = \frac{F_{41}(\lambda)}{F_{42}(\lambda)} - \frac{\tau_1}{\lambda}, \tag{41}$$

where

$$\begin{aligned}
F_{41}(\lambda) &= 5B_5\lambda^4 + 4B_4\lambda^3 + 3B_3\lambda^2 + 2B_2\lambda + B_1 \\
&+ \left(\left(4D_4 - \tau_2 D_3\right)\lambda^3 - \tau_2 D_4\lambda^4 + \left(3D_3 - \tau_2 D_2\right)\lambda^2\right. \\
&\left. + \left(2D_2 - D_1\right)\lambda + D_1 - \tau_2 D_0\right) e^{-\lambda\tau_2} + \left(6\lambda^5\right. \\
&\left. + 5A_5\lambda^4 + 4A_4\lambda^3 + 3A_3\lambda^2 + 2A_2\lambda + A_1\right) e^{\lambda\tau_1} \\
&+ \left(\left(3E_3 - 2\tau_2 E_2\right)\lambda^2 - 2\tau_2 E_3\lambda^3 + 2\left(E_2 - \tau_2 E_1\right)\lambda\right. \\
&\left. + E_1 - 2\tau_2 E_0\right) e^{-2\lambda\tau_2} + \left(\left(5C_5 - \tau_2 C_4\right)\lambda^4 - \tau_2 C_5\lambda^5\right. \\
&\left. + \left(4C_4 - \tau_2 C_3\right)\lambda^3 + \left(3C_3 - \tau_2 C_2\right)\lambda^2\right. \\
&\left. + \left(2C_2 - \tau_2 C_1\right)\lambda + C_1 - \tau_2 C_0\right) e^{\lambda(\tau_1 - \tau_2)} + \left(4F_4\lambda^3\right. \\
&\left. + 3F_3\lambda^2 + 2F_2\lambda + F_1\right) e^{-\lambda\tau_1} + \left(\left(3H_3 - \tau_2 H_2\right)\lambda^2\right. \\
&\left. - \tau_2 H_3\lambda^3 + \left(2H_2 - \tau_2 H_1\right)\lambda + H_1 - \tau_2 H_0\right) \\
&\cdot e^{-\lambda(\tau_1 + \tau_2)} + \left(\left(4G_4 - 2\tau_2 G_3\right)\lambda^3 - 2\tau_2 G_4\lambda^4\right. \\
&\left. + \left(3G_3 - \tau_2 G_2\right)\lambda^2 + 2\left(G_2 - \tau_2 G_1\right)\lambda + G_1\right. \\
&\left. - 2\tau_2 G_0\right) e^{\lambda(\tau_1 - 2\tau_2)} + \left(2\left(I_2 - \tau_2 I_1\right)\lambda - 2\tau_2 I_2\lambda^2 + I_1\right. \\
&\left. - 2\tau_2 I_0\right) e^{-\lambda(\tau_1 + 2\tau_2)},
\end{aligned} \tag{42}$$

$$\begin{aligned}
F_{42}(\lambda) &= \left(F_4\lambda^5 + F_3\lambda^4 + F_2\lambda^3 + F_1\lambda^2 + F_0\lambda\right) e^{-\lambda\tau_1} \\
&+ \left(H_3\lambda^4 + H_2\lambda^3 + H_1\lambda^2 + H_0\lambda\right) e^{-\lambda(\tau_1 + \tau_2)} + \left(I_2\lambda^3\right. \\
&\left. + I_1\lambda^2 + I_0\lambda\right) e^{-\lambda(\tau_1 + 2\tau_2)} - \left(\lambda^7 + A_5\lambda^6 + A_4\lambda^5\right. \\
&\left. + A_3\lambda^4 + A_2\lambda^3 + A_1\lambda^2 + A_0\lambda\right) e^{\lambda\tau_1} - \left(C_5\lambda^6\right. \\
&\left. + C_4\lambda^5 + C_3\lambda^4 + C_2\lambda^3 + C_1\lambda^2 + C_0\lambda\right) e^{\lambda(\tau_1 - \tau_2)} \\
&- \left(G_4\lambda^5 + G_3\lambda^4 + G_2\lambda^3 + G_1\lambda^2 + G_0\lambda\right) e^{\lambda(\tau_1 - 2\tau_2)}.
\end{aligned}$$

Define

$$\operatorname{Re}\left[\frac{d\lambda}{d\tau_1}\right]^{-1}_{\lambda = i\omega_{10}^*} = \frac{G_{4R} \times H_{4R} + G_{4I} \times H_{4I}}{H_{4R}^2 + H_{4I}^2}. \tag{43}$$

Similar to Case 2, we know that if condition (H_{42}) $G_{4R} \times H_{4R} + G_{4I} \times H_{4I} \neq 0$ holds, then $\operatorname{Re}[d\lambda/d\tau_1]_{\lambda = i\omega_{10}^*} \neq 0$. Thus, we have the following results.

Theorem 3. *Let $\tau_2 \in (0, \tau_{20})$ and suppose that conditions (H_1), (H_{41}), and (H_{42}) hold for system (2). The viral equilibrium $P_*(S_*, E_*, I_*, Q_*, R_*, V_*)$ is locally asymptotically stable when $\tau_1 \in [0, \tau_{10}^*)$ and a Hopf bifurcation occurs at the viral equilibrium $P_*(S_*, E_*, I_*, Q_*, R_*, V_*)$ when $\tau_1 = \tau_{10}^*$.*

Case 5 ($\tau_1 \in (0, \tau_{10})$; $\tau_2 > 0$). Regarding τ_2 as the bifurcation parameter when $\tau_1 \in (0, \tau_{10})$, multiplying by $e^{\lambda\tau_2}$, (6) becomes

$$\begin{aligned}
&C_5\lambda^5 + C_4\lambda^4 + C_3\lambda^3 + C_2\lambda^2 + C_1\lambda + C_0 + \left(D_4\lambda^4\right. \\
&\left. + D_3\lambda^3 + D_2\lambda^2 + D_1\lambda + D_0\right) e^{-\lambda\tau_1} + \left(H_3\lambda^3\right. \\
&\left. + H_2\lambda^2 + H_1\lambda + H_0\right) e^{-2\lambda\tau_1} + \left(G_4\lambda^4 + G_3\lambda^3\right. \\
&\left. + G_2\lambda^2 + G_1\lambda + G_0\right) e^{-\lambda\tau_2} + \left(\lambda^6 + A_5\lambda^5 + A_4\lambda^4\right. \\
&\left. + A_3\lambda^3 + A_2\lambda^2 + A_1\lambda + A_0\right) e^{\lambda\tau_2} + \left(B_5\lambda^5 + B_4\lambda^4\right. \\
&\left. + B_3\lambda^3 + B_2\lambda^2 + B_1\lambda + B_0\right) e^{\lambda(\tau_2 - \tau_1)} + \left(E_3\lambda^3\right. \\
&\left. + E_2\lambda^2 + E_1\lambda + E_0\right) e^{-\lambda(\tau_2 + \tau_1)} + \left(F_4\lambda^4 + F_3\lambda^3\right. \\
&\left. + F_2\lambda^2 + F_1\lambda + F_0\right) e^{\lambda(\tau_2 - 2\tau_1)} + \left(I_2\lambda^2 + I_1\lambda + I_0\right) \\
&\cdot e^{-\lambda(\tau_2 + 2\tau_1)}.
\end{aligned} \tag{44}$$

Let $\lambda = i\omega_2^*$ ($\omega_2^* > 0$) be the root of (44), and for the convenience we still denote ω_2^* as ω_2; then,

$$\begin{aligned}
L_{51}(\omega_2)\cos\tau_2\omega_2 - L_{52}(\omega_1)\sin\tau_2\omega_2 &= L_{53}(\omega_2), \\
L_{54}(\omega_2)\sin\tau_2\omega_2 + L_{55}(\omega_1)\cos\tau_2\omega_2 &= L_{56}(\omega_2),
\end{aligned} \tag{45}$$

where

$$\begin{aligned}
L_{51}(\omega_2) &= \left(A_4 + G_4\right)\omega_2^4 - \omega_2^6 - \left(A_2 + G_2\right)\omega_2^2 + A_0 + G_0 \\
&+ \left(B_4\omega_2^4 - \left(B_2 + E_2\right)\omega_2^2 + B_0 + E_0\right)\cos\tau_1\omega_2 \\
&+ \left(B_5\omega_2^5 - \left(B_3 + E_3\right)\omega_2^3 + \left(B_1 - E_1\right)\omega_2\right)\sin\tau_1\omega_2 \\
&+ \left(F_4\omega_2^4 - \left(F_2 + I_2\right)\omega_2^2 + F_0 + I_0\right)\cos 2\tau_1\omega_2 \\
&+ \left(\left(F_1 + I_1\right)\omega_2 - F_3\omega_2^3\right)\sin 2\tau_1\omega_2, \\
L_{52}(\omega_2) &= A_5\omega_2^5 - \left(A_3 - G_3\right)\omega_2^3 + \left(A_1 - G_1\right)\omega_2 \\
&+ \left(\left(B_2 - E_2\right)\omega_2^2 - B_4\omega_2^4 + E_0 - B_0\right)\sin\tau_1\omega_2 \\
&+ \left(B_5\omega_2^5 - \left(B_3 - E_3\right)\omega_2^3 + \left(B_1 - E_1\right)\omega_2\right)\cos\tau_1\omega_2 \\
&- \left(F_4\omega_2^4 - \left(F_2 - I_2\right)\omega_2^2 + F_0 - I_0\right)\sin 2\tau_1\omega_2 \\
&+ \left(\left(F_1 - I_1\right)\omega_2 - F_3\omega_2^3\right)\cos 2\tau_1\omega_2,
\end{aligned}$$

$$
\begin{aligned}
&L_{53}(\omega_2)\\
&= C_2\omega_2^2 - C_4\omega_2^4 - C_0 + \left(D_3\omega_2^3 - D_1\omega_2\right)\sin\tau_1\omega_2\\
&\quad + \left(D_2\omega_2^2 - D_4\omega_2^4 - D_0\right)\cos\tau_1\omega_2\\
&\quad + \left(H_3\omega_2^3 - H_1\omega_2\right)\sin 2\tau_1\omega_2\\
&\quad + \left(H_2\omega_2^2 - H_0\right)\cos 2\tau_1\omega_2,\\
&L_{54}(\omega_2)\\
&= \left(A_4 - G_4\right)\omega_2^4 - \omega_2^6 - \left(A_2 - G_2\right)\omega_2^2 + A_0 - G_0\\
&\quad + \left(B_4\omega_2^4 - \left(B_2 - E_2\right)\omega_2^2 + B_0 - E_0\right)\cos\tau_1\omega_2\\
&\quad + \left(B_5\omega_2^5 - \left(B_3 - E_3\right)\omega_2^3 + \left(B_1 - E_1\right)\omega_2\right)\sin\tau_1\omega_2\\
&\quad + \left(F_4\omega_2^4 - \left(F_2 - I_2\right)\omega_2^2 + F_0 - I_0\right)\cos 2\tau_1\omega_2\\
&\quad + \left(\left(F_1 - I_1\right)\omega_2 - F_3\omega_2^3\right)\sin 2\tau_1\omega_2,\\
&L_{55}(\omega_2)\\
&= A_5\omega_2^5 - \left(A_3 + G_3\right)\omega_2^3 + \left(A_1 + G_1\right)\omega_2\\
&\quad - \left(B_4\omega_2^4 - \left(B_2 + E_2\right)\omega_2^2 + E_0 + B_0\right)\sin\tau_1\omega_2\\
&\quad + \left(B_5\omega_2^5 - \left(B_3 + E_3\right)\omega_2^3 + \left(B_1 + E_1\right)\omega_2\right)\cos\tau_1\omega_2\\
&\quad - \left(F_4\omega_2^4 - \left(F_2 + I_2\right)\omega_2^2 + F_0 - I_0\right)\sin 2\tau_1\omega_2\\
&\quad + \left(\left(F_1 + I_1\right)\omega_2 - F_3\omega_2^3\right)\cos 2\tau_1\omega_2,\\
&L_{56}(\omega_2)\\
&= C_3\omega_2^3 - C_5\omega_2^5 - C_1\omega_2\\
&\quad + \left(D_3\omega_2^3 - D - 1\omega_2\right)\cos\tau_1\omega_2\\
&\quad - \left(D_2\omega_2^2 - D_4\omega_2^4 - D_0\right)\sin\tau_1\omega_2\\
&\quad + \left(H_3\omega_2^3 - H_1\omega_2\right)\cos 2\tau_1\omega_2\\
&\quad - \left(H_2\omega_2^2 - H_0\right)\sin 2\tau_1\omega_2.
\end{aligned}
\tag{46}
$$

Thus,

$$
\begin{aligned}
&\cos\tau_2\omega_2\\
&\quad = \frac{L_{52}(\omega_2)\times L_{56}(\omega_2) + L_{53}(\omega_2)\times L_{54}(\omega_2)}{L_{51}(\omega_2)\times L_{54}(\omega_2) + L_{52}(\omega_2)\times L_{55}(\omega_2)},\\
&\sin\tau_2\omega_2\\
&\quad = \frac{L_{51}(\omega_2)\times L_{56}(\omega_2) - L_{53}(\omega_2)\times L_{55}(\omega_2)}{L_{51}(\omega_2)\times L_{54}(\omega_2) + L_{52}(\omega_2)\times L_{55}(\omega_2)}.
\end{aligned}
\tag{47}
$$

Then, we get

$$
\cos^2\tau_2\omega_2 + \sin^2\tau_2\omega_2 = 1. \tag{48}
$$

If (H_{51}) holds, then there exists $\omega_{20}^* > 0$ such that (35) has a pair of purely imaginary roots $\pm i\omega_{20}^*$. For ω_{20}^*,

$$
\begin{aligned}
\tau_{20}^* &= \frac{1}{\omega_{20}^*}\\
&\quad\times \arccos\left\{\frac{L_{52}(\omega_{20}^*)\times L_{56}(\omega_{20}^*) + L_{53}(\omega_{20}^*)\times L_{54}(\omega_{20}^*)}{L_{51}(\omega_{20}^*)\times L_{54}(\omega_{20}^*) + L_{52}(\omega_{20}^*)\times L_{55}(\omega_{20}^*)}\right\}.
\end{aligned}
\tag{49}
$$

Differentiating (25) with respect to τ_2, one can get

$$
\left[\frac{d\lambda}{d\tau_2}\right]^{-1} = \frac{F_{51}(\lambda)}{F_{52}(\lambda)} - \frac{\tau_2}{\lambda}, \tag{50}
$$

where

$$
\begin{aligned}
F_{51}(\lambda) &= 5C_5\lambda^4 + 4C_4\lambda^3 + 3C_3\lambda^2 + 2C_2\lambda + C_1\\
&\quad + \left(\left(4D_4 - \tau_1 D_3\right)\lambda^3 - \tau_1 D_4\lambda^4 + \left(3D_3 - \tau_1 D_2\right)\lambda^2\right.\\
&\quad \left. + \left(2D_2 - \tau_1 D_1\right)\lambda + D_1 - \tau_1 D_0\right)e^{-\lambda\tau_1}\\
&\quad + \left(\left(3H_3 - 2\tau_1 H_2\right)\lambda^2 - 2\tau_1 H_3\lambda^3\right.\\
&\quad \left. + 2\left(H_2 - \tau_1 H_1\right)\lambda + H_1 - 2\tau_1 H_0\right)e^{-2\lambda\tau_1} + \left(4G_4\lambda^3\right.\\
&\quad \left. + 3G_3\lambda^2 + 2G_2\lambda + G_1\right)e^{-\lambda\tau_2} + \left(6\lambda^5 + 5A_5\lambda^4\right.\\
&\quad \left. + 4A_4\lambda^3 + 3A_3\lambda^2 + 2A_2\lambda + A_1\right)e^{\lambda\tau_2}\\
&\quad + \left(\left(5B_5 - \tau_1 B_4\right)\lambda^4 - \tau_1 B_5\lambda^5 + \left(4B_4 - \tau_1 B_3\right)\lambda^3\right.\\
&\quad + \left(3B_3 - \tau_1 B_2\right)\lambda^2 + \left(2B_2 - \tau_1 B_1\right)\lambda + B_1 - \tau_1 B_0\Big)\\
&\quad \cdot e^{\lambda(\tau_2 - \tau_1)} + \left(\left(3E_3 - \tau_1 E_2\right)\lambda^2 - \tau_1 E_3\lambda^3\right.\\
&\quad \left. + \left(2E_2 - \tau_1 E_1\right)\lambda + E_1 - \tau_1 E_0\right)e^{-\lambda(\tau_2 + \tau_1)}\\
&\quad + \left(\left(4F_4 - 2\tau_1 F_3\right)\lambda^3 - 2\tau_1 F_4\lambda^4 + \left(3F_3 - 2\tau_1 F_2\right)\lambda^2\right.\\
&\quad \left. + \left(2F_2 - 2\tau_1 F_1\right)\lambda + F_1 - 2\tau_1 F_0\right)e^{\lambda(\tau_2 - 2\tau_1)}\\
&\quad + \left(2\left(I_2 - \tau_1 I_1\right)\lambda - 2\tau_1 I_2\lambda^2 + I_1 - 2\tau_1 I_0\right)e^{\lambda(\tau_2 + 2\tau_1)},\\
F_{52}(\lambda) &= \left(G_4\lambda^5 + G_3\lambda^4 + G_2\lambda^3 + G_1\lambda^2 + G_0\lambda\right)e^{-\lambda\tau_2}\\
&\quad + \left(E_3\lambda^4 + E_2\lambda^3 + E_1\lambda^2 + E_0\lambda\right)e^{-\lambda(\tau_2 + \tau_1)} + \left(I_2\lambda^3\right.\\
&\quad \left. + I_1\lambda^2 + I_0\lambda\right)e^{-\lambda(\tau_2 + 2\tau_1)} - \left(F_4\lambda^5 + F_3\lambda^4 + F_2\lambda^3\right.\\
&\quad \left. + F_1\lambda^2 + F_0\lambda\right)e^{\lambda(\tau_2 - 2\tau_1)} - \left(B_5\lambda^6 + B_4\lambda^5 + B_3\lambda^4\right.\\
&\quad \left. + B_2\lambda^3 + B_1\lambda^2 + B_0\lambda\right)e^{\lambda(\tau_2 - \tau_1)} - \left(\lambda^7 + A_5\lambda^6\right.\\
&\quad \left. + A_4\lambda^5 + A_3\lambda^4 + A_2\lambda^3 + A_1\lambda^2 + A_0\lambda\right)e^{\lambda\tau_2}.
\end{aligned}
\tag{51}
$$

Thus,

$$\mathrm{Re}\left[\frac{d\lambda}{d\tau_2}\right]^{-1}_{\lambda=i\omega_{20}^*} = \frac{G_{3R}\times H_{3R} + G_{3I}\times H_{3I}}{H_{3R}^2 + H_{3I}^2}. \quad (52)$$

Therefore, we know that if condition (H_{52}) $G_{5R}\times H_{5R} + G_{5I}\times H_{5I} \neq 0$ holds, then $\mathrm{Re}[d\lambda/d\tau_2]_{\lambda=i\omega_{20}^*} \neq 0$. Then, we have the following results.

Theorem 4. *Let $\tau_1 \in (0,\tau_{10})$ and suppose that conditions (H_1), (H_{51}), and (H_{52}) hold for system (2). The viral equilibrium $P_*(S_*,E_*,I_*,Q_*,R_*,V_*)$ is locally asymptotically stable when $\tau_2 \in [0,\tau_{20}^*)$ and a Hopf bifurcation occurs at the viral equilibrium $P_*(S_*,E_*,I_*,Q_*,R_*,V_*)$ when $\tau_2 = \tau_{20}^*$.*

3. Properties of the Hopf Bifurcation

In this section, we shall investigate direction and stability of the Hopf bifurcation under the case where $\tau_1 \in (0,\tau_{10})$ and $\tau_2 > 0$. Set $u_1(t) = S(t)-S_*$, $u_2(t) = E(t)-E_*$, $u_3(t) = I(t)-I_*$, $u_4(t) = Q(t)-Q_*$, $u_5(t) = R(t)-R_*$, $u_6(t) = V(t)-V_*$, and $t \to (t/\tau_2)$. For convenience, we assume that $\tau_1^* \in (0,\tau_{10}) < \tau_{20}^*$ throughout this section. Then, system (2) becomes functional differential equations in $C = C([-1,0],R^6)$:

$$\dot{u}(t) = L_\mu u_t + F(\mu,u_t), \quad (53)$$

with

$$L_\mu\phi = (\tau_{20}^*+\mu)\left(A\phi(0) + B\phi\left(-\frac{\tau_1^*}{\tau_{20}^*}\right) + C\phi(-1)\right),$$
$$F(\mu,\phi) = (\tau_{20}^*+\mu)\begin{pmatrix} -\beta\phi_1(0)\phi_3(0) \\ \beta\phi_1(0)\phi_3(0) \\ 0 \\ 0 \\ 0 \\ 0 \end{pmatrix}, \quad (54)$$

where

$$A = \begin{pmatrix} a_1 & 0 & a_2 & 0 & 0 & 0 \\ a_3 & a_4 & a_5 & 0 & 0 & 0 \\ 0 & a_6 & a_7 & 0 & 0 & 0 \\ 0 & 0 & a_8 & a_9 & 0 & 0 \\ 0 & 0 & 0 & 0 & a_{10} & 0 \\ a_{11} & 0 & 0 & 0 & 0 & a_{12} \end{pmatrix},$$
$$B = \begin{pmatrix} 0 & 0 & 0 & 0 & 0 & 0 \\ 0 & 0 & 0 & 0 & 0 & 0 \\ 0 & 0 & b_1 & 0 & 0 & 0 \\ 0 & 0 & 0 & b_2 & 0 & 0 \\ 0 & 0 & b_3 & b_4 & 0 & 0 \\ 0 & 0 & 0 & 0 & 0 & 0 \end{pmatrix},$$
$$C = \begin{pmatrix} 0 & 0 & 0 & 0 & c_1 & c_2 \\ 0 & 0 & 0 & 0 & 0 & 0 \\ 0 & 0 & 0 & 0 & 0 & 0 \\ 0 & 0 & 0 & 0 & 0 & 0 \\ 0 & 0 & 0 & c_3 & 0 & 0 \\ 0 & 0 & 0 & 0 & 0 & c_4 \end{pmatrix}. \quad (55)$$

Based on the Riesz representation theorem, there exists a 6×6 function $\eta(\theta,\mu) : [-1,0] \to R^{6\times6}$ such that

$$L_\mu\phi = \int_{-1}^{0} d\eta(\theta,\mu)\phi(\theta), \quad \phi \in C. \quad (56)$$

In fact, we choose

$$\eta(\theta,\mu) = \begin{cases} (\tau_{20}^*+\mu)(A+B+B), & \theta = 0, \\ (\tau_{20}^*+\mu)(B+C), & \theta \in \left[-\frac{\tau_1^*}{\tau_{20}^*},0\right), \\ (\tau_{20}^*+\mu)B, & \theta \in \left(-1,-\frac{\tau_1^*}{\tau_{20}^*}\right), \\ 0, & \theta = -1. \end{cases} \quad (57)$$

For $\phi \in C([-1,0],R^6)$, we define

$$A(\mu)\phi = \begin{cases} \dfrac{d\phi(\theta)}{d\theta}, & -1 \le \theta < 0, \\ \displaystyle\int_{-1}^{0} d\eta(\theta,\mu)\phi(\theta), & \theta = 0, \end{cases}$$
$$R(\mu)\phi = \begin{cases} 0, & -1 \le \theta < 0, \\ F(\mu,\phi), & \theta = 0. \end{cases} \quad (58)$$

Then, system (53) becomes

$$\dot{u}(t) = A(\mu)u_t + R(\mu)u_t, \quad (59)$$

where $u_t(\theta) = u(t+\theta)$ for $\theta \in [-1,0]$.

Define A^* as follows:

$$A^*(\varphi) = \begin{cases} -\dfrac{d\varphi(s)}{ds}, & 0 < s \le 1, \\ \displaystyle\int_{-1}^{0} d\eta^T(s,0)\varphi(-s), & s = 0, \end{cases} \quad (60)$$

and a bilinear form

$$\langle\varphi(s),\phi(\theta)\rangle = \overline{\varphi}(0)\phi(0) - \int_{\theta=-1}^{0}\int_{\xi=0}^{\theta}\overline{\varphi}(\xi-\theta)\,d\eta(\theta)\phi(\xi)\,d\xi, \quad (61)$$

where $\eta(\theta) = \eta(\theta,0)$.

Let $q(\theta) = (1, q_2, q_3, q_4, q_5, q_6)^T e^{i\omega_{20}^*\tau_{20}^*\theta}$ be the eigenvector of $A(0)$ with $+i\omega_{20}^*\tau_{20}^*$ and let $q^*(s) = D(1, q_2^*, q_3^*, q_4^*, q_5^*)e^{i\omega_{20}^*\tau_{20}^* s}$ be the eigenvector of $A^*(0)$ with $-i\omega_{20}^*\tau_{20}^*$. Then, according to the definition of $A(0)$ and $A^*(0)$, we obtain

$$
\begin{aligned}
q_2 &= \frac{a_3 + a_5 q_3}{i\omega_{20}^* - a_3},\\
q_3 &= \frac{a_3 a_6}{\left(i\omega_{20}^* - a_3\right)\left(i\omega_{20}^* - a_7 - b_1 e^{-i\tau_1^*\omega_{20}^*}\right) - a_5 a_6},\\
q_4 &= \frac{a_8 q_3}{i\omega_{20}^- a_9 - b_2 e^{-i\tau_1^*\omega_{20}^*}},\\
q_5 &= \frac{i\omega_{20}^* - a_1 - a_2 q_3 - c_2 e^{-i\tau_{20}^*\omega_{20}^*}}{c_1 e^{-i\tau_{20}^*\omega_{20}^*}},\\
q_6 &= \frac{i\omega_{20}^* - a_{11}}{a_{12} + c_4 e^{-i\tau_{20}^*\omega_{20}^*}},\\
q_2^* &= -\frac{i\omega_{20}^* + a_1}{a_3},\\
q_3^* &= \frac{\left(i\omega_{20}^* + a_1\right)\left(i\omega_{20}^* + a_4\right)}{a_3 a_6},\\
q_4^* &= -\frac{\left(i\omega_{20}^* + a_7 + b_1 e^{i\tau_1^*\omega_{20}^*}\right) q_3}{a_8}\\
&\quad + \frac{a_2 a_3 + \left(i\omega_{20}^* + a_1\right) a_5}{a_3 a_8}\\
&\quad + \frac{b_3\left(i\omega_{20}^* + a_9 + b_2 e^{i\tau_1^*\omega_{20}^*}\right)}{a_8 b_4},\\
q_5 &= -\frac{\left(i\omega_{20}^* + a_9 + b_2 e^{i\tau_1^*\omega_{20}^*}\right) q_4}{b_4 e^{i\tau_1^*\omega_{20}^*}},\\
q_6^* &= -\frac{c_2 e^{i\tau_{20}^*\omega_{20}^*}}{i\omega_{20}^* + a_{12} + c_4 e^{i\tau_{20}^*\omega_{20}^*}}.
\end{aligned}
\tag{62}
$$

In addition, from (61), we have

$$
\begin{aligned}
&\left\langle q^*(s), q(\theta)\right\rangle = \overline{q}(0)\, q(0)\\
&\quad - \int_{-1}^{0}\int_{\xi=0}^{\theta} \overline{q}^*(\xi - \theta)\, d\eta(\theta)\, q(\xi)\, d\xi\\
&\quad = \overline{D}\left(1, \overline{q}_2^*, \overline{q}_3^*, \overline{q}_4^*, \overline{q}_5^*, \overline{q}_6^*\right)\left(1, q_2, q_3, q_4, q_5, q_6\right)^T\\
&\quad - \int_{-1}^{0}\int_{\xi=0}^{\theta} \overline{D}\left(1, \overline{q}_2^*, \overline{q}_3^*, \overline{q}_4^*, \overline{q}_5^*, \overline{q}_6^*\right)\\
&\quad \cdot e^{-i\tau_1^*\omega_{20}^*(\xi-\theta)} d\eta(\theta)\left(1, q_2, q_3, q_4, q_5, q_6\right)^T e^{i\tau_1^*\omega_{20}^*\xi} d\xi\\
&\quad - \int_{-1}^{0}\int_{\xi=0}^{\theta} \overline{D}\left(1, \overline{q}_2^*, \overline{q}_3^*, \overline{q}_4^*, \overline{q}_5^*, \overline{q}_6^*\right)\\
&\quad \cdot e^{-i\tau_{20}^*\omega_{20}^*(\xi-\theta)} d\eta(\theta)\left(1, q_2, q_3, q_4, q_5, q_6\right)^T e^{i\tau_{20}^*\omega_{20}^*\xi} d\xi\\
&\quad = \overline{D}\Big[1 + q_2\overline{q}_2^* + q_3\overline{q}_3^* + q_4\overline{q}_4^* + q_5\overline{q}_5^* + q_6\overline{q}_6^*\\
&\quad + \tau_1^* e^{i\tau_1^*\omega_{20}^*}\int_{-1}^{0}\left(1, \overline{q}_2^*, \overline{q}_3^*, \overline{q}_4^*, \overline{q}_5^*, \overline{q}_6^*\right)\\
&\quad \cdot B\left(1, q_2, q_3, q_4, q_5, q_6\right)^T\\
&\quad + \tau_1^* e^{i\tau_2^*\omega_{20}^*}\int_{-1}^{0}\left(1, \overline{q}_2^*, \overline{q}_3^*, \overline{q}_4^*, \overline{q}_5^*, \overline{q}_6^*\right)\\
&\quad \cdot C\left(1, q_2, q_3, q_4, q_5, q_6\right)^T\Big] = \overline{D}\Big[1 + q_2\overline{q}_2^* + q_3\overline{q}_3^*\\
&\quad + q_4\overline{q}_4^* + q_5\overline{q}_5^* + q_6\overline{q}_6^*\\
&\quad + \tau_1^* e^{-i\tau_1^*\omega_{20}^*}\left(b_3\left(b_1\overline{q}_3^* + b_3\overline{q}_5^*\right) + b_4\left(b_2\overline{q}_4^* + b_4\overline{q}_5^*\right)\right)\\
&\quad + \tau_{20}^* e^{-i\tau_{20}^*\omega_{20}^*}\left(c_1\overline{q}_5^* + c_2\overline{q}_6^* + c_3 q_5\overline{q}_5^* + c_4 q_6\overline{q}_6^*\right)\Big].
\end{aligned}
\tag{63}
$$

Thus, we can choose

$$
\begin{aligned}
\overline{D} = \Big[&1 + q_2\overline{q}_2^* + q_3\overline{q}_3^* + q_4\overline{q}_4^* + q_5\overline{q}_5^* + q_6\overline{q}_6^*\\
&+ \tau_1^* e^{-i\tau_1^*\omega_{20}^*}\left(b_3\left(b_1\overline{q}_3^* + b_3\overline{q}_5^*\right) + b_4\left(b_2\overline{q}_4^* + b_4\overline{q}_5^*\right)\right)\\
&+ \tau_{20}^* e^{-i\tau_{20}^*\omega_{20}^*}\left(c_1\overline{q}_5^* + c_2\overline{q}_6^* + c_3 q_5\overline{q}_5^* + c_4 q_6\overline{q}_6^*\right)\Big]^{-1},
\end{aligned}
\tag{64}
$$

such that $\langle q^*, q\rangle = 1$, $\langle q^*, \overline{q}\rangle = 0$.

Then, using the algorithms from Hassard et al. [25] and the similar computation process in [26–29], we obtain

$$
\begin{aligned}
g_{20} &= 2\beta\tau_{20}^*\overline{D}q_3\left(\overline{q}_2^* - 1\right),\\
g_{11} &= \beta\tau_{20}^*\overline{D}\,\mathrm{Re}\left\{q_3\right\}\left(\overline{q}_2^* - 1\right),\\
g_{02} &= 2\beta\tau_{20}^*\overline{D}\overline{q}_3\left(\overline{q}_2^* - 1\right),\\
g_{21} &= 2\beta\tau_{20}^*\overline{D}\left(\overline{q}_2^* - 1\right)\Big(W_{11}^{(1)}(0)\, q_3 + \frac{1}{2}W_{20}^{(1)}(0)\,\overline{q}_3\\
&\quad + W_{11}^{(3)}(0) + \frac{1}{2}W_{20}^{(3)}(0)\Big),
\end{aligned}
\tag{65}
$$

with

$$
\begin{aligned}
W_{20}(\theta) &= \frac{ig_{20}q(0)}{\tau_{20}^*\omega_{20}^*}e^{i\tau_{20}^*\omega_{20}^*\theta} + \frac{i\overline{g}_{02}\overline{q}(0)}{3\tau_{20}^*\omega_{20}^*}e^{-i\tau_{20}^*\omega_{20}^*\theta} + E_1 e^{2i\tau_{20}^*\omega_{20}^*\theta},\\
W_{11}(\theta) &= -\frac{ig_{11}q(0)}{\tau_{20}^*\omega_{20}^*}e^{i\tau_{20}^*\omega_{20}^*\theta} + \frac{i\overline{g}_{11}\overline{q}(0)}{\tau_{20}^*\omega_{20}^*}e^{-i\tau_{20}^*\omega_{20}^*\theta} + E_2,
\end{aligned}
$$

$$E_1 = 2\begin{pmatrix} a_1' & 0 & -a_2 & 0 & -c_1 e^{-2i\tau_{20}^*\omega_{20}^*} & -c_2 e^{-2i\tau_{20}^*\omega_{20}^*} \\ -a_3 & a_2' & -a_5 & 0 & 0 & 0 \\ 0 & -a_6 & a_3' & 0 & 0 & 0 \\ 0 & 0 & -a_8 & a_4' & 0 & 0 \\ 0 & 0 & -b_3 e^{-2i\tau_1^*\omega_{20}^*} & -b_4 e^{-2i\tau_1^*\omega_{20}^*} & a_5' & 0 \\ -a_{11} & 0 & 0 & 0 & 0 & a_6' \end{pmatrix}^{-1} \times \begin{pmatrix} -\beta q_3 \\ \beta q_3 \\ 0 \\ 0 \\ 0 \\ 0 \end{pmatrix},$$

$$E_2 = -\begin{pmatrix} a_1 & 0 & a_2 & 0 & c_1 & c_2 \\ a_3 & a_4 & a_5 & 0 & 0 & 0 \\ 0 & a_6 & a_7 + b_1 & 0 & 0 & 0 \\ 0 & 0 & a_8 & a_9 + b_2 & 0 & 0 \\ 0 & 0 & b_3 & b_4 & a_{10} + c_3 & 0 \\ a_{11} & 0 & 0 & 0 & 0 & a_{12} + c_4 \end{pmatrix}^{-1} \times \begin{pmatrix} -\beta \operatorname{Re}\{q_3\} \\ \beta \operatorname{Re}\{q_3\} \\ 0 \\ 0 \\ 0 \\ 0 \end{pmatrix}, \tag{66}$$

where

$$\begin{aligned} a_1' &= 2i\omega_{20}^* - a_1, \\ a_2' &= 2i\omega_{20}^* - a_4, \\ a_3' &= 2i\omega_{20}^* - a_7 - b_1 e^{-2i\tau_1^*\omega_{20}^*}, \\ a_4' &= 2i\omega_{20}^* - a_9 - b_2 e^{-2i\tau_1^*\omega_{20}^*}, \\ a_5' &= 2i\omega_{20}^* - a_{10} - c_3 e^{-2i\tau_{20}^*\omega_{20}^*}, \\ a_6' &= 2i\omega_{20}^* - a_{12} - c_4 e^{-2i\tau_{20}^*\omega_{20}^*}. \end{aligned} \tag{67}$$

Then, we can get the following coefficients:

$$\begin{aligned} C_1(0) &= \frac{i}{2\tau_{20}^*\omega_{20}^*}\left(g_{11}g_{20} - 2|g_{11}|^2 - \frac{|g_{02}|^2}{3}\right) \\ &\quad + \frac{g_{21}}{2}, \\ \mu_2 &= -\frac{\operatorname{Re}\{C_1(0)\}}{\operatorname{Re}\{\lambda'(\tau_{20}^*)\}}, \\ \rho_2 &= 2\operatorname{Re}\{C_1(0)\}, \\ T_2 &= -\frac{\operatorname{Im}\{C_1(0)\} + \mu_2 \operatorname{Im}\{\lambda'(\tau_{20}^*)\}}{\tau_{20}^*\omega_{20}^*}. \end{aligned} \tag{68}$$

Thus, we have the following results.

Theorem 5. *The sign of μ_2 determines direction of the Hopf bifurcation: if $\mu_2 > 0$ ($\mu_2 < 0$), then the Hopf bifurcation is supercritical (subcritical); the sign of ρ_2 determines stability of the bifurcating periodic solutions: if $\rho_2 < 0$ ($\rho_2 > 0$), then the bifurcating periodic solutions are stable (unstable); the sign of T_2 determines period of the bifurcating solutions: if $T_2 > 0$ ($T_2 < 0$), then the period of the bifurcating periodic solutions increases (decreases).*

4. Numerical Simulation

In this section, we present some numerical results of system (2) in order to validate the analytical predictions obtained in Sections 2 and 3. We choose a set of parameters as follows: $A = 100$, $\beta = 0.009$, $d = 0.05$, $\rho = 0.65$, $\theta = 0.05$, $\chi = 0.55$, $\gamma = 0.45$, $\alpha = 0.035$, $\delta = 0.1$, $\eta = 0.35$, and $\varepsilon = 0.07$, and consider the following special case of (2):

$$\begin{aligned} \frac{dS(t)}{dt} &= 100 - 0.009S(t)I(t) - 0.05S(t) - 0.65S(t) \\ &\quad + 0.05R(t-\tau_2) + 0.55V(t-\tau_2), \\ \frac{dE(t)}{dt} &= 0.009S(t)I(t) - 0.05E(t) - 0.45E(t), \\ \frac{dI(t)}{dt} &= 0.45E(t) - 0.05I(t) - 0.035I(t) - 0.1I(t) \\ &\quad - 0.35I(t-\tau_1), \\ \frac{dQ(t)}{dt} &= \delta I(t) - 0.05Q(t) - 0.035Q(t) \\ &\quad - 0.07Q(t-\tau_1), \\ \frac{dR(t)}{dt} &= 0.07Q(t-\tau_1) - 0.05R(t) - 0.05R(t-\tau_2) \\ &\quad + 0.35I(t-\tau_1), \\ \frac{dV(t)}{dt} &= 0.65S(t) - 0.05V(t) - 0.55V(t-\tau_2), \end{aligned} \tag{69}$$

from which we can get the unique viral equilibrium $P_*(66.0494, 277.7978, 233.6617, 150.7495, 923.3406, 71.7439)$.

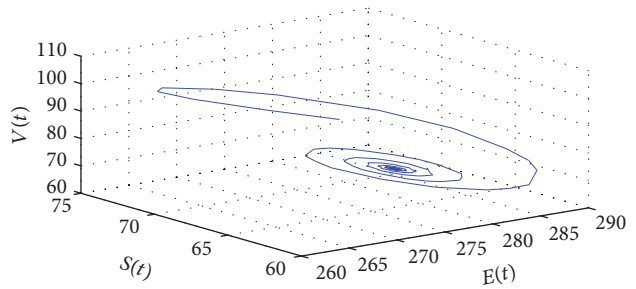

Figure 1: The projection of the phase portrait of system (69) in (S, E, V)-space with $\tau_1 = 3.605$.

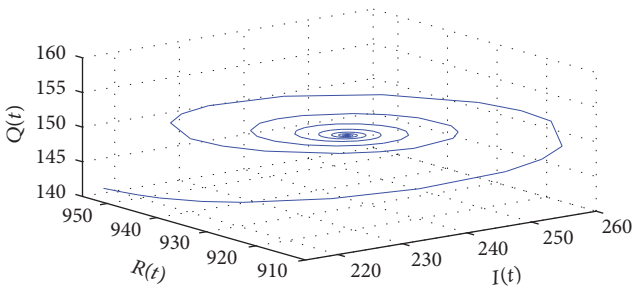

Figure 2: The projection of the phase portrait of system (69) in (I, Q, R)-space with $\tau_1 = 3.605$.

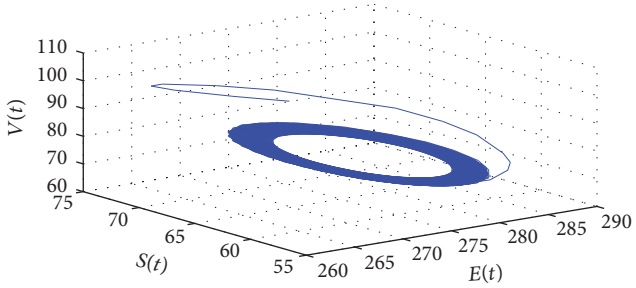

Figure 3: The projection of the phase portrait of system (69) in (S, E, V)-space with $\tau_1 = 4.60$.

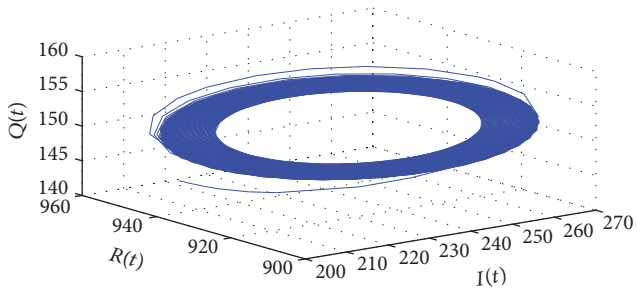

Figure 4: The projection of the phase portrait of system (69) in (I, Q, R)-space with $\tau_1 = 4.60$.

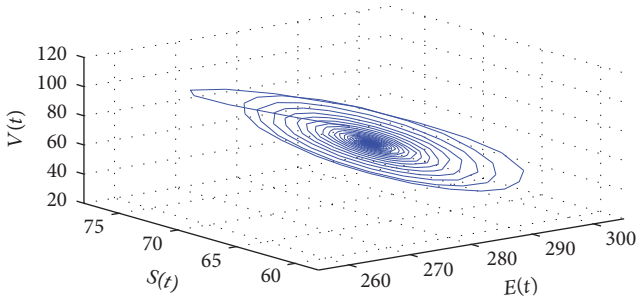

Figure 5: The projection of the phase portrait of system (69) in (S, E, V)-space with $\tau_2 = 3.65$.

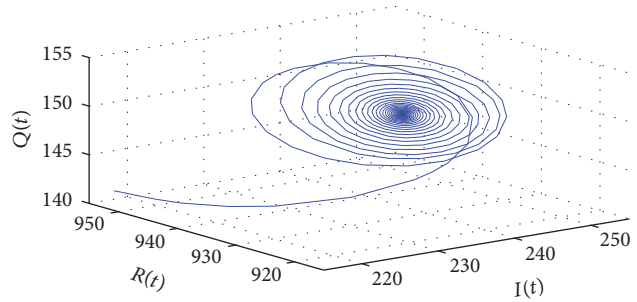

Figure 6: The projection of the phase portrait of system (69) in (I, Q, R)-space with $\tau_2 = 3.65$.

It can be easily verified that condition (H_1) is satisfied when $\tau_1 = \tau_2 = 0$.

By computation, we have $\omega_{10} = 0.8554$ and $\tau_{10} = 4.1056$. Then, we get $\lambda'(\tau_{10}) = 2.3686 + i1.0212$. Thus, we know that conditions (H_{21}) and (H_{22}) hold. We can conclude that all roots that cross the imaginary axis at $i\omega_{10}$ cross from left to right as τ_1 increases by the theory in [22]. According to Theorem 1, $P_*(66.0494, 277.7978, 233.6617, 150.7495, 923.3406, 71.7439)$ is asymptotically stable when $\tau_1 \in (0, \tau_{10})$. This property can be illustrated by Figures 1 and 2. In this case, spreading law of the computer viruses can be predicted and the viruses can be controlled and eliminated. However, once the value of τ_1 passes through the critical value τ_{10}, $P_*(66.0494, 277.7978, 233.6617, 150.7495, 923.3406, 71.7439)$ loses its stability and a Hopf bifurcation occurs, which can be shown in Figures 3 and 4. The occurrence of a Hopf bifurcation means that the state of computer viruses propagation changes from the viral equilibrium point to a limit cycle. This makes spreading of the computer viruses be out of control.

Similarly, we have the following: $\omega_{20} = 1.8255$ and $\tau_{20} = 3.7424$ when $\tau_1 = 0$ and $\tau_2 > 0$; $\omega_{10}^* = 0.9665$ and $\tau_{10}^* = 3.1862$ when $\tau_1 > 0$ and $\tau_2 = 2.25 \in (0, \tau_{20})$; $\omega_{20}^* = 2.4217$ and $\tau_{20}^* = 3.0254$ when $\tau_2 > 0$ and $\tau_1 = 2.45 \in (0, \tau_{10})$. The corresponding phase plots are shown in Figures 5–8, Figures 9–12, and Figures 13–16, respectively. In addition, for $\tau_2 > 0$ and $\tau_1 = 2.45 \in (0, \tau_{10})$, we have $C_1(0) = -17.2982 + i13.5056$ and $\lambda'(\tau_{20}^*) = 0.3796 + i2.0581$ by some complex computation. Based on (68), we get $\mu_2 = 45.5692 > 0$, $\rho_2 = -34.5964 < 0$, and $T_2 = -14.6441 < 0$. Therefore, the Hopf bifurcation is supercritical, the bifurcating periodic solutions are stable, and the period of the bifurcating periodic solutions decreases.

According to the numerical simulation results, we know that the time delay should remain less than the corresponding threshold in order to control and predict the viruses' propagation by decreasing the period that antivirus software uses

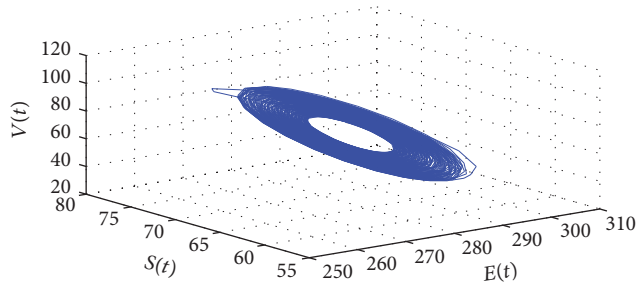

Figure 7: The projection of the phase portrait of system (69) in (S, E, V)-space with $\tau_2 = 3.805$.

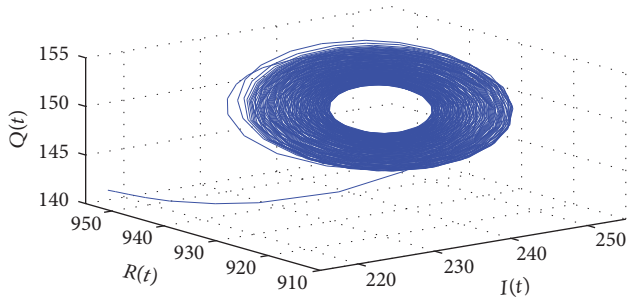

Figure 8: The projection of the phase portrait of system (69) in (I, Q, R)-space with $\tau_2 = 3.805$.

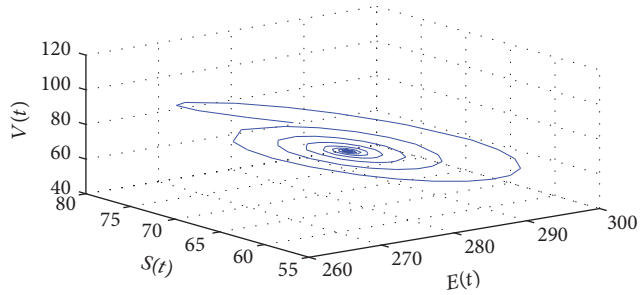

Figure 9: The projection of the phase portrait of system (69) in (S, E, V)-space with $\tau_1 = 2.86$ and $\tau_2 = 2.25 \in (0, \tau_{20})$.

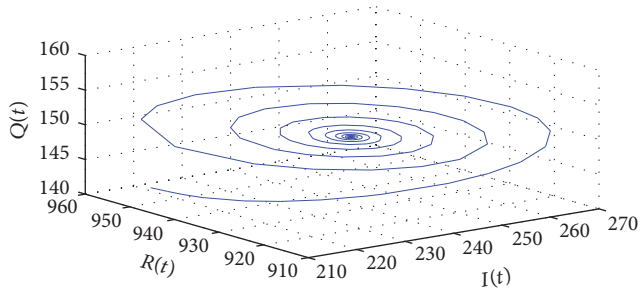

Figure 10: The projection of the phase portrait of system (69) in (I, Q, R)-space with $\tau_1 = 2.86$ and $\tau_2 = 2.25 \in (0, \tau_{20})$.

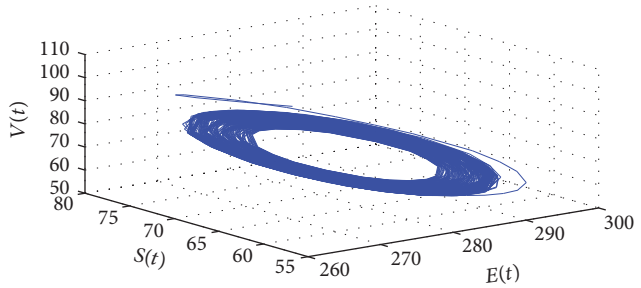

Figure 11: The projection of the phase portrait of system (69) in (S, E, V)-space with $\tau_1 = 3.574$ and $\tau_2 = 2.25 \in (0, \tau_{20})$.

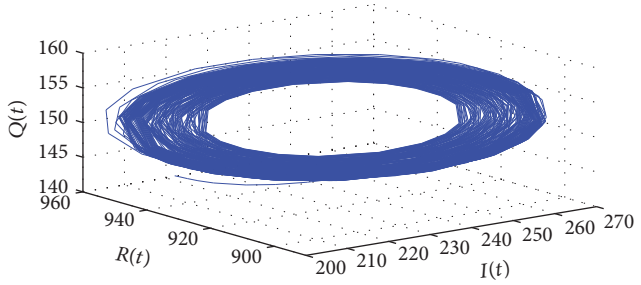

Figure 12: The projection of the phase portrait of system (69) in (I, Q, R)-space with $\tau_1 = 3.574$ and $\tau_2 = 2.25 \in (0, \tau_{20})$.

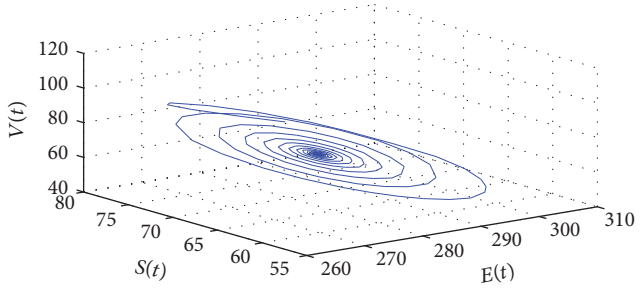

Figure 13: The projection of the phase portrait of system (69) in (S, E, V)-space with $\tau_2 = 2.862$ and $\tau_1 = 2.45 \in (0, \tau_{10})$.

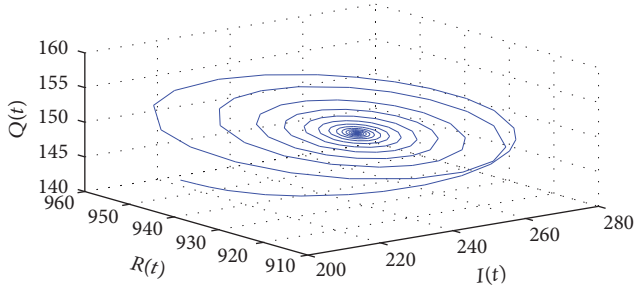

Figure 14: The projection of the phase portrait of system (69) in (I, Q, R)-space with $\tau_2 = 2.862$ and $\tau_1 = 2.45 \in (0, \tau_{10})$.

to clean the computer viruses and the temporary immunity period of the recovered and the vaccinated computers. To this end, we can adjust the parameters of our proposed model in real-world networks, such as timely updating the antivirus software on computers, properly controlling the number of computers attached to the network, and timely disconnecting computers from the network when the connections are unnecessary. Of course, in the next step, we also need to collect large amount of relevant data and estimate the parameters involved in our proposed model through statistical analysis in real-world networks. Namely, we have to adjust the parameters in the model so as to control viruses' propagation effectively if it is necessary.

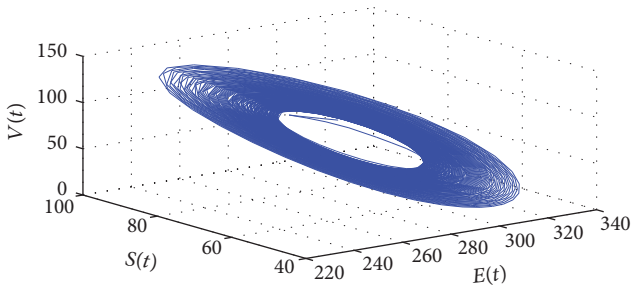

Figure 15: The projection of the phase portrait of system (69) in (S, E, V)-space with $\tau_2 = 3.225$ and $\tau_1 = 2.45 \in (0, \tau_{10})$.

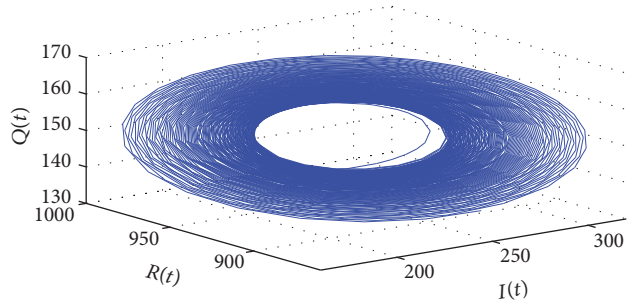

Figure 16: The projection of the phase portrait of system (69) in (I, Q, R)-space with $\tau_2 = 3.225$ and $\tau_1 = 2.45 \in (0, \tau_{10})$.

5. Conclusions

It is definitely an interesting work to consider the effect of delays on dynamical systems, because a stability switch occurs even when an ignored delay is small for a dynamical system. Based on this fact, we introduce the time delay due to the period that antivirus software uses to clean the computer viruses in the infectious and quarantined computers (τ_1) and the time delay due to the temporary immunity period of the recovered and the vaccinated computers (τ_2) into the SEIQRS-V computer virus propagation model considered in [21]. We obtain some conditions for local stability and Hopf bifurcation occurring by analyzing distribution of roots of the associated characteristic equation.

By computation, there exists a corresponding critical value of the time delay below which system (2) is stable and above which system (2) is unstable. When the system is stable, the characteristics of the propagation of computer viruses can be easily predicted and then the computer viruses can get eliminated. Otherwise, the propagation of the computer viruses is out of control. Therefore, stability of the computer virus propagation system must be guaranteed in practice. In addition, we find that the effect of τ_2 on system (2) is marked compared with τ_1, because the critical value of τ_2 is much smaller when we only consider it. At last, we have also derived the explicit formula which can determine direction and stability of the Hopf bifurcation under the case where $\tau_1 \in (0, \tau_{10})$ and $\tau_2 > 0$.

Conflicts of Interest

The authors declare that there are no conflicts of interest regarding the publication of this paper.

Acknowledgments

This work was supported by Natural Science Foundation of Anhui Province (nos. 1608085QF151, 1608085QF145, and 1708085MA17) and Natural Science Foundation of the Higher Education Institutions of Anhui Province (nos. KJ2014A006 and KJ2015A144).

References

[1] L.-X. Yang and X. Yang, "The effect of infected external computers on the spread of viruses: A Compartment Modeling Study," *Physica A. Statistical Mechanics and its Applications*, vol. 392, no. 24, pp. 6523–6535, 2013.

[2] P. Szor, *The Art of Computer Virus Research and Defense*, Addison-Wesley Education Publishers Inc., Boston, Mass, USA, 2005.

[3] H. Yuan and G. Chen, "Network virus-epidemic model with the point-to-group information propagation," *Applied Mathematics and Computation*, vol. 206, no. 1, pp. 357–367, 2008.

[4] B. K. Mishra and S. K. Pandey, "Dynamic model of worms with vertical transmission in computer network," *Applied Mathematics and Computation*, vol. 217, no. 21, pp. 8438–8446, 2011.

[5] L.-X. Yang, X. Yang, L. Wen, and J. Liu, "A novel computer virus propagation model and its dynamics," *International Journal of Computer Mathematics*, vol. 89, no. 17, pp. 2307–2314, 2012.

[6] J. Ren, X. Yang, Q. Zhu, L.-X. Yang, and C. Zhang, "A novel computer virus model and its dynamics," *Nonlinear Analysis. Real World Applications*, vol. 13, no. 1, pp. 376–384, 2012.

[7] C. Gan, X. Yang, W. Liu, Q. Zhu, and X. Zhang, "Propagation of computer virus under human intervention: a dynamical model," *Discrete Dynamics in Nature and Society*, vol. 2012, Article ID 106950, 8 pages, 2012.

[8] L. X. Yang, M. Draief, and X. F. Yang, "Heterogeneous virus propagation in networks: a theoretical study," *Mathematical Methods in the Applied Sciences*, vol. 40, no. 5, pp. 1396–1413, 2017.

[9] C. Zhang, Y. Zhao, Y. Wu, and S. Deng, "A stochastic dynamic model of computer viruses," *Discrete Dynamics in Nature and Society*, vol. 2012, Article ID 264874, 16 pages, 2012.

[10] A. Jafarabadi and M. A. Azgomi, "A stochastic epidemiological model for the propagation of active worms considering the dynamicity of network topology," *Peer-to-Peer Networking and Applications*, vol. 8, no. 6, pp. 1008–1022, 2015.

[11] J. Amador, "The stochastic *SIRA* model for computer viruses," *Applied Mathematics and Computation*, vol. 232, pp. 1112–1124, 2014.

[12] J. Amador and J. R. Artalejo, "Stochastic modeling of computer virus spreading with warning signals," *Journal of the Franklin Institute. Engineering and Applied Mathematics*, vol. 350, no. 5, pp. 1112–1138, 2013.

[13] Y. Yao, X.-W. Xie, H. Guo, G. Yu, F.-X. Gao, and X.-J. Tong, "Hopf bifurcation in an Internet worm propagation model with time delay in quarantine," *Mathematical and Computer Modelling*, vol. 57, no. 11-12, pp. 2635–2646, 2013.

[14] J. Ren and Y. Xu, "Stability and bifurcation of a computer virus propagation model with delay and incomplete antivirus ability," *Mathematical Problems in Engineering*, vol. 2014, Article ID 475934, 2014.

[15] J. Liu, "Hopf bifurcation in a delayed SEIQRS model for the transmission of malicious objects in computer network," *Journal of Applied Mathematics*, vol. 2014, Article ID 492198, 8 pages, 2014.

[16] L. Feng, X. Liao, H. Li, and Q. Han, "Hopf bifurcation analysis of a delayed viral infection model in computer networks," *Mathematical and Computer Modelling*, vol. 56, no. 7-8, pp. 167–179, 2012.

[17] Y. Muroya, Y. Enatsu, and H. Li, "Global stability of a delayed SIRS computer virus propagation model," *International Journal of Computer Mathematics*, vol. 91, no. 3, pp. 347–367, 2014.

[18] J. G. Ren, X. F. Yang, L.-X. Yang, Y. H. Xu, and F. Z. Yang, "A delayed computer virus propagation model and its dynamics," *Chaos, Solitons and Fractals*, vol. 45, no. 1, pp. 74–79, 2012.

[19] L. Yang and X. Yang, "The effect of network topology on the spread of computer viruses: A Modelling Study," *International Journal of Computer Mathematics*, pp. 1–18, 2016.

[20] L.-X. Yang, X. Yang, and Y. Wu, "The impact of patch forwarding on the prevalence of computer virus: a theoretical assessment approach," *Applied Mathematical Modelling*, vol. 43, pp. 110–125, 2017.

[21] C. Gan, "Modeling and analysis of the effect of network eigenvalue on viral spread," *Nonlinear Dynamics*, vol. 84, no. 3, pp. 1727–1733, 2016.

[22] C. Gan, X. Yang, W. Liu, and Q. Zhu, "A propagation model of computer virus with nonlinear vaccination probability," *Communications in Nonlinear Science and Numerical Simulation*, vol. 19, no. 1, pp. 92–100, 2014.

[23] C. Gan, X. Yang, and Q. Zhu, "Global stability of a computer virus propagation model with two kinds of generic nonlinear probabilities," *Abstract and Applied Analysis*, vol. 2014, Article ID 735327, 7 pages, 2014.

[24] M. Kumar, B. K. Mishra, and T. C. Panda, "Effect of quarantine & vaccination on infectious nodes in computer network," *International Journal of Computer Networks and Applications*, vol. 2, pp. 92–97, 2015.

[25] B. D. Hassard, N. D. Kazarinoff, and Y. H. Wan, *Theory and Applications of Hopf Bifurcation*, vol. 41 of *London Mathematical Society Lecture Note Series*, Cambridge University Press, Cambridge, UK, 1981.

[26] X.-Y. Meng, H.-F. Huo, X.-B. Zhang, and H. Xiang, "Stability and Hopf bifurcation in a three-species system with feedback delays," *Nonlinear Dynamics*, vol. 64, no. 4, pp. 349–364, 2011.

[27] C. Xu, X. Tang, and M. Liao, "Stability and bifurcation analysis of a six-neuron BAM neural network model with discrete delays," *Neurocomputing*, vol. 74, no. 5, pp. 689–707, 2011.

[28] C. Bianca and L. Guerrini, "Existence of limit cycles in the Solow model with delayed-logistic population growth," *The Scientific World Journal*, vol. 2014, Article ID 207806, 2014.

[29] C. Xu, X. Tang, and M. Liao, "Stability and bifurcation analysis on a ring of five neurons with discrete delays," *Journal of Dynamical and Control Systems*, vol. 19, no. 2, pp. 237–275, 2013.

Hindawi
Discrete Dynamics in Nature and Society
Volume 2017, Article ID 8390784, 14 pages
https://doi.org/10.1155/2017/8390784

Research Article

On the Optimal Dynamic Control Strategy of Disruptive Computer Virus

Jichao Bi,[1] Xiaofan Yang,[1] Yingbo Wu,[1] Qingyu Xiong,[1] Junhao Wen,[1] and Yuan Yan Tang[2]

[1]*College of Software Engineering, Chongqing University, Chongqing 400044, China*
[2]*Department of Computer and Information Science, The University of Macau, Macau*

Correspondence should be addressed to Xiaofan Yang; xfyang1964@gmail.com

Received 14 December 2016; Revised 13 February 2017; Accepted 23 February 2017; Published 19 March 2017

Academic Editor: Yong Deng

Copyright © 2017 Jichao Bi et al. This is an open access article distributed under the Creative Commons Attribution License, which permits unrestricted use, distribution, and reproduction in any medium, provided the original work is properly cited.

Disruptive computer viruses have inflicted huge economic losses. This paper addresses the development of a cost-effective dynamic control strategy of disruptive viruses. First, the development problem is modeled as an optimal control problem. Second, a criterion for the existence of an optimal control is given. Third, the optimality system is derived. Next, some examples of the optimal dynamic control strategy are presented. Finally, the performance of actual dynamic control strategies is evaluated.

1. Introduction

The proliferation of computer networks has brought huge benefits to human society. Meanwhile, it offers a shortcut to spread computer viruses, inflicting large economic losses [1]. Consequently, containing the prevalence of digital viruses has been one of the major concerns in the field of cybersecurity. The spreading dynamics of computer virus has been widely adopted as the standard method for assessing the viral prevalence [2]. Since the seminal work by Kephart and White [3, 4], a multitude of computer virus-spreading models, ranging from the population-level models [5–12] and the network-level models [13–17] to the node-level models [18–22], have been proposed.

One of the central tasks in cybersecurity is to develop control strategies of computer virus so that, subject to limited budgets, the losses caused by computer infections are minimized [23]. In recent years, the optimal design problem of virus control strategies has been modeled as static optimization problems [24–28]. The optimal static control strategies, however, only apply to the small-timescale situations where the network state keeps unchanged. In the realistic situations where the network state is varying over time, the optimal design problem of virus control strategies can be modeled as dynamic optimal control problems [29–33]. The optimal dynamic control strategies outperform their static counterparts, because the former not only are more cost-effective but apply to different timescales.

A disruptive computer virus is defined as a computer virus whose life period consists of two consecutive phases: the latent phase and the disruptive phase. In the latent phase, a disruptive virus staying in a host does not perform any disruptive operations. Rather, the virus tries to infect as many hosts as possible by sending its copies to them. In the disruptive phase, a disruptive virus staying in a host performs a variety of operations that disrupt the host, such as distorting data, deleting data or files, and destroying the operating system. To assess the prevalence of disruptive viruses, a number of virus-spreading models, which are referred to as the Susceptible-Latent-Bursting-Susceptible (SLBS) models, have been suggested [34–38]. The main distinction between the SLBS models and the traditional SEIS models lies in that the latent hosts in the former possess strong infecting capability, whereas the exposed individuals in the latter possess no infecting capability at all. Recently, the basic SLBS models have been extended towards different directions [39–43]. At the population-level, Chen et al. [44] developed an optimal dynamic control strategy of disruptive viruses.

All of the above-mentioned SLBS models are population-level; that is, they are based on the assumption that every infected host in the population is equally likely to infect any other susceptible host. These models have two striking defects: (a) the personalized features of different hosts cannot be taken into consideration and (b) the impact of the structure of the virus-propagating network on the viral prevalence cannot be revealed by studying the models. To overcome these defects, Yang et al. [45] presented a node-level SLBS model. In our opinion, optimal dynamic control strategies of disruptive viruses should be developed at the node-level, so as to achieve the best cost-efficiency.

This paper is intended to develop at the node-level an optimal dynamic control strategy of disruptive computer viruses. First, the development problem is modeled as an optimal control problem. Second, a criterion for the existence of an optimal control for the optimal control problem is given. Third, the optimality system for the optimal control problem is presented. Next, some exemplar optimal dynamic control strategies are given. Finally, the difference between the cost-efficiency of an arbitrary control strategy and that of the optimal dynamic strategy is estimated.

The subsequent materials of this work are organized as follows. Section 2 presents the preliminary knowledge on optimal control theory. Sections 3 and 4 formulate and study the optimal control problem, respectively. Some numerical examples are given in Section 5. Section 6 estimates the aforementioned difference. Finally, Section 7 closes this work.

2. Fundamental Knowledge

For fundamental knowledge on optimal control theory, see [46].

Consider the following optimal control problem.

$$\begin{aligned} \underset{\mathbf{u}(\cdot)\in\mathcal{U}}{\text{Minimize}} \quad & J\left(\mathbf{u}\left(t\right)\right) \\ & = \int_0^T F\left(\mathbf{x}\left(t\right), \mathbf{u}\left(t\right)\right) dt \\ \text{subject to} \quad & \frac{d\mathbf{x}\left(t\right)}{dt} = \mathbf{f}\left(\mathbf{x}\left(t\right), \mathbf{u}\left(t\right)\right), \\ & 0 \le t \le T. \end{aligned} \tag{P}$$

Lemma 1. *Problem* (P) *has an optimal control if the following five conditions hold simultaneously.*

(C_1) $\mathcal{U}$ *is closed and convex.*

(C_2) *There is* $\mathbf{u}(\cdot) \in \mathcal{U}$ *such that the adjunctive dynamical system is solvable.*

(C_3) $\mathbf{f}(\mathbf{x}, \mathbf{u})$ *is bounded by a linear function in* $\mathbf{x}$.

(C_4) $F(\mathbf{x}, \mathbf{u})$ *is convex on* $\mathcal{U}$.

(C_5) $F(\mathbf{x}, \mathbf{u}) \ge c_1\|\mathbf{u}\|^\rho + c_2$ *for some vector norm* $\|\cdot\|$, $\rho > 1, c_1 > 0$, *and* c_2.

3. Formulation of the Optimal Control Problem

Consider a population of N hosts (nodes) labelled $1, 2, \ldots, N$. As with the traditional SLBS models, assume that at any time every node in the population is in one of three possible states: *susceptible*, *latent*, and *disruptive*. Susceptible nodes are those that are not infected with any disruptive computer virus. Latent nodes are those that are infected with some disruptive viruses and all of them are in the latent phase. Disruptive nodes are those that are infected with some disruptive viruses and some of them are in the disruptive phase. Let $X_i(t) = 0$, 1, and 2 denote that at time t node i is susceptible, latent, and disruptive, respectively. Let

$$\begin{aligned} S_i\left(t\right) &= \Pr\left\{X_i\left(t\right) = 0\right\}, \\ L_i\left(t\right) &= \Pr\left\{X_i\left(t\right) = 1\right\}, \\ B_i\left(t\right) &= \Pr\left\{X_i\left(t\right) = 2\right\}. \end{aligned} \tag{1}$$

As $S_i(t) + L_i(t) + B_i(t) \equiv 1$ $(1 \le i \le N)$, the vector

$$\begin{aligned} &\mathbf{I}\left(t\right) \\ &\quad = \left(L_1\left(t\right), \ldots, L_N\left(t\right), B_1\left(t\right), \ldots, B_N\left(t\right)\right)^T \end{aligned} \tag{2}$$

probabilistically captures the state of the population at time t.

Suppose a dynamic control strategy will be carried out during the time frame $[0, T]$. Let us impose a set of statistical hypotheses as follows.

(H_1) A susceptible node i is infected by a latent node j at rate $\beta_{L,ij} \ge 0$. Let $\mathbf{A}_L = (\beta_{L,ij})_{N\times N}$.

(H_2) A susceptible node i is infected by a disruptive node j at rate $\beta_{B,ij} \ge 0$. Let $\mathbf{A}_B = (\beta_{B,ij})_{N\times N}$.

(H_3) Due to the outburst of latent viruses, a latent node i becomes disruptive at rate $\alpha_i > 0$. Let $\overline{\alpha} = \max_i \alpha_i$.

(H_4) Due to the action of new patches, at time t a latent node i becomes susceptible at a controllable rate $\gamma_{L,i}(t) \in L^2[0, T]$ and $\underline{\gamma_L} \le \gamma_{L,i}(t) \le \overline{\gamma_L}$. Hereafter, the symbol $L^2[0, T]$ stands for the set of all Lebesgue square integrable functions defined on the interval $[0, T]$. Moreover, the cost needed to achieve the rate at the infinitesimal time interval $[t, t + dt)$ is $p_i\gamma_{L,i}^\theta(t)dt$, $p_i > 0$, and $\theta > 0$. This accords with the intuition that the cost increases with $\gamma_{L,i}(t)$.

(H_5) Due to the action of new patches, at time t a disruptive node i becomes susceptible at a controllable rate $\gamma_{B,i}(t) \in L^2[0, T]$ and $\underline{\gamma_B} \le \gamma_{B,i}(t) \le \overline{\gamma_B}$. Moreover, the cost needed to achieve the rate at the infinitesimal time interval $[t, t + dt)$ is $q_i\gamma_{B,i}^\theta(t)dt$, $q_i > 0$. This conforms to the intuition that the cost increases with $\gamma_{B,i}(t)$.

Figure 1 shows hypotheses (H_1)–(H_5) schematically.

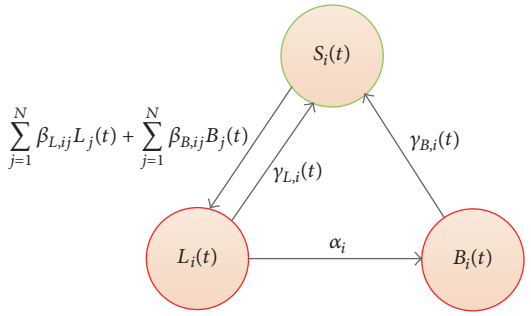

Figure 1: Diagram of assumptions (H_1)–(H_5).

Let $\Delta t > 0$ denote a very small time interval. Hypotheses (H_1)–(H_5) imply the following relations.

$$\begin{aligned}
&\Pr\{X_i(t+\Delta t) = 1 \mid X_i(t) = 0\} \\
&\quad = \Delta t \sum_{j=1}^{N} \beta_{L,ij} L_j(t) + \Delta t \sum_{j=1}^{N} \beta_{B,ij} B_j(t) + o(\Delta t), \\
&\Pr\{X_i(t+\Delta t) = 2 \mid X_i(t) = 0\} = o(\Delta t), \\
&\Pr\{X_i(t+\Delta t) = 2 \mid X_i(t) = 1\} = \alpha_i \Delta t + o(\Delta t), \\
&\Pr\{X_i(t+\Delta t) = 0 \mid X_i(t) = 1\} = \gamma_{L,i}(t)\Delta t + o(\Delta t), \\
&\Pr\{X_i(t+\Delta t) = 0 \mid X_i(t) = 2\} = \gamma_{B,i}(t)\Delta t + o(\Delta t), \\
&\Pr\{X_i(t+\Delta t) = 1 \mid X_i(t) = 2\} = o(\Delta t).
\end{aligned} \tag{3}$$

As a result, we have

$$\begin{aligned}
&\Pr\{X_i(t+\Delta t) = 0 \mid X_i(t) = 0\} \\
&\quad = 1 - \Delta t \sum_{j=1}^{N} \beta_{L,ij} L_j(t) \\
&\qquad - \Delta t \sum_{j=1}^{N} \beta_{B,ij} B_j(t) + o(\Delta t), \\
&\Pr\{X_i(t+\Delta t) = 1 \mid X_i(t) = 1\} \\
&\quad = 1 - \alpha_i \Delta t - \gamma_{L,i}(t)\Delta t + o(\Delta t), \\
&\Pr\{X_i(t+\Delta t) = 2 \mid X_i(t) = 2\} \\
&\quad = 1 - \gamma_{B,i}(t)\Delta t + o(\Delta t).
\end{aligned} \tag{4}$$

By the total probability formula, we get

$$\begin{aligned}
&L_i(t+\Delta t) \\
&\quad = S_i(t) \Pr\{X_i(t+\Delta t) = 1 \mid X_i(t) = 0\} \\
&\qquad + L_i(t) \Pr\{X_i(t+\Delta t) = 1 \mid X_i(t) = 1\} \\
&\qquad + B_i(t) \Pr\{X_i(t+\Delta t) = 1 \mid X_i(t) = 2\} \\
&\quad = [1 - L_i(t) - B_i(t)]\Delta t \sum_{j=1}^{N} \left[\beta_{L,ij} L_j(t) + \beta_{B,ij} B_j(t)\right] \\
&\qquad + L_i(t) - \Delta t [\alpha_i + \gamma_{L,i}(t)] L_i(t) + o(\Delta t), \\
&B_i(t+\Delta t) \\
&\quad = S_i(t) \Pr\{X_i(t+\Delta t) = 2 \mid X_i(t) = 0\} \\
&\qquad + L_i(t) \Pr\{X_i(t+\Delta t) = 2 \mid X_i(t) = 1\} \\
&\qquad + B_i(t) \Pr\{X_i(t+\Delta t) = 2 \mid X_i(t) = 2\} \\
&\quad = \alpha_i \Delta t L_i(t) + B_i(t) - \gamma_{B,i}(t)\Delta t B_i(t) + o(\Delta t).
\end{aligned} \tag{5}$$

Transposing the terms $L_i(t)$ and $B_i(t)$ from the right to the left and dividing both sides by Δt, we get

$$\begin{aligned}
&\frac{L_i(t+\Delta t) - L_i(t)}{\Delta t} \\
&\quad = [1 - L_i(t) - B_i(t)] \sum_{j=1}^{N} \left[\beta_{L,ij} L_j(t) + \beta_{B,ij} B_j(t)\right] \\
&\qquad - [\alpha_i + \gamma_{L,i}(t)] L_i(t) + \frac{o(\Delta t)}{\Delta t}, \\
&\frac{B_i(t+\Delta t) - B_i(t)}{\Delta t} = \alpha_i L_i(t) - \gamma_{B,i}(t) B_i(t) + \frac{o(\Delta t)}{\Delta t}.
\end{aligned} \tag{6}$$

Letting $\Delta t \to 0$, we get the following dynamical model.

$$\begin{aligned}
&\frac{dL_i(t)}{dt} \\
&\quad = [1 - L_i(t) - B_i(t)] \sum_{j=1}^{N} \left[\beta_{L,ij} L_j(t) + \beta_{B,ij} B_j(t)\right] \\
&\qquad - [\alpha_i + \gamma_{L,i}(t)] L_i(t), \\
&\frac{dB_i(t)}{dt} = \alpha_i L_i(t) - \gamma_{B,i}(t) B_i(t),
\end{aligned} \tag{7}$$

where $t \geq 0$, $1 \leq i \leq N$. We refer to the model as the *controlled SLBS model*, where the control,

$$\gamma(t) = \left(\gamma_{L,1}(t), \ldots, \gamma_{L,N}(t), \gamma_{B,1}(t), \ldots, \gamma_{B,N}(t)\right)^T, \tag{8}$$

stands for a dynamic control strategy of disruptive computer viruses. The admissible set of controls is

$$\Gamma = \left\{\gamma(t) \in \left(L^2[0,T]\right)^{2N} \mid \underline{\gamma_L} \leq \gamma_{L,i}(t) \leq \overline{\gamma_L}, \underline{\gamma_B} \leq \gamma_{B,i}(t) \leq \overline{\gamma_B},\ 0 \leq t \leq T,\ 1 \leq i \leq N\right\}. \tag{9}$$

Model (7) can be written in matrix notation as

$$\frac{d\mathbf{I}(t)}{dt} = \mathbf{f}\left(\mathbf{I}(t), \gamma(t)\right), \quad 0 \leq t \leq T. \tag{10}$$

Given a dynamic control strategy $\gamma(\cdot)$. The total loss can be measured by $\int_0^T \sum_{i=1}^N [L_i(t) + B_i(t)]dt$, and the total cost can be gauged by $\int_0^T \sum_{i=1}^N [p_i\gamma_{L,i}^{\theta}(t) + q_i\gamma_{B,i}^{\theta}(t)]dt$. As a result, the performance of a dynamic control strategy $\gamma(\cdot)$ can be measured by

$$J\left(\gamma(\cdot)\right) = \int_0^T \sum_{i=1}^N \left[L_i(t) + B_i(t) + p_i\gamma_{L,i}^{\theta}(t) + q_i\gamma_{B,i}^{\theta}(t)\right] dt. \tag{11}$$

Hence, developing an optimal dynamic control strategy of disruptive viruses can be modeled as solving the following optimal control problem.

$$\begin{aligned} \underset{\gamma(\cdot)\in\Gamma}{\text{Minimize}} \quad & J\left(\gamma(\cdot)\right) = \int_0^T \sum_{i=1}^N \left[L_i(t) + B_i(t) + p_i\gamma_{L,i}^{\theta}(t) + q_i\gamma_{B,i}^{\theta}(t)\right] dt \\ \text{subject to} \quad & \frac{d\mathbf{I}(t)}{dt} = \mathbf{f}\left(\mathbf{I}(t), \gamma(t)\right), \quad 0 \leq t \leq T, \\ & \mathbf{I}(0) = \mathbf{I}_0. \end{aligned} \tag{P*}$$

A solution to the optimal control problem (P*) stands for an optimal dynamic control strategy of disruptive viruses. For convenience, let

$$F\left(\mathbf{I}(t), \gamma(t)\right) = \sum_{i=1}^N \left[L_i(t) + B_i(t) + p_i\gamma_{L,i}^{\theta}(t) + q_i\gamma_{B,i}^{\theta}(t)\right]. \tag{12}$$

4. A Theoretical Study of the Optimal Control Problem

In this section, we shall study the optimal control problem (P*) presented in the previous section.

4.1. Existence of an Optimal Control. As a solution to the optimal control problem (P*) stands for an optimal dynamic control strategy of disruptive viruses, it is critical to show that there is such an optimal control. For that purpose, let us show that the five conditions in Lemma 1 hold true simultaneously.

Lemma 2. *The admissible set* Γ *is closed.*

Proof. Let $\gamma(t) = (\gamma_{L,1}(t), \ldots, \gamma_{L,N}(t), \gamma_{B,1}(t), \ldots, \gamma_{B,N}(t))^T$ be a limit point of Γ,

$$\gamma^{(n)}(t) = \left(\gamma_{L,1}^{(n)}(t), \ldots, \gamma_{L,N}^{(n)}(t), \gamma_{B,1}^{(n)}(t), \ldots, \gamma_{B,N}^{(n)}(t)\right)^T, \quad n = 1, 2, \ldots, \tag{13}$$

a sequence of points in Γ such that

$$\left\|\gamma^{(n)}(t) - \gamma(t)\right\|_2 = \left[\int_0^T \left|\gamma^{(n)}(t) - \gamma(t)\right|^2 dt\right]^{1/2} < \frac{1}{n}. \tag{14}$$

The completeness of $(L^2(0,T))^{2N}$ implies $\gamma(t) \in L^2(0,T)^{2N}$. Hence, the claim follows from the observation that

$$\begin{aligned} \underline{\gamma_L} \leq \gamma_{L,i}(t) = \lim_{n\to\infty} \gamma_{L,i}^{(n)}(t) \leq \overline{\gamma_L}, \\ \underline{\gamma_B} \leq \gamma_{B,i}(t) = \lim_{n\to\infty} \gamma_{B,i}^{(n)}(t) \leq \overline{\gamma_B}, \\ 1 \leq i \leq N. \end{aligned} \tag{15}$$

□

Lemma 3. *The admissible set* Γ *is convex.*

Proof. Let

$$\begin{aligned}\gamma^{(1)}(t) &= \left(\gamma_{L,1}^{(1)}(t), \ldots, \gamma_{L,N}^{(1)}(t), \gamma_{B,1}^{(1)}(t), \ldots, \gamma_{B,N}^{(1)}(t)\right)^T \\ &\in \Gamma, \\ \gamma^{(2)}(t) &= \left(\gamma_{L,1}^{(2)}(t), \ldots, \gamma_{L,N}^{(2)}(t), \gamma_{B,1}^{(2)}(t), \ldots, \gamma_{B,N}^{(2)}(t)\right)^T \\ &\in \Gamma,\end{aligned} \tag{16}$$

and $0 < \kappa < 1$. As $(L^2[0,T])^{2N}$ is a real vector space, we get

$$\begin{aligned}&(1-\kappa)\gamma^{(1)}(t) + \kappa\gamma^{(2)}(t) \\ &\in \left(L^2\left[0,T\right]\right)^{2N}.\end{aligned} \tag{17}$$

So, the claim follows from the observation that

$$\begin{aligned}\underline{\gamma_L} \le (1-\kappa)\gamma_{L,i}^{(1)}(t) + \kappa\gamma_{L,i}^{(2)}(t) \le \overline{\gamma_L}, \\ \underline{\gamma_B} \le (1-\kappa)\gamma_{B,i}^{(1)}(t) + \kappa\gamma_{B,i}^{(2)}(t) \le \overline{\gamma_B}, \\ 1 \le i \le N.\end{aligned} \tag{18}$$

□

Lemma 4. *There is $\gamma \in \Gamma$ such that model (7) is solvable.*

Proof. Substituting $\gamma(t) \equiv \overline{\gamma} = (\overline{\gamma_L}, \ldots, \overline{\gamma_L}, \overline{\gamma_B}, \ldots, \overline{\gamma_B})^T$ into model (7), we get

$$\frac{d\mathbf{I}(t)}{dt} = \mathbf{f}\left(\mathbf{I}(t), \overline{\gamma}\right), \quad 0 \le t \le T. \tag{19}$$

As $\mathbf{f}(\mathbf{I}, \overline{\gamma})$ is continuously differentiable, the claim follows from the Continuation Theorem for Differential Systems [47]. □

Lemma 5. $\mathbf{f}(\mathbf{I}, \gamma)$ *is bounded by a linear function in* $\mathbf{I}$.

Proof. The claim follows from the observation that, for $i = 1, 2, \ldots, N$,

$$\begin{aligned}&(1 - L_i - B_i)\sum_{j=1}^{N}\left(\beta_{L,ij}L_j + \beta_{B,ij}B_j\right) \\ &\quad - \left(\alpha_i + \gamma_{L,i}\right)L_i \le \sum_{j=1}^{N}\beta_{L,ij}L_j \\ &\quad + \sum_{j=1}^{N}\beta_{B,ij}B_j - \left(\alpha_i + \underline{\gamma_L}\right)L_i, \\ &\alpha_i L_i - \gamma_{B,i}B_i \le \alpha_i L_i - \underline{\gamma_B}B_i.\end{aligned} \tag{20}$$

□

Lemma 6. $F(\mathbf{I}, \gamma)$ *is convex on* Γ *if* $\theta \ge 1$.

Proof. The Hessian of F with respect to γ,

$$\begin{bmatrix} \frac{\partial^2 F}{\partial \gamma_{L,1}^2} & \cdots & \frac{\partial^2 F}{\partial \gamma_{L,1}\partial \gamma_{L,N}} & \frac{\partial^2 F}{\partial \gamma_{L,1}\partial \gamma_{B,1}} & \cdots & \frac{\partial^2 F}{\partial \gamma_{L,1}\partial \gamma_{B,N}} \\ \vdots & \ddots & \vdots & \vdots & \ddots & \vdots \\ \frac{\partial^2 F}{\partial \gamma_{L,N}\partial \gamma_{L,1}} & \cdots & \frac{\partial^2 F}{\partial \gamma_{L,N}^2} & \frac{\partial^2 F}{\partial \gamma_{L,N}\partial \gamma_{B,1}} & \cdots & \frac{\partial^2 F}{\partial \gamma_{L,N}\partial \gamma_{B,N}} \\ \frac{\partial^2 F}{\partial \gamma_{B,1}\partial \gamma_{L,1}} & \cdots & \frac{\partial^2 F}{\partial \gamma_{B,1}\partial \gamma_{L,N}} & \frac{\partial^2 F}{\partial \gamma_{B,1}^2} & \cdots & \frac{\partial^2 F}{\partial \gamma_{B,1}\partial \gamma_{B,N}} \\ \vdots & \ddots & \vdots & \vdots & \ddots & \vdots \\ \frac{\partial^2 F}{\partial \gamma_{B,N}\partial \gamma_{L,1}} & \cdots & \frac{\partial^2 F}{\partial \gamma_{B,N}\partial \gamma_{L,N}} & \frac{\partial^2 F}{\partial \gamma_{B,N}\partial \gamma_{B,1}} & \cdots & \frac{\partial^2 F}{\partial \gamma_{B,N}^2} \end{bmatrix} \tag{21}$$

$$= \theta(\theta-1)\begin{bmatrix} p_1\gamma_{L,1}^{\theta-2} & \cdots & 0 & 0 & \cdots & 0 \\ \vdots & \ddots & \vdots & \vdots & \ddots & \vdots \\ 0 & \cdots & p_N\gamma_{L,N}^{\theta-2} & 0 & \cdots & 0 \\ 0 & \cdots & 0 & q_1\gamma_{B,1}^{\theta-2} & \cdots & 0 \\ \vdots & \ddots & \vdots & \vdots & \ddots & \vdots \\ 0 & \cdots & 0 & 0 & \cdots & q_N\gamma_{B,N}^{\theta-2} \end{bmatrix},$$

is always positive semidefinite. This implies the convexity of F. □

Lemma 7. *$F(\mathbf{I}, \gamma) \geq \min_i\{c_i, d_i\}\|\mathbf{I}\|_\theta^\theta$, where $\|\cdot\|_\theta$ stands for the θ-norm of vectors.*

Proof. We have

$$\begin{aligned} F\left(\mathbf{I}, \gamma\right) &= \sum_{i=1}^{N}\left(L_i + B_i + p_i\gamma_{L,i}^{\theta} + q_i\gamma_{B,i}^{\theta}\right) \\ &\geq \min_{1\leq i\leq N}\left\{p_i, q_i\right\}\sum_{i=1}^{N}\left(\gamma_{L,i}^{\theta} + \gamma_{B,i}^{\theta}\right) \\ &= \min_{1\leq i\leq N}\left\{p_i, q_i\right\}\left\|\mathbf{I}\right\|_\theta^\theta. \end{aligned} \tag{22}$$

□

We are ready to present the main result of this subsection.

Theorem 8. *Problem* (P*) *has an optimal control if $\theta > 1$.*

Proof. Lemmas 2–7 show that the five conditions in Lemma 1 are all met. Hence, the existence of an optimal control follows from Lemma 1. □

4.2. The Optimality System. As the optimality system for the optimal control problem (P*) offers a method for numerically solving the problem, it is critical to determine the optimality system. For that purpose, consider the corresponding Hamiltonian

$$\begin{aligned} &H\left(\mathbf{I}\left(t\right), \gamma\left(t\right), \lambda\left(t\right)\right) \\ &= \sum_{i=1}^{N}\left[L_i\left(t\right) + B_i\left(t\right) + p_i\gamma_{L,i}^{\theta}\left(t\right) + q_i\gamma_{2i}^{\theta}\left(t\right)\right] \\ &+ \sum_{i=1}^{N}\lambda_{L,i}\left(t\right) \\ &\cdot\left\{\left[1 - L_i\left(t\right) - B_i\left(t\right)\right]\sum_{j=1}^{N}\left[\beta_{L,ij}L_j\left(t\right) + \beta_{B,ij}B_j\left(t\right)\right]\right. \\ &\left. - \left[\alpha_i + \gamma_{L,i}\left(t\right)\right]L_i\left(t\right)\right\} + \sum_{i=1}^{N}\lambda_{B,i}\left(t\right)\left[\alpha_i L_i\left(t\right)\right. \\ &\left. - \gamma_{B,i}\left(t\right)B_i\left(t\right)\right], \end{aligned} \tag{23}$$

where $\lambda(\cdot) = (\lambda_{L,1}(\cdot), \ldots, \lambda_{L,N}(\cdot), \lambda_{B,1}(\cdot), \ldots, \lambda_{B,N}(\cdot))^T$ is the adjoint.

Theorem 9. *Suppose $\gamma^*(\cdot)$ is an optimal control for problem* (P*) *with $\theta > 1$; $\mathbf{I}^*(\cdot)$ is the solution to the controlled SLBS model with $\gamma(\cdot) = \gamma^*(\cdot)$. Then, there exists $\lambda^*(\cdot)$ with $\lambda^*(T) = \mathbf{0}$ such that*

$$\begin{aligned} \frac{d\lambda_{L,i}^*\left(t\right)}{dt} &= -1 + \lambda_{L,i}^*\left(t\right)\left\{\alpha_i + \gamma_{L,i}^*\left(t\right)\right. \\ &\left. + \sum_{j=1}^{N}\left[\beta_{L,ij}L_j^*\left(t\right) + \beta_{B,ij}B_j^*\left(t\right)\right]\right\} \\ &- \sum_{j=1}^{N}\beta_{L,ji}\left[1 - L_j^*\left(t\right) - B_j^*\left(t\right)\right]\lambda_{L,j}^*\left(t\right) \\ &- \alpha_i\lambda_{B,i}^*\left(t\right), \\ \frac{d\lambda_{B,i}^*\left(t\right)}{dt} &= -1 + \gamma_{B,i}^*\left(t\right)\lambda_{B,i}^*\left(t\right) + \lambda_{L,i}^*\left(t\right) \\ &\cdot\sum_{j=1}^{N}\left[\beta_{L,ij}L_j^*\left(t\right) + \beta_{B,ij}B_j^*\left(t\right)\right] \\ &- \sum_{j}\beta_{B,ji}\left[1 - L_j^*\left(t\right) - B_j^*\left(t\right)\right]\lambda_{L,j}^*\left(t\right), \\ \gamma_{L,i}^*\left(t\right) &= \max\left\{\min\left\{\left[\frac{\lambda_{L,i}^*\left(t\right)L_i^*\left(t\right)}{\theta p_i}\right]^{1/(\theta-1)}, \right.\right. \\ &\left.\left.\overline{\gamma_L}\right\}, \underline{\gamma_L}\right\}, \\ \gamma_{B,i}^*\left(t\right) &= \max\left\{\min\left\{\left[\frac{\lambda_{B,i}^*\left(t\right)B_i^*\left(t\right)}{\theta q_i}\right]^{1/(\theta-1)}, \right.\right. \\ &\left.\left.\overline{\gamma_B}\right\}, \underline{\gamma_B}\right\}, \end{aligned} \tag{24}$$

where $0 \leq t \leq T$ and $1 \leq i \leq N$.

Proof. According to the Pontryagin Minimum Principle [26], there exists $\lambda^*(t)$ such that

$$\frac{d\lambda_{L,i}^*\left(t\right)}{dt} = -\frac{\partial H\left(\mathbf{I}^*\left(t\right), \gamma^*\left(t\right), \lambda^*\left(t\right)\right)}{\partial L_i},$$

$$0 \leq t \leq T,\ 1 \leq i \leq N,$$

$$\frac{d\lambda^*_{B,i}(t)}{dt} = -\frac{\partial H\left(\mathbf{I}^*(t), \gamma^*(t), \lambda^*(t)\right)}{\partial B_i}, \quad 0 \le t \le T,\ 1 \le i \le N. \tag{25}$$

Thus, the first $2N$ equations in the claim follow by direct calculations. As the terminal cost is unspecified and the final state is free, the transversality condition $\lambda^*(T) = \mathbf{0}$ holds. By using the optimality condition

$$\gamma^*(t) = \arg\min_{\gamma(t)\in\Gamma} H\left(\mathbf{I}^*(t), \gamma(t), \lambda^*(t)\right), \tag{26}$$

we get (a) either

$$\frac{\partial H\left(\mathbf{I}^*(t), \gamma^*(t), \lambda^*(t)\right)}{\partial \gamma_{L,i}} = \theta p_i \left(\gamma^*_{L,i}(t)\right)^{\theta-1} - \lambda^*_{L,i}(t) L^*_i(t) = 0 \tag{27}$$

or $\gamma^*_{L,i}(t) = \underline{\gamma_L}$ or $\gamma^*_{L,i}(t) = \overline{\gamma_L}$ and (b) either

$$\frac{\partial H\left(\mathbf{I}^*(t), \gamma^*(t), \lambda^*(t)\right)}{\partial \gamma_{B,i}} = \theta q_i \left(\gamma^*_{B,i}(t)\right)^{\theta-1} - \lambda^*_{B,i}(t) B^*_i(t) = 0 \tag{28}$$

or $\gamma^*_{B,i}(t) = \underline{\gamma_B}$ or $\gamma^*_{B,i}(t) = \overline{\gamma_B}$. So, the last $2N$ equations in the claim follow.

By combining the above discussions, we get the optimality system for problem (P*) with $\theta > 1$ as follows.

$$\begin{aligned}
\frac{dL_i(t)}{dt} &= \left[1 - L_i(t) - B_i(t)\right] \cdot \sum_{j=1}^{N} \left[\beta_{L,ij} L_j(t) + \beta_{B,ij} B_j(t)\right] - \left[\alpha_i + \gamma_{L,i}(t)\right] L_i(t), \\
\frac{dB_i(t)}{dt} &= \alpha_i L_i(t) - \gamma_{B,i}(t) B_i(t), \\
\frac{d\lambda_{L,i}(t)}{dt} &= -1 + \lambda_{L,i}(t) \left\{\alpha_i + \gamma_{L,i}(t) + \sum_{j=1}^{N} \left[\beta_{L,ij} L_j(t) + \beta_{B,ij} B_j(t)\right]\right\} \\
&\quad - \sum_{j=1}^{N} \beta_{L,ji} \left[1 - L_j(t) - B_j(t)\right] \lambda_{L,j}(t) - \alpha_i \lambda_{B,i}(t), \\
\frac{d\lambda_{B,i}(t)}{dt} &= -1 + \gamma_{B,i}(t) \lambda_{B,i}(t) + \lambda_{L,i}(t) \cdot \sum_{j=1}^{N} \left[\beta_{L,ij} L_j(t) + \beta_{B,ij} B_j(t)\right] \\
&\quad - \sum_{j=1}^{N} \beta_{B,ji} \left[1 - L_j(t) - B_j(t)\right] \lambda_{L,j}(t), \\
\gamma_{L,i}(t) &= \max\left\{\min\left\{\left[\frac{\lambda_{L,i}(t) L_i(t)}{\theta p_i}\right]^{1/(\theta-1)}, \overline{\gamma_L}\right\}, \underline{\gamma_L}\right\}, \\
\gamma_{B,i}(t) &= \max\left\{\min\left\{\left[\frac{\lambda_{B,i}(t) B_i(t)}{\theta q_i}\right]^{1/(\theta-1)}, \overline{\gamma_B}\right\}, \underline{\gamma_B}\right\},
\end{aligned} \tag{29}$$

where $\mathbf{I}(0) = \mathbf{I}_0$, $\lambda(T) = \mathbf{0}$, $0 \le t \le T$, $1 \le i \le N$.

By applying the forward-backward Euler scheme to the optimality system, we can obtain the numerical solution to the optimal control problem (P*), that is, an optimal dynamic control strategy of disruptive viruses. □

5. Numerical Examples

This section gives some examples of the optimal dynamic control strategy of disruptive computer viruses. Given a dynamic control strategy $\gamma(t)$. Define the average control (AC) function, the average cumulative loss (ACL) function, the average cumulative cost (ACC) function, and the average cumulative performance (ACP) function as follows.

$$\mathrm{AC}(t) = \frac{1}{N} \sum_{i=1}^{N} \left[\gamma_{L,i}(t) + \gamma_{B,i}(t)\right], \quad 0 \le t \le T,$$

$$\mathrm{ACL}(t) = \frac{1}{N}\sum_{i=1}^{N}\int_0^t \left[L_i(s) + B_i(s)\right] ds, \quad 0 \le t \le T,$$

$$\mathrm{ACC}(t) = \frac{1}{N}\sum_{i=1}^{N}\int_0^t \left[p_i \gamma_{L,i}^{\theta}(s) + q_i \gamma_{B,i}^{\theta}(s)\right] ds, \quad 0 \le t \le T,$$

$$\mathrm{ACP}(t) = \frac{1}{N}\sum_{i=1}^{N}\int_0^t \left[L_i(s) + B_i(s) + p_i \gamma_{L,i}^{\theta}(s) + q_i \gamma_{B,i}^{\theta}(s)\right] ds, \quad 0 \le t \le T. \tag{30}$$

These functions form an evaluation criterion of dynamic control strategies of disruptive viruses.

5.1. Scale-Free Network. Scale-free networks are a large class of networks having widespread applications. For our purpose, generate a scale-free network G with $N = 100$ nodes using the Barabasi-Albert method [48].

Example 10. Consider an optimal control problem (P*) on the virus-spreading network G, where the parameters and the initial conditions are set as follows.

(a) $T = 200$, $\theta = 2$, $\underline{\gamma_L} = 0$, $\overline{\gamma_L} = 0.2$, $\underline{\gamma_B} = 0.1$, and $\overline{\gamma_B} = 0.3$.

(b) $\beta_{L,ij} = 0.005$ and $\beta_{B,ij} = 0.001$, $(i, j) \in E(G)$.

(c) $\alpha_i = 0.1$ and $p_i = q_i = 1$, $i \in V(G)$.

(d) $L_i(0) = 0.1$ and $B_i(0) = 0$, $1 \le i \le N$.

For the optimal dynamic control strategy to the optimal control problem and some static control strategies, the AC functions, the ACL functions, the ACC functions, and the ACP function are shown in Figure 2.

5.2. Small-World Network. Small-world networks are another large class of networks having widespread applications. For our purpose, generate a small-world network G with $N = 100$ nodes using the Watts-Strogatz method [49].

Example 11. Consider an optimal control problem (P*) on the virus-spreading network G, where the parameters and the initial conditions are set as follows.

(a) $T = 200$, $\theta = 2$, $\underline{\gamma_L} = 0$, $\overline{\gamma_L} = 0.2$, $\underline{\gamma_B} = 0.1$, and $\overline{\gamma_B} = 0.3$.

(b) $\beta_{L,ij} = 0.005$ and $\beta_{B,ij} = 0.001$, $(i, j) \in E(G)$.

(c) $\alpha_i = 0.1$ and $p_i = q_i = 1$, $i \in V(G)$.

(d) $L_i(0) = 0.1$ and $B_i(0) = 0$, $1 \le i \le N$.

For the optimal dynamic control strategy to the optimal control problem and some static control strategies, the AC functions, the ACL functions, the ACC functions, and the ACP function are shown in Figure 3.

5.3. Realistic Network. Consider a network G with $N = 300$ nodes cut out from the database of Stanford University [50].

Example 12. Consider an optimal control problem (P*) on the virus-spreading network G, where the parameters and the initial conditions are set as follows.

(a) $T = 200$, $\theta = 2$, $\underline{\gamma_L} = 0$, $\overline{\gamma_L} = 0.2$, $\underline{\gamma_B} = 0.1$, and $\overline{\gamma_B} = 0.3$.

(b) $\beta_{L,ij} = 0.005$ and $\beta_{B,ij} = 0.001$, $(i, j) \in E(G)$.

(c) $\alpha_i = 0.1$ and $p_i = q_i = 1$, $i \in V(G)$.

(d) $L_i(0) = 0.1$ and $B_i(0) = 0$, $1 \le i \le N$.

For the optimal dynamic control strategy to the optimal control problem and some static control strategies, the AC functions, the ACL functions, the ACC functions, and the ACP function are shown in Figure 4.

6. Performance Evaluation

The previous discussions manifest that if the parameters in the optimal control problem (P*) are all available, then an optimal dynamic control strategy can be obtained by numerically solving the optimality system. In realistic scenarios, however, some of these parameters might be unavailable. In such situations, it is necessary to estimate the performance of an actual dynamical control strategy in comparison with that of the optimal dynamical control strategy. Now let us present such an estimation.

Theorem 13. *Consider the optimal control problem* (P*). *Let* $\gamma^*(\cdot)$ *be the optimal dynamic control strategy,* $\gamma(\cdot)$ *an arbitrary dynamic control strategy. Then,*

$$\begin{aligned}\left|J\left(\gamma(\cdot)\right) - J\left(\gamma^*(\cdot)\right)\right| &\le \frac{2Nc_1}{c_2}\left(e^{c_2 T} - 1 - c_2 T - \frac{c_2^2 T^2}{2}\right) \\ &+ \sum_{i=1}^{N} p_i \int_0^T \left|\gamma_{L,i}^{\theta}(t) - \gamma_{L,i}^{*\theta}(t)\right| dt \\ &+ \sum_{i=1}^{N} q_i \int_0^T \left|\gamma_{B,i}^{\theta}(t) - \gamma_{B,i}^{*\theta}(t)\right| dt,\end{aligned} \tag{31}$$

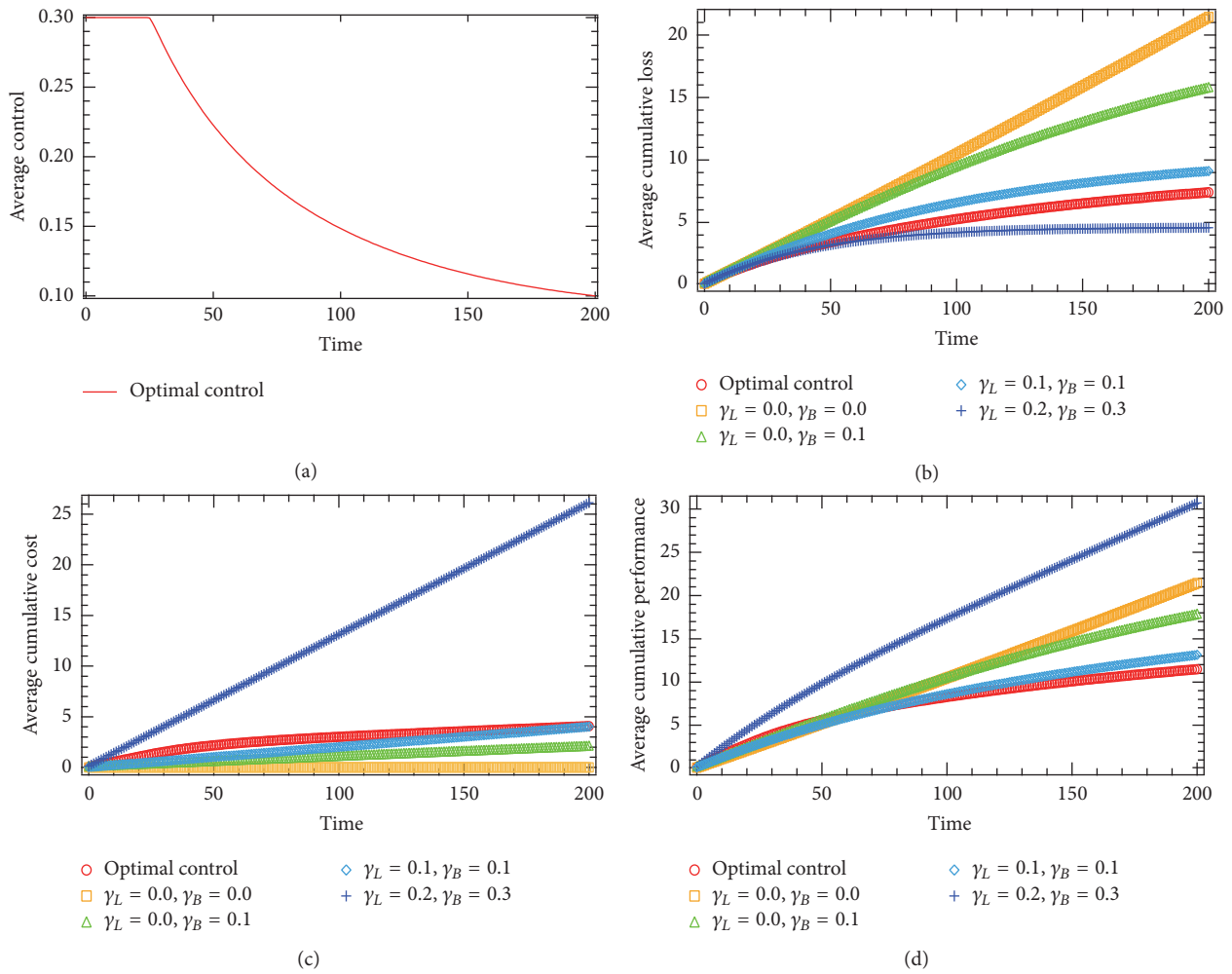

Figure 2: (a) The AC functions, (b) the ACL functions, (c) the ACC functions, and (d) the ACP functions for the optimal dynamic control strategies in Example 10.

where

$$c_1 = \max\left\{2\max_{1\le i\le N}\left\{\sum_{j=1}^{N}\left|\beta_{L,ij}\right|\right\} + 2\max_{1\le i\le N}\left\{\sum_{j=1}^{N}\left|\beta_{B,ij}\right|\right\} + \overline{\gamma_L} - \underline{\gamma_L}, \overline{\gamma_B} - \underline{\gamma_B}\right\},$$

$$c_2 = 2\max_{1\le i\le N}\left\{\sum_{j=1}^{N}\left|\beta_{L,ij}\right|\right\} + \overline{\alpha} + \overline{\gamma_L} + \max\left\{2\max_{1\le i\le N}\left\{\sum_{j=1}^{N}\left|\beta_{B,ij}\right|\right\}, \overline{\gamma_B}\right\}. \tag{32}$$

Proof. Let $\|\cdot\|$ denote the ∞-norm. Let $\mathbf{I}^*(\cdot) = (\mathbf{L}^*(\cdot)^T, \mathbf{B}^*(\cdot)^T)^T$ denote the solution to the SLBS model with control $\gamma^*(t)$ and $\mathbf{I}(\cdot) = (\mathbf{L}(\cdot)^T, \mathbf{B}(\cdot)^T)^T$ the solution to the SLBS model with control $\gamma(\cdot)$. As

$$\begin{aligned}\mathbf{L}(t) = \mathbf{L}_0^* &+ \int_0^t \operatorname{diag}\left(1 - B_i(s) - L_i(s)\right) \cdot \mathbf{A}_L \mathbf{L}(s)\, ds \\ &+ \int_0^t \operatorname{diag}\left(1 - B_i(s) - L_i(s)\right) \cdot \mathbf{A}_B \mathbf{B}(s)\, ds \\ &- \int_0^t \operatorname{diag}\left(\alpha_i + \gamma_{L,i}(s)\right) \mathbf{L}(s)\, ds,\end{aligned}$$

$$\begin{aligned}\mathbf{L}^*(t) = \mathbf{L}_0^* &+ \int_0^t \operatorname{diag}\left(1 - B_i^*(s) - L_i^*(s)\right) \cdot \mathbf{A}_L \mathbf{L}^*(s)\, ds\end{aligned}$$

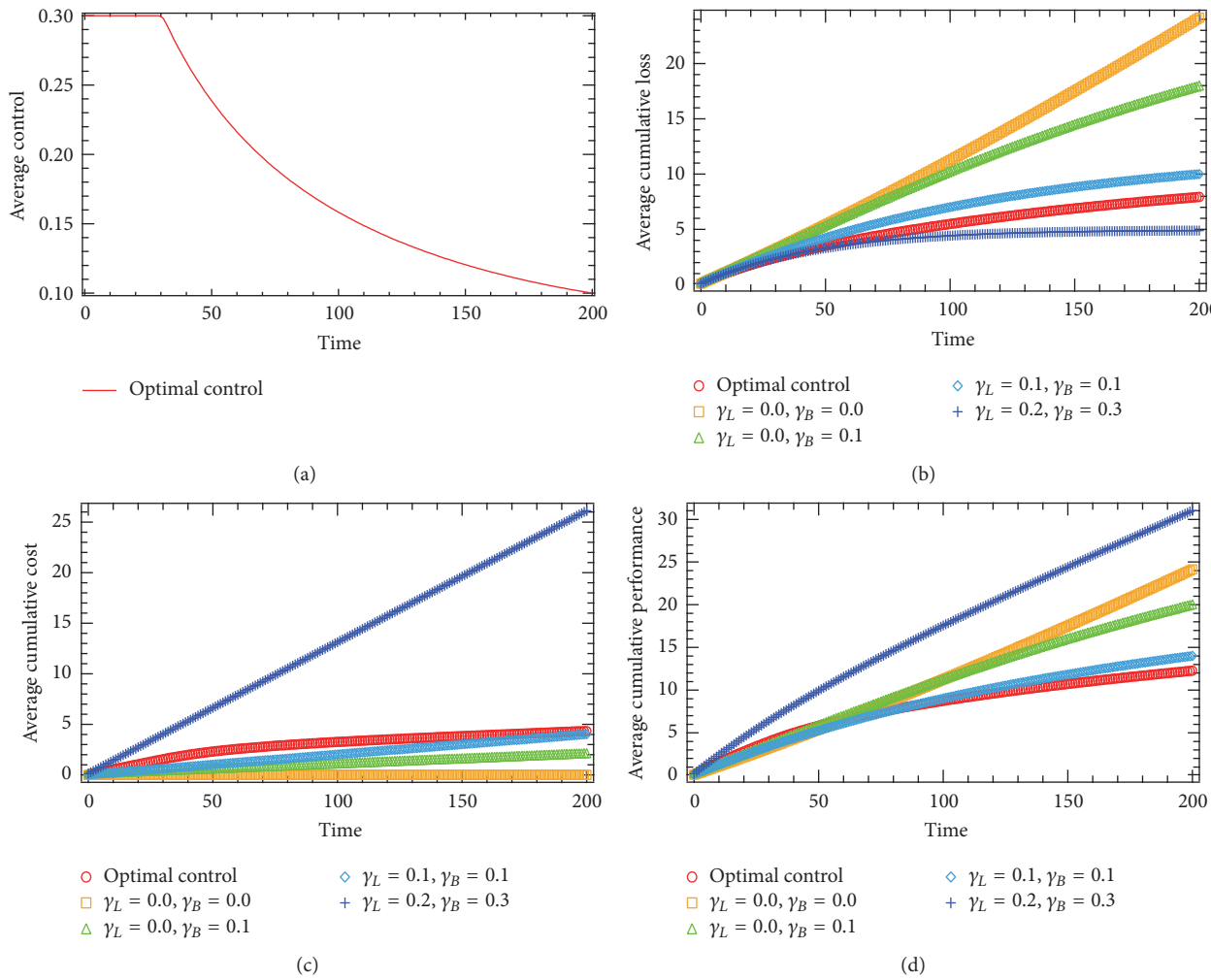

FIGURE 3: (a) The AC functions, (b) the ACL functions, (c) the ACC functions, and (d) the ACP functions for the optimal dynamic control strategies in Example 11.

$$
\begin{aligned}
&+ \int_0^t \operatorname{diag}\left(1 - B_i^*(s) - L_i^*(s)\right) \\
&\cdot \mathbf{A}_B \mathbf{B}^*(s)\, ds \\
&- \int_0^t \operatorname{diag}\left(\alpha_i + \gamma_{L,i}^*(s)\right) \mathbf{L}^*(s)\, ds,
\end{aligned} \tag{33}
$$

we get

$$
\begin{aligned}
\mathbf{L}(t) - \mathbf{L}^*(t) &= \int_0^t \operatorname{diag}\left(1 - B_i(s) - L_i(s)\right) \\
&\cdot \mathbf{A}_L \left[\mathbf{L}(s) - \mathbf{L}^*(s)\right] ds \\
&+ \int_0^t \operatorname{diag}\left(1 - B_i(s) - L_i(s)\right) \\
&\cdot \mathbf{A}_B \left[\mathbf{B}(s) - \mathbf{B}^*(s)\right] ds \\
&- \int_0^t \operatorname{diag}\left(L_i(s) - L_i^*(s) + B_i(s) - B_i^*(s)\right) \\
&\cdot \mathbf{A}_L \mathbf{L}^*(s)\, ds \\
&- \int_0^t \operatorname{diag}\left(L_i(s) - L_i^*(s) + B_i(s) - B_i^*(s)\right) \\
&\cdot \mathbf{A}_B \mathbf{B}^*(s)\, ds - \int_0^t \operatorname{diag}\left(\alpha_i + \gamma_{L,i}(s)\right) \\
&\cdot \left[\mathbf{L}(s) - \mathbf{L}^*(s)\right] ds - \int_0^t \operatorname{diag}\left(\gamma_{L,i}(s) - \gamma_{L,i}^*(s)\right) \\
&\cdot \mathbf{L}^*(s)\, ds.
\end{aligned} \tag{34}
$$

So,

$$
\begin{aligned}
\left\|\mathbf{L}(t) - \mathbf{L}^*(t)\right\| &\le \left\|\mathbf{A}_L\right\| \int_0^t \left\|\operatorname{diag}\left(1 - B_i(s) - L_i(s)\right)\right\| \\
&\cdot \left\|\mathbf{L}(s) - \mathbf{L}^*(s)\right\| ds + \left\|\mathbf{A}_B\right\| \\
&\cdot \int_0^t \left\|\operatorname{diag}\left(1 - B_i(s) - L_i(s)\right)\right\| \\
&\cdot \left\|\mathbf{B}(s) - \mathbf{B}^*(s)\right\| ds + \left\|\mathbf{A}_L\right\|
\end{aligned}
$$

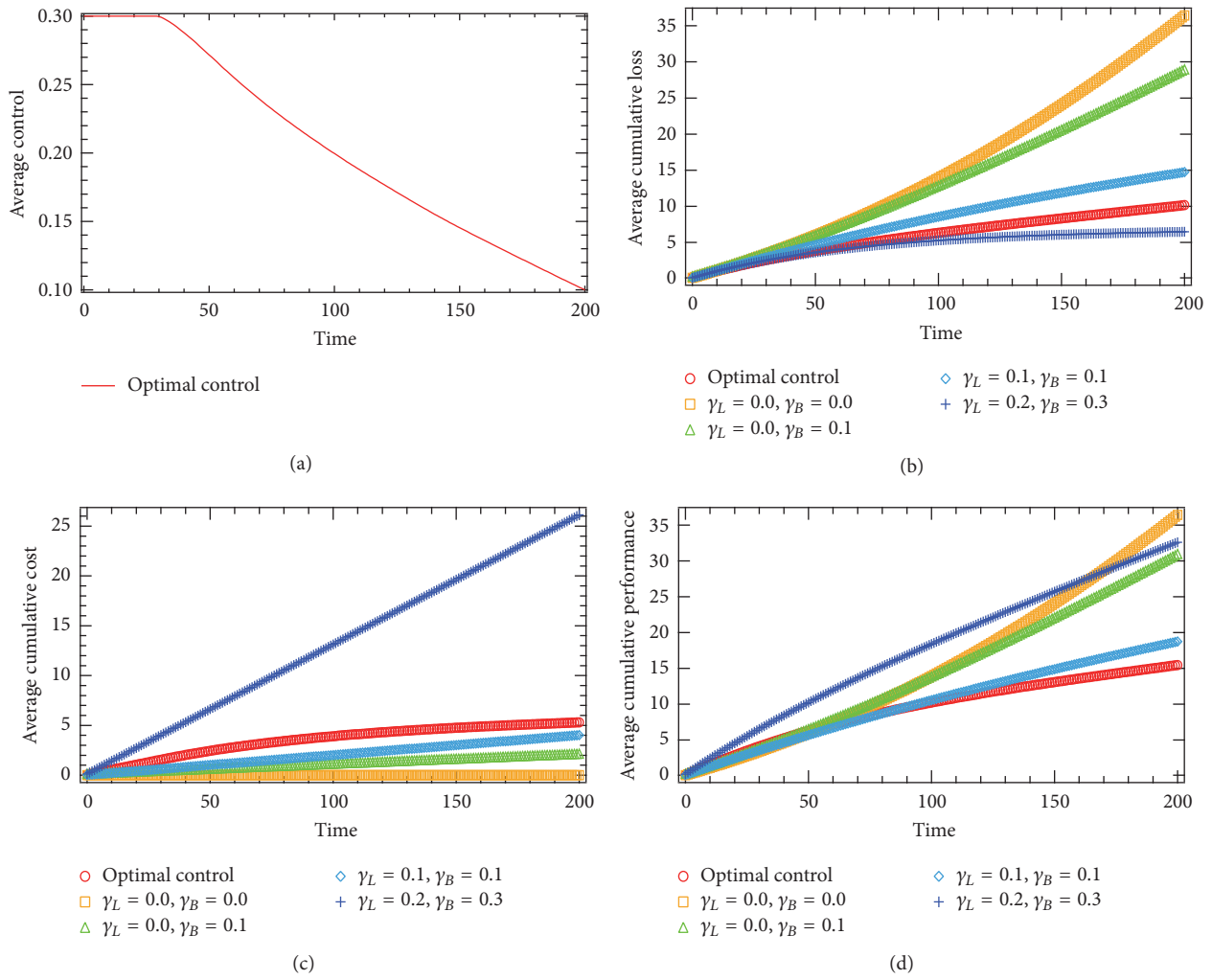

Figure 4: (a) The AC functions, (b) the ACL functions, (c) the ACC functions, and (d) the ACP functions for the optimal dynamic control strategies in Example 12.

$$
\begin{aligned}
&\cdot \int_0^t \left\| \operatorname{diag}\left(L_i(s) - L_i^*(s) + B_i(s) - B_i^*(s)\right)\right\| \\
&\cdot \left\|\mathbf{L}^*(s)\right\| ds + \left\|\mathbf{A}_B\right\| \\
&\cdot \int_0^t \left\| \operatorname{diag}\left(L_i(s) - L_i^*(s) + B_i(s) - B_i^*(s)\right)\right\| \\
&\cdot \left\|\mathbf{B}^*(s)\right\| ds + \int_0^t \left\| \operatorname{diag}\left(\alpha_i + \gamma_{L,i}(s)\right)\right\| \\
&\cdot \left\|\mathbf{L}(s) - \mathbf{L}^*(s)\right\| ds \\
&+ \int_0^t \left\| \operatorname{diag}\left(\gamma_{L,i}(s) - \gamma_{L,i}^*(s)\right)\right\| \cdot \left\|\mathbf{L}^*(s)\right\| ds \\
&\le \left(2\left\|\mathbf{A}_L\right\| + 2\left\|\mathbf{A}_B\right\| + \overline{\gamma_L} - \underline{\gamma_L}\right) t + \left(\left\|\mathbf{A}_L\right\| + \overline{\alpha} + \overline{\gamma_L}\right) \\
&\cdot \int_0^t \left\|\mathbf{L}(s) - \mathbf{L}^*(s)\right\| ds + \left\|\mathbf{A}_B\right\| \\
&\cdot \int_0^t \left\|\mathbf{B}(s) - \mathbf{B}^*(s)\right\| ds.
\end{aligned} \tag{35}
$$

As

$$
\begin{aligned}
\mathbf{B}(t) &= \mathbf{B}_0^* + \int_0^t \operatorname{diag}\left(\alpha_i\right) \mathbf{L}(s)\, ds \\
&\quad - \int_0^t \operatorname{diag}\left(\gamma_{B,i}(s)\right) \mathbf{B}(s)\, ds, \\
\mathbf{B}^*(t) &= \mathbf{B}_0^* + \int_0^t \operatorname{diag}\left(\alpha_i\right) \mathbf{L}^*(s)\, ds \\
&\quad - \int_0^t \operatorname{diag}\left(\gamma_{B,i}^*(s)\right) \cdot \mathbf{B}^*(s)\, ds,
\end{aligned} \tag{36}
$$

we get

$$\begin{aligned}
&\mathbf{B}(t) - \mathbf{B}^*(t) \\
&= \int_0^t \operatorname{diag}(\alpha_i)\left[\mathbf{L}(s) - \mathbf{L}^*(s)\right] ds \\
&- \int_0^t \operatorname{diag}\left(\gamma_{B,i}(s)\right)\left[\mathbf{B}(s) - \mathbf{B}^*(s)\right] ds \\
&- \int_0^t \operatorname{diag}\left(\gamma_{B,i}(s) - \gamma_{B,i}^*(s)\right)\mathbf{B}^*(s)\, ds.
\end{aligned} \tag{37}$$

Thus,

$$\begin{aligned}
&\left\|\mathbf{B}(t) - \mathbf{B}^*(t)\right\| \\
&\le \int_0^t \left\|\operatorname{diag}(\alpha_i)\right\| \cdot \left\|\mathbf{L}(s) - \mathbf{L}^*(s)\right\| ds \\
&+ \int_0^t \left\|\operatorname{diag}\left(\gamma_{B,i}(s)\right)\right\| \cdot \left\|\mathbf{B}(s) - \mathbf{B}^*(s)\right\| ds \\
&+ \int_0^t \left\|\operatorname{diag}\left(\gamma_{B,i}(s) - \gamma_{B,i}^*(s)\right)\right\| \cdot \left\|\mathbf{B}^*(s)\right\| ds \\
&\le \left(\overline{\gamma_B} - \underline{\gamma_B}\right) t + \overline{\alpha} \int_0^t \left\|\mathbf{L}(s) - \mathbf{L}^*(s)\right\| ds \\
&+ \overline{\gamma_B} \int_0^t \left\|\mathbf{B}(s) - \mathbf{B}^*(s)\right\| ds.
\end{aligned} \tag{38}$$

As $\|\mathbf{I}(t) - \mathbf{I}^*(t)\| = \max\{\|\mathbf{L}(t) - \mathbf{L}^*(t)\|, \|\mathbf{B}(t) - \mathbf{B}^*(t)\|\}$, we get

$$\begin{aligned}
\left\|\mathbf{I}(t) - \mathbf{I}^*(t)\right\| &\le \max\left\{2\left\|\mathbf{A}_L\right\| + 2\left\|\mathbf{A}_B\right\|\right. \\
&+ \overline{\gamma_L} - \underline{\gamma_L}, \overline{\gamma_B} - \underline{\gamma_B}\Big\} t + \left(\left\|\mathbf{A}_L\right\| + \overline{\alpha}\right. \\
&+ \left.\overline{\gamma_L}\right) \int_0^t \left\|\mathbf{L}(s) - \mathbf{L}^*(s)\right\| ds \\
&+ \max\left\{\left\|\mathbf{A}_B\right\|, \overline{\gamma_B}\right\} \\
&\cdot \int_0^t \left\|\mathbf{B}(s) - \mathbf{B}^*(s)\right\| ds \le c_1 t \\
&+ c_2 \int_0^t \left\|\mathbf{I}(s) - \mathbf{I}^*(s)\right\| ds.
\end{aligned} \tag{39}$$

Applying the Gronwall inequality [47], we get

$$\begin{aligned}
\left\|\mathbf{I}(t) - \mathbf{I}^*(t)\right\| &\le c_1 t + c_1 c_2 \int_0^t s e^{c_2(t-s)} ds \\
&= \frac{c_1}{c_2}\left(e^{c_2 t} - 1 - c_2 t\right).
\end{aligned} \tag{40}$$

Hence, we deduce that

$$\begin{aligned}
&\left|J(\gamma(\cdot)) - J(\gamma^*(\cdot))\right| \\
&\le \sum_{i=1}^N \int_0^T \left|L_i(t) - L_i^*(t)\right| dt \\
&+ \sum_i \int_0^T \left|B_i(t) - B_i^*(t)\right| dt \\
&+ \sum_i p_i \int_0^T \left|\gamma_{L,i}^{\theta}(t) - \gamma_{L,i}^{*\theta}(t)\right| dt \\
&+ \sum_{i=1}^N q_i \int_0^T \left|\gamma_{B,i}^{\theta}(t) - \gamma_{B,i}^{*\theta}(t)\right| dt \\
&\le 2N \int_0^T \left\|\mathbf{I}(t) - \mathbf{I}^*(t)\right\| dt \\
&+ \sum_{i=1}^N p_i \int_0^T \left|\gamma_{L,i}^{\theta}(t) - \gamma_{L,i}^{*\theta}(t)\right| dt \\
&+ \sum_{i=1}^N q_i \int_0^T \left|\theta_i^k(t) - \theta_i^{*k}(t)\right| dt \\
&\le \frac{2Nc_1}{c_2}\left(e^{c_2 T} - 1 - c_2 T - \frac{c_2^2 T^2}{2}\right) \\
&+ \sum_{i=1}^N p_i \int_0^T \left|\gamma_{L,i}^{\theta}(t) - \gamma_{L,i}^{*\theta}(t)\right| dt \\
&+ \sum_{i=1}^N q_i \int_0^T \left|\gamma_{B,i}^{\theta}(t) - \gamma_{B,i}^{*\theta}(t)\right| dt.
\end{aligned} \tag{41}$$

□

Although this estimation is rough, it takes the first step towards the accurate performance evaluation of actual dynamic control strategies of disruptive computer viruses.

7. Conclusions and Remarks

This paper has studied the problem of containing disruptive computer viruses in a cost-effective way. The problem has been modeled as an optimal control problem. A criterion for the existence of an optimal control has been given, and the optimality system has been derived. Some examples of the optimal dynamic control strategy have been presented. Finally, the performance of an actual control strategy of disruptive viruses has been estimated.

Towards this direction, there are a number of problems that are worth studying. First, the bandwidth resources consumed in the virus control process should be measured and incorporated in the cost. Second, the optimal dynamic control problem should be investigated under sophisticated epidemic models such as the impulsive epidemic models [51, 52], the stochastic epidemic models [53–55], and the epidemic models on time-varying networks [56–58]. Last,

it is rewarding to apply the methodology developed in this paper to the optimal dynamic control of rumor spreading [59–61].

Conflicts of Interest

The authors declare that there are no conflicts of interest regarding the publication of this paper.

Acknowledgments

This work is supported by Natural Science Foundation of China (Grant nos. 61572006, 71301177), National Sci-Tech Support Plan (Grant no. 2015BAF05B03), Basic and Advanced Research Program of Chongqing (Grant no. cstc2013jcyjA1658), and Fundamental Research Funds for the Central Universities (Grant no. 106112014CDJZR008823).

References

[1] P. Szor, *The Art of Computer Virus Research and Defense*, Addison-Wesley Education Publishers, 2005.

[2] Y. Wang, S. Wen, Y. Xiang, and W. Zhou, "Modeling the propagation of worms in networks: a survey," *IEEE Communications Surveys and Tutorials*, vol. 16, no. 2, pp. 942–960, 2014.

[3] J. O. Kephart and S. R. White, "Directed-graph epidemiological models of computer viruses," in *Proceedings of the IEEE Computer Society Symposium on Research in Security and Privacy*, pp. 343–359, Oakland, Calif, USA, May 1991.

[4] J. O. Kephart and S. R. White, "Measuring and modeling computer virus prevalence," in *Proceedings of the IEEE Computer Society Symposium on Research in Security and Privacy*, pp. 2–15, Oakland, Calif, USA, May 1993.

[5] J. R. Piqueira and V. O. Araujo, "A modified epidemiological model for computer viruses," *Applied Mathematics and Computation*, vol. 213, no. 2, pp. 355–360, 2009.

[6] B. K. Mishra and S. K. Pandey, "Dynamic model of worms with vertical transmission in computer network," *Applied Mathematics and Computation*, vol. 217, no. 21, pp. 8438–8446, 2011.

[7] Y. Yao, W. Xiang, A. Qu, G. Yu, and F. Gao, "Hopf bifurcation in an SEIDQV worm propagation model with quarantine strategy," *Discrete Dynamics in Nature and Society*, vol. 2012, Article ID 304868, 18 pages, 2012.

[8] L. Feng, X. Liao, Q. Han, and L. Song, "Modeling and analysis of peer-to-peer botnets," *Discrete Dynamics in Nature and Society*, vol. 2012, Article ID 865075, 18 pages, 2012.

[9] Y. Li, J. Pan, L. Song, and Z. Jin, "The influence of user protection behaviors on the control of internet worm propagation," *Abstract and Applied Analysis*, vol. 2013, Article ID 531781, 13 pages, 2013.

[10] Y. Yao, X.-W. Xie, H. Guo, G. Yu, F.-X. Gao, and X.-J. Tong, "Hopf bifurcation in an Internet worm propagation model with time delay in quarantine," *Mathematical and Computer Modelling*, vol. 57, no. 11-12, pp. 2635–2646, 2013.

[11] Y. Muroya, Y. Enatsu, and H. Li, "Global stability of a delayed SIRS computer virus propagation model," *International Journal of Computer Mathematics*, vol. 91, no. 3, pp. 347–367, 2014.

[12] Z. Zhang and H. Yang, "Hopf bifurcation of an SIQR computer virus model with time delay," *Discrete Dynamics in Nature and Society*, vol. 2015, Article ID 101874, 8 pages, 2015.

[13] R. Pastor-Satorras and A. Vespignani, "Epidemic spreading in scale-free networks," *Physical Review Letters*, vol. 86, no. 14, pp. 3200–3203, 2001.

[14] M. Barthélemy, A. Barrat, R. Pastor-Satorras, and A. Vespignani, "Velocity and hierarchical spread of epidemic outbreaks in scale-free networks," *Physical Review Letters*, vol. 92, no. 17, Article ID 178701, 2004.

[15] M. Yang, G. Chen, and X. Fu, "A modified SIS model with an infective medium on complex networks and its global stability," *Physica A: Statistical Mechanics and Its Applications*, vol. 390, no. 12, pp. 2408–2413, 2011.

[16] J. Ren, Y. Xu, and J. Liu, "Investigation of dynamics of a virus-antivirus model in complex network," *Physica A: Statistical Mechanics and its Applications*, vol. 421, pp. 533–540, 2015.

[17] J. Ren, J. Liu, and Y. Xu, "Modeling the dynamics of a network-based model of virus attacks on targeted resources," *Communications in Nonlinear Science and Numerical Simulation*, vol. 31, no. 1–3, pp. 1–10, 2016.

[18] P. Van Mieghem, J. Omic, and R. Kooij, "Virus spread in networks," *IEEE/ACM Transactions on Networking*, vol. 17, no. 1, pp. 1–14, 2009.

[19] P. Van Mieghem, "The N-intertwined SIS epidemic network model," *Computing*, vol. 93, no. 2, pp. 147–169, 2011.

[20] S. Xu, W. Lu, and Z. Zhan, "A stochastic model of multivirus dynamics," *IEEE Transactions on Dependable and Secure Computing*, vol. 9, no. 1, pp. 30–45, 2012.

[21] F. D. Sahneh, F. N. Chowdhury, and C. M. Scoglio, "On the existence of a threshold for preventive behavioral responses to suppress epidemic spreading," *Scientific Reports*, vol. 2, article 632, 2012.

[22] P. Van Mieghem, "Approximate formula and bounds for the time-varying susceptible-infected-susceptible prevalence in networks," *Physical Review E—Statistical, Nonlinear, and Soft Matter Physics*, vol. 93, no. 5, Article ID 052312, 2016.

[23] C. Nowzari, V. M. Preciado, and G. J. Pappas, "Analysis and control of epidemics: a survey of spreading processes on complex networks," *IEEE Control Systems*, vol. 36, no. 1, pp. 26–46, 2016.

[24] V. M. Preciado, F. D. Sahneh, and C. Scoglio, "A convex framework for optimal investment on disease awareness in social networks," in *Proceedings of the 1st IEEE Global Conference on Signal and Information Processing (GlobalSIP '13)*, pp. 851–854, Austin, Tex, USA, December 2013.

[25] V. M. Preciado, M. Zargham, C. Enyioha, A. Jadbabaie, and G. J. Pappas, "Optimal resource allocation for network protection against spreading processes," *IEEE Transactions on Control of Network Systems*, vol. 1, no. 1, pp. 99–108, 2014.

[26] C. Nowzari, M. Ogura, V. M. Preciado, and G. J. Pappas, "Optimal resource allocation for containing epidemics on time-varying networks," in *Proceedings of the 49th Asilomar Conference on Signals, Systems and Computers (ACSSC '15)*, pp. 1333–1337, Pacific Grove, Calif, USA, November 2015.

[27] H. Shakeri, F. D. Sahneh, C. Scoglio, P. Poggi-Corradini, and V. M. Preciado, "Optimal information dissemination strategy to promote preventive behaviors in multilayer epidemic networks," *Mathematical Biosciences and Engineering. MBE*, vol. 12, no. 3, pp. 609–623, 2015.

[28] N. J. Watkins, C. Nowzari, V. M. Preciado, and G. J. Pappas, "Optimal resource allocation for competitive spreading processes on bilayer networks," *IEEE Transactions on Control of Network Systems*, 2016.

[29] E. Hansen and T. Day, "Optimal control of epidemics with limited resources," *Journal of Mathematical Biology*, vol. 62, no. 3, pp. 423–451, 2011.

[30] M. H. R. Khouzani, S. Sarkar, and E. Altman, "Optimal dissemination of security patches in mobile wireless networks," *IEEE Transactions on Information Theory*, vol. 58, no. 7, pp. 4714–4732, 2012.

[31] S. Eshghi, M. H. R. Khouzani, S. Sarkar, and S. S. Venkatesh, "Optimal patching in clustered malware epidemics," *IEEE/ACM Transactions on Networking*, vol. 24, no. 1, pp. 283–298, 2016.

[32] A. Khanafer and T. Basar, "An optimal control problem over infected networks," in *Proceedings of the International Conference of Control, Dynamic Systems, and Robotics*, Ottawa, Canada, May 2014.

[33] L.-X. Yang, M. Draief, and X. Yang, "The optimal dynamic immunization under a controlled heterogeneous node-based SIRS model," *Physica A. Statistical Mechanics and Its Applications*, vol. 450, pp. 403–415, 2016.

[34] L.-X. Yang and X. Yang, "Propagation behavior of virus codes in the situation that infected computers are connected to the internet with positive probability," *Discrete Dynamics in Nature and Society*, vol. 2012, Article ID 693695, 13 pages, 2012.

[35] L.-X. Yang and X. Yang, "The spread of computer viruses under the influence of removable storage devices," *Applied Mathematics and Computation*, vol. 219, no. 8, pp. 3914–3922, 2012.

[36] L.-X. Yang, X. Yang, L. Wen, and J. Liu, "A novel computer virus propagation model and its dynamics," *International Journal of Computer Mathematics*, vol. 89, no. 17, pp. 2307–2314, 2012.

[37] L.-X. Yang, X. Yang, Q. Zhu, and L. Wen, "A computer virus model with graded cure rates," *Nonlinear Analysis: Real World Applications*, vol. 14, no. 1, pp. 414–422, 2013.

[38] Y. Muroya and T. Kuniya, "Global stability of nonresident computer virus models," *Mathematical Methods in the Applied Sciences*, vol. 38, no. 2, pp. 281–295, 2015.

[39] M. Yang, Z. Zhang, Q. Li, and G. Zhang, "An SLBRS model with vertical transmission of computer virus over the Internet," *Discrete Dynamics in Nature and Society*, vol. 2012, Article ID 925648, 17 pages, 2012.

[40] L.-X. Yang, X. Yang, J. Liu, Q. Zhu, and C. Gan, "Epidemics of computer viruses: a complex-network approach," *Applied Mathematics and Computation*, vol. 219, no. 16, pp. 8705–8717, 2013.

[41] L.-X. Yang and X. Yang, "A new epidemic model of computer viruses," *Communications in Nonlinear Science and Numerical Simulation*, vol. 19, no. 6, pp. 1935–1944, 2014.

[42] C. Zhang, W. Liu, J. Xiao, and Y. Zhao, "Hopf bifurcation of an improved SLBS model under the influence of latent period," *Mathematical Problems in Engineering*, vol. 2013, Article ID 196214, 10 pages, 2013.

[43] L.-X. Yang and X. Yang, "The impact of nonlinear infection rate on the spread of computer virus," *Nonlinear Dynamics. An International Journal of Nonlinear Dynamics and Chaos in Engineering Systems*, vol. 82, no. 1-2, pp. 85–95, 2015.

[44] L. Chen, K. Hattaf, and J. Sun, "Optimal control of a delayed SLBS computer virus model," *Physica A. Statistical Mechanics and Its Applications*, vol. 427, pp. 244–250, 2015.

[45] L.-X. Yang, M. Draief, and X. Yang, "The impact of the network topology on the viral prevalence: a node-based approach," *PLoS ONE*, vol. 10, no. 7, Article ID e0134507, 2015.

[46] D. Liberzon, *Calculus of Variations and Optimal Control Theory*, Princeton University Press, Princeton, NJ, USA, 2012.

[47] R. C. Robinson, *An Introduction to Dynamical Systems: Continuous and Discrete*, Pearson Prentice Hall, Upper Saddle River, NJ, USA, 2005.

[48] A.-L. Barabási and R. Albert, "Emergence of scaling in random networks," *Science*, vol. 286, no. 5439, pp. 509–512, 1999.

[49] D. J. Watts and S. H. Strogatz, "Collective dynamics of 'small-world' networks," *Nature*, vol. 393, no. 6684, pp. 440–442, 1998.

[50] https://snap.stanford.edu/data/egonets-Facebook.html.

[51] Y. Yao, L. Guo, H. Guo, G. Yu, F.-X. Gao, and X.-J. Tong, "Pulse quarantine strategy of internet worm propagation: modeling and analysis," *Computers and Electrical Engineering*, vol. 38, no. 5, pp. 1047–1061, 2012.

[52] Y. Yao, X. Feng, W. Yang, W. Xiang, and F. Gao, "Analysis of a delayed Internet worm propagation model with impulsive quarantine strategy," *Mathematical Problems in Engineering*, vol. 2014, Article ID 369360, 18 pages, 2014.

[53] T. Britton, "Stochastic epidemic models: a survey," *Mathematical Biosciences*, vol. 225, no. 1, pp. 24–35, 2010.

[54] J. Amador and J. R. Artalejo, "Stochastic modeling of computer virus spreading with warning signals," *Journal of the Franklin Institute. Engineering and Applied Mathematics*, vol. 350, no. 5, pp. 1112–1138, 2013.

[55] J. Amador, "The stochastic SIRA model for computer viruses," *Applied Mathematics and Computation*, vol. 232, pp. 1112–1124, 2014.

[56] Y. Schwarzkopf, A. Rakos, and D. Mukamel, "Epidemic spreading in evolving networks," *Physical Review E*, vol. 82, no. 3, pp. 336–354, 2010.

[57] E. Valdano, L. Ferreri, C. Poletto, and V. Colizza, "Analytical computation of the epidemic threshold on temporal networks," *Physical Review X*, vol. 5, no. 2, Article ID 021005, 2015.

[58] M. Ogura and V. M. Preciado, "Stability of spreading processes over time-varying large-scale networks," *IEEE Transactions on Network Science and Engineering*, vol. 3, no. 1, pp. 44–57, 2016.

[59] J. R. Piqueira, "Rumor propagation model: An Equilibrium Study," *Mathematical Problems in Engineering*, vol. 2010, Article ID 631357, 7 pages, 2010.

[60] S. Nizamani, N. Memon, and S. Galam, "From public outrage to the burst of public violence: an epidemic-like model," *Physica A: Statistical Mechanics and Its Applications*, vol. 416, pp. 620–630, 2014.

[61] J. Xu, M. Zhang, and J. Ni, "A coupled model for government communication and rumor spreading in emergencies," *Advances in Difference Equations*, vol. 2016, article 208, 2016.

Hindawi
Discrete Dynamics in Nature and Society
Volume 2017, Article ID 4232971, 22 pages
https://doi.org/10.1155/2017/4232971

Research Article

On a New Epidemic Model with Asymptomatic and Dead-Infective Subpopulations with Feedback Controls Useful for Ebola Disease

M. De la Sen,[1] A. Ibeas,[2] S. Alonso-Quesada,[1] and R. Nistal[1]

[1] *Institute of Research and Development of Processes IIDP, University of the Basque Country, Campus of Leioa, P.O. Box 48940, Leioa, Bizkaia, Spain*
[2] *Department of Telecommunications and Systems Engineering, Universitat Autònoma de Barcelona (UAB), 08193 Barcelona, Spain*

Correspondence should be addressed to M. De la Sen; manuel.delasen@ehu.eus

Received 13 December 2016; Revised 9 January 2017; Accepted 15 January 2017; Published 19 February 2017

Academic Editor: Lu-Xing Yang

Copyright © 2017 M. De la Sen et al. This is an open access article distributed under the Creative Commons Attribution License, which permits unrestricted use, distribution, and reproduction in any medium, provided the original work is properly cited.

This paper studies the nonnegativity and local and global stability properties of the solutions of a newly proposed SEIADR model which incorporates asymptomatic and dead-infective subpopulations into the standard SEIR model and, in parallel, it incorporates feedback vaccination plus a constant term on the susceptible and feedback antiviral treatment controls on the symptomatic infectious subpopulation. A third control action of impulsive type (or "culling") consists of the periodic retirement of all or a fraction of the lying corpses which can become infective in certain diseases, for instance, the Ebola infection. The three controls are allowed to be eventually time varying and contain a total of four design control gains. The local stability analysis around both the disease-free and endemic equilibrium points is performed by the investigation of the eigenvalues of the corresponding Jacobian matrices. The global stability is formally discussed by using tools of qualitative theory of differential equations by using Gauss-Stokes and Bendixson theorems so that neither Lyapunov equation candidates nor the explicit solutions are used. It is proved that stability holds as a parallel property to positivity and that disease-free and the endemic equilibrium states cannot be simultaneously either stable or unstable. The periodic limit solution trajectories and equilibrium points are analyzed in a combined fashion in the sense that the endemic periodic solutions become, in particular, equilibrium points if the control gains converge to constant values and the control gain for culling the infective corpses is asymptotically zeroed.

1. Introduction

Relevant attention is being paid in the last two decades to the study of mathematical epidemic models which are modelled by integro-differential equations and/or difference equations. Those models describe the evolution of the various subpopulations considered as the disease under study progresses. Typically, the models have three essential subpopulations (namely, susceptible, infected, and recovered by immunity) whose dynamics are mutually coupled. There are different degrees of complexity in the statement of the models. The simplest ones have only "susceptible" (S) and "infected" (I) subpopulations and are referred to as SI-models. A second degree of complexity adds a third one said to be the "recovered by immunity" subpopulation and those models are said to be SIR-models. A further complexity degree splits the infected into two subpopulations (or compartments), namely, the so-called "infected" or "exposed" (E) subpopulation (those having the disease but do not present yet external symptoms) and the "infectious" or "infective" subpopulation (those having external symptoms). The generic acronym used for this last category of models is SEIR, being referred to as SEIR epidemic models. General description of epidemic models and some mathematical analysis on them is given in some classical books. See, for instance, [1–3] and for more recent models, see, for instance, [4–11] and references therein. The positivity of the solution is investigated in a number of works. See, for instance, [6–9, 12] and some references therein. The use of nonlinear incidence rates in the models is also investigated in a number of papers. See, for instance, [13–15]. The presence of perturbations is also investigated in many models. See, for instance, [9, 15–17]

to give some of them. Also, certain robustness studies of stability and positivity under deviations of the equilibrium points due to Wiener noise are performed in [9]. The stability properties and the convergence of the solutions to equilibrium states are a major analysis tool in most of the works. In particular, the asymptotic solution behaviors including associated diffusion effects have been provided in [18, 19] and some references therein. The use of vaccination rules to improve the infection behavior has been also proposed in the literature. See, for instance, [6–8, 11, 20–23] and references therein. In particular, two control actions are proposed in [20], namely, a vaccination action of the susceptible and a therapeutic treatment of the infectious subpopulation with constant and nonconstant controls and impulsive controls are proposed in [22, 23]. The stability and optimal control under a subpopulation of infective in treatment with vaccination is investigated in [24] and a model with delay, latent period and saturation incidence rate and impulsive vaccination is proposed and discussed in [25].

On the other hand, it turns out as known due to medical experience that there are individuals who are infective but do not have significant external symptoms, that is, the so-called the "asymptomatic" (A) subpopulation, [26]. This occurs even in the common known influenza disease. If such an asymptomatic subpopulation is considered in the model, then it turns out that the exposed subpopulation have different transitions to the symptomatic infectious subpopulation and to the asymptomatic ones so that a part of the exposed become subpopulation asymptomatic infectious after a certain time while others become symptomatic infectious. Finally, it is well known that in the case of Ebola disease, the lying dead corpses are infective [27, 28] which causes serious sanitary problems in third world tropical countries with low or scarce sanitary means when an Ebola disease spreads thoroughly specially when it is transmitted from rural areas to high populated urban ones. The dead corpses can be considered in the model as a new subpopulation "D."

The paper is organized as follows. Section 2 defines the SEIADR model with the six subpopulations (S, E, I, A, D, R) under controls in terms of vaccination control on the susceptible and antiviral treatment on the symptomatic infectious subpopulation. The vaccination control possesses feedback-independent (which can be constant, in particular) and feedback linear terms while the antiviral treatment control is implemented via proportional gain acting on the symptomatic infectious population. There is also a third control which consists of an impulsive control action of retirement of corpses to reduce the risks of dead-contagion to the living uninfected population. The three mentioned controls have feedback information taken on line from their respective subpopulations. The nonconstant control terms are based on feedback information of the respective subpopulations. Section 2 also discusses later on some nonnegativity and stability properties of the model, under the various controls, in a linked way in the sense that the nonnegativity of the subpopulations, under nonzero initial conditions, and the boundedness of the total population both together guarantee the boundedness of all the subpopulations for all time as a result. Section 3 deals with the disease-free and endemic equilibrium points and the periodic limit solutions of the controlled epidemic model as well as the associated local stability properties. The dependence of the resulting disease-free and endemic equilibrium states is seen to be dependent on the limiting vaccination control gains. On the other hand, the global stability is also investigated by using qualitative theory of stability of differential equations by using Gauss-Stokes and Bendixson theorems while neither Lyapunov functions nor the explicit solutions of the differential model are invoked at this stage. Finally, some numerical examples are given in Section 4 with attention to oscillatory behaviors under periodic culling action of dead infectious corpses and some conclusions end the paper.

1.1. Notation

$\mathbf{R}_+ = \{r \in \mathbf{R} : r > 0\}$; $\mathbf{R}_{0+} = \{r \in \mathbf{R} : r \geq 0\}$,

$\mathbf{C}$ is the complex plane,

$\vee$ and $\wedge$ stand, respectively, for logic "or" and "and,"

C^0 and PC^0 are, respectively, the sets of continuous and piecewise-continuous functions of domain I and image X. The functions $f : I \to X$ in those sets are denoted, respectively, by $f \in C^0(I, X)$ and $f \in PC^0(I, X)$,

$\text{card}(A)$ denotes the cardinal of the set A,

$\text{card}(A) = \aleph_0$ indicates that the cardinal of a denumerable set A is infinite as opposed to $\text{card}(A) = \infty$, denoting the infinity cardinal of a nondenumerable set A,

$\mathbf{I}_n$ is nth identity matrix,

$\delta(t)$ denotes the Dirac distribution at $t = 0$,

$\overline{m} = \{1, 2, \ldots, m\}$.

2. The SEIADR Epidemic Model: Some Results on Nonnegativity, Stability, and Equilibrium Solution Trajectories

The proposed SEIADR model is an extended SEIR model with the following characteristics and novelties:

(a) Apart from the classical subpopulations of "susceptible" (S), "exposed" who are infected but not yet infective (E), "symptomatic infectious" (I), and "recovered" (R) subpopulation, it has two extra additional subpopulations, namely, "asymptomatic infectious" (A) and "dead-infective" (D). The so-called asymptomatic are a group of infective individuals (which are modelled as a distinct group of the I-infective subpopulation), characterized by small or null level of infection, with acquired immunity, but who can transmit the infective disease to others. The so-called dead-infective subpopulation are dead individuals (spread corpses in the distribution disease habitat) which transmit the illness because of lack of good sanitary performance or practice in certain infective

illnesses (e.g., the Ebola disease) as it is a common situation in some third world countries with scarce technical and economic means.

(b) It incorporates three combined control actions which can be of a feedback nature as follows: (1) the standard vaccination control V of the susceptible which consists of two terms, one of them being a nonfeedback gain and another feedback term with a gain being proportional to the susceptible, (2) the antiviral treatment ξ of the infective subpopulation with a proportional gain on the symptomatic infectious subpopulation, and (3) the dead-infective culling which has a feedback impulsive nature modulated by a control gain in the sense that it is not applied at all time but at certain periods where either voluntary or civil-servant staff can become involved on this duty. The three controls contain together four, eventually time varying, design control gains which is a novel contribution of the paper related to the background literature while another novelty is the global stability analysis outlined from qualitative theory of differential equations.

It has been pointed out that the coexistence of an asymptomatic infectious subpopulation, often known in some well-known diseases as influenza, and a dead-infective subpopulation (e.g., in the case of the Ebola) can occur. See, for instance, a related UK medical report [29] and see also [27]. Recent work on the incorporation of infective corpses and asymptomatic infectious type as new subpopulation is discussed, for instance, in [26, 28]. The epidemic SEIADR model with vaccination and antiviral treatment together with infective corpses culling is as follows:

$$\dot{S}(t) = b_1 - \left(b_2 + \beta I(t) + \beta_A A(t) + \beta_D D(t)\right) S(t) + \eta R(t) - V(t), \tag{1}$$

$$\dot{E}(t) = -\left(b_2 + \gamma\right) E(t) + \left(\beta I(t) + \beta_A A(t) + \beta_D D(t)\right) S(t), \tag{2}$$

$$\dot{I}(t) = -\left(b_2 + \alpha + \tau_0\right) I(t) + \gamma p E(t) - \xi(t), \tag{3}$$

$$\dot{A}(t) = -\left(b_2 + \tau_0\right) A(t) + \gamma\left(1 - p\right) E(t), \tag{4}$$

$$\dot{D}(t) = -\mu D(t) + b_2 (I(t) + A(t)) + \alpha I(t) - \rho_D(t) D(t) \sum_{t_i \in \mathrm{Imp}D} \delta\left(t - t_i\right), \tag{5}$$

$$\dot{R}(t) = -\left(b_2 + \eta\right) R(t) + \tau_0 (I(t) + A(t)) + \xi(t) + V(t), \tag{6}$$

$$V(t) = V_0(t) + K_V(t) S(t), \tag{7}$$

$$\xi(t) = K_\xi(t) I(t); \tag{8}$$

$$\forall t \in \mathbf{R}_{0+} \tag{9}$$

with initial conditions satisfying $\min(S(0), E(0), I(0), A(0), D(0), R(0)) \geq 0$, where $\mathrm{Imp}D = \{t \in \mathbf{R}_{0+} : D(t) \neq D(t^-)\} = \bigcup_{t \in \mathbf{R}_{0+}} \mathrm{Imp}D(t)$ is the total set of impulsive ("culling") time instants for removal of infective corpses (note that the notation for $f(t^+)$ is simplified to $f(t)$). The vaccination $V(t)$ and (7) consist of feedback-independent term, which can be constant, plus a linear feedback term injected on the susceptible subpopulation while the antiviral action is a linear feedback control applied to the symptomatic infectious subpopulation. Besides,

$$\mathrm{Imp}D\left(t^-\right) = \left\{\sigma \in \mathrm{Imp}D : \sigma < t\right\},$$

$$\mathrm{Imp}D(t) = \left\{\sigma \in \mathrm{Imp}D : \sigma \leq t\right\} = \mathrm{Imp}D\left(t^-\right) \quad \text{if } t \notin \mathrm{Imp}D, \tag{10}$$

$$\mathrm{Imp}D(t) = \left\{\sigma \in \mathrm{Imp}D : \sigma \leq t\right\} = \mathrm{Imp}D\left(t^-\right) \cup \{t\} \quad \text{if } t \in \mathrm{Imp}D$$

and the (nonnegative) parameters and controls are the following:

b_1 is the recruitment rate.

b_2 is the natural average death rate.

β, β_A, β_D are the various disease transmission coefficients to the susceptible from the respective symptomatic infectious, asymptomatic, and infective corpses subpopulations.

η is a parameter such that $1/\eta$ is the average duration of the immunity period reflecting a transition from the recovered to the susceptible.

γ is the transition rate from the exposed to all (i.e., both symptomatic and asymptomatic) infectious subpopulation.

α is the average extra mortality associated with the symptomatic infectious subpopulation.

τ_0 is the natural immune response rate for the whole infectious subpopulation (i.e., $A + I$), respectively; p is the fraction of the exposed which become symptomatic infectious subpopulation.

$1 - p$ is the fraction of the exposed which becomes asymptomatic infectious subpopulation.

$1/\mu$ is the average period of infectiousness after death.

$V(t)$ and $\xi(t)$ are, respectively, the vaccination and antiviral treatment controls and $\rho_D(t_i)D(t_i)$ is the impulsive action of removal of corpses (or "culling") for all $t_i \in \mathrm{Imp}D$ with some piecewise continuous $\rho_D(t) \in [0, 1]$. The controls can be of different types including constant and feedback actions. It turns out that a well-posed epidemic model has to be positive and with bounded solutions to be useful for potential applications. The subsequent results are, respectively, related to the nonnegativity under nonnegative initial conditions and some smoothness conditions on the controls and boundedness of the solutions of the

model. Note that the positivity of the trajectory solutions as well as that of the equilibrium solutions is a crucial "a priori" basic requirement for model validation in many different biological problems. See, for instance, [6–9, 12, 18, 30–32].

Theorem 1. *The solutions of the SEIADR model (1) to (8) are uniquely defined and if* $\min(S(0), E(0), I(0), A(0), R(0), D(0)) \geq 0$, $V_0(t) \in [0, b_1 + \eta R(t)]$, $\rho_D, V, K_V, K_\xi \in PC^0(\mathbf{R}_{0+}, \mathbf{R}_{0+})$ *and* $\rho_D : \mathbf{R}_{0+} \to [0,1]$, *then such solutions are, furthermore, nonnegative for any given nonnegative initial conditions defined by:*

$$S(t) = e^{-(b_2 t + \int_0^t (K_V(\sigma) + \beta I(\sigma) + \beta_A A(\sigma) + \beta_D D(\sigma)) d\sigma)} \times \left(S(0) + \int_0^t e^{\int_0^\sigma (b_2 + K_V(\theta) + \beta I(\theta) + \beta_A A(\theta) + \beta_D D(\theta)) d\theta} (b_1 + \eta R(\sigma) - V_0(\sigma)) d\sigma \right); \quad \forall t \in \mathbf{R}_{0+}, \tag{11}$$

$$E(t) = e^{-(b_2+\gamma)t} \left(E(0) + \int_0^t e^{(b_2+\gamma)\sigma} (\beta I(\sigma) + \beta_A A(\sigma) + \beta_D D(\sigma)) S(\sigma) d\sigma \right); \quad \forall t \in \mathbf{R}_{0+}, \tag{12}$$

$$I(t) = e^{-((b_2+\alpha+\tau_0)t + \int_0^t K_\xi(\sigma) d\sigma)} \left(I(0) + \gamma p \int_0^t e^{\int_0^\sigma (b_2+\alpha+\tau_0+K_\xi(\theta)) d\theta} E(\sigma) d\sigma \right); \quad \forall t \in \mathbf{R}_{0+}, \tag{13}$$

$$A(t) = e^{-(b_2+\tau_0)t} \left(A(0) + \gamma(1-p) \cdot \int_0^t e^{(b_2+\tau_0)\sigma} E(\sigma) d\sigma \right); \quad \forall t \in \mathbf{R}_{0+}, \tag{14}$$

$$R(t) = e^{-(b_2+\eta)t} \left(R(0) + \int_0^t e^{(b_2+\eta)\sigma} (\tau_0 (I(\sigma) + A(\sigma)) + K_\xi(\sigma) I(\sigma) + V_0(\sigma) + K_V(\sigma) S(\sigma)) d\sigma \right); \quad \forall t \in \mathbf{R}_{0+}, \tag{15}$$

$$D(t) = e^{-\mu(t-t_i)} \left(D(t_i) + \int_{t_i}^t e^{\mu(\sigma - t_i)} [(b_2+\alpha) I(\sigma) + b_2 A(\sigma)] d\sigma \right); \quad \forall t \in [t_i, t_{i+1}), \ \forall t_i \in \mathrm{Imp}D \tag{16}$$

with

$$D(t_{i+1}^-) = e^{-\mu T_i} \left(D(t_i) + \int_{t_i}^{t_{i+1}} e^{\mu(\sigma - t_i)} [(b_2+\alpha) I(\sigma) + b_2 A(\sigma)] d\sigma \right) \tag{17}$$

while

$$\begin{aligned} D(t_{i+1}) &= D(t_{i+1}^-) - \int_{t_{i+1}^-}^{t_{i+1}} \rho_D(\sigma) D(\sigma) \delta(\sigma - t_{i+1}) d\sigma \\ &= (1 - \rho_D(t_{i+1})) D(t_{i+1}^-) = (1 - \rho_D(t_{i+1})) \\ &\cdot e^{-\mu T_i} \left(D(t_i) + \int_{t_i}^{t_{i+1}} e^{\mu(\sigma - t_i)} [(b_2+\alpha) I(\sigma) + b_2 A(\sigma)] d\sigma \right), \end{aligned} \tag{18}$$

where $T_i = t_{i+1} - t_i$; $\forall t_i \in \mathrm{Imp}D$. *Furthermore,* $S, E, I, A, R \in C^0(\mathbf{R}_{0+}, \mathbf{R}_{0+})$ *are everywhere differentiable in* $\mathbf{R}_{0+}$ *and* $D \in PC^0(\mathbf{R}_{0+}, \mathbf{R}_{0+})$ *and it is time-differentiable in* $\bigcup_{t_i \in \mathrm{Imp}D} (t_i, t_{i+1})$.

Proof. The replacements of (7) into (1) and (8) into (3) yield

$$\dot{S}(t) = b_1 - (b_2 + K_V(t) + \beta I(t) + \beta_A A(t) + \beta_D D(t)) S(t) + \eta R(t) - V_0(t), \tag{19}$$

$$\dot{I}(t) = -\left(b_2 + \alpha + \tau_0 + K_\xi(t)\right) I(t) + \gamma p E(t); \tag{20}$$

$$\forall t \in \mathbf{R}_{0+}. \tag{21}$$

The solutions of (19), (2), (20), and (4)–(6) follow via direct calculus and are unique and nonnegative resulting in (11)–(18) for any given set of nonnegative initial conditions. Also, $S, E, I, A, R \in C^0(\mathbf{R}_{0+}, \mathbf{R}_{0+})$ since their first respective time derivatives exist everywhere in $\mathbf{R}_{0+}$ from (1)–(4) and (6). Furthermore, note from (5) and the fact that its impulsive ("culling") control $\rho_D : \mathbf{R}_{0+} \to [0,1]$ yields a unique piecewise solution $D \in PC^0(\mathbf{R}_{0+}, \mathbf{R}_{0+})$ for each given $D(0)$. □

The boundedness of all the subpopulations for all time and the asymptotic infection removal under a feedback, in general, time-varying linear antiviral control law, is addressed by the subsequent result.

Theorem 2. *The following properties hold under the assumptions of Theorem 1:*

(i) $\limsup_{t\to\infty} I(t) \leq b_1/\alpha$, $\sup_{t\in\mathbf{R}_{0+}} I(t) < +\infty$, $\sup_{t\in\mathbf{R}_{0+}} N(t) \leq N(0) + b_1/b_2 < +\infty$; $\forall t \in \mathbf{R}_{0+}$ *where* $N(t) = S(t) + E(t) + I(t) + A(t) + R(t)$; $\forall t \in \mathbf{R}_{0+}$ *is the total alive population, and*

$$\begin{aligned} &\max\left(\sup_{t\in\mathbf{R}_{0+}} S(t), \sup_{t\in\mathbf{R}_{0+}} E(t), \sup_{t\in\mathbf{R}_{0+}} I(t), \sup_{t\in\mathbf{R}_{0+}} A(t), \sup_{t\in\mathbf{R}_{0+}} D(t), \sup_{t\in\mathbf{R}_{0+}} R(t) \right) \leq \sup_{t\in\mathbf{R}_{0+}} \overline{N}(t) \\ &\leq \max\left(\sup_{t\in\mathbf{R}_{0+}} N(t), \sup_{t\in\mathbf{R}_{0+}} D(t) \right) < +\infty, \end{aligned} \tag{22}$$

(ii) *for any* $t \in \mathbf{R}_{0+}$, *assume that* $K_\xi(t) = 0$ *if* $I(t) = 0$, *and the antiviral control gain is chosen to be*

$$K_\xi(t) = \frac{\xi(t)}{I(t)} = \frac{1}{I(t)}\left[(\alpha+\tau_0)E(t) + \alpha A(t) + \left(\beta_A A(t) + \beta_D D(t)\right)S(t)\right] + \beta S(t) \quad \text{if } I(t) \neq 0. \tag{23}$$

Then, $K_\xi(t) = O(I(t))$, *implying also that* $\sup_{t\in\mathbf{R}_{0+}} K_\xi(t) < +\infty$, *and the following limits exist:*

$$\lim_{t\to\infty}(E(t)+I(t)+A(t)+D(t)) = 0,$$
$$\lim_{t\to\infty}(S(t)+R(t)) = \lim_{t\to\infty}\overline{N}(t) = \lim_{t\to\infty}N(t) = \frac{b_1}{b_2}, \tag{24}$$

where $\overline{N}(t) = N(t) + D(t)$; $\forall t \in \mathbf{R}_{0+}$ *is the total population including infective corpses.*

(iii) *If, furthermore,* $V_0(t)$ *satisfies the most stringent constraint* $\limsup_{t\to\infty}(V_0(t) - b_1 - \eta R(t) + \varepsilon_V) \leq 0$ *for any fixed* $\varepsilon_V (\leq b_1 - \eta R(t)) \in \mathbf{R}_+$, *then* $\min(\liminf_{t\to\infty} S(t), \liminf_{t\to\infty} R(t)) > 0$.

Proof. Assume that $\limsup_{t\to\infty} I(t) > b_1/\alpha$ and proceed by contradiction. By summing up (1) to (4) and adding (6), one gets $\dot{N}(t) = -b_2 N(t) + b_1 - \alpha I(t)$; $\forall t \in \mathbf{R}_{0+}$ which concludes that

$$\limsup_{t\to\infty}\left(\int_0^t e^{-b_2(t-\sigma)}\left(\alpha I(\sigma) - b_1\right)d\sigma + N(t)\right) = 0. \tag{25}$$

Since $\limsup_{t\to\infty} I(t) > b_1/\alpha$ and $N \in C^0(\mathbf{R}_{0+}, \mathbf{R}_{0+})$, which is derived from the result of Theorem 1, it follows a contradiction to (25) since $\limsup_{t\to\infty}(\int_0^t e^{-b_2(t-\sigma)}(\alpha I(\sigma) - b_1)d\sigma + N(t)) > 0$. Therefore, $\limsup_{t\to\infty} I(t) \leq b_1/\alpha < +\infty$. Also, the boundedness of $N(t)$ follows directly since $I(t) \geq 0$; $\forall t \in \mathbf{R}_{0+}$ from the standard comparison theorem for $\dot{N}(t) \leq \dot{N}_0(t) = -b_2 N_0(t) + b_1$ leading to $N(t) \leq e^{-b_2 t}N(0) + (1 - e^{-b_2 t})(b_1/b_2) \leq N(0) + b_1/b_2 < +\infty$; $\forall t \in \mathbf{R}_{0+}$ provided that $N_0(0) = N(0)$ and $\limsup_{t\to\infty} N(t) = b_1/b_2$. From Theorem 1, all the subpopulations are nonnegative for all time for any given nonnegative initial conditions. Since the model is nonnegative for all time then all the living subpopulations are bounded for all time since $N(t) < +\infty$. From (17)-(18) the lying corpses subpopulation is nonnegative and bounded for all time since both the symptomatic and asymptomatic infectious subpopulations are bounded for all time. As a result, the total population is also bounded for all time as they are all the subpopulations. Property (i) is proved. To prove Property (ii), one gets from (2), (3), and (4) under the given antiviral treatment control law that

$$\begin{aligned}
&\dot{E}(t) + \dot{I}(t) + \dot{A}(t)\\
&\quad = -b_2(E(t) + I(t) + A(t))\\
&\qquad + \left(\beta I(t) + \beta_A A(t) + \beta_D D(t)\right)S(t)\\
&\qquad - (\alpha+\tau_0)I(t) - \xi(t) - \tau_0 A(t)\\
&\quad = -(b_2 + \tau_0 + \alpha)(E(t) + I(t) + A(t))\\
&\qquad + \left(\beta I(t) + \beta_A A(t) + \beta_D D(t)\right)S(t)\\
&\qquad + (\alpha+\tau_0)E(t) + \alpha A(t) - K_\xi(t)I(t)\\
&\quad = -(b_2 + \tau_0 + \alpha)(E(t) + I(t) + A(t));\\
&\qquad\qquad \forall t \in \mathbf{R}_{0+}
\end{aligned} \tag{26}$$

so that it exists the limit $\lim_{t\to\infty}(E(t) + I(t) + A(t)) = e^{-(b_2+\tau_0+\alpha)t}(E(0) + I(0) + A(0)) = 0$. Thus, $\lim_{t\to\infty}E(t) = \lim_{t\to\infty}I(t) = \lim_{t\to\infty}A(t) = 0$ since the three subpopulations are nonnegative for all time under any given nonnegative initial conditions. This also implies as a result that $\lim_{t\to\infty}(S(t) + R(t)) = \lim_{t\to\infty}\overline{N}(t) = \lim_{t\to\infty}N(t) = b_1/b_2$ since from (16)–(18), $\lim_{t\to\infty}D(t) = 0$. It remains to prove that $K_\xi(t) = O(I(t)) = O(\max(I(t), S(t)) < +\infty)$. First, note that $I(t)$ is uniformly bounded since it is nonnegative and the total population is uniformly bounded. Thus, to prove that $K_\xi(t) = O(I(t)) = O(I(t), S(t))$, it suffices to prove, in view of (23), that $I \leq \max(o(E), o(A), o(D))$. Since $\lim_{t\to\infty}(E(t) + I(t) + A(t)) = 0$, then $\lim_{t\to\infty}(E(t) + A(t)) = 0$. On the other hand, note from (13) that $I(t) \to 0$ as $t \to t_1$ for any $t_1 \in \mathbf{R}_{0+}$ implies $\int_0^{t_1} e^{-((b_2+\alpha+\tau_0)(t_1-\sigma) + \int_\sigma^{t_1} K_\xi(\sigma)d\sigma)}E(\sigma)d\sigma \to 0$ and $E(t_1) \to 0$. If, in addition $I(0) > 0$ then $t_1 \to \infty$. On the other hand, from (12) if $E(t) \to 0$ as $t \to \infty$, then $I(t), A(t), D(t) \to 0$ as $t \to \infty$. Thus, $E(t)/I(t)$ and $A(t)/I(t)$ cannot diverge as $t \to \infty$ if $E(t) \to 0$ as $t \to \infty$. Thus, if $I(t) \to 0$ then $E(t), A(t), D(t) \to 0$ and if $E(t) \to 0$ or $A(t) \to 0$ (see also (14)), then $I(t) \to 0$. Then, $K_\xi(t) = O(I(t)) = O(I(t), S(t))$. Property (ii) has been proved. On the other hand, if $\liminf_{t\to\infty}(b_1 - \varepsilon_V + \eta R(t) - V_0(t)) \geq 0$ then $\liminf_{t\to\infty} S(t) > 0$ from (11) which leads to $\liminf_{t\to\infty} R(t) > 0$ from (15). Hence, Property (iii) is proved. □

Remark 3. Note that the condition $\liminf_{t\to\infty}(b_1 - \varepsilon_V + \eta R(t) - V_0(t)) \geq 0$ for $\varepsilon_V = 0$ of Theorem 2(iii) is guaranteed if $V_0(t) \in [0, b_1)$; $\forall t \in \mathbf{R}_{0+}$.

3. Disease-Free and Endemic Equilibrium Points, Limit Periodic Equilibrium Trajectories, and Local and Global Stability

Define the linearized error of the trajectory solution with respect to any equilibrium x^* by

$$\tilde{x}(t) = x(t) - x^*(t); \quad \forall t \in \mathbf{R}_{0+} \setminus \mathrm{Imp}D, \tag{27}$$

where $x(t)$ is the linearized state-trajectory solution in $\mathbf{R}^6_{0+}$ whose six components are defined by $S(t)$, $E(t)$, $I(t)$, $A(t)$, $D(t)$, and $R(t)$ in this order. In particular, $x^*_{\mathrm{df}}(t) = x^*_{\mathrm{df}} = (S^*_{\mathrm{df}}, 0, 0, 0, 0, R^*_{\mathrm{df}})^T$ for any $t \in \mathbf{R}_{0+}$ is the disease-free equilibrium solution, which is an equilibrium point, and $x^*_{\mathrm{end}}(t) = (S^*_{\mathrm{end}}(t), E^*_{\mathrm{end}}(t), I^*_{\mathrm{end}}(t), A^*_{\mathrm{end}}(t), D^*_{\mathrm{end}}(t), R^*_{\mathrm{end}}(t))^T$ for any $t \in [0, T^*_D]$ is an equilibrium periodic trajectory of period T^*_D if $\rho_D(t) \to \rho^*_D \in (0, 1)$ and $(t_{i+1} - t_i) \to T^*_D (> 0)$ as $t_i (\in \mathrm{Imp}D) \to \infty$. If $\rho^*_D = 0$ or $\mathrm{card}\,\mathrm{Imp}D < \chi_0$

(i.e., the cardinal of impulsive time instants is numerable finite), then $x^*_{\text{end}}(t) = x^*_{\text{end}}$; $\forall t \in \mathbf{R}_{0+}$ (i.e., the limit periodic endemic solution is just an endemic equilibrium point). The following result holds and is concerned with the eventually periodic asymptotic behavior of the dead-infective lying corpses subpopulation under constant limiting values of the culling removal fraction and culling period. It is also obtained the intuitively obvious result that if all the lying infective corpses are removed by the culling control then the dead corpses infective subpopulation is asymptotically zeroed at the culling time instants.

Theorem 4. *The following properties hold:*

(i) *Assume that* $(t_{i+1} - t_i) \to T^*_D (> 0)$, $V_0(t) = V_0$; $\forall t \in \mathbf{R}_{0+}$, *and* $\rho_D(t_i) \to \rho^*_D (\in [0,1])$ *as* $t_i (\in \text{Imp}D) \to \infty$. *Then, a periodic limit solution of period* T^*_D *of the form*

$$\begin{aligned}\lim_{n\to\infty} D\left(nT^*_D + \theta\right) &= D^*\left(T^*_D + \theta\right)\\ &= \frac{e^{-\mu\theta}}{\mu}\left[\left(b_2+\alpha\right)I^*_{av} + b_2 A^*_{av}\right]\\ &\cdot\left[\frac{\left(1-\rho^*_D\right)\left(1-e^{-\mu\theta}\right)}{\left(1-\left(1-\rho^*_D\right)e^{-\mu\theta}\right)} - 1 + e^{\mu\theta}\right];\quad \forall\theta\in\left[0,T^*_D\right]\end{aligned} \tag{28}$$

exists for the dead-infective corpses subpopulation, where the subscript "av" stands for a mean value of the corresponding subpopulation on the period $[0, T^*_D)$ *with existing right and left limits*

$$\begin{aligned}D^*\left(T^{*}_D + \theta\right) &= \lim_{n\to\infty} D\left(nT^*_D + \theta\right) = \lim_{t_i\to\infty} D\left(t_i + \theta\right);\\ &\qquad \forall\theta\in\left[0,T^*_D\right),\\ D^*\left(T^{*-}_D\right) &= D\left(0^-\right) = \lim_{\theta\to 0^-}\lim_{n\to\infty} D\left(nT^*_D + \theta\right)\\ &= \lim_{\theta\to 0^-}\lim_{t_i\to\infty} D\left(t_i - \theta\right)\end{aligned} \tag{29}$$

possessing eventual discontinuities $D^*(T^*_D) \neq D^*(T^{*-}_D)$ *which satisfy*

$$\begin{aligned}&D^*\left(T^*_D\right) = \left(1-\rho^*_D\right)D^*\left(T^{*-}_D\right);\\ &D^*\left(T^{*-}_D\right)\\ &= \frac{1-e^{-\mu T^*_D}}{\mu\left(1-\left(1-\rho^*_D\right)e^{-\mu T^*_D}\right)}\left[\left(b_2+\alpha\right)I^*_{av} + b_2 A^*_{av}\right].\end{aligned} \tag{30}$$

(ii) *If* $T^*_D = +\infty$, *or if* Imp$D$ *has a finite cardinal, then*

$$\begin{aligned}D^*\left(T^{*-}_D\right) &= \frac{1}{\mu}\left[\left(b_2+\alpha\right)I^*_{av} + b_2 A^*_{av}\right];\\ D^*\left(T^*_D\right) &= \frac{1-\rho^*_D}{\mu}\left[\left(b_2+\alpha\right)I^*_{av} + b_2 A^*_{av}\right].\end{aligned} \tag{31}$$

If, furthermore $\rho^*_D = 1$, *then* $D^*(T^*_D) = 0$.

For the disease-free equilibrium, $D^*_{df}(T^*_D) = D^*_{df}(T^{*-}_D) = 0$ *irrespective of* T^*_D *and* ρ^*_D.

If, furthermore $\rho^*_D = 0$, *then the endemic equilibrium periodic solution is an endemic equilibrium point* $D^*_{end} = ((b_2+\alpha)I^*_{end} + b_2 A^*_{end})/\mu$.

(iii) *The limit periodic solution* $D^*(T^*_D + \theta)$ *for* $\theta \in [0, T^*_D)$ *induces limit periodic oscillations of the susceptible and immune which obey the relationships:*

$$\begin{aligned}S^*(\theta) &= \frac{b_1 - V_0 + \eta R^*(\theta)}{b_2 + K^*_V(\theta) + \beta I^*(\theta) + \beta_A A^*(\theta) + \beta_D D^*(\theta)},\\ R^*(\theta) &= \frac{N^*_R(\theta)}{D^*_R(\theta)},\end{aligned} \tag{32}$$

where

$$\begin{aligned}N^*_R(\theta) &= \left(b_2 + \beta I^*(\theta) + \beta_A A^*(\theta) + \beta_D D^*(\theta)\right)\\ &\cdot\left(\left(\tau_0 + K^*_\xi(\theta)\right)I^*(\theta) + \tau_0 A^*(\theta) + V^*_0(\theta)\right)\\ &+ K^*_V(\theta)\left(\left(\tau_0 + K^*_\xi(\theta)\right)I^*(\theta) + \tau_0 A^*(\theta) + b_1\right),\\ D^*_R(\theta) &= \left(b_2+\eta\right)\\ &\cdot\left(b_2 + \beta I^*(\theta) + \beta_A A^*(\theta) + \beta_D D^*(\theta)\right)\\ &+ b_2 K^*_V(\theta);\\ &\qquad \forall\theta\in\left[0,T^*_D\right]\end{aligned} \tag{33}$$

provided that $V_0(nT^*_D + \theta) \to V^*_0(\theta)$, $K_V(nT^*_D + \theta) \to K^*_V(\theta)$, *and* $K_\xi(nT^*_D + \theta) \to K^*_\xi(\theta)$ *for any* $\theta \in [0, T^*_D]$ *as* $n(\in \mathbf{Z}_+) \to \infty$. *If* $\rho^*_D = 0$, $V^*_0(\theta) = V^*_0$, $K^*_V(\theta) = K^*_V$, *and* $K_\xi(\theta) = K^*_\xi$; $\forall\theta \in [0, T^*_D]$ *then the endemic equilibrium solution is an endemic equilibrium point.*

Proof. Note from (18) that if $(t_{i+1} - t_i) \to T^*_D$ and $\rho_D(t_i) \to \rho^*_D \in [0,1]$ as $t_i (\in \text{Imp}D) \to \infty$ then the right limits $D(T^*_D + \theta) = \lim_{n\to\infty} D(nT^*_D + \theta) = \lim_{t_i\to\infty} D(t_i + \theta)$ exist for $\theta \in [0, T^*_D)$ as well as the left limits $D(T^{*-}_D) = \lim_{\theta\to 0^-}\lim_{n\to\infty} D(nT^*_D + \theta) = \lim_{\theta\to 0^-}\lim_{t_i\to\infty} D(t_i - \theta)$ with eventual discontinuities $D(T^*_D) \neq D(T^{*-}_D)$. So, we have in the steady state

$$\begin{aligned}D\left(t_{i+1}\right) = D\left(t_i\right) &= D\left(T^*_D\right) = \left(1-\rho^*_D\right)D\left(t^-_{i+1}\right)\\ &= \left(1-\rho^*_D\right)e^{-\mu T^*_D}D\left(T^*_D\right) + \left(1-\rho^*_D\right)\\ &\cdot\left(\int_0^{T^*_D} e^{-\mu\left(T^*_D-\sigma\right)}\left[\left(b_2+\alpha\right)I^*(\sigma) + b_2 A^*(\sigma)\right]d\sigma\right)\end{aligned} \tag{34}$$

so that, from the mean value theorem since the limit the periodic oscillation is bounded, there is a mean value of the symptomatic and asymptomatic infectious subpopulation such that

$$\begin{aligned}&\left[1-\left(1-\rho^*_D\right)e^{-\mu T^*_D}\right]D^*\left(T^*_D\right) = \left(1-\rho^*_D\right)\\ &\cdot\frac{1-e^{-\mu T^*_D}}{\mu}\left[\left(b_2+\alpha\right)I^*_{\text{av}} + b_2 A^*_{\text{av}}\right],\end{aligned} \tag{35}$$

$$D^*\left(T_D^*+\theta\right)=e^{-\mu\theta}D^*\left(T_D^*\right)+\left[\left(b_2+\alpha\right)I_{\text{av}}^*+b_2A_{\text{av}}^*\right]\cdot\left(\int_0^\theta e^{-\mu(\theta-\sigma)}d\sigma\right)=\frac{e^{-\mu\theta}}{\mu}\left[\left(b_2+\alpha\right)I_{\text{av}}^*+b_2A_{\text{av}}^*\right]\cdot\left[\frac{\left(1-\rho_D^*\right)\left(1-e^{-\mu\theta}\right)}{\left(1-\left(1-\rho_D^*\right)e^{-\mu\theta}\right)}-1+e^{\mu\theta}\right];\quad\forall\theta\in\left[0,T_D^*\right]. \tag{36}$$

If $\rho_D^*=0$, one gets from (36) that

$$\lim_{t_i(\in\text{Imp}D)\to\infty}D\left(t_i+\theta\right)=\left[\left(b_2+\alpha\right)I_{\text{av}}^*+b_2A_{\text{av}}^*\right]\cdot\lim_{t_i(\in\text{Imp}D)\to\infty}\left(\int_{t_i}^{t_i+T_D^*}e^{-\mu\left(T_D^*+\theta-\sigma\right)}d\sigma\right)=D^*\left(T_D^*+\theta\right)=\frac{\left(b_2+\alpha\right)I_{\text{av}}^*+b_2A_{\text{av}}^*}{\mu};\quad\forall\theta\in\left[0,T_D^*\right) \tag{37}$$

so that $D(t)\to 0$ as $t\to\infty$ if the disease-free equilibrium point is globally asymptotically attractive and $D(t)\to D_{\text{end}}^*=((b_2+\alpha)I_{\text{end}}^*+b_2A_{\text{end}}^*)/\mu$ if the endemic equilibrium state, which is an equilibrium point, is globally asymptotically attractive. The proofs of Properties (i)-(ii) are complete. To prove Property (iii), the inspection of (1) and (6) at any equilibrium yields that S and R have periodic oscillation if D is periodic. So, we can get from (1) and (6) that if $V_0(\theta)=V_0^*(\theta)$, $K_V(\theta)=K_V^*(\theta)$, and $K_\xi(\theta)=K_\xi^*(\theta)$, for any $\theta\in[0,T_D^*]$, the relations

$$\begin{aligned}S^*(\theta)&=\frac{b_1-V_0^*(\theta)+\eta R^*(\theta)}{b_2+K_V^*(\theta)+\beta I^*(\theta)+\beta_AA^*(\theta)+\beta_DD^*(\theta)},\\R^*(\theta)&=\frac{\left(\tau_0+K_\xi^*(\theta)\right)I^*(\theta)+\tau_0A^*(\theta)+V_0^*(\theta)}{b_2+\eta}+\frac{K_V^*(\theta)}{b_2+\eta}S^*(\theta)\\&=\frac{\left(\tau_0+K_\xi^*(\theta)\right)I^*(\theta)+\tau_0A^*(\theta)+V_0^*(\theta)}{b_2+\eta}+\frac{K_V^*(\theta)}{b_2+\eta}\cdot\frac{b_1-V_0^*(\theta)+\eta R^*(\theta)}{b_2+K_V^*(\theta)+\beta I^*(\theta)+\beta_AA^*(\theta)+\beta_DD^*(\theta)}\end{aligned} \tag{38}$$

lead to

$$\left(1-\frac{K_V^*(\theta)\eta}{(b_2+\eta)\left(b_2+K_V^*(\theta)+\beta I^*(\theta)+\beta_AA^*(\theta)+\beta_DD^*(\theta)\right)}\right)\cdot R^*(\theta)=\frac{1}{b_2+\eta}\left[\left(\tau_0+K_\xi^*(\theta)\right)I^*(\theta)+\tau_0A^*(\theta)+V_0^*(\theta)+\frac{K_V^*(\theta)\left(b_1-V_0^*(\theta)\right)}{\left(b_2+K_V^*(\theta)+\beta I^*(\theta)+\beta_AA^*(\theta)+\beta_DD^*(\theta)\right)}\right] \tag{39}$$

which may be simplified as $R^*(\theta)=N_R^*(\theta)/D_R^*(\theta)$; $\forall\theta\in[0,T_D^*)$. Thus, Property (iii) follows. □

On the other hand, the linearized error of the trajectory solution with respect to an equilibrium trajectory is defined by

$$\begin{aligned}\dot{\widetilde{x}}(t)&=\mathbf{A}^*\widetilde{x}(t),\\\widetilde{x}\left(t_i\right)&=\left(\mathbf{I}_6-\mathbf{M}^*\right)\widetilde{x}\left(t_i^-\right);\quad\forall t\in\left[t_i,t_{i+1}\right),\ \forall t_i\in\text{Imp}D,\end{aligned} \tag{40}$$

where $\widetilde{x}(0^-)=\widetilde{x}_0$ and $\mathbf{M}^*$ are $\mathbf{R}^6\times\mathbf{R}^6$ matrix taking account of the impulses, where $(\mathbf{M}^*)_{55}=\rho_D^*$ as $\rho_D(t)\to\rho_D^*$ as $t\to\infty$ and its remaining entries being zero. The following result, concerning the disease-free and endemic equilibrium points, holds if the control gains converge to constant values and $\rho_D^*=0$.

Theorem 5. *Assume that $V_0(t)\to V_0$, $K_V(t)\to K_V^*$, $K_\xi(t)\to K_\xi^*$ and $\rho_D(t_i)\to\rho_D^*=0$, and $(t_{i+1}-t_i)\to T_D^*$ as $t,t_i(\in\text{Imp}D)\to\infty$. Then, the following properties hold:*

(i) *There is a unique disease-free equilibrium point satisfying*

$$\begin{aligned}x_{df}^*&:=\lim_{t\to\infty}x(t)=\left(S_{df}^*,E_{df}^*,I_{df}^*,A_{df}^*,D_{df}^*,R_{df}^*\right)^T\\&=\left(S_{df}^*,0,0,0,0,R_{df}^*\right)^T\end{aligned} \tag{41}$$

with

$$\begin{aligned}S_{df}^*&=\frac{b_2\left(b_1-V_0\right)+\eta b_1}{b_2\left(b_2+\eta+K_V^*\right)}=\frac{b_1+\eta N_{df}^*-V_0}{b_2+\eta+K_V^*},\\R_{df}^*&=\frac{b_2V_0+K_V^*b_1}{b_2\left(b_2+\eta+K_V^*\right)}=\frac{K_V^*N_{df}^*+V_0}{b_2+\eta+K_V^*}\\&=\frac{K_V^*S_{df}^*+V_0}{b_2+\eta}=N_{df}^*-S_{df}^*\end{aligned} \tag{42}$$

leading to an associated limit total population

$$\overline{N}_{df}^*=N_{df}^*=S_{df}^*+R_{df}^*=\frac{b_1}{b_2} \tag{43}$$

under a vaccination disease-free limiting control $V_{df}^* = V_0 + K_V^* S_{df}^*$ *and a zero antiviral treatment control.*

(ii) *There exists some large enough threshold* β_{cend} *such that if* $\beta > \beta_{cend}$ *then there is a unique endemic equilibrium point with all its components being positive such that*

$$N_{df}^* > S_{end}^* = \frac{\mu(b_2+\gamma)(b_2+\tau_0)\left(b_2+\alpha+\tau_0+K_\xi^*\right)}{\beta\left(\gamma p(b_2+\tau_0)(\mu+\beta_{Dr}(b_2+\alpha))+\gamma(1-p)\left(b_2+\alpha+\tau_0+K_\xi^*\right)\left(\beta_{Ar}\mu+\beta_{Dr}b_2\right)\right)} > 0, \tag{44}$$

$$S_{end}^* = \frac{b_2+\gamma}{\beta\left(C_I+\beta_{Ar}C_A+\beta_{Dr}C_D\right)} = \frac{b_1-V_0+\eta R_{end}^*}{b_2+K_V^*+\beta\left(C_I+\beta_{Ar}C_A+\beta_{Dr}C_D\right)E_{end}^*}, \tag{45}$$

$$R_{end}^* = \frac{\left(\left(\tau_0+K_\xi^*\right)C_I+\tau_0C_A\right)E_{end}^*+V_0+K_V^*S_{end}^*}{b_2+\eta}, \tag{46}$$

$$\overline{N}_{end}^* = \frac{\left(\tau_0+K_\xi^*\right)I_{end}^*+\tau_0A_{end}^*+V_0}{b_2+\eta}+\left(1+\frac{K_V^*}{b_2+\eta}\right)S_{end}^*+\left(C_I+C_A+C_D+1\right)E_{end}^*, \tag{47}$$

where $\beta_{Ar} = \beta_A/\beta$ *and* $\beta_{Dr} = \beta_D/\beta$ *are relative disease coefficient transmission rates of the asymptomatic infectious and lying infective corpses with respect to the symptomatic infectious one, and*

$$C_I = \frac{\gamma p}{b_2+\alpha+\tau_0+K_\xi^*},$$

$$C_A = \frac{\gamma(1-p)}{b_2+\tau_0},$$

$$C_D = \frac{1}{\mu}\left[\frac{(b_2+\alpha)\gamma p}{b_2+\alpha+\tau_0+K_\xi^*}+\frac{b_2\gamma(1-p)}{b_2+\tau_0}\right]. \tag{48}$$

(iii) *The disease-free and endemic equilibrium dynamics matrices are, respectively, given by*

$$\mathbf{A}_{df}^* = \begin{bmatrix} -\left(b_2+K_V^*\right) & 0 & -\beta S_{df}^* & -\beta_A S_{df}^* & -\beta_D S_{df}^* & \eta \\ 0 & -(b_2+\gamma) & \beta S_{df}^* & \beta_A S_{df}^* & \beta_D S_{df}^* & 0 \\ 0 & \gamma p & -\left(b_2+\alpha+\tau_0+K_\xi^*\right) & 0 & 0 & 0 \\ 0 & \gamma(1-p) & 0 & -(b_2+\tau_0) & 0 & 0 \\ 0 & 0 & b_2+\alpha & b_2 & -\mu & 0 \\ K_V^* & 0 & \tau_0+K_\xi^* & \tau_0 & 0 & -(b_2+\eta) \end{bmatrix}, \tag{49}$$

$$\mathbf{A}_{end}^* = \begin{bmatrix} -\left(b_2+\beta I_{end}^*+\beta_A A_{end}^*+\beta_D D_{end}^*+K_V^*\right) & 0 & -\beta S_{end}^* & -\beta_A S_{end}^* & -\beta_D S_{end}^* & \eta \\ \beta I_{end}^*+\beta_A A_{end}^*+\beta_D D_{end}^* & -(b_2+\gamma) & \beta S_{end}^* & \beta_A S_{end}^* & \beta_D S_{end}^* & 0 \\ 0 & \gamma p & -\left(b_2+\alpha+\tau_0+K_\xi^*\right) & 0 & 0 & 0 \\ 0 & \gamma(1-p) & 0 & -(b_2+\tau_0) & 0 & 0 \\ 0 & 0 & b_2+\alpha & b_2 & -\mu & 0 \\ K_V^* & 0 & \tau_0+K_\xi^* & \tau_0 & 0 & -(b_2+\eta) \end{bmatrix}. \tag{50}$$

Note that the endemic equilibrium linearized dynamics can also be described equivalently by

$$\overline{A}^*_{end} = \begin{bmatrix} -(b_2+K_V^*) & 0 & -(\beta+1)S^*_{end} & -(\beta_A+1)S^*_{end} & -(\beta_D+1)S^*_{end} & \eta \\ 0 & -(b_2+\gamma) & (\beta+1)S^*_{end} & (\beta_A+1)S^*_{end} & (\beta_D+1)S^*_{end} & 0 \\ 0 & \gamma p & -\left(b_2+\alpha+\tau_0+K_\xi^*\right) & 0 & 0 & 0 \\ 0 & \gamma(1-p) & 0 & -(b_2+\tau_0) & 0 & 0 \\ 0 & 0 & b_2+\alpha & b_2 & -\mu & 0 \\ K_V^* & 0 & \tau_0+K_\xi^* & \tau_0 & 0 & -(b_2+\eta) \end{bmatrix}. \tag{51}$$

(iv) *If $\rho_D^* \in (0,1)$ then the endemic equilibrium steady state $x^*_{end}(\theta)$ for $\theta \in [0, T_D^*)$ is periodic of period T_D^* leading to a matrix of dynamics $\mathbf{A}^*_{end} : [0, T_D^*) \to \mathbf{R}^{6\times 6}$ with $\mathbf{A}^*_{end}(T_D^*) = \mathbf{A}^*_{end}(0)$ and $\mathbf{A}^*_{end}(T_D^{*-}) = \mathbf{A}^*_{end}(0^-) \neq \mathbf{A}^*_{end}(0)$. Equations (45)–(47) and (50)-(51) remain valid with the change $x^*_{end} \to x^*_{end}(\theta)$ and the corresponding changes in the two first rows of (50) and (51) for $\theta \in [0, T_D^*)$.*

If the limit control gains $V_0^*(\cdot)$, $K_V^*(\cdot)$, and $K_\xi^*(\cdot)$ are periodic functions of period T_D^* then the disease-free equilibrium state has periodic susceptible and immune components defined as in Property (i) with the replacements $K_V^* \to K_V^*(\theta)$ and $K_\xi^* \to K_\xi^*(\theta)$ for $\theta \in [0, T_D^*)$ and $\mathbf{A}^*_{df} : [0, T_D^*) \to \mathbf{R}^{6\times 6}$ in (49). In this case, the endemic equilibrium state, if it exists, is also periodic of period T_D^*.

Proof. The disease-free equilibrium point is obtained directly from (1) to (7) from the constraints $E^*_{\mathrm{df}} = I^*_{\mathrm{df}} = A^*_{\mathrm{df}} = D^*_{\mathrm{df}} = 0$ and it is seen to be trivially unique. The Jacobian matrix of the linearized system at such a disease-free equilibrium point is (49). The proof of Property (i) follows directly. To prove the existence of an endemic equilibrium point (Property (ii)) some calculations are now performed to see the compatibility of the model with the existence of an equilibrium with exposed subpopulation $E^*_{\mathrm{end}} > 0$ implying the remaining subpopulations to be nonnegative. Direct calculations by zeroing in (3) to (5) the time derivatives of the subpopulations by taking into account (7)-(8) yield

$$\begin{aligned} &E^*_{\mathrm{end}} > 0 \Longleftrightarrow I^*_{\mathrm{end}} = C_I E^*_{\mathrm{end}} > 0, \\ &E^*_{\mathrm{end}} > 0 \Longleftrightarrow A^*_{\mathrm{end}} = C_A E^*_{\mathrm{end}} > 0, \\ &E^*_{\mathrm{end}} > 0 \Longleftrightarrow D^*_{\mathrm{end}} = C_D E^*_{\mathrm{end}} > 0 \end{aligned} \tag{52}$$

with the above constants defined in (48). From (2), one gets if $E^*_{\mathrm{end}} > 0$ implying that $I^*_{\mathrm{end}} > 0$ that (44) holds since

$$\begin{aligned} &E^*_{\mathrm{end}} > 0 \Longleftrightarrow \\ &\left[\left(I^*_{\mathrm{end}} > 0\right) \wedge \left(A^*_{\mathrm{end}} > 0\right) \wedge \left(D^*_{\mathrm{end}} > 0\right)\right] \Longrightarrow \\ &S^*_{\mathrm{end}} = \frac{b_2+\gamma}{\beta\left(C_I + \beta_{Ar}C_A + \beta_{Dr}C_D\right)E^*_{\mathrm{end}}} E^*_{\mathrm{end}}. \end{aligned} \tag{53}$$

This proves the first part of Property (ii) since $N^*_{\mathrm{end}} < N^*_{\mathrm{df}}$. Now, note from (44) that if $\beta \leq \beta_{\mathrm{cend}}$ for a small enough threshold β_{cend} for some existing small enough threshold β_{cend}, then $S^*_{\mathrm{end}} \geq N^*_{\mathrm{end}}$ from (44). This implies that $S^*_{\mathrm{end}} > 0$ from (44) but $E^*_{\mathrm{end}} \leq 0$ (then either the endemic equilibrium point does not exist, since it has negative components, or it coincides with the disease-free one) since (46) leads to $E^*_{\mathrm{end}} > 0$ and $S^*_{\mathrm{end}} > 0$ implies $R^*_{\mathrm{end}} > 0$ and $R^*_{\mathrm{end}} < 0$ with $S^*_{\mathrm{end}} > 0$ if and only if $E^*_{\mathrm{end}} < 0$. Therefore, $E^*_{\mathrm{end}} > 0 \Leftrightarrow (N^*_{\mathrm{end}} > S^*_{\mathrm{end}} > 0)$ if and only if $\beta > \beta_{\mathrm{cend}}$. Now, summing up (1), (2), and (6), by taking into account (7)-(8) at the endemic equilibrium point yield (45)–(47) since

$$\begin{aligned} &b_2\left(S^*_{\mathrm{end}} + R^*_{\mathrm{end}}\right) \\ &\quad = b_1 + \left[\left(\tau_0 + K_\xi^*\right)C_I + \tau_0 C_A - b_2 - \gamma\right]E^*_{\mathrm{end}}, \\ &R^*_{\mathrm{end}} - \frac{K_V^* S^*_{\mathrm{end}} + V_0}{b_2+\eta} = \frac{\left(\tau_0 + K_\xi^*\right)I^*_{\mathrm{end}} + \tau_0 A^*_{\mathrm{end}}}{b_2+\eta} \\ &\quad = \frac{\left(\tau_0 + K_\xi^*\right)C_I + \tau_0 C_A}{b_2+\eta} E^*_{\mathrm{end}}, \\ &\overline{N}^*_{\mathrm{end}} = R^*_{\mathrm{end}} + S^*_{\mathrm{end}} + \left(I^*_{\mathrm{end}} + A^*_{\mathrm{end}} + D^*_{\mathrm{end}} + E^*_{\mathrm{end}}\right) \\ &\quad = \frac{\left(\tau_0 + K_\xi^*\right)I^*_{\mathrm{end}} + \tau_0 A^*_{\mathrm{end}} + V_0}{b_2+\eta} \\ &\qquad + \left(1 + \frac{K_V^*}{b_2+\eta}\right)S^*_{\mathrm{end}} + \left(C_I + C_A + C_D + 1\right)E^*_{\mathrm{end}} \end{aligned} \tag{54}$$

which completes the proof of Property (ii). The proof of Property (iii) is direct by taking the respective Jacobian matrices at the disease-free equilibrium point and the endemic equilibrium. The respective Jacobian matrices are (49) and (50). The use of (51), replacing (50), as the matrix of linearized dynamics around the endemic equilibrium point is legitimated via the identity:

$$\begin{aligned} &\left(\beta I^*_{\mathrm{end}} + \beta_A A^*_{\mathrm{end}} + \beta_D D^*_{\mathrm{end}}\right)S^*_{\mathrm{end}} \\ &\qquad = \left[\beta S^*_{\mathrm{end}} \quad \beta_A S^*_{\mathrm{end}} \quad \beta_D S^*_{\mathrm{end}}\right] \begin{bmatrix} I^*_{\mathrm{end}} \\ A^*_{\mathrm{end}} \\ D^*_{\mathrm{end}} \end{bmatrix}. \end{aligned} \tag{55}$$

Property (iv) follows directly from Property (iii) and Theorem 4 with the replacement $x^*_{\text{end}} \to x^*_{\text{end}}(\theta)$ and $C_I = C_I(\theta)$ and $C_D = C_D(\theta)$ in (48) for $\theta \in [0, T^*_D)$ and, eventually, $S^*_{\text{df}} \to S^*_{\text{df}}(\theta)$ and $R^*_{\text{df}} \to R^*_{\text{df}}(\theta)$ if the control gains converge to periodic values of period T^*_D. □

Theorem 5 is useful for the study under linearization of the solution trajectories around the disease-free equilibrium point if $\rho^*_D = 0$ under limit gains of the other controls. However, if the above limit gain is nonzero and less than one, then the trajectory solutions are asymptotically periodic. It is also proved the existence and uniqueness of the endemic equilibrium point if the coefficient transmission rates exceed a certain minimum threshold β_{cend}. It is also deduced from the disease-free equilibrium expressions that the susceptible disease-free equilibrium numbers can be decreased, and correspondingly the immune equilibrium numbers increased, by increasing the constant vaccination and/or the linear vaccination gains.

A constraint for the endemic equilibrium solution, if it exists, is discussed and given in the subsequent result. The existence constraints are easy to test under the form $S^*_{\text{end}}(\theta) < b_1/b_2 - V^*_0(\theta)$, $\forall\theta \in [0, T^*_D)$, or some equivalent constraints, where T^*_D is the limit interculling action period.

Theorem 6. *Assume that* $(t_{i+1} - t_i) \to T^*_D$, $\rho_D(nT^*_D) \to \rho^*_D \in [0, 1)$, $V_0(nT^*_D + \theta) \to V^*_0(\theta)$, $K_V(nT^*_D + \theta) \to K^*_V(\theta)$ *and* $K_\xi(nT^*_D + \theta) \to K^*_\xi(\theta)$ *as* $n \to \infty$, $\forall\theta \in [0, T^*_D]$ *as* $t \to \infty$, $t_i (\in \text{Imp}D) \to \infty$, *and* $n (\in \mathbf{Z}_+) \to \infty$. *Then, the following properties hold:*

(i) *The endemic equilibrium state* $x^*_{end} = x^*_{end}(\theta)$ *for* $\theta \in [0, T^*_D]$, *being a point if* $\rho^*_D = 0$, *equivalently if* $\text{card}\,\text{Imp}D < \aleph_0$ *(i.e., it is finite), and a periodic limit oscillation if* $\rho^*_D \in (0, 1]$ *has the subsequent components:*

$$S^*_{end}(\theta) = \frac{B_A B_I(\theta) B_E}{\beta f + \beta_A f_A(\theta) + \beta_D f_D(\theta)} = \frac{b_2 + \gamma}{\beta\left(C_I(\theta) + \beta_{Ar} C_A + \beta_{Dr} C_D(\theta)\right)},$$

$$E^*_{end}(\theta) = B_A B_I(\theta) C_0(\theta) \cdot \left(B_R\left(S^*_{df}(\theta) - S^*_{end}(\theta)\right) + K^*_V(\theta) S^*_{df}\right),$$

$$I^*_{end}(\theta) = C_I(\theta) E^*_{end}(\theta) = f C_0(\theta) \cdot \left(B_R\left(S^*_{df}(\theta) - S^*_{end}(\theta)\right) + K^*_V(\theta) S^*_{df}(\theta)\right),$$

$$A^*_{end}(\theta) = C_A E^*_{end}(\theta) = f C_0(\theta) \cdot \left(B_R\left(S^*_{df}(\theta) - S^*_{end}(\theta)\right) + K^*_V(\theta) S^*_{df}(\theta)\right),$$

$$D^*_{end}(\theta) = C_D(\theta) E^*_{end}(\theta) = f_D(\theta) C_0(\theta) \cdot \left(B_R\left(S^*_{df}(\theta) - S^*_{end}(\theta)\right) + K^*_V S^*_{df}(\theta)\right),$$

$$R^*_{end}(\theta) = \left(S^*_{df}(\theta) - S^*_{end}(\theta)\right) + \left(R^*_{df}(\theta) - \left(E^*_{end}(\theta) + \frac{\mu}{b_2} D^*_{end}(\theta)\right)\right); \quad \forall\theta \in [0, T^*_D]. \tag{56}$$

Being real constants if $\rho^*_D = 0$, *where*

$$B_A = b_2 + \tau_0;$$
$$B_I(\theta) = b_2 + \tau_0 + \alpha + K^*_\xi(\theta),$$
$$B_R = b_2 + \eta;$$
$$B_E = b_2 + \gamma,$$
$$f = \gamma p B_A;$$
$$f_A(\theta) = \gamma(1 - p) B_I(\theta),$$
$$f_D(\theta) = \frac{1}{\mu}\left(b_2 f_A(\theta) + (b_2 + \alpha) f\right) = \frac{\gamma}{\mu}\left(b_2(1 - p) B_I(\theta) + p(b_2 + \alpha) B_A\right),$$
$$C_0(\theta) = \frac{b_2}{b_2 B_A B_I(\theta)(\gamma + B_R) + \eta\mu f_D(\theta)}; \quad \forall\theta \in [0, T^*_D), \tag{57}$$

where $C_I = C_I(\theta)$ *and* $C_D = C_D(\theta)$ *in (48) since* $K^*_\xi = K^*_\xi(\theta)$ *for* $\theta \in [0, T^*_D)$. *If* $S^*_{end}(\theta) < ((B_R + K^*_V(\theta))/B_R) S^*_{df}(\theta) = (1 + K^*_V(\theta)/(b_2 + \eta)) S^*_{df}(\theta)$; $\forall\theta \in [0, T^*_D)$, *then the endemic equilibrium state exists, while being distinct of the disease-free equilibrium state. This existence condition of the endemic equilibrium state is equivalent to* $S^*_{end}(\theta) < b_1/b_2 - V^*_0(\theta)$; $\forall\theta \in [0, T^*_D)$.

If $S^*_{end}(\theta) > (1 + K^*_V(\theta)/(b_2 + \eta)) S^*_{df}(\theta)$; $\forall\theta \in [0, T^*_D)$ *then the endemic equilibrium state does not exist in the sense that it has some negative components. On the contrary, the opposed condition*

$$S^*_{end}(\theta) < \left(1 + \frac{K^*_V(\theta)}{b_2 + \eta}\right) S^*_{df}(\theta) = \frac{b_2\left(b_1 - V^*_0(\theta)\right) + \eta b_1}{b_2(b_2 + \eta)}; \quad \theta \in [0, T^*_D) \tag{58}$$

yields the existence of such an endemic equilibrium state. In the case when the limit control gains are constant, the disease-free equilibrium state is an equilibrium point. If, in addition, $\rho^*_D = 0$ *then the endemic equilibrium solution, if it exists, is also an equilibrium point.*

(ii)

$$N^*_{end}(\theta) < N^*_{df} = \frac{b_1}{b_2} \tag{59}$$

and the dependence on $\theta \in [0, T_D^*)$ is removed in the case that the endemic equilibrium state is an equilibrium point.

Proof. The values of the components of the endemic equilibrium state follow by direct elementary calculations form (45) and (48) and have been verified under symbolic calculation with the Mathematica package. Note that in the general case when the control gains converge to periodic functions of period T_D^* both the disease-free and endemic equilibrium solutions are periodic with such a period [see Theorem 5(iv)]. The endemic equilibrium exists while it is distinct from the disease-free one if (58) holds. To prove Property (ii), note by zeroing (1) to (4) and (6) while summing them up and the use of (7) at the disease-free and endemic equilibrium states that

$$N_{\text{end}}^*(\theta) = S_{\text{end}}^*(\theta) + R_{\text{end}}^*(\theta) + E_{\text{end}}^*(\theta) + I_{\text{end}}^*(\theta) + A_{\text{end}}^*(\theta) < N_{\text{df}}^* = S_{\text{df}}^* + R_{\text{df}}^*; \quad \forall\theta \in [0, T_D^*) \tag{60}$$

since $\dot{N}(t) = -b_2 N(t) + b_1 - \alpha I(t)$; $\forall t \in \mathbf{R}_{0+}$. Thus, since $(E_{\text{end}}^*(\theta) + I_{\text{end}}^*(\theta) + A_{\text{end}}^*(\theta)) > 0$; $\forall\theta \in [0, T_D^*)$ implied by $E_{\text{end}}^*(\theta) > 0$, $\forall\theta \in [0, T_D^*)$ if the endemic equilibrium state exists then $N_{\text{end}}^*(\theta) < N_{\text{df}}^*$; $\forall\theta \in [0, T_D^*)$. Property (ii) is proved. □

Note from the components of the endemic equilibrium expressions given in Theorem 6(i) that the equilibrium number of the endemic susceptible increases while correspondingly those of all the infective subpopulations decrease as the limit antiviral control gain K_ξ^* increases. This is an interesting tool to control the infection in the case that the endemic equilibrium exists and the disease-free one is unstable so unreachable in practice if the coefficient transmission rate is large enough exceeding the threshold β_{cend} of Theorem 5.

Remark 7. Note that we can write the linearized equation around the endemic equilibrium state as

$$\dot{\widetilde{x}}(\theta) = \left[\mathbf{A}_{\text{df}}^*(\theta) + \left(\mathbf{A}_{\text{end}}^*(\theta) - \mathbf{A}_{\text{df}}^*(\theta)\right)\right]\widetilde{x}(\theta) = \left[\mathbf{A}_{\text{df}}^*(\theta) + \left(\overline{\mathbf{A}}_{\text{end}}^*(\theta) - \mathbf{A}_{\text{df}}^*(\theta)\right)\right]\widetilde{x}(\theta); \quad \forall\theta \in [0, T_D^*) \tag{61}$$

with

$$\widetilde{x}(0) = \widetilde{x}(T_D^*) = (1 - \rho_D^*)\,\widetilde{x}(T_D^{*-}), \tag{62}$$

where

$$\overline{\mathbf{A}}_{\text{end}}^*(\theta) - \mathbf{A}_{\text{df}}^*(\theta) = \begin{bmatrix} 0 & 0 & -a_{13}(\theta) & -a_{14}(\theta) & -a_{15}(\theta) & 0 \\ 0 & 0 & a_{13}(\theta) & a_{14}(\theta) & a_{15}(\theta) & 0 \\ & & & \mathbf{0}_{4\times 6} & & \end{bmatrix} \tag{63a}$$

with

$$\begin{aligned} a_{13}(\theta) &= (\beta + 1)\,S_{\text{end}}^*(\theta) - \beta S_{\text{df}}^*(\theta), \\ a_{14}(\theta) &= (\beta\beta_{Ar} + 1)\,S_{\text{end}}^*(\theta) - \beta\beta_{Ar} S_{\text{df}}^*(\theta), \\ a_{15}(\theta) &= (\beta\beta_{Dr} + 1)\,S_{\text{end}}^*(\theta) - \beta\beta_{Dr} S_{\text{df}}^*(\theta); \\ &\qquad \forall\theta \in [0, T_D^*) \end{aligned} \tag{63b}$$

since

$$\begin{aligned} \mathbf{A}_{\text{end}}^*(\theta)\,x_{\text{end}}^*(\theta) &= \overline{\mathbf{A}}_{\text{end}}^*(\theta)\,x_{\text{end}}^*(\theta) \\ &= \left[\mathbf{A}_{\text{df}}^*(\theta) + \left(\overline{\mathbf{A}}_{\text{end}}^*(\theta) - \mathbf{A}_{\text{df}}^*(\theta)\right)\right] x_{\text{end}}^*(\theta); \\ &\qquad \forall\theta \in [0, T_D^*) \end{aligned} \tag{64}$$

by using (49)–(51) and (55). If $\mathbf{A}_{\text{df}}^*(\theta)$ is nonsingular then $\overline{\mathbf{A}}_{\text{end}}^*(\theta) = \mathbf{A}_{\text{df}}^*(\theta)[\mathbf{I}_6 + \mathbf{A}_{\text{df}}^{*-1}(\theta)(\overline{\mathbf{A}}_{\text{end}}^*(\theta) - \mathbf{A}_{\text{df}}^*(\theta))]$ is also nonsingular if

$$\left\|\overline{\mathbf{A}}_{\text{end}}^*(\theta) - \mathbf{A}_{\text{df}}^*(\theta)\right\|_2^2 = 2\left[a_{13}^2(\theta) + a_{13}^2(\theta) + a_{15}^2(\theta)\right] < 1; \quad \forall\theta \in [0, T_D^*). \tag{65}$$

Therefore, if $\mathbf{A}_{\text{df}}^*(\theta)$ is a stability matrix (then, nonsingular) and (65) holds then $\overline{\mathbf{A}}_{\text{end}}^*(\theta)$ and $\mathbf{A}_{\text{end}}^*(\theta)$ are stability matrices.

The following results give easily testable sufficiency-type local instability and local stability tests for the endemic equilibrium point based on the stability properties of the disease-free matrix of dynamics of the linearized system about the disease-free equilibrium. The extension to the case of oscillatory periodic endemic equilibrium solution would follow "mutatis-mutandis."

Theorem 8. *Assume that the control limits V_0^*, K_V^*, K_ξ^*, and $\rho_D^* = 0$ exist and define the amounts*

$$\begin{aligned} \vartheta &= \frac{1}{2}\left\|A_{df}^{*-1}\right\|_1 \left\|\overline{A}_{end}^* - A_{df}^*\right\|_1, \\ \kappa_\vartheta &= \left\|A_{df}^{*-1}\right\|_1 \frac{b_2(b_1 - V_0) + \eta b_1}{b_2(b_2 + \eta + K_V^*)}\left[\frac{K_V^*}{b_2 + \eta}(1 + \beta\max(1, \beta_{Ar}, \beta_{Dr})) + 1\right]. \end{aligned} \tag{66}$$

The following properties hold:

(i) *The endemic equilibrium point exists and it is unstable if A_{df}^* is instability nonsingular matrix (i.e., it has at least one eigenvalue in $\text{Re}\, s > 0$) and $\kappa_\vartheta < 1/2$.*

(ii) *The endemic equilibrium point, provided that it exists, is locally asymptotically stable if A_{df}^* is a stability matrix and $\kappa_\vartheta < 1/2$.*

Proof. Elementary calculation yields $\overline{A}_{\text{end}}^* = A_{\text{df}}^*[\mathbf{I}_6 + A_{\text{df}}^{*-1}(\overline{A}_{\text{end}}^* - A_{\text{df}}^*)]$ if A_{df}^* is nonsingular. If, furthermore, A_{df}^* is instability matrix then $\overline{A}_{\text{end}}^*$ is also instability matrix if

$1 > \|A_{\text{df}}^{*-1}(\overline{A}_{\text{end}}^{*} - A_{\text{df}}^{*})\|_1$, which is equivalent to $\kappa_\vartheta < 1/2$, from Banach's Perturbation Lemma [33], since $\overline{A}_{\text{end}}^{*}$ is nonsingular and the eigenvalues are continuous functions with respect to any matrix entry thus $\overline{A}_{\text{end}}^{*}$ is instability matrix. In the same way, if A_{df}^{*} is a stability matrix (then nonsingular) and $\kappa_\vartheta < 1/2$ then $\overline{A}_{\text{end}}^{*}$ is nonsingular and then stable by similar reasoning.

It has to be pointed out that Theorem 10, which is stated and proved later on, establishes that both equilibrium points cannot be simultaneously stable. As a result, one concludes via Theorem 8(ii) that if A_{df}^{*} is a stability matrix and $\kappa_\vartheta < 1/2$ then the endemic equilibrium point does not exist. By linking this observation with Theorem 6(i), one concludes as well that $S_{\text{end}}^{*} > (1 + K_V^{*}/(b_2 + \eta))S_{\text{df}}^{*}$ and the only existing equilibrium point is the disease-free one which is globally asymptotically stable. □

Theorem 8 can be reformulated for the use of ℓ_∞-norms by using the identity:

$$\begin{aligned}\left\|\overline{A}_{\text{end}}^{*} - A_{\text{df}}^{*}\right\|_\infty &= \left|S_{\text{end}}^{*} + \beta\left(S_{\text{end}}^{*} - S_{\text{df}}^{*}\right)\right| \\ &\quad + \left|S_{\text{end}}^{*} + \beta\beta_{Ar}\left(S_{\text{end}}^{*} - S_{\text{df}}^{*}\right)\right| \\ &\quad + \left|S_{\text{end}}^{*} + \beta\beta_{Dr}\left(S_{\text{end}}^{*} - S_{\text{df}}^{*}\right)\right|\end{aligned} \tag{67}$$

and for the use of ℓ_2-norms by using the square root of the sum of the squares of the three right-hand-side terms in the above identity as replacement of it. A simple sufficient condition for the local stability of the disease-free equilibrium follows.

Theorem 9. *Assume that β is small enough according to $\beta < \beta_{cdf}$ with respect to the threshold:*

$$\begin{aligned}\beta_{cdf} &= \frac{1 + \beta_{Ar} + \beta_{Dr}}{S_{df}^{*}}\left[b_2 + \min\left(\gamma, K_V^{*} - \eta\right)\right] \\ &= \frac{b_2\left(b_2 + \eta + K_V^{*}\right)}{\left(1 + \beta_{Ar} + \beta_{Dr}\right)\left[b_2\left(b_1 - V_0\right) + \eta b_1\right]}\left(b_2\right. \\ &\quad \left. + \min\left(\gamma, K_V^{*} - \eta\right)\right).\end{aligned} \tag{68}$$

Thus, the disease-free equilibrium point is locally asymptotically stable provided that

$$\begin{aligned}&\alpha < \mu; \\ &K_V^{*} > \eta - b_2, \\ &b_2 \in \left(\max\left(\eta - K_V^{*}, K_V^{*} + 2\tau_0 + K_\xi^{*} - \mu, \gamma\left(1 - p\right)\right.\right. \\ &\quad \left.\left. - \tau_0, \gamma p - \alpha - \tau_0 - K_\xi^{*}, 0\right), \frac{\mu - \alpha}{2}\right).\end{aligned} \tag{69}$$

Proof. Note from (49) that $\mathbf{A}_{\text{df}}^{*}$ is a stability matrix since $\text{diag}(\mathbf{A}_{\text{df}}^{*})$ is a stability matrix and $\mathbf{A}_{\text{df}}^{*}$ is diagonally row dominant if (68)-(69) hold. □

Note that Theorem 9 can be combined with Theorem 5 in practical situations in the following sense. If the threshold $\beta < \beta_{\text{cdf}} \leq \beta_{\text{cend}}$ then the disease-free equilibrium is locally asymptotically stable and no endemic equilibrium point exists. If $\beta \geq \beta_{\text{cdf}} \geq \beta_{\text{cend}}$ then the endemic equilibrium point is locally asymptotically stable while the disease-free one is unstable. This local result has a global stability version as discussed in the following. The subsequent global stability result is proved in Appendix and it is based on the qualitative theory of differential equations in the sense that Lyapunov equation candidates are not used. The solution explicit formulas are not invoked to construct the proof but only the trajectory separating properties of eventually existing stable, semistable, or unstable limit cycles around equilibrium points are addressed and used.

Theorem 10 (global uniform asymptotic stability). *Assume that $\rho_D(t) \to \rho_D^{*} = 0$ as $t(\in \text{Im}pD) \to \infty$. Thus, the following properties hold:*

(i) *If the disease-free equilibrium point is locally asymptotically stable while the endemic equilibrium state does not exist then the epidemic model is globally uniformly asymptotically stable and all the solution trajectories converge asymptotically to the disease-free equilibrium point.*

(ii) *If the disease-free equilibrium point is unstable and the endemic equilibrium state exists then the system is globally uniformly asymptotically stable and all the solution trajectories converge to the endemic equilibrium point.*

(iii) *The disease-free and the endemic equilibrium states cannot be simultaneously either stable or unstable.*

4. Numerical Simulations

It is now presented a set of numerical simulation work. The parameters of the model are obtained from real data from a study of Ebola disease [29]. The recruitment rate and the natural average death rate are $b_1 = b_2 = 1/(70 \times 365) \times \text{days}^{-1}$ while the disease transmission coefficients are $\beta = 0.16$, $\beta_A = 0.05$, and $\beta_D = 0.5$ ($\times\text{days}^{-1}$), respectively. The average duration of the immunity period reflecting a transition from the recovered subpopulation to the susceptible subpopulation is determined by $1/\eta = 1000$ days, the average transition rate from the exposed to both infectious subpopulations is $\gamma = 1/15.8 \times \text{days}^{-1}$, the average extra mortality of the symptomatic infectious is $\alpha = 1/13.3 \times \text{days}^{-1}$, the natural immune response is $\tau_0 = 1/12 \times \text{days}^{-1}$, the fraction of the exposed subpopulation becoming symptomatic infectious one is $p = 0.9$, and the average duration of infection is $1/\mu = 20$ days. The initial conditions are given by $S(0) = 1000/1050$, $E(0) = 10/1050$, $I(0) = 30/1050$, $A(0) = D(0) = 0$, and $R(0) = 10/1050$ so that the initial total living population is normalized to unity, $N(0) = S(0) + E(0) + I(0) + A(0) + D(0) + R(0) = 1$. Figure 1 displays the natural evolution of the disease in the absence of any external action. It is observed that the number of infective and infectious subpopulations increases implying an increase of infective corpses as well. The result of the natural evolution of the epidemics is the dead of individuals so that the total living population decreases with

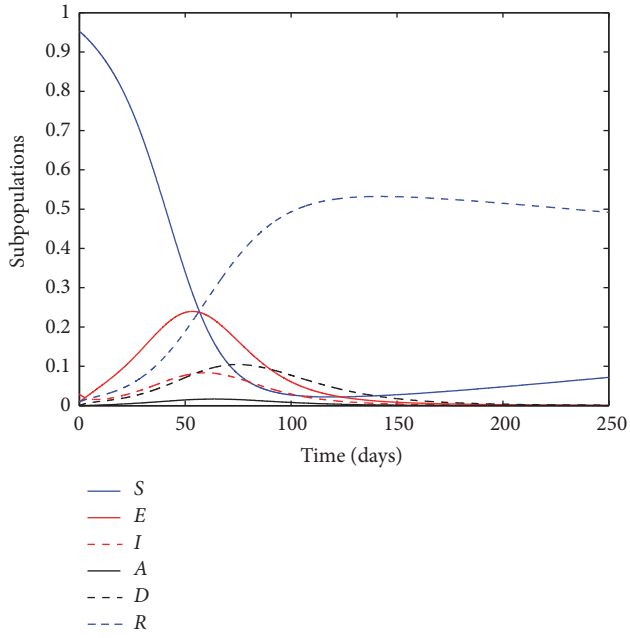

Figure 1: Natural evolution of the subpopulations.

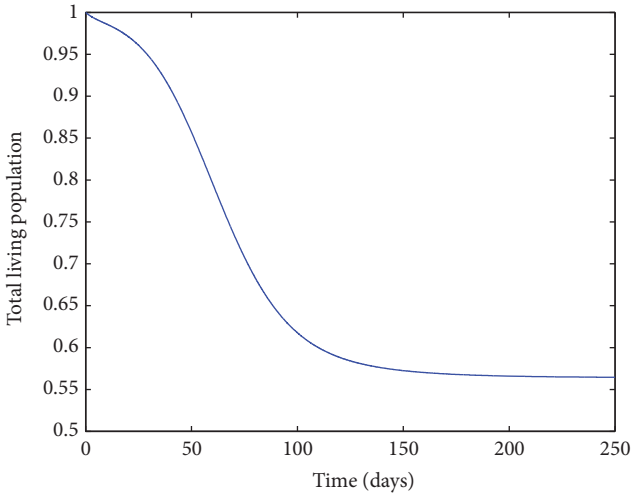

Figure 2: Natural evolution of the total alive population.

time as Figure 2 shows. After 250 days, the total living population is only 56.47% of the initial one. Three control mechanisms of fighting against Ebola have been considered in the previous subsections. The effect of these control policies is now illustrated through simulation examples. Initially, corpse culling (impulsive action on D) is considered as the only action to modify the natural behavior of the disease. Figures 3 and 4 show the effect of corpse culling on the system with different culling rates. In this way, Figure 3 considers the case when corpses are removed once daily at a rate of $\rho_D = 0.1$ (i.e., 10% of corpses are removed daily) while Figure 4 shows the behavior of the system when the daily culling rate is $\rho_D = 0.8$.

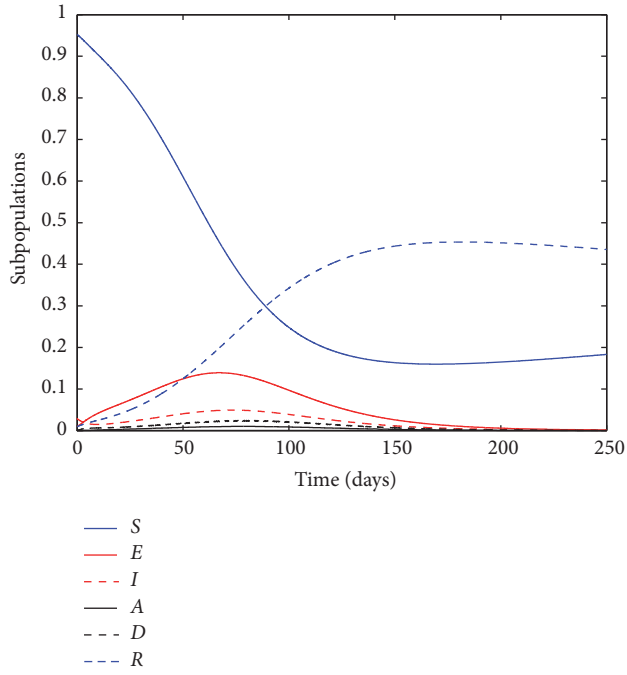

Figure 3: Evolution of the subpopulations with a daily culling rate of $\rho_D = 0.1$.

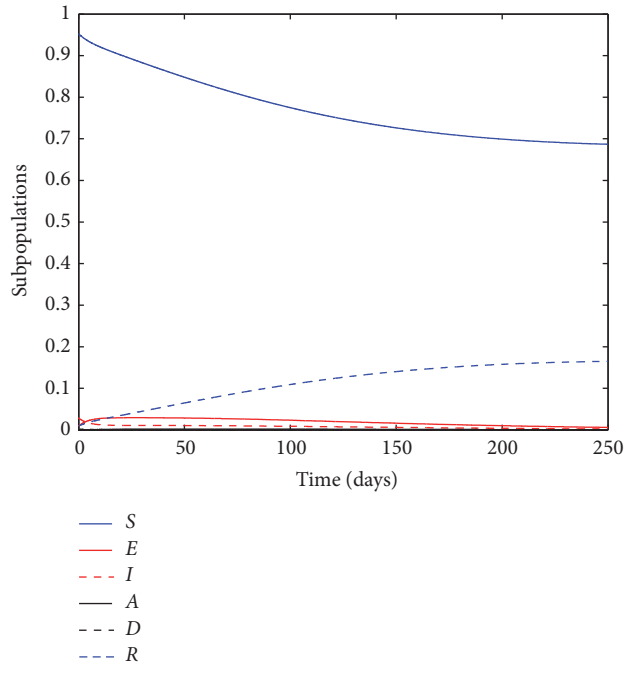

Figure 4: Evolution of the subpopulations with a daily culling rate of $\rho_D = 0.8$.

It can be deduced from Figures 3 and 4 that corpse culling has a high impact on the evolution of the disease since all the infected populations reduce their peak values due to the application of culling. The direct consequence of this fact is that the number of casualties is reduced as Figures 5 and 6 reveal for the total living population. Therefore, when the culling rate is $\rho_D = 0.1$, the total living population after 250

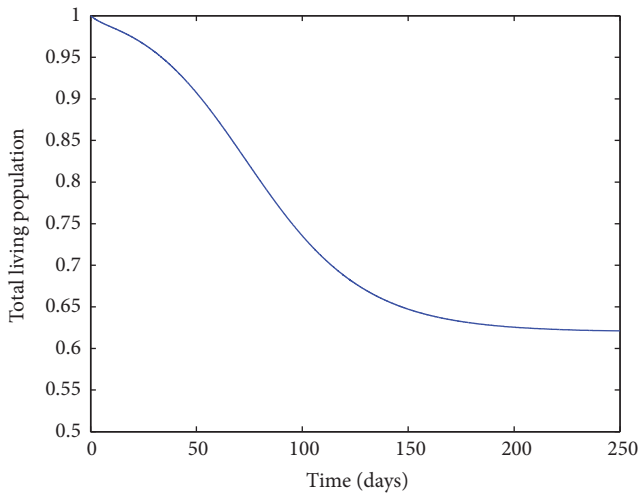

Figure 5: Evolution of the total alive population with a daily culling rate of $\rho_D = 0.1$.

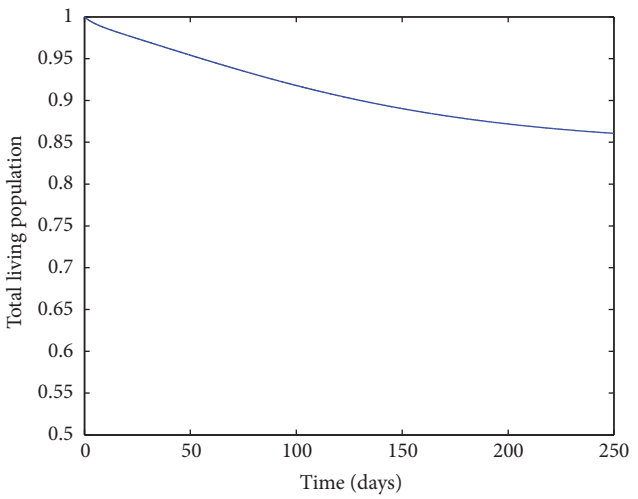

Figure 6: Evolution of the total alive population with a daily culling rate of $\rho_D = 0.8$.

days is 62.10% of the initial one while when $\rho_D = 0.8$ the total living population after 250 days is 86.07% of the initial one. On the other hand, Figures 7 and 8 show the effect of culling when applied every other day instead of daily.

If we now compare Figures 6 and 8 it can be noticed that the spacing of the culling action reduces the total living population after 250 days of epidemics. Thus, from Figures 5, 6, and 8 it is obtained the intuitive conclusion that it is recommendable to perform culling as frequently as possible with the highest possible rate. Hence, the proposed mathematical model (1)–(6) captures and illustrates the effect of culling in reality. Figures 9, 10, and 11 display the culling effort corresponding to the cases considered in Figures 3, 4, and 7, respectively. The culling effort is higher during the first time instants for a higher culling rate while decreases afterwards. Thus, a greater number of corpses are removed initially, fact that reduces the number of deaths caused by the infection, which in turn reduces the number of new corpses.

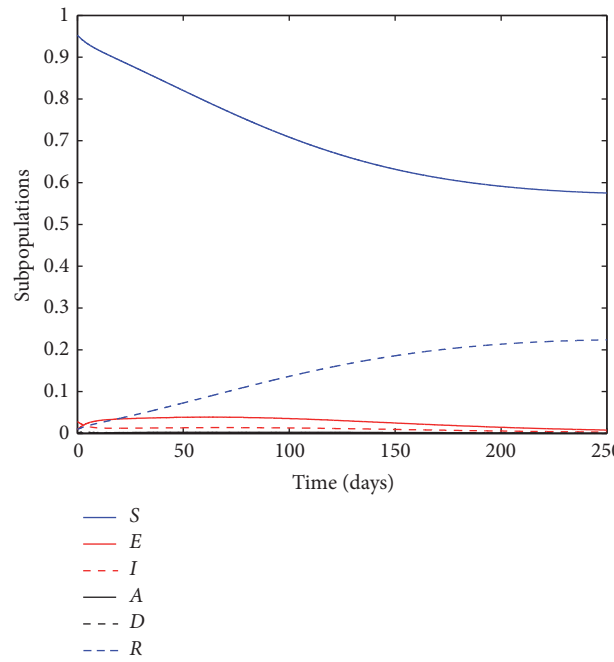

Figure 7: Evolution of the subpopulations with an every other day culling rate of $\rho_D = 0.8$.

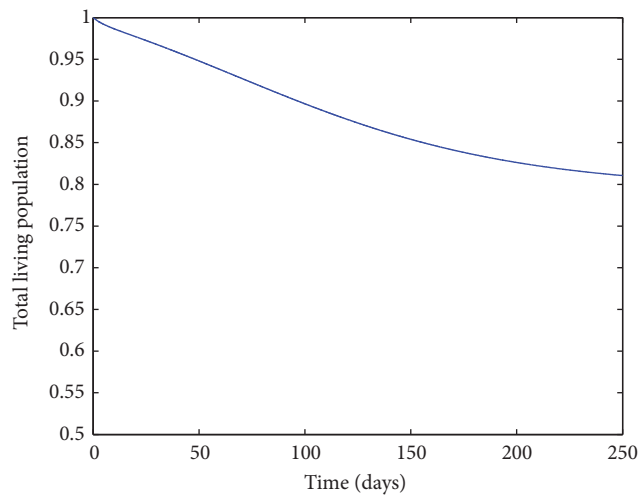

Figure 8: Evolution of the total alive population with an every other day culling rate of $\rho_D = 0.8$.

As a consequence, the number of corpses to be removed reduces as time goes by. On the other hand, a smaller culling rate causes a peak in the culling effort during the evolution of the disease, as Figure 9 shows.

Furthermore, vaccination can also be used in addition to culling to fight against disease. In this way, Figures 12–15 show the effect of a constant vaccination on the system when a culling rate of $\rho_D = 0.1$ is also applied. The constant vaccination is expressed in both cases as a multiple of b_1, being of $V = V_0 = 0.2b_1$ for Figures 12 and 13 and $V = V_0 = 0.8b_1$ for Figures 14 and 15.

It can be noted from Figures 5, 13, and 15 that the proposed constant vaccinations do not alter significantly the

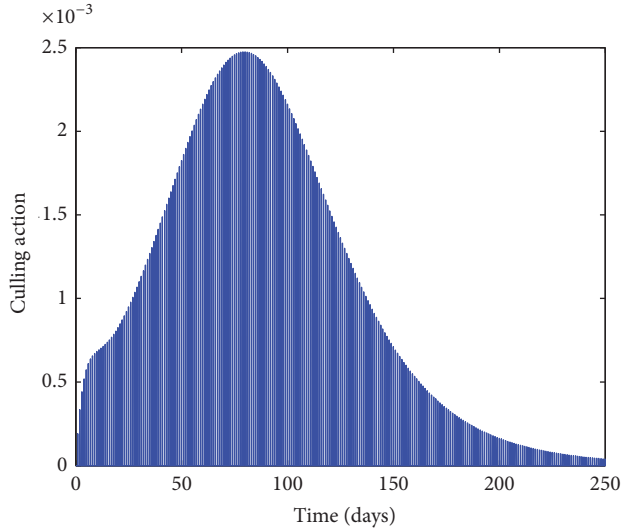

Figure 9: Culling effort $\rho_D D(t)$ with a daily culling rate of $\rho_D = 0.1$.

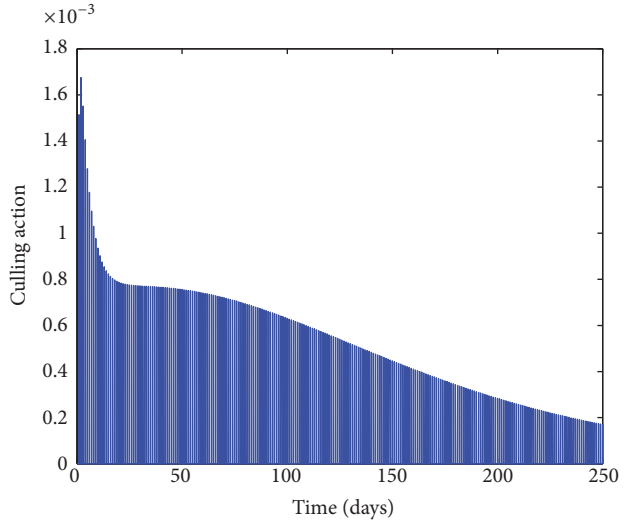

Figure 10: Culling effort $\rho_D D(t)$ with a daily culling rate of $\rho_D = 0.8$.

behavior of the system where the culling action has been applied. This result points out that it may be difficult to tune the constant vaccination term V_0 in order to obtain an appropriate behavior of the controlled system. The proposed feedback vaccination given by (7) in Section 2 contributes to solving this tuning problem since it relates the vaccination effort to the actual evolution of the system in such a way that the amplitude of vaccination is calculated based on the current value of susceptible. Thus, Figures 16 and 17 show the system evolution when a feedback vaccination with a constant of $K_V = 0.002$ is applied along with the constant vaccination term.

From Figures 12 and 16 we conclude that the feedback vaccination law calculated from the value of susceptible modifies significantly the behavior of the system while Figures 13 and 17 reveal that the total living population is largely improved by the action of feedback control. As a consequence, the main recommendation related to vaccination campaign design is to

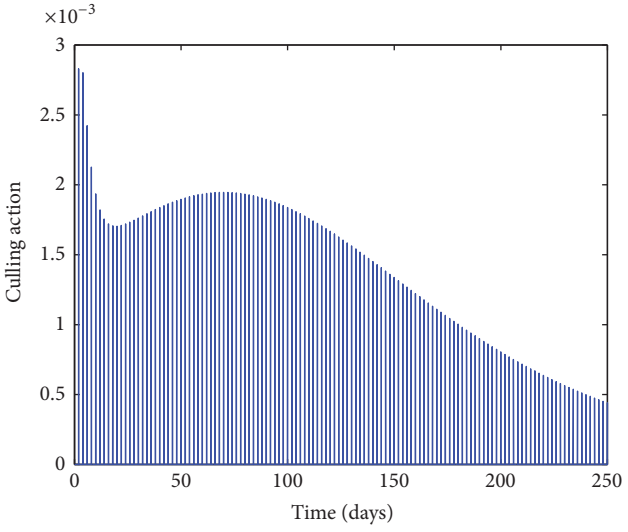

Figure 11: Culling effort $\rho_D D(t)$ with an every other culling rate of $\rho_D = 0.8$.

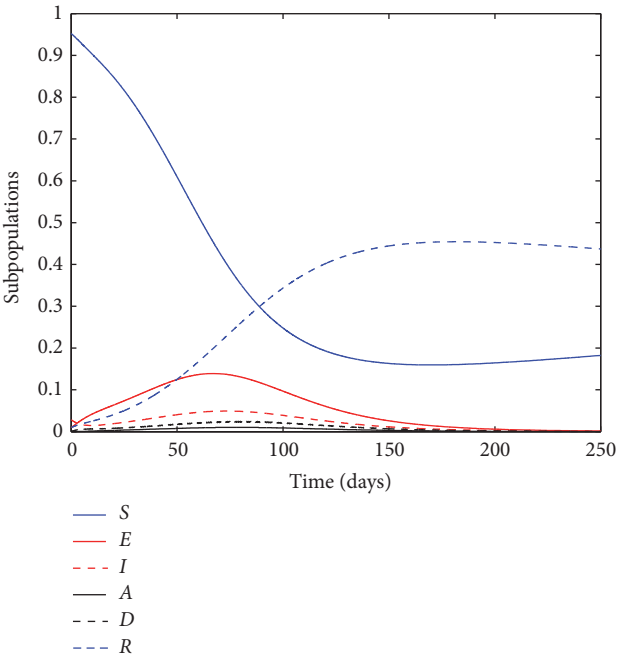

Figure 12: Evolution of the subpopulations with daily culling rate of $\rho_D = 0.1$ and constant vaccination of $V = V_0 = 0.2b_1$.

dynamically calculate the amount of vaccines to be applied by using the proposed feedback law (7). The vaccination control action is shown in Figure 18 while the culling effort corresponding to this case is depicted in Figure 19. It can be observed in Figure 19 that the culling action vanishes as a direct consequence of $D(t)$ tending to zero asymptotically. Therefore, the combination of culling and feedback vaccination allows stopping the mortality associated with the disease. Finally, we can also add antivirals to fight against Ebola. Antiviral action is given by (8) which is a feedback control law based on the symptomatic infectious subpopulation. In this case, we consider the constant linear value of $\xi(t) = K_\xi I(t) =$

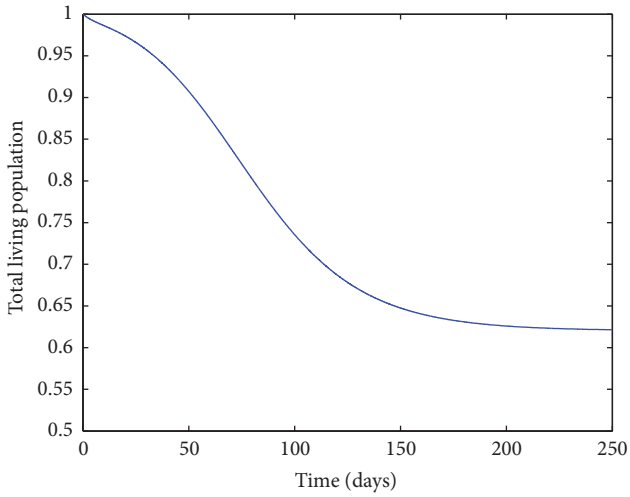

Figure 13: Evolution of the total alive population with daily culling rate of $\rho_D = 0.1$ and constant vaccination of $V = V_0 = 0.2b_1$.

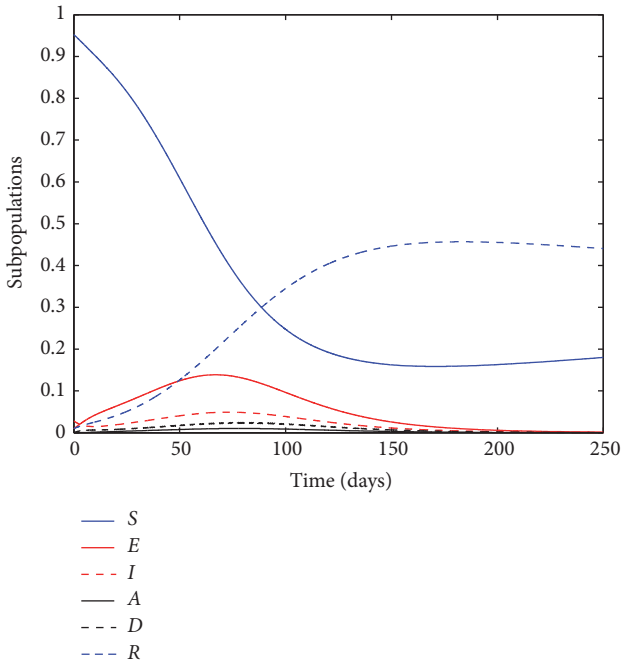

Figure 14: Evolution of the subpopulations with daily culling rate of $\rho_D = 0.1$ and constant vaccination of $V = V_0 = 0.8b_1$.

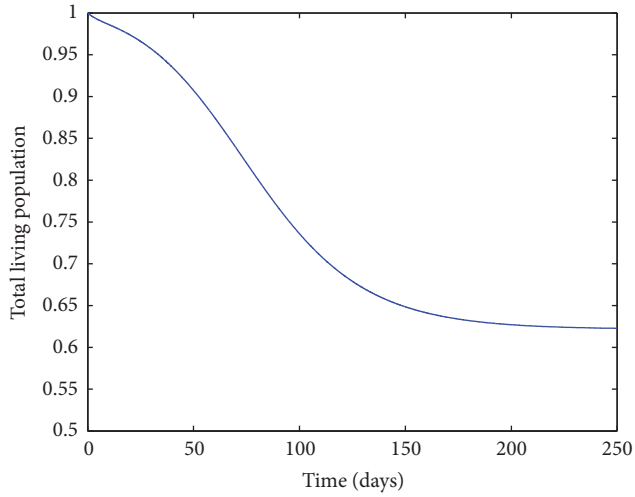

Figure 15: Evolution of the total alive population with daily culling rate of $\rho_D = 0.1$ and constant vaccination of $V = V_0 = 0.8b_1$.

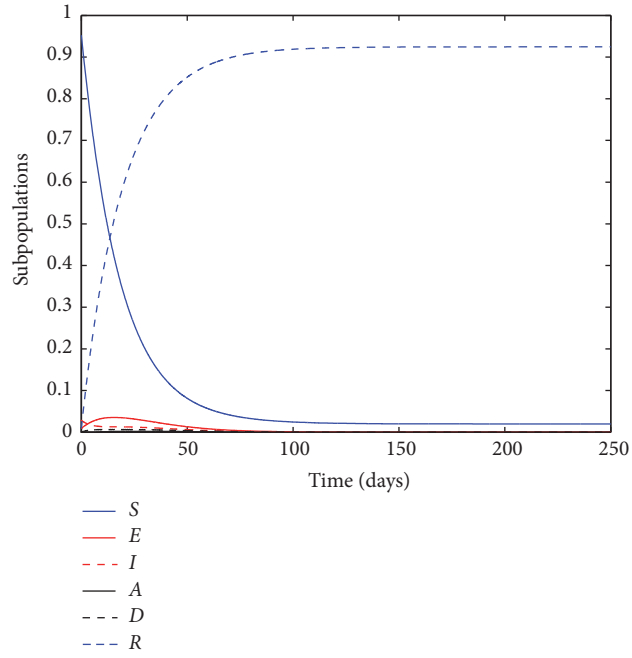

Figure 16: Evolution of the subpopulations with daily culling rate of $\rho_D = 0.1$ and feedback vaccination of $V = 0.2b_1 + 0.002S(t)$.

$0.01I(t)$ to show its effect on the system. Figures 20 and 21 show the combined effect of the three external actions.

From Figures 17 and 21 it is observed that the total living population is improved thanks to the use of antivirals while the deaths associated with the disease are stopped due to the use of the proposed approach. Moreover, it is now worth comparing the behavior of the natural system without any kind of external action with the evolution of the system when culling, vaccination, and antivirals are applied, especially Figures 2 and 21. After 250 days of epidemics, the total living population without any external action is of 56.47% while it is of 98.74% when the proposed dedicated policies are applied. These values show the great success in the application of control measurements to lessen the impact of epidemics in society. Moreover, Figures 22, 23, and 24 show the control efforts associated with each one of the therapies. It is shown that the culling and antiviral actions vanish asymptotically so that they are only applied for a limited period of time while vaccination needs to be maintained since it converges to a positive constant.

Figures 25–28 show the behaviors of the asymptomatic and lying infective corpses under a culling rate of $\rho_D = 0.1$. The oscillatory nature of the solution due to the impulsive culling action on infective corpses is better figured out in Figure 28 which is ran on longer observation time intervals.

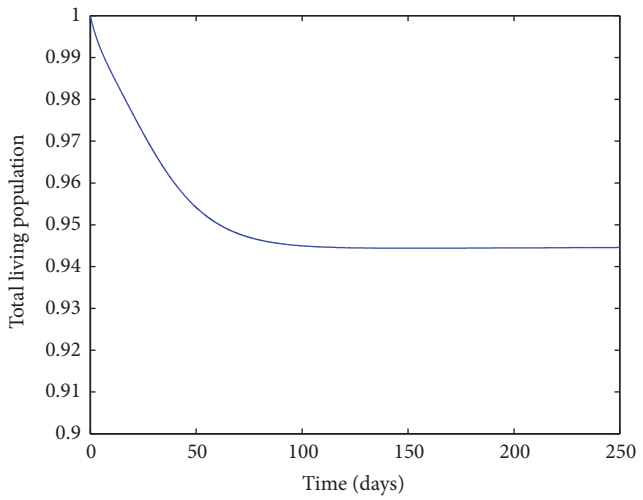

FIGURE 17: Evolution of the total alive population with daily culling rate of $\rho_D = 0.1$ and feedback vaccination of $V = 0.2b_1 + 0.002S(t)$.

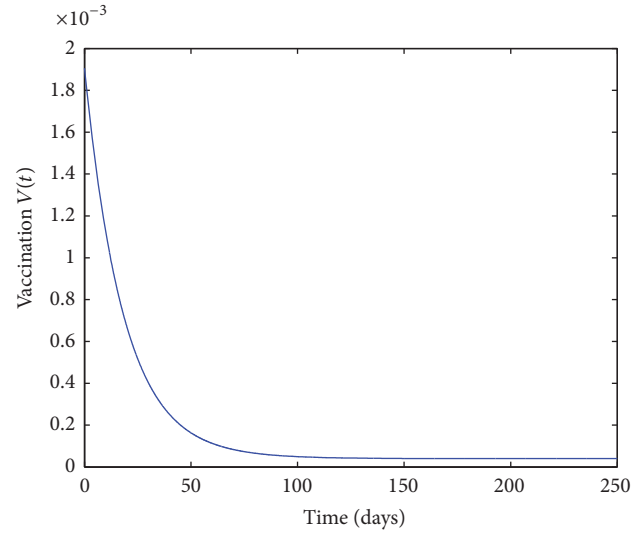

FIGURE 18: Vaccination function $V = 0.2b_1 + 0.002S(t)$ when a daily culling rate of $\rho_D = 0.1$ is also applied.

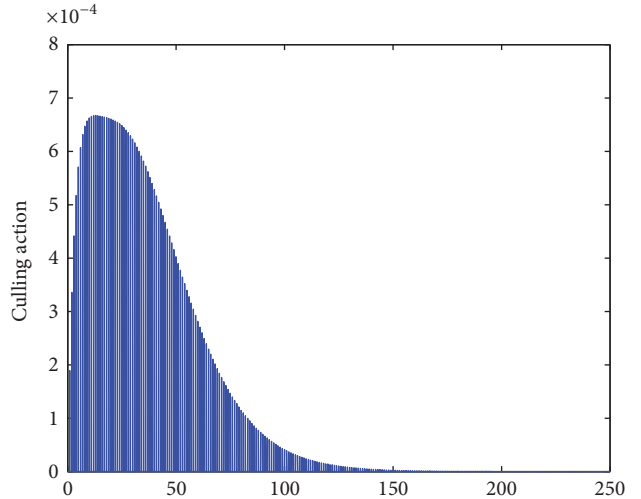

FIGURE 19: Culling effort $\rho_D D(t)$ when a daily culling rate of $\rho_D = 0.1$ and vaccination law $V = 0.2b_1 + 0.002S(t)$ are applied.

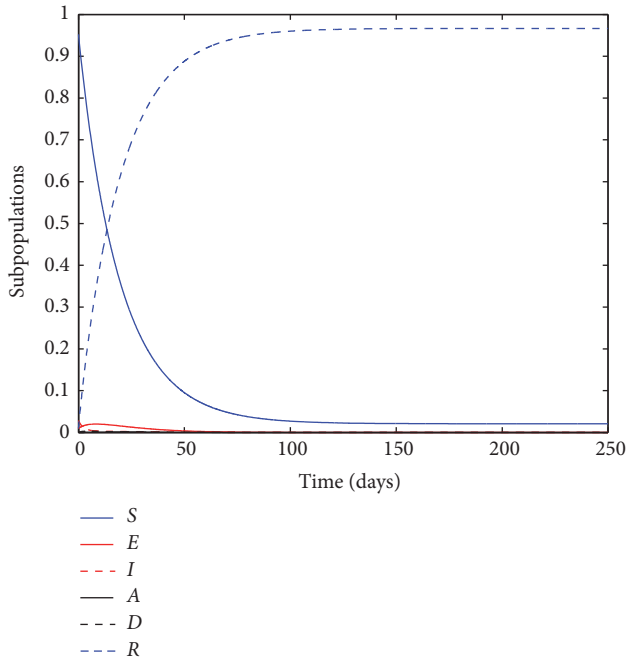

FIGURE 20: Evolution of the subpopulations with daily culling rate of $\rho_D = 0.1$, feedback vaccination $V = 0.2b_1 + 0.002S(t)$, and antiviral treatment $\xi(t) = K_\xi I(t) = 0.01I(t)$.

5. Conclusions

A new epidemic model is proposed with six subpopulations by incorporating the asymptomatic infectious and the dead corpses into a basic SEIR model of four subpopulations. The model is driven by three simultaneous controls in terms of a vaccination control on the susceptible which is based on linear time-varying feedback plus a constant term, an antiviral treatment on the symptomatic infectious subpopulation with infection feedback information, and a culling action of impulsive type on the infective dead corpses. The vaccination controls are combinations of feedback-independent (which can be constant, in particular) and feedback time-varying linear terms and the antiviral treatment control is of a time-varying linear feedback nature. There is also an impulsive time-dependent control action consisting of the retirement of corpses so as to reduce the risks of dead-contagion to the living uninfected population.

An identification and analysis of the endemic and disease-free equilibrium points and equilibrium oscillations are performed in the case that the control gains are constant. The equilibrium oscillations arise as a generalization of the equilibrium points when the dead corpses recovery action has a periodic nature. The parameterizations of those mentioned steady-state solutions are investigated as being dependent on the control gains as they converge to constant values. The local stability properties of the steady states and the global

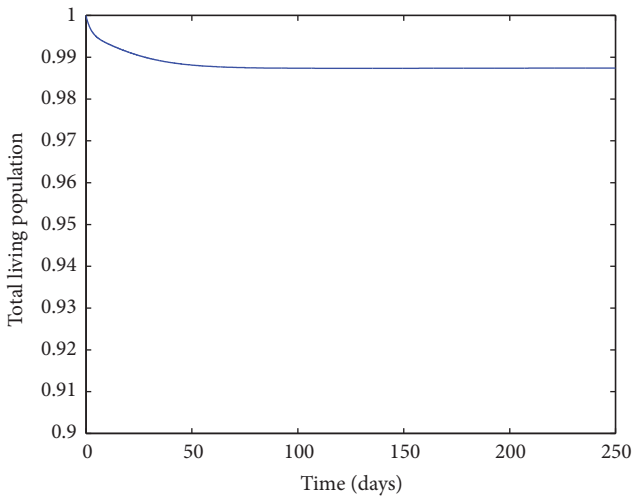

FIGURE 21: Evolution of the total alive population with daily culling rate of $\rho_D = 0.1$, feedback vaccination $V = 0.2b_1 + 0.002S(t)$, and antiviral treatment $\xi(t) = K_\xi I(t) = 0.01I(t)$.

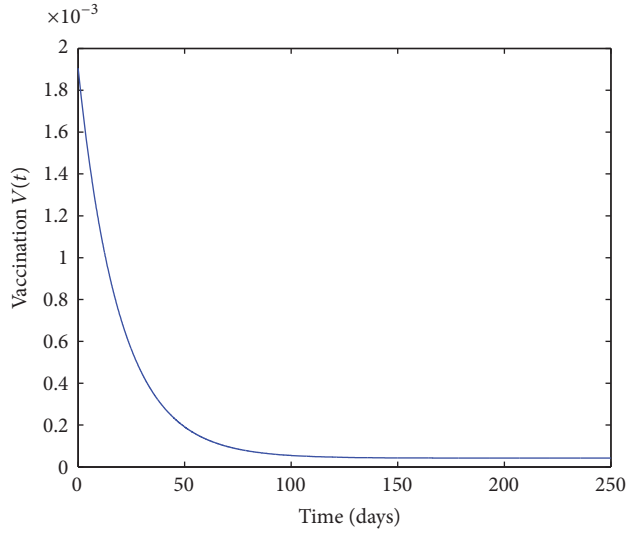

FIGURE 22: Vaccination function $V = 0.2b_1 + 0.002S(t)$ when a daily culling rate of $\rho_D = 0.1$ and antiviral treatment $\xi(t) = K_\xi I(t) = 0.01I(t)$ are applied.

stability are investigated. The main novelties of the paper are (a) the incorporation of the asymptomatic infectious subpopulation and dead corpses as extra subpopulations with study of their steady states being either equilibrium points or oscillations; (b) the design of three distinct controls on the above proposed extended SEIADR model which can be time varying and with feedback information on the susceptible, symptomatic infections and dead corpses; (c) the performance of the global stability analysis based on qualitative theory of differential equations rather than on the analysis of Lyapunov functionals; and (d) the emphasis, supported within a variety of performed simulations, that the infection evolution might be very sensitive to the corpses culling action (impulsive control) parameters.

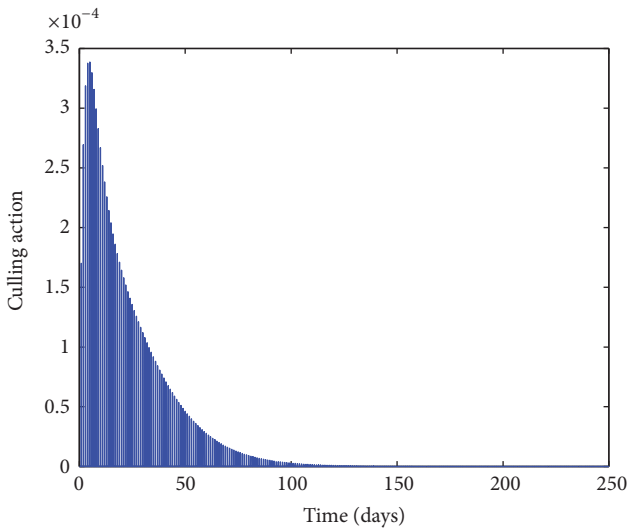

FIGURE 23: Culling effort $\rho_D D(t)$ when a daily culling rate of $\rho_D = 0.1$, vaccination law $V = 0.2b_1 + 0.002S(t)$ and antiviral treatment $\xi(t) = K_\xi I(t) = 0.01I(t)$ are applied.

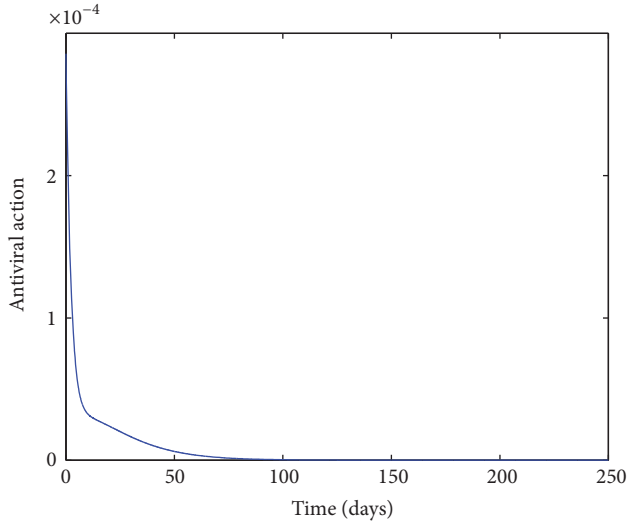

FIGURE 24: Antiviral action when a daily culling rate of $\rho_D = 0.1$, vaccination law $V = 0.2b_1 + 0.002S(t)$, and antiviral treatment $\xi(t) = K_\xi I(t) = 0.01I(t)$ are applied.

Appendix

Proof of Theorem 10. Rewrite (2) equivalently as

$$\begin{aligned}
&\dot{E}(t) - (\beta I(t) + \beta_A A(t) + \beta_D D(t)) S(t) \\
&\quad = F_1(E(t), I(t) + A(t)) = F_1(E(t), 0) \\
&\quad := -(b_2 + \gamma) E(t)
\end{aligned} \tag{A.1}$$

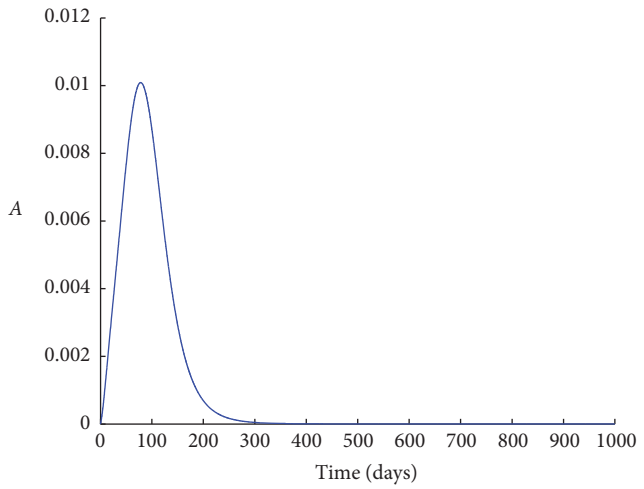

FIGURE 25: Evolution of the asymptomatic subpopulation with a daily culling rate of $\rho_D = 0.1$.

while one gets from (3), (4), and (8)

$$\begin{aligned}\dot{I}(t) + \dot{A}(t) + \left(\alpha + K_\xi^* + \widetilde{K}_\xi(t)\right) I(t) &= F_2(E(t), I(t) + A(t)) \\ &:= \gamma E(t) - (b_2 + \tau_0)(I(t) + A(t)),\end{aligned} \tag{A.2}$$

where $\widetilde{K}_\xi(t) = K_\xi(t) - K_\xi^*$. Note from (A.1)-(A.2) that $F_1(E(t), 0)$ and $F_2(E(t), I(t) + A(t))$ are continuous with continuous partial derivatives with respect to their arguments in any simply connected region $\mathbf{C}_{\text{int}}$ of $\mathbf{R}^2$

$$\begin{aligned}&\frac{\partial F_1(E(t), 0)}{\partial E(t)} + \frac{\partial F_2(E(t), I(t) + A(t))}{\partial (I(t) + A(t))} \\ &= -(2b_2 + \gamma + \tau_0) < 0; \quad \forall t \in \mathbf{R}_{0+}.\end{aligned} \tag{A.3}$$

Any such region $\mathbf{C}_{\text{int}}$ cannot contain a closed trajectory $\mathbf{C}$ (limit cycle) from Gauss-Stokes theorem since then

$$\begin{aligned}&\oint_{\mathbf{C}} \left[F_1(E(t), 0)\, d(I(t) + A(t)) - F_2(E(t), I(t) + A(t))\, dE(t)\right] \\ &= \iint_{\mathbf{C}_{\text{int}_\mathbf{C}}} \left(\frac{\partial F_1(E(t), 0)}{\partial E(t)} + \frac{\partial F_2(E(t), I(t) + A(t))}{\partial (I(t) + A(t))}\right) dE(t)\, d(I(t) + A(t)) < 0;\end{aligned} \tag{A.4}$$

from (A.3) if $\mathbf{C}_{\text{int}_\mathbf{C}}$ is the interior of the set defined by the simple curve $\mathbf{C}$, a contradiction, (Bendixson's criterion of nonexistence of limit cycles [34] or Bendixson's first theorem, implies that the above integral has to be null for closed trajectories) then it should hold $\dot{\overline{F}}_2(t) d\overline{F}_1(t) - \dot{\overline{F}}_1(t) d\overline{F}_2(t) = 0$ along the orbit $\mathbf{C}$ and this is impossible from (A.4), where

$$\begin{aligned}\overline{F}_1(t) &= E(t) - E(0) - \int_0^t \left(\beta I(\sigma) + \beta_A A(\sigma) + \beta_D D(\sigma)\right) S(\sigma)\, d\sigma \\ &= -(b_2 + \gamma) \int_0^t E(\sigma)\, d\sigma, \\ \overline{F}_2(t) &= I(t) + A(t) - I(0) - A(0) + \int_0^t \left(\alpha + K_\xi^* + \widetilde{K}_\xi(\sigma)\right) I(\sigma)\, d\sigma \\ &= \int_0^t \left(\gamma E(\sigma) - (b_2 + \tau_0)(I(\sigma) + A(\sigma))\right) d\sigma\end{aligned} \tag{A.5}$$

from (A.1)-(A.2). Since $\widetilde{K}_\xi(t) \to 0$ as $t \to \infty$ one has from (A.1) and (A.2) and (A.4) that

$$\begin{aligned}\lim_{t\to\infty} \Big[&\dot{I}(t) + \dot{A}(t) + \left(\alpha + K_\xi^*\right) I(t) \\ &- F_2(E(t), I(t) + A(t))\Big] = 0,\end{aligned} \tag{A.6}$$

$$\begin{aligned}\lim_{t\to\infty} \Big[&\dot{E}(t) - \left(\beta I(t) + \beta_A A(t) + \beta_D D(t)\right) S(t) \\ &- F_1(E(t), 0)\Big] = 0.\end{aligned} \tag{A.7}$$

Taking Laplace transforms in (A.6) by neglecting initial conditions and using (48), one gets from (A.6) that $\widehat{E}(s) = \widehat{F}_2(s)/((C_I + C_A)s + (\alpha + K_\xi^*)C_I)$, where the superscript "hat" denotes the Laplace transform in the Laplace argument "s" of $F_2(\cdot)$. Since $F_2(t)$ is not asymptotically periodic the Laplace antitransform of $\widehat{E}(s)$, that is, $E(t)$, is not asymptotically periodic from the above expression. Since $E(t)$ is not asymptotically periodic then $I(t)$ and $A(t)$ and $D(t)$ are not asymptotically periodic (note the assumption $\rho_D^* = 0$). On the other hand, one gets from (6) to (8) as $t \to \infty$, since $K_V(t) \to K_V^*$ and $K_\xi(t) \to K_\xi^*$ as $t \to \infty$ that

$$\begin{aligned}&\dot{R}(t) + (b_2 + \eta) R(t) - V_0 - K_V^* S(t) \\ &= \tau_0 A(t) + \left(\tau_0 + K_\xi^*\right) I(t)\end{aligned} \tag{A.8}$$

while summing up (1) and (6) by taking into account (2) and (48) yields

$$\begin{aligned}&\dot{S}(t) + \dot{R}(t) + b_2 (S(t) + R(t)) \\ &= -\dot{E}(t) + b_1 + \left(\tau_0 C_A + \left(\tau_0 + K_\xi^*\right) C_I - (b_2 + \gamma)\right) E(t).\end{aligned} \tag{A.9}$$

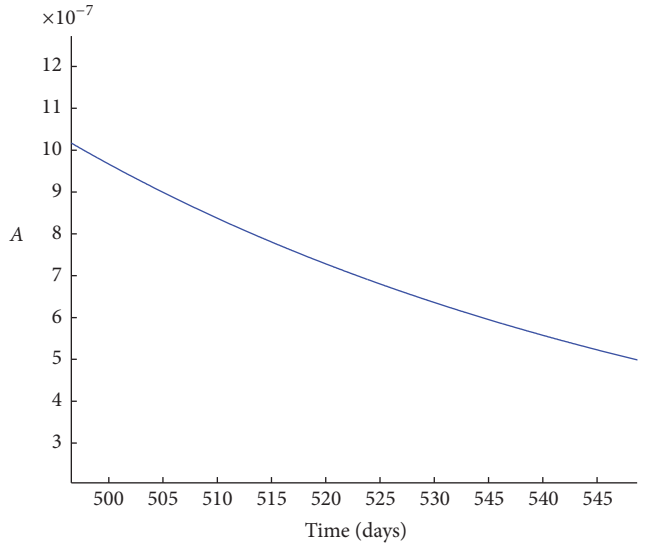

Figure 26: Zoom on the evolution of the asymptomatic subpopulation with a daily culling rate of $\rho_D = 0.1$.

Subtracting (A.8) from (A.9) and rewriting (A.9) in an equivalent form yields

$$\dot{S}(t) + \dot{E}(t) + (b_2 + \gamma) E(t) - b_1 + V_0 = F_3(S(t), R(t)) := -(b_2 + K_V^*) S(t) + \eta R(t), \quad \text{(A.10)}$$

$$\dot{S}(t) + \dot{R}(t) + \dot{E}(t) - b_1 + \left(b_2 + \gamma - \tau_0 C_A - \left(\tau_0 + K_\xi^*\right) C_I\right) E(t) = F_4(S(t), R(t)) := -b_2 (S(t) + R(t)), \quad \text{(A.11)}$$

$$\frac{\partial F_3(S(t), R(t))}{\partial S(t)} + \frac{\partial F_4(S(t), R(t))}{\partial R(t)} = -(2b_2 + K_V^*) < 0; \quad \forall t \in \mathbf{R}_{0+}. \quad \text{(A.12)}$$

Since $\text{sign}((\partial F_3(S(t), R(t)))/\partial S(t) + (\partial F_4(S(t), R(t)))/\partial R(t))$ is constant along state-trajectory solutions in $\mathbf{R}^2$, one has again that no closed trajectory (then no limit cycle) can exist surrounding any region with Poincaré's index +1. In view of (A.11)-(A.12), the functions $\dot{S}(t)+\dot{E}(t)+(b_2+\gamma)E(t)-b_1+V_0$ and $\dot{S}(t)+\dot{R}(t)+\dot{E}(t)-b_1+(b_2+\gamma-\tau_0 C_A-(\tau_0+K_\xi^*)C_I)E(t)$ are not asymptotically periodic. Since $E(t)$ and $\dot{E}(t)$ have been proved to be nonasymptotically periodic then $(\dot{S}(t)+\dot{R}(t))$, $\dot{S}(t)$, $\dot{R}(t)$, and then their time-integral solutions are not asymptotically periodic either.

The above arguments, together with the property of uniform boundedness of the total population and that of the nonnegativity of the solution, conclude that if only the disease-free equilibrium point exists while it is locally asymptotically stable then it is globally asymptotically stable as well since no limit cycle can exist around it in any plane in $\mathbf{R}_{0+}^2$ associated with any two of the state variables. On the other hand, assume that the endemic equilibrium state

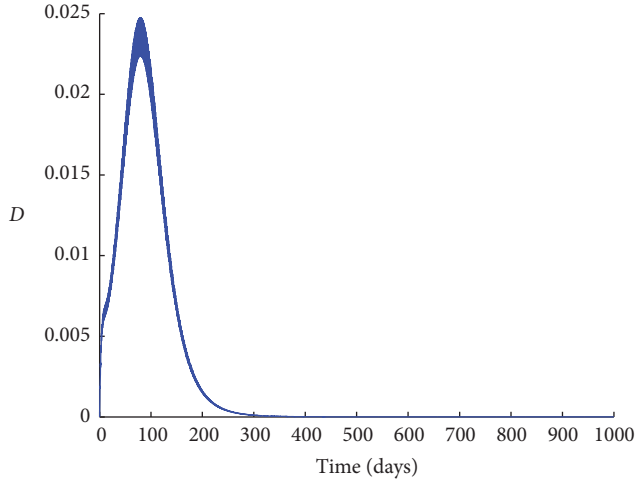

Figure 27: Evolution of the infective lying corpses with a daily culling rate of $\rho_D = 0.1$.

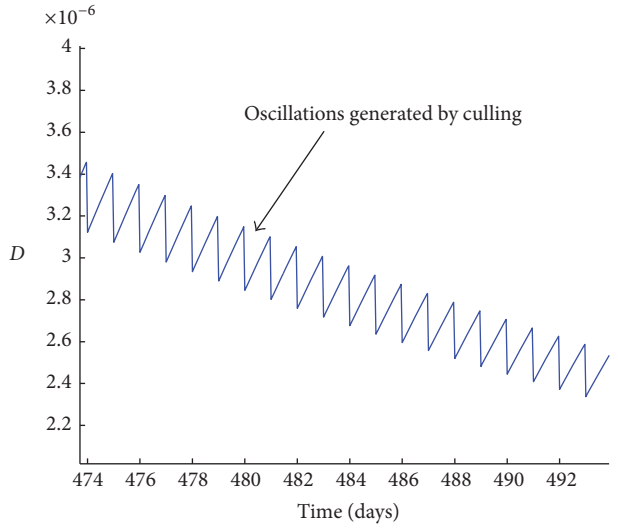

Figure 28: Zoom on the evolution of the infective corpses with a daily culling rate of $\rho_D = 0.1$.

is not a stable attractor while the disease-free is unstable. Then, an unstable limit cycle around it cannot exist from the above discussion (which excludes both stable and instable limit cycles) and, due to the nonnegativity of the solution and to the uniform boundedness of the whole population, then the trajectory converges asymptotically to it so that it is a stable attractor.

If the disease-free equilibrium point is unstable and the endemic equilibrium exists then the endemic equilibrium point is a stable attractor and the system is globally asymptotically stable with any state-trajectory solution converging to it.

Two other possible stability/instability combinations of the stability of both equilibrium states are excluded as follows leading to Property (ii):

(1) The case that both equilibrium states are simultaneously locally stable is excluded. Since there is no

closed trajectory solution then there is no semistable limit cycle separating the domains of attraction of both equilibrium states within the first orthant of $\mathbf{R}^6$.

(2) The case that both equilibrium states are simultaneously unstable is excluded as well since the system is globally stable if it is positive.

□

Competing Interests

The authors declare that they do not have any competing interests.

Authors' Contributions

All the authors contributed equally to all the parts of the manuscript.

Acknowledgments

This research is supported by the Spanish Government and the European Fund of Regional Development FEDER through Grant DPI2015-64766-R.

References

[1] D. Mollison, Ed., *Epidemic Models: Their Structure and Relation to Data*, Publications of the Newton Institute, Cambridge University Press, 1995, (transferred to digital printing 2003).

[2] M. J. Keeling and P. Rohani, *Modeling Infectious Diseases in Humans and Animals*, Princeton University Press, Princeton, NJ, USA, 2008.

[3] D. J. Daley and J. Gani, *Epidemic Modelling. An Introduction*, vol. 15 of *Cambridge Studies in Mathematical Biology*, Cambridge University Press, New York, NY, USA, 2005.

[4] H. Khan, R. N. Mohapatra, K. Vajravelu, and S. J. Liao, "The explicit series solution of SIR and SIS epidemic models," *Applied Mathematics and Computation*, vol. 215, no. 2, pp. 653–669, 2009.

[5] X. Song, Y. Jiang, and H. Wei, "Analysis of a saturation incidence SVEIRS epidemic model with pulse and two time delays," *Applied Mathematics and Computation*, vol. 214, no. 2, pp. 381–390, 2009.

[6] M. De la Sen, R. P. Agarwal, A. Ibeas, and S. Alonso-Quesada, "On the existence of equilibrium points, boundedness, oscillating behavior and positivity of a SVEIRS epidemic model under constant and impulsive vaccination," *Advances in Difference Equations*, vol. 2011, Article ID 748608, 2011.

[7] M. De la Sen, R. P. Agarwal, A. Ibeas, and S. Alonso-Quesada, "On a generalized time-varying SEIR epidemic model with mixed point and distributed time-varying delays and combined regular and impulsive vaccination," *Advances in Difference Equations*, vol. 2010, Article ID 281612, 2010.

[8] M. De la Sen and S. Alonso-Quesada, "Vaccination strategies based on feedback control techniques for a general SEIR-epidemic model," *Applied Mathematics and Computation*, vol. 218, no. 7, pp. 3888–3904, 2011.

[9] M. de la Sen, S. Alonso-Quesada, and A. Ibeas, "On the stability of an SEIR epidemic model with distributed time-delay and a general class of feedback vaccination rules," *Applied Mathematics and Computation*, vol. 270, pp. 953–976, 2015.

[10] Z. Fitriah and A. Suryanto, "Nonstandard finite difference scheme for SIRS epidemic model with disease- related death," in *Proceedings of the Symposium on Biomathematics (SYMOMATH '15)*, vol. 1723 of *AIP Conference Proceedings*, Bandung, Indonesia, 2015.

[11] J. P. Tripathi and S. Abbas, "Global dynamics of autonomous and nonautonomous SI epidemic models with nonlinear incidence rate and feedback controls," *Nonlinear Dynamics*, vol. 86, no. 1, pp. 337–351, 2016.

[12] Z. Wei and M. Le, "Existence and convergence of the positive solutions of a discrete epidemic model," *Discrete Dynamics in Nature and Society*, vol. 2015, Article ID 434537, 10 pages, 2015.

[13] X. Wang, "An SIRS epidemic model with vital dynamics and a ratio-dependent saturation incidence rate," *Discrete Dynamics in Nature and Society. An International Multidisciplinary Research and Review Journal*, vol. 2015, Article ID 720682, 9 pages, 2015.

[14] L. Wang, Z. Liu, and X. Zhang, "Global dynamics of an SVEIR epidemic model with distributed delay and nonlinear incidence," *Applied Mathematics and Computation*, vol. 284, pp. 47–65, 2016.

[15] F. Wei and F. Chen, "Stochastic permanence of an SIQS epidemic model with saturated incidence and independent random perturbations," *Physica A: Statistical Mechanics and Its Applications*, vol. 453, pp. 99–107, 2016.

[16] L. Shaikhet and A. Korobeinikov, "Stability of a stochastic model for HIV-1 dynamics within a host," *Applicable Analysis*, vol. 95, no. 6, pp. 1228–1238, 2016.

[17] L. Shaikhet, "Stability of equilibrium states for a stochastically perturbed exponential type system of difference equations," *Journal of Computational and Applied Mathematics*, vol. 290, pp. 92–103, 2015.

[18] R. Peng and F. Yi, "Asymptotic profile of the positive steady state for an SIS epidemic reaction-diffusion model: effects of epidemic risk and population movement," *Physica D. Nonlinear Phenomena*, vol. 259, pp. 8–25, 2013.

[19] R. Peng, "Asymptotic profiles of the positive steady state for an SIS epidemic reaction–diffusion model. Part I," *Journal of Differential Equations*, vol. 247, no. 4, pp. 1096–1119, 2009.

[20] B. Buonomo, D. Lacitignola, and C. Vargas-De-Leon, "Qualitative analysis and optimal control of an epidemic model with vaccination and treatment," *Mathematics and Computers in Simulation*, vol. 100, pp. 88–102, 2014.

[21] K. Mcculloch, M. G. Roberts, and C. R. Laing, "Exact analytical expressions for the final epidemic size of an SIR model on small networks," *The ANZIAM Journal*, vol. 57, no. 4, pp. 429–444, 2016.

[22] L. Ling, G. Jiang, and T. Long, "The dynamics of an SIS epidemic model with fixed-time birth pulses and state feedback pulse treatments," *Applied Mathematical Modelling*, vol. 39, no. 18, pp. 5579–5591, 2015.

[23] Y. He, S. Gao, and D. Xie, "An SIR epidemic model with time-varying pulse control schemes and saturated infectious force," *Applied Mathematical Modelling*, vol. 37, no. 16-17, pp. 8131–8140, 2013.

[24] S. Sharma and G. P. Samanta, "Stability analysis and optimal control of an epidemic model with vaccination," *International*

Journal of Biomathematics, vol. 8, no. 3, Article ID 1550030, 28 pages, 2015.

[25] G. P. Samanta, "A delayed hand-foot-mouth disease model with pulse vaccination strategy," *Computational and Applied Mathematics*, vol. 34, no. 3, pp. 1131–1152, 2015.

[26] M. R. de Pinho, I. Kornienko, and H. Maurer, "Optimal control of a SEIR model with mixed constraints and L^1 cost," in *CONTROLO '2014—Proceedings of the 11th Portuguese Conference on Automatic Control*, vol. 321 of *Lecture Notes in Electrical Engineering*, Springer, Basel, Switzerland, 2015.

[27] E. Santermans, E. Robesyn, T. Ganyani et al., "Spatiotemporal evolution of Ebola virus disease at sub-national level during the 2014 West Africa epidemic: model scrutiny and data meagreness," *PLoS ONE*, vol. 11, no. 1, Article ID e0147172, 2016.

[28] I. Al-Darabsah and Y. Yuan, "A time-delayed epidemic model for Ebola disease transmission," *Applied Mathematics and Computation*, vol. 290, pp. 307–325, 2016.

[29] S. E. Bellan, J. R. C. Pulliam, J. Dushoff, and L. A. Meyers, "Ebola control: effect of asymptomatic infection and acquired immunity," *The Lancet*, vol. 384, no. 9953, pp. 1499–1500, 2014.

[30] M. de la Sen, "Preserving positive realness through discretization," *Positivity*, vol. 6, no. 1, pp. 31–45, 2002.

[31] B. Xie, Z. Wang, Y. Xue, and Z. Zhang, "The dynamics of a delayed predator-prey model with double Allee effect," *Discrete Dynamics in Nature and Society*, vol. 2015, Article ID 102597, 8 pages, 2015.

[32] X. Wen, Y. Chen, and H. Yin, "Positive solutions of a diffusive predator-prey system including disease for prey and equipped with Dirichlet boundary condition," *Discrete Dynamics in Nature and Society*, vol. 2016, Article ID 2323752, 10 pages, 2016.

[33] J. M. Ortega, *Numerical Analysis*, Academic Press, New York, NY, USA, 1972.

[34] J. E. Gibson, *Nonlinear Automatic Control*, McGraw-Hill, New York, NY, USA, 1963.

Hindawi
Discrete Dynamics in Nature and Society
Volume 2017, Article ID 7571017, 9 pages
https://doi.org/10.1155/2017/7571017

Research Article

Global Dynamics and Optimal Control of a Viral Infection Model with Generic Nonlinear Infection Rate

Chenquan Gan,[1,2] Maobin Yang,[1] Zufan Zhang,[1] and Wanping Liu[1,2]

[1]*School of Communication and Information Engineering, Chongqing University of Posts and Telecommunications, Chongqing 400065, China*
[2]*College of Computer Science and Engineering, Chongqing University of Technology, Chongqing 400054, China*

Correspondence should be addressed to Wanping Liu; lwphe@163.com

Received 16 October 2016; Revised 5 December 2016; Accepted 25 December 2016; Published 13 February 2017

Academic Editor: Jose R. C. Piqueira

Copyright © 2017 Chenquan Gan et al. This is an open access article distributed under the Creative Commons Attribution License, which permits unrestricted use, distribution, and reproduction in any medium, provided the original work is properly cited.

This paper is devoted to exploring the combined impact of a generic nonlinear infection rate and infected removable storage media on viral spread. For that purpose, a novel dynamical model with an external compartment is proposed, and the explanations of the main model assumptions (especially the generic nonlinear infection rate) are also examined. The existence and global stability of the unique equilibrium of the model are fully investigated, from which it can be seen that computer virus would persist. On this basis, a next-best approach to controlling the level of infected computers is suggested, and the theoretical analysis of optimal control of the model is also performed. Additionally, some numerical examples are given to illustrate the main results.

1. Introduction

In the wake of developments in computer and network technologies, computer virus has become more capable of conquering computer system. In the meantime, the study of fighting against computer virus has in the past few decades been paid more attention. In reality, there is no doubt that antivirus software and firewall are the most effective prevention measures. However, they are incompetent to inhibit computer virus diffusion over the Internet [1]. To deal with this problem, a wide variety of mathematical models have been widely studied (for the related references, see, e.g., [2–15]).

The infection rate is an important and essential system parameter in computer virus propagation models. However, the dominating majority of previous models assume a bilinear incidence rate (for the related references, see, e.g., [16–20]) or a nonlinear increasing incidence rate (for the related references, see, e.g., [21]). The former assumption is suitable for the case where the proportion of infected computers is small. The latter assumption neglects the fact that, due to active protection measures taken during viral spread, the infection rate would be decreasing, while the infected computers may be increasing. In order to depict the case where the infection rate could be decreasing with the infected computers and inspired by the previous work (e.g., [22, 23]), the proposed model of this paper adopts a nonlinear function $\sigma(I) = \beta I/f(I)$, where $\beta > 0$ and function $f \in C^2[0, +\infty)$ with $f' \geq 0$, $f'' < 0$, and $f(0) = 1$ (see also the model assumption (A3) in the next section).

External computers (i.e., computers outside the Internet) and infected removable storage media play an important role in viral spread (for the related references, see, e.g., [24, 25]). In [24], the impact of infected removable storage media is considered, but the influence of external computers is insufficient. In [25], a dynamical model, in which all external computers are regarded as a separate compartment, was proposed. Unfortunately, this model ignores the effects of generic nonlinear infection rate and infected removable storage media. Consequently, it is necessary to consider the combined impact of a generic nonlinear infection rate and infected removable storage media on viral spread.

In addition, optimal control theory is often applied to control virus prevalence (for the related references, see, e.g., [14, 26–28]). In [14, 27], a susceptible-latent-breaking-outside-susceptible (SLBOS) model and a susceptible-latent-breaking-susceptible (SLBS) model were studied,

respectively. References [26, 28] considered a susceptible-infected-recovered-susceptible (SIRS) model in a fully connected network and a complex network, respectively. To our knowledge, there is no susceptible-infected-external-susceptible (SIES) model that has been examined by applying optimal control theory.

Combining the above discussions, a novel SIES model with two kinds of incidence rates, which are caused by infected computers and infected removable storage media, is established in this paper. A systematic analysis of the proposed model shows that the unique (viral) equilibrium is globally asymptotically stable. This result indicates that any effort in eradicating computer virus cannot succeed. In this regard, theoretical analysis of a next-best approach and optimal control of the model is performed. Numerical analysis of the model is also included.

The remaining materials of this paper are organized as follows: Section 2 formulates the model. Section 3 considers the viral equilibrium and its global stability. In Section 4, a theoretical analysis of optimal control of the model is performed. Finally, Section 5 concludes the contributions of this work and points out some further works that are worth doing.

2. Model Characterization

In this paper, the proposed model consists of three compartments (see (i)–(iii)), and the assumptions of it are also made (see (A1)–(A8)):

(i) S-compartment: the set of all S-computers (susceptible internal computers, i.e., computers in the Internet)

(ii) I-compartment: the set of all I-computers (infected internal computers)

(iii) E-compartment: the set of all E-computers (external computers, i.e., computers outside the Internet)

(A1) Every computer is out of use with probability per unit time $\mu > 0$

(A2) Every S- or I-computer leaves the Internet with probability per unit time $\gamma_1 > 0$

(A3) Due to possible communication with I-computers over the Internet, every S-computer is infected with probability per unit time $\sigma(I) = \beta I/f(I)$, where $\beta > 0$ and function $f \in C^2[0, +\infty)$ with $f' \geq 0$, $f'' < 0$, and $f(0) = 1$

(A4) Due to possible effect of infected removable storage media, every S-computer is infected with probability per unit time $\theta \geq 0$

(A5) Due to treatment, every I-computer is cured with probability per unit time $\gamma_2 > 0$

(A6) The rate of all newly accessed E-computers is $\delta > 0$

(A7) Every E-computer is either susceptible or infected when it enters the Internet

(A8) Every susceptible (or infected) E-computer enters the Internet with probability per unit time $\eta_2 > 0$ (or $\eta_1 > 0$)

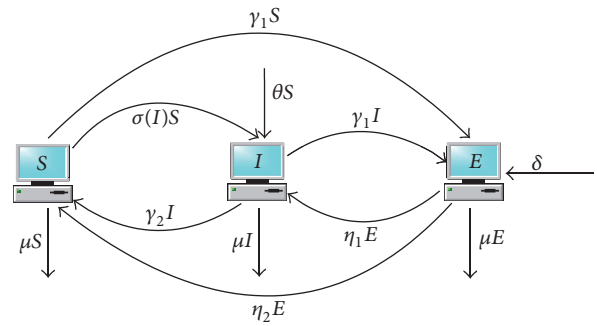

Figure 1: The transfer diagram of the proposed model.

For convenience, let S, I, and E represent the average number of computers in S-compartment, I-compartment, and E-compartment at time t, respectively. Collecting the foregoing hypotheses, the proposed model can be depicted by Figure 1 or the differential system

$$\begin{aligned} \dot{S} &= \gamma_2 I + \eta_2 E - \mu S - \sigma(I) S - \gamma_1 S - \theta S, \\ \dot{I} &= \sigma(I) S + \theta S - \mu I - \gamma_1 I - \gamma_2 I + \eta_1 E, \\ \dot{E} &= \delta + \gamma_1 S + \gamma_1 I - \mu E - \eta_1 E - \eta_2 E, \end{aligned} \tag{1}$$

with initial condition $(S(0), I(0), E(0)) \in R^3_+$.

3. Model Analysis

Let $N = S + I + E$. System (1) can be rewritten as

$$\begin{aligned} \dot{N} &= \delta - \mu N, \\ \dot{I} &= \sigma(I)(N - I - E) + \theta(N - I - E) - \mu I - \gamma_1 I \\ &\quad - \gamma_2 I + \eta_1 E, \\ \dot{E} &= \delta + \gamma_1 N - \gamma_1 E - \mu E - \eta_1 E - \eta_2 E, \end{aligned} \tag{2}$$

with initial condition $(N(0), I(0), E(0)) \in R^3_+$.

Let $N^* = \delta/\mu$ and $E^* = \delta(\mu + \gamma_1)/\mu(\mu + \gamma_1 + \eta_1 + \eta_2)$. Solving the first and third equations of system (2), we get $\lim_{t\to+\infty} N(t) = N^*$ and $\lim_{t\to+\infty} E(t) = E^*$. System (2) can be reduced to the limiting system [29]

$$\dot{I} = \sigma(I)(A - I) - (\mu + \gamma_1 + \gamma_2 + \theta) I + B, \tag{3}$$

where $A = N^* - E^* = \delta(\eta_1 + \eta_2)/\mu(\mu + \gamma_1 + \eta_1 + \eta_2) > 0$ and $B = \eta_1 E^* + \theta A > 0$.

Clearly, system (3) has no virus-free equilibrium. Thus, this section mainly addresses the existence and global stability of viral equilibrium of system (3) with respect to positively invariant region: $\Omega = \{I \mid 0 \leq I \leq N^*\}$.

3.1. Equilibrium

Theorem 1. *System (3) has a unique viral equilibrium I^*, where I^* is the unique root in $(0, N^*)$ of the equation*

$$F(x) = \sigma(x)(A - x) - (\mu + \gamma_1 + \gamma_2 + \theta) x + B = 0. \tag{4}$$

Proof. If I^* is a viral equilibrium of system (3), then it satisfies (4). Now, it suffices to show that (4) has a unique root in $(0, N^*)$. As $\sigma(x) = \beta x/f(x)$ and $\sigma'(x) = \beta((f(x) - xf'(x))/f^2(x))$, we proceed by treating two possibilities.

Case 1. $f(x) - xf'(x) \le 0$; namely, $\sigma'(x) \le 0$. Note that

$$\begin{aligned} F(0) &= B > 0, \\ F(A) &= B - (\mu + \gamma_1 + \gamma_2 + \theta) A \\ &= -\frac{\delta(\eta_2(\mu + \gamma_1 + \gamma_2) + \gamma_2\eta_1)}{\mu(\mu + \gamma_1 + \eta_1 + \eta_2)} < 0, \\ F'(x) &= \beta\frac{(A - 2x) f(x) - (A - x) xf'(x)}{f^2(x)} \\ &\quad - (\mu + \gamma_1 + \gamma_2 + \theta) \\ &= \beta\frac{A(f(x) - xf'(x)) - x[2f(x) - xf'(x)]}{f^2(x)} \\ &\quad - (\mu + \gamma_1 + \gamma_2 + \theta). \end{aligned} \tag{5}$$

Let $G(x) = 2f(x) - xf'(x)$; then $G(0) = 2f(0) > 0$. $f(x) - xf'(x) \le 0$, $f' \ge 0$; $f'' < 0$ implies that $G'(x) = f'(x) - xf''(x) > 0$. Hence, $G(x) > 0$; $F'(x) < 0$ implies that $F(x)$ has a unique root in $(0, N^*)$.

Case 2. $f(x) - xf'(x) > 0$; namely, $\sigma'(x) > 0$. Let

$$\begin{aligned} F_1(x) &= \frac{f(x)}{x} F(x) \\ &= \beta(A - x) + B\frac{f(x)}{x} - (\mu + \gamma_1 + \gamma_2 + \theta) f(x) \\ &= 0. \end{aligned} \tag{6}$$

Then,

$$\begin{aligned} F_1(0^+) &= \lim_{x \to 0^+} F_1(x) = +\infty > 0, \\ F_1(A) &= B\frac{f(A)}{A} - (\mu + \gamma_1 + \gamma_2 + \theta) f(A) < 0, \\ F_1'(x) &= -\beta + B\frac{xf'(x) - f(x)}{x^2} \\ &\quad - (\mu + \gamma_1 + \gamma_2 + \theta) f'(x) < 0. \end{aligned} \tag{7}$$

Thus, $F(x)$ has a unique root in $(0, N^*)$. The claimed result follows by the above discussions. □

Remark 2. It follows from the above proof that $0 < I^* < A$.

3.2. Global Stability

Theorem 3. *I^* is globally asymptotically stable with respect to Ω.*

Proof. Consider the Lyapunov function

$$V = \int_I^{I^*} \frac{u - I^*}{u} du. \tag{8}$$

Then,

$$\begin{aligned} \dot{V}\big|_{(3)} &= \frac{I - I^*}{I} [\sigma(I)(A - I) - (\mu + \gamma_1 + \gamma_2 + \theta) I + B] \\ &= \frac{I - I^*}{I} [\sigma(I)(A - I) - \sigma(I^*)(A - I^*) \\ &\quad - (\mu + \gamma_1 + \gamma_2 + \theta)(I - I^*)] \\ &= \frac{I - I^*}{I} [(A - I^*)(\sigma(I) - \sigma(I^*)) - \sigma(I)(I - I^*) \\ &\quad - (\mu + \gamma_1 + \gamma_2 + \theta)(I - I^*)] \\ &= \frac{(I - I^*)^2}{I} \left[(A - I^*)\frac{\sigma(I) - \sigma(I^*)}{I - I^*} - \sigma(I) \right. \\ &\quad \left. - (\mu + \gamma_1 + \gamma_2 + \theta)\right]. \end{aligned} \tag{9}$$

Here, we proceed by treating two cases.

Case 1. If $\sigma'(I) \le 0$, namely, $f(I) - If'(I) \le 0$, then it follows from the Lagrange mean value theorem that $(\sigma(I) - \sigma(I^*))/(I - I^*) = \sigma'(\xi) \le 0$, $\xi \in (I, I^*)$, or $\xi \in (I^*, I)$. As $A - I^* = N^* - E^* - I^* > 0$, $\dot{V}|_{(3)} \le 0$ and $\dot{V}|_{(3)} = 0$ if and only if $I = I^*$. Thus, the claimed result follows from LaSalle's Invariance Principle [30].

Case 2. If $\sigma'(I) > 0$, namely, $f(I) - If'(I) > 0$, let

$$\begin{aligned} H(I) &= (A - I^*)\frac{\sigma(I) - \sigma(I^*)}{I - I^*} - \sigma(I) \\ &\quad - (\mu + \gamma_1 + \gamma_2 + \theta). \end{aligned} \tag{10}$$

Then,

$$\begin{aligned} H(0) &= (A - I^*)\frac{\sigma(I^*)}{I^*} - (\mu + \gamma_1 + \gamma_2 + \theta) = -\frac{B}{I^*} \\ &< 0, \\ H'(I) &= (A - I^*)\frac{\sigma'(I)(I - I^*) - [\sigma(I) - \sigma(I^*)]}{(I - I^*)^2} \\ &\quad - \sigma'(I). \end{aligned} \tag{11}$$

Next, we need to further distinguish two subcases.

Subcase 2.1. If $I > I^*$, it follows from the Lagrange mean value theorem that $\sigma(I) - \sigma(I^*) = \sigma'(\zeta)(I - I^*)$, $\zeta \in (I^*, I)$. As $f'' < 0$, $\sigma'' < 0$. Then, for $\epsilon \in (\zeta, I)$,

$$\begin{aligned} H'(I) &= (A - I^*)\frac{\sigma'(I) - \sigma'(\zeta)}{I - I^*} - \sigma'(I) \\ &= (A - I^*)\frac{\sigma''(\epsilon)(I - \zeta)}{I - I^*} - \sigma'(I) < 0. \end{aligned} \tag{12}$$

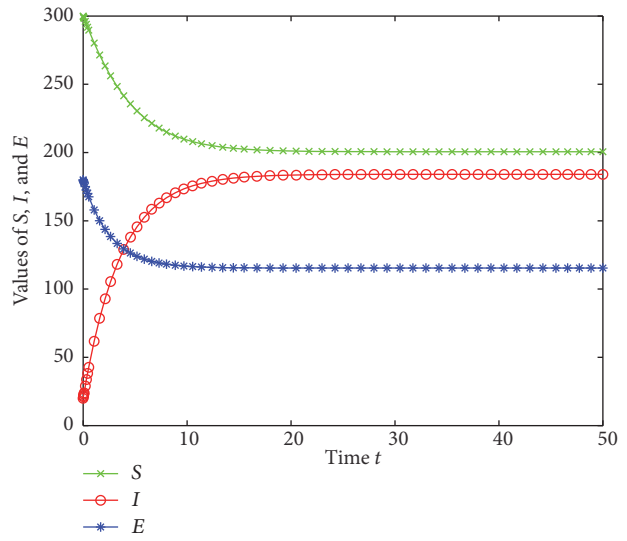

Figure 2: Time plots of $S(t)$, $I(t)$, and $E(t)$ for system (1) given in Example 4.

Subcase 2.2. If $I \le I^*$, it follows from the Lagrange mean value theorem that $\sigma(I) - \sigma(I^*) = \sigma'(\varepsilon)(I - I^*)$, $\varepsilon \in (I, I^*)$. As $f'' < 0, \sigma'' < 0$. Then, for $\varsigma \in (I, \varepsilon)$,

$$H'(I) = (A - I^*)\frac{\sigma'(I) - \sigma'(\varepsilon)}{I - I^*} - \sigma'(I) = (A - I^*)\frac{\sigma''(\varsigma)(I - \varepsilon)}{I - I^*} - \sigma'(I) < 0. \tag{13}$$

It follows from (12)-(13) that $H(I) \le H(0) < 0$. Thus, $\dot{V}|_{(3)} \le 0$. Furthermore, $\dot{V}|_{(3)} = 0$ if and only if $I = I^*$. The claimed result also follows from LaSalle's Invariance Principle [30]. The proof is complete. □

Example 4. Consider system (1) with $\delta = 5$, $\mu = 0.01$, $\eta_1 = 0.1$, $\eta_2 = 0.2$, $\gamma_1 = 0.08$, $\gamma_2 = 0.08895$, $\theta = 0.01$, and $\sigma(I) = 0.04487I/(1 + \sqrt{I})$. Figure 2 displays the time plot of this system with initial condition $(S(0), I(0), E(0)) = (300, 20, 180)$. From Figure 2, the values of $S(t)$, $I(t)$, and $E(t)$ tend to a constant, respectively. Furthermore, $I(t)$ tends to a positive constant. This shows that I^* is globally asymptotically stable.

Remark 5. Theorem 3 reveals that $I(t)$ tends to a positive constant I^*. From an epidemiological standpoint, it indicates that computer virus would persist in network. Thus, one can conclude that any effort in eradicating computer virus is doomed to failure. Thus, the best achievable goal is to make the number of infected computers below an acceptable level (i.e., as low as possible). Note that I^* cannot be expressed in a specific formula, and it follows from Remark 2 that $0 < I^* < A$. Then, one could keep the value of A below an acceptable threshold. To this end, the following result is made.

Theorem 6. *From Equation (3),* $A = \delta(\eta_1 + \eta_2)/\mu(\mu + \gamma_1 + \eta_1 + \eta_2)$. *Then* $\partial A/\partial\mu < 0$, $\partial A/\partial\gamma_1 < 0$, $\partial A/\partial\delta > 0$, $\partial A/\partial\eta_1 > 0$, *and* $\partial A/\partial\eta_2 > 0$.

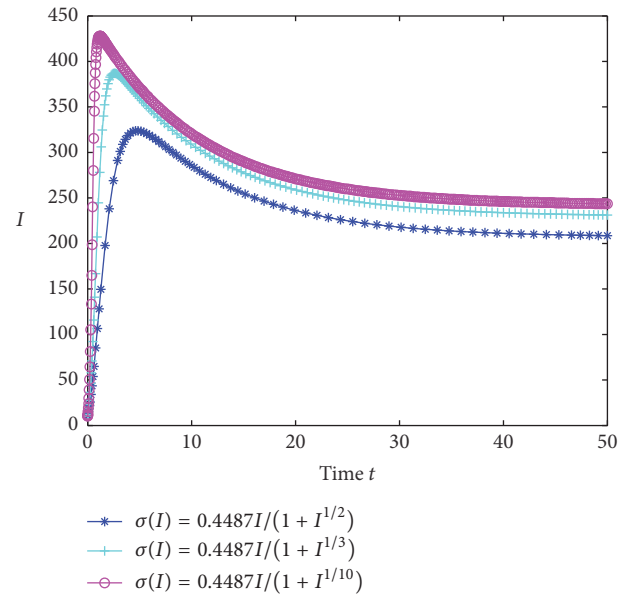

Figure 3: An illustration of the impact of $\sigma(I)$ on $I(t)$ for system (1) given in Example 8.

Proof. Since $A = \delta(\eta_1 + \eta_2)/\mu(\mu + \gamma_1 + \eta_1 + \eta_2)$, then

$$\frac{\partial A}{\partial \mu} = -\frac{\delta(\eta_1 + \eta_2)(2\mu + \gamma_1 + \eta_1 + \eta_2)}{\mu^2(\mu + \gamma_1 + \eta_1 + \eta_2)^2} < 0,$$

$$\frac{\partial A}{\partial \gamma_1} = -\frac{\delta(\eta_1 + \eta_2)}{\mu(\mu + \gamma_1 + \eta_1 + \eta_2)^2} < 0,$$

$$\frac{\partial A}{\partial \delta} = \frac{\eta_1 + \eta_2}{\mu(\mu + \gamma_1 + \eta_1 + \eta_2)} > 0, \tag{14}$$

$$\frac{\partial A}{\partial \eta_1} = \frac{\delta(\mu + \gamma_1)}{\mu(\mu + \gamma_1 + \eta_1 + \eta_2)^2} > 0,$$

$$\frac{\partial A}{\partial \eta_2} = \frac{\delta(\mu + \gamma_1)}{\mu(\mu + \gamma_1 + \eta_1 + \eta_2)^2} > 0.$$

Thus, the proof is complete. □

Remark 7. Theorem 6 implies the effects of some system parameters on the value of A.

In addition, the following two examples exhibit the impacts of $\sigma(I)$ and θ on I, respectively.

Example 8. Consider system (1) with $\delta = 5$, $\mu = 0.01$, $\eta_1 = 0.01$, $\eta_2 = 0.04$, $\gamma_1 = 0.04$, $\gamma_2 = 0.08895$, and $\theta = 0.01$. Figure 3 demonstrates the time plot of this system with initial condition $(S(0), I(0), E(0)) = (450, 10, 40)$.

Example 9. Consider system (1) with $\delta = 5$, $\mu = 0.01$, $\eta_1 = 0.04$, $\eta_2 = 0.08$, $\gamma_1 = 0.08$, $\gamma_2 = 0.08895$, and $\sigma(I) = 0.004487I/(1+\sqrt{I})$. Figure 4 shows the time plot of this system with initial condition $(S(0), I(0), E(0)) = (450, 10, 40)$.

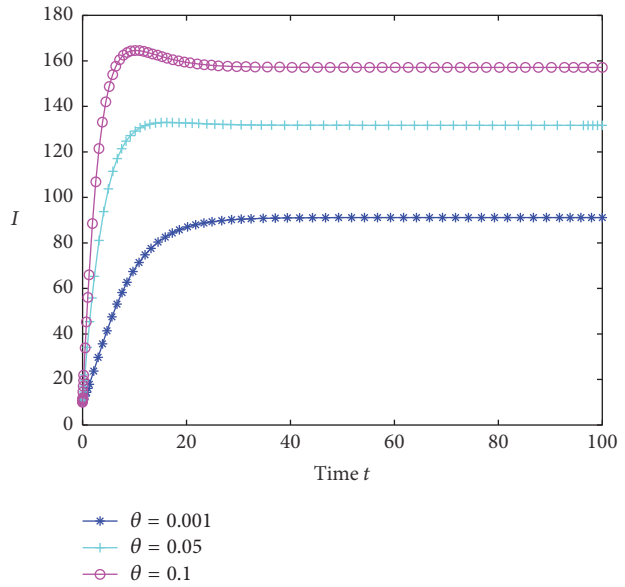

FIGURE 4: An illustration of the impact of θ on $I(t)$ for system (1) given in Example 9.

Figures 3 and 4 show the effects of different infection rates and infected removable media on virus diffusion, respectively.

4. Optimal Control of the Model

To make a tradeoff between control cost and control effect, the control variable $u(t)$ meaning the control strategy is applied in the proposed model (system (1)). Then, one can get the controlled dynamical system

$$\begin{aligned}\dot{S} &= \gamma_2 I + \eta_2 E - \mu S - \sigma(I) S - \gamma_1 S - \theta S,\\ \dot{I} &= \sigma(I) S + \theta S - \mu I - \gamma_1 I - u(t) I + \eta_1 E,\\ \dot{E} &= \delta + \gamma_1 S + \gamma_1 I - \mu E - \eta_1 E - \eta_2 E,\end{aligned} \tag{15}$$

with initial condition $(S(0), I(0), E(0))^T \in \Omega'$, where

$$\Omega' = \left\{(S, I, E)^T \in R_+^3 \mid S + I + E \le \frac{\delta}{\mu}\right\}. \tag{16}$$

The admissible control set is

$$U = \left\{u(\cdot) \in L^2[0, T] \mid \underline{\gamma_2} \le u(\cdot) \le \overline{\gamma}_2\right\}, \tag{17}$$

where $\underline{\gamma_2}$ and $\overline{\gamma}_2$ are positive constants and $0 < \underline{\gamma_2} < \overline{\gamma}_2 < 1$.

Let $\mathbf{x}(t) = (S(t), I(t), E(t))^T$. Then system (15) can be written in matrix notation as

$$\frac{d\mathbf{x}(t)}{dt} = \mathbf{f}(\mathbf{x}(t), u(t)), \quad 0 \le t \le T, \tag{18}$$

with initial condition $\mathbf{x}(0) \in \Omega'$.

Now, the objective is to find a control variable $u(\cdot)$ so as to minimize both the number of infected computers and the total budget for treatment and vaccination during the time period $[0, T]$. That is, it suffices to solve the optimal control problem.

$$\text{Minimize}_{u(\cdot)\in U} \quad J(u(\cdot)) = \int_0^T L(\mathbf{x}(t), u(t))\, dt \tag{19}$$

subject to system (18), where

$$L(\mathbf{x}, u) = I + \frac{\epsilon u^2}{2} \tag{20}$$

is the Lagrangian and $\epsilon > 0$ is a tradeoff factor based on the control cost and control effect.

Theorem 10. *The optimal control problem (19) has an optimal control.*

Proof. From equations (19) and (20), one can get that

(1) there exist $u(\cdot) \in U$ such that system (18) is solvable,

(2) the admissible control set U is convex and closed,

(3) the right-hand side of system (18) is bounded by a linear function in $\mathbf{x}$,

(4) $L(\mathbf{x}, u)$ is convex on U,

(5) there exist $\rho = 2$, $c_1 = \epsilon/2$, and $c_2 = 0$ such that $L(\mathbf{x}, u) \ge (\epsilon/2)\|u\|_2^2$.

Thus, the claimed result follows directly from [31]. □

Theorem 11. *Suppose $\widetilde{u}(\cdot)$ is an optimal control for the optimal control problem (19), and $(\widetilde{S}(t), \widetilde{I}(t), \widetilde{E}(t))^T$ is the solution to system (18) with $u(\cdot) = \widetilde{u}(\cdot)$. Then, there exist functions $\widetilde{\lambda_1}(t)$, $\widetilde{\lambda_2}(t)$, and $\widetilde{\lambda_3}(t)$, $0 \le t \le T$, such that*

$$\begin{aligned}\frac{d\widetilde{\lambda_1}(t)}{dt} &= \widetilde{\lambda_1}(t)\left(\mu + \gamma_1 + \theta + \sigma\left(\widetilde{I}(t)\right)\right) - \gamma_1 \widetilde{\lambda_3}(t)\\ &\quad - \widetilde{\lambda_2}(t)\left(\theta + \sigma\left(\widetilde{I}(t)\right)\right),\\ \frac{d\widetilde{\lambda_2}(t)}{dt} &= -1 - \widetilde{\lambda_1}(t)\left(\mu - C\widetilde{S}(t)\right) - \gamma_1 \widetilde{\lambda_3}(t)\\ &\quad + \widetilde{\lambda_2}(t)\left(\mu + \gamma_1 + \widetilde{u}(t) - C\widetilde{S}(t)\right),\\ \frac{d\widetilde{\lambda_3}(t)}{dt} &= -\eta_2 \widetilde{\lambda_1}(t) - \eta_1 \widetilde{\lambda_2}(t) + (\mu + \eta_1 + \eta_2)\widetilde{\lambda_3}(t),\\ &\qquad 0 \le t \le T,\end{aligned} \tag{21}$$

with transversality conditions $\widetilde{\lambda_1}(T) = \widetilde{\lambda_2}(T) = \widetilde{\lambda_3}(T) = 0$, where

$$C = \frac{\beta f\left(\widetilde{I}(t)\right) - \beta \widetilde{I}(t) f'\left(\widetilde{I}(t)\right)}{f^2\left(\widetilde{I}(t)\right)}. \tag{22}$$

Furthermore, we have

$$u^{*}(t) = \max\left\{\min\left\{\frac{\left(\widetilde{\lambda}_2(t) - \widetilde{\lambda}_1(t)\right)\widetilde{I}(t)}{\epsilon}, \overline{\gamma}_2\right\}, \underline{\gamma_2}\right\}, \quad 0 \le t \le T. \tag{23}$$

Proof. Note that the Hamiltonian is

$$H(S, I, E, \lambda_1, \lambda_2, \lambda_3, u) = I + \frac{\epsilon}{2}u^2 + \lambda_1\frac{dS}{dt} + \lambda_2\frac{dI}{dt} + \lambda_3\frac{dE}{dt}, \tag{24}$$

where λ_1, λ_2, and λ_3 are undetermined.

Then, applying the Pontryagin Minimum Principle [32], there exist functions $\widetilde{\lambda_1}(t)$, $\widetilde{\lambda_2}(t)$, and $\widetilde{\lambda_3}(t)$, $0 \le t \le T$, such that

$$\begin{aligned}
\frac{d\widetilde{\lambda_1}(t)}{dt} &= -\frac{\partial H\left(\widetilde{S}(t), \widetilde{I}(t), \widetilde{E}(t), \widetilde{\lambda_1}(t), \widetilde{\lambda_2}(t), \widetilde{\lambda_3}(t), \widetilde{u}(t)\right)}{\partial S},\\
\frac{d\widetilde{\lambda_2}(t)}{dt} &= -\frac{\partial H\left(\widetilde{S}(t), \widetilde{I}(t), \widetilde{E}(t), \widetilde{\lambda_1}(t), \widetilde{\lambda_2}(t), \widetilde{\lambda_3}(t), \widetilde{u}(t)\right)}{\partial I},\\
\frac{d\widetilde{\lambda_3}(t)}{dt} &= -\frac{\partial H\left(\widetilde{S}(t), \widetilde{I}(t), \widetilde{E}(t), \widetilde{\lambda_1}(t), \widetilde{\lambda_2}(t), \widetilde{\lambda_3}(t), \widetilde{u}(t)\right)}{\partial E},\\
&\qquad 0 \le t \le T.
\end{aligned} \tag{25}$$

Hence, system (21) follows by a straightforward calculation. As the terminal cost is unspecified and the final state is free, the transversality conditions hold.

Note that the optimality condition $H(\widetilde{S}(\cdot), \widetilde{I}(\cdot), \widetilde{E}(\cdot), \widetilde{\lambda_1}(\cdot), \widetilde{\lambda_2}(\cdot), \widetilde{\lambda_3}(\cdot), \widetilde{u}(\cdot)) = \min_{u(\cdot)\in U} H(\widetilde{S}(\cdot), \widetilde{I}(\cdot), \widetilde{E}(\cdot), \widetilde{\lambda_1}(\cdot), \widetilde{\lambda_2}(\cdot), \widetilde{\lambda_3}(\cdot), u(\cdot))$. Then, either

$$\begin{aligned}
&\frac{\partial H\left(\widetilde{S}(t), \widetilde{I}(t), \widetilde{E}(t), \widetilde{\lambda_1}(t), \widetilde{\lambda_2}(t), \widetilde{\lambda_3}(t), \widetilde{u}(t)\right)}{\partial u}\\
&\quad = \epsilon\widetilde{u}(t) + \widetilde{\lambda_1}(t)\widetilde{I}(t) - \widetilde{\lambda_2}(t)\widetilde{I}(t) = 0
\end{aligned} \tag{26}$$

or $\widetilde{u}(t) = \underline{\gamma_2}$ or $\widetilde{u}(t) = \overline{\gamma}_2$. Thus, the proof is complete. □

By combining the above discussions, the optimality system for the optimal control problem (19) can be derived as follows:

$$\begin{aligned}
\frac{dS(t)}{dt} &= u(t)I(t) + \eta_2 E(t) - \mu S(t) - \sigma(I(t))S(t)\\
&\quad - \gamma_1 S(t) - \theta S(t),\\
\frac{dI(t)}{dt} &= \sigma(I(t))S(t) + \theta S(t) - \mu I(t) - \gamma_1 I(t)\\
&\quad - u(t)I(t) + \eta_1 E(t),\\
\frac{dE(t)}{dt} &= \delta + \gamma_1 S(t) + \gamma_1 I(t) - \mu E(t) - \eta_1 E(t) - \eta_2 E(t),\\
\frac{d\lambda_1(t)}{dt} &= \lambda_1(t)\left(\mu + \gamma_1 + \theta + \sigma(I(t))\right)\\
&\quad - \lambda_2(t)\left(\theta + \sigma(I(t))\right) - \gamma_1\lambda_3(t),\\
\frac{d\lambda_2(t)}{dt} &= -1 - \lambda_1(t)\left(\mu - CS(t)\right)\\
&\quad + \lambda_2(t)\left(\mu + \gamma_1 + u(t) - CS(t)\right) - \gamma_1\lambda_3(t),\\
\frac{d\lambda_3(t)}{dt} &= -\eta_2\lambda_1(t) - \eta_1\lambda_2(t) + \left(\mu + \eta_1 + \eta_2\right)\lambda_3(t),\\
u(t) &= \max\left\{\min\left\{\frac{\left(\lambda_2(t) - \lambda_1(t)\right)I(t)}{\epsilon}, \overline{\gamma}_2\right\}, \underline{\gamma_2}\right\},\\
&\qquad 0 \le t \le T,
\end{aligned} \tag{27}$$

with $(S(0), I(0), E(0))^T \in \Omega'$, and $\lambda_1(T) = \lambda_2(T) = \lambda_3(T) = 0$.

Next, the effectiveness of optimal control will be examined. Here we have to point out that all parameter values are chosen hypothetically due to the unavailability of real-world data.

Example 12. Suppose that $\delta = 2$, $\mu = 0.01$, $\eta_1 = 0.012$, $\eta_2 = 0.021$, $\gamma_1 = 0.01$, $\theta = 0.015$, $\underline{\gamma_2} = 0.001$, $\overline{\gamma}_2 = 0.8$, $\sigma(I) = 0.005I/(1 + \sqrt{I})$, $\epsilon = 15$, and $T = 100$. The optimality system (18) with $(S(0), I(0), E(0)) = (100, 60, 40)$ is to be numerically solved with the backward-forward Runge-Kutta fourth-order scheme. Then Figures 5–7 and Table 1 are obtained.

Figures 5 and 6 exhibit the evolution of S and I with different control strategies, respectively. From these two figures, it is natural to see that the optimal control $\widetilde{u}$ is superior to others.

Table 1: The values of I and objective function J under different control strategies u.

	$u = \widetilde{u}$	$u = 0.001$	$u = 0.2$	$u = 0.4$	$u = 0.6$	$u = 0.8$
$I(u)$	5.5	104.1	19.9	9.5	6.1	4.3
$J(u)$	748.1	9894.8	2637.1	1671.4	1373.1	1322.9

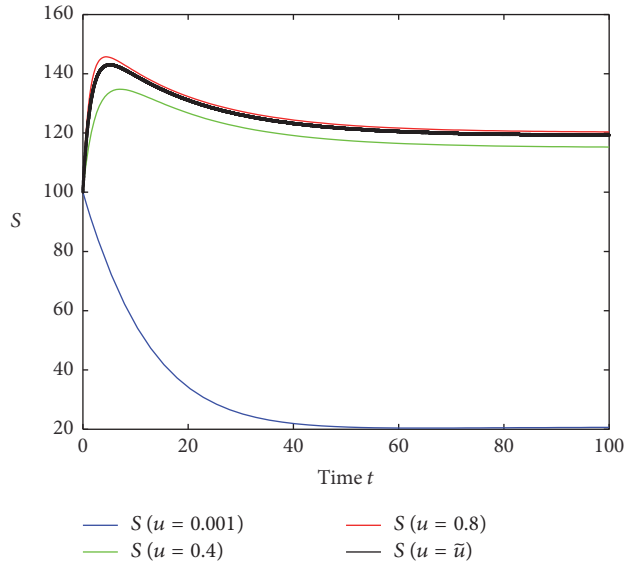

Figure 5: Evolution of number of susceptible computers with different control strategies.

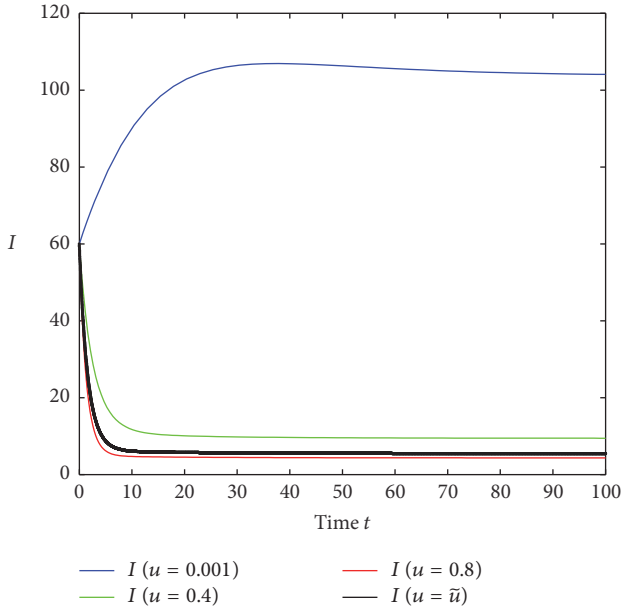

Figure 6: Evolution of number of infected computers with different control strategies.

Figure 7 shows the corresponding optimal control strategy.

Table 1 lists the values of infected computers I and objective function J under different control strategies. It is easy to conclude that $\widetilde{u}$ is the best choice.

5. Conclusions and Prospects

This paper has investigated an SIES model with generic nonlinear infection rate. A thorough analysis shows that the unique (viral) equilibrium is globally asymptotically stable. This result implies that any effort in eradicating computer virus is inoperative. As a result, a countermeasure, which mainly aims to maintain the number of infected computers at an acceptable level, and optimal control analysis of the proposed model have been posed. Some numerical examples are also included.

The study of this model not only implies some new practical measures but also gives a theoretical support to the usefulness of some existing antivirus strategies and provides the basis to developing many other more elaborated models.

The study can be continued in several directions. First of all, it would be interesting for complex network (e.g., scale-free network) because our model is a homogeneous model. Next, delays (or pulses) could be incorporated in our model so as to characterize the delay in the development of new vaccine (or the emergency of new virus). Finally, our model involves a relatively large number of parameters, which are very difficult to establish with accuracy. Therefore, it is appropriate to modify our model by considering the parameters to be random variables.

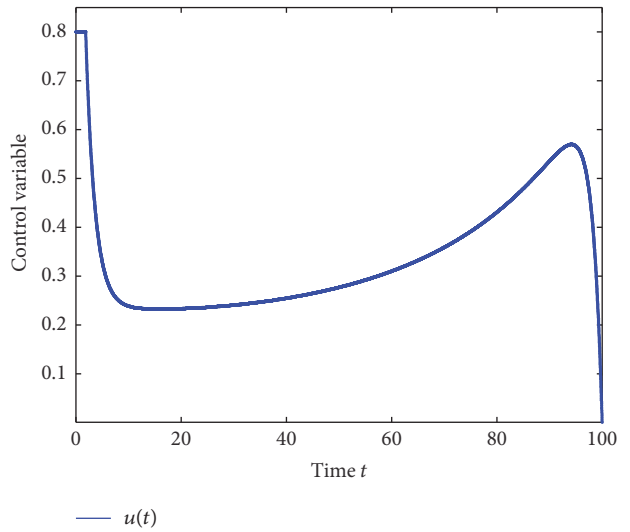

Figure 7: An optimal control function for system (18).

Competing Interests

The authors declare that there are no competing interests regarding the publication of this paper.

Acknowledgments

This work is supported by Natural Science Foundation of China (Grant nos. 11547148, 61603065, and 61503307), Innovation Project of the Common Key Technology of Chongqing Science and Technology Industry (Grant no. cstc2015zdcy-ztzx40008), Scientific and Technological Research Program of Chongqing Municipal Education Commission (Grant nos. KJ1500415 and KJ1500904), and Doctoral Scientific Research Foundation of Chongqing University of Posts and Telecommunications (Grant nos. A2015-02 and A2016-10).

References

[1] Z.-h. Zuo, Q.-x. Zhu, and M.-t. Zhou, "On the time complexity of computer viruses," *Institute of Electrical and Electronics Engineers. Transactions on Information Theory*, vol. 51, no. 8, pp. 2962–2966, 2005.

[2] J. O. Kephart and S. R. White, "Directed-graph epidemiological models of computer viruses," in *Proceedings of the IEEE Computer Society Symposium on Research in Security and Privacy*, pp. 343–358, May 1991.

[3] J. O. Kephart and S. R. White, "Measuring and modeling computer virus prevalence," in *Proceedings of the 1993 IEEE Computer Society Symposium on Research in Security and Privacy*, Oakland, Calif, USA, May 1993.

[4] L. Feng, X. Liao, H. Li, and Q. Han, "Hopf bifurcation analysis of a delayed viral infection model in computer networks," *Mathematical and Computer Modelling*, vol. 56, no. 7-8, pp. 167–179, 2012.

[5] C. Gan, X. Yang, W. Liu, Q. Zhu, and X. Zhang, "Propagation of computer virus under human intervention: a dynamical model," *Discrete Dynamics in Nature and Society*, vol. 2012, Article ID 106950, 8 pages, 2012.

[6] Q. Zhu, X. Yang, and J. Ren, "Modeling and analysis of the spread of computer virus," *Communications in Nonlinear Science and Numerical Simulation*, vol. 17, no. 12, pp. 5117–5124, 2012.

[7] C. Gan, X. Yang, W. Liu, and Q. Zhu, "A propagation model of computer virus with nonlinear vaccination probability," *Communications in Nonlinear Science and Numerical Simulation*, vol. 19, no. 1, pp. 92–100, 2014.

[8] J. Amador, "The stochastic SIRA model for computer viruses," *Applied Mathematics and Computation*, vol. 232, pp. 1112–1124, 2014.

[9] J. Ren and Y. Xu, "Stability and bifurcation of a computer virus propagation model with delay and incomplete antivirus ability," *Mathematical Problems in Engineering*, vol. 2014, Article ID 475934, 9 pages, 2014.

[10] B. K. Mishra and S. K. Pandey, "Dynamic model of worm propagation in computer network," *Applied Mathematical Modelling*, vol. 38, no. 7-8, pp. 2173–2179, 2014.

[11] Y. Yao, X. Feng, W. Yang, W. Xiang, and F. Gao, "Analysis of a delayed Internet worm propagation model with impulsive quarantine strategy," *Mathematical Problems in Engineering*, vol. 2014, Article ID 369360, 18 pages, 2014.

[12] C. Gan, "Modeling and analysis of the effect of network eigenvalue on viral spread," *Nonlinear Dynamics*, vol. 84, no. 3, pp. 1727–1733, 2016.

[13] W. Liu, C. Liu, Z. Yang, X. Liu, Y. Zhang, and Z. Wei, "Modeling the propagation of mobile malware on complex networks," *Communications in Nonlinear Science and Numerical Simulation*, vol. 37, pp. 249–264, 2016.

[14] C. Zhang and H. Huang, "Optimal control strategy for a novel computer virus propagation model on scale-free networks," *Physica A. Statistical Mechanics and its Applications*, vol. 451, pp. 251–265, 2016.

[15] B. K. Mishra, K. Haldar, and D. N. Sinha, "Impact of information based classification on network epidemics," *Scientific Reports*, vol. 6, Article ID 28289, 2016.

[16] J. R. C. Piqueira, A. A. de Vasconcelos, C. E. C. J. Gabriel, and V. O. Araujo, "Dynamic models for computer viruses," *Computers and Security*, vol. 27, no. 7-8, pp. 355–359, 2008.

[17] J. R. C. Piqueira and V. O. Araujo, "A modified epidemiological model for computer viruses," *Applied Mathematics and Computation*, vol. 213, no. 2, pp. 355–360, 2009.

[18] X. Han and Q. Tan, "Dynamical behavior of computer virus on internet," *Applied Mathematics and Computation*, vol. 217, no. 6, pp. 2520–2526, 2010.

[19] B. K. Mishra and S. K. Pandey, "Dynamic model of worms with vertical transmission in computer network," *Applied Mathematics and Computation*, vol. 217, no. 21, pp. 8438–8446, 2011.

[20] Q. Zhu, X. Yang, L.-X. Yang, and X. Zhang, "A mixing propagation model of computer viruses and countermeasures," *Nonlinear Dynamics*, vol. 73, no. 3, pp. 1433–1441, 2013.

[21] L.-X. Yang and X. Yang, "The impact of nonlinear infection rate on the spread of computer virus," *Nonlinear Dynamics*, vol. 82, no. 1-2, pp. 85–95, 2015.

[22] A. Lahrouz, L. Omari, D. Kiouach, and A. Belmaâti, "Complete global stability for an SIRS epidemic model with generalized non-linear incidence and vaccination," *Applied Mathematics and Computation*, vol. 218, no. 11, pp. 6519–6525, 2012.

[23] C. Gan, X. Yang, W. Liu, Q. Zhu, and X. Zhang, "An epidemic model of computer viruses with vaccination and generalized nonlinear incidence rate," *Applied Mathematics and Computation*, vol. 222, pp. 265–274, 2013.

[24] L.-X. Yang and X. Yang, "The spread of computer viruses under the influence of removable storage devices," *Applied Mathematics and Computation*, vol. 219, no. 8, pp. 3914–3922, 2012.

[25] C. Gan, X. Yang, Q. Zhu, J. Jin, and L. He, "The spread of computer virus under the effect of external computers," *Nonlinear Dynamics*, vol. 73, no. 3, pp. 1615–1620, 2013.

[26] Q. Zhu, X. Yang, L.-X. Yang, and C. Zhang, "Optimal control of computer virus under a delayed model," *Applied Mathematics and Computation*, vol. 218, no. 23, pp. 11613–11619, 2012.

[27] L. Chen, K. Hattaf, and J. Sun, "Optimal control of a delayed SLBS computer virus model," *Physica A*, vol. 427, no. 1, pp. 244–250, 2015.

[28] L.-X. Yang, M. Draief, and X. Yang, "The optimal dynamic immunization under a controlled heterogeneous node-based SIRS model," *Physica A. Statistical Mechanics and its Applications*, vol. 450, pp. 403–415, 2016.

[29] H. R. Thieme, "Asymptotically autonomous differential equations in the plane," *The Rocky Mountain Journal of Mathematics*, vol. 24, no. 1, pp. 351–380, 1994.

[30] R. C. Robinson, *An Introduction to Dynamical System: Continuous and Discrete*, Prentice Hall, New York, NY, USA, 2004.

[31] M. I. Kamien and N. L. Schwartz, *Dynamic Optimization: The Calculus of Variations and Optimal Control in Economics and Management*, Elsevier Science, Amsterdam, The Netherlands, 2000.

[32] D. Liberzon, *Calculus of Variations and Optimal Control Theory: A Concise Introduction*, Princeton University Press, Princeton, NJ, USA, 2012.